Cardiff University

School of Biosciences

Enhanced molecular assays using strand-displacing polymerases and loop mediated amplification (LAMP) with Bioluminescent Assay in Real Time (BART) reporter

Tomasz Lasota

September 2017

A thesis submitted in partial fulfilment of the requirements for the degree of Doctor of Philosophy

Preface

DECLARATION

This work has not been submitted in substance for any other degree or award at this or any other university or place of learning, nor is being submitted concurrently in candidature for any degree or other award.

Signed …… (candidate) Date ……

STATEMENT 1

This thesis is being submitted in partial fulfillment of the requirements for the degree of ……(insert MCh, MD, MPhil, PhD etc, as appropriate)

Signed …… (candidate) Date ……

STATEMENT 2

This thesis is the result of my own independent work/investigation, except where otherwise stated.

Other sources are acknowledged by explicit references. The views expressed are my own.

Signed …… (candidate) Date ……

STATEMENT 3

I hereby give consent for my thesis, if accepted, to be available for photocopying and for inter-library loan, and for the title and summary to be made available to outside organisations.

Signed …… (candidate) Date ……

STATEMENT 4: PREVIOUSLY APPROVED BAR ON ACCESS

I hereby give consent for my thesis, if accepted, to be available for photocopying and for inter-library loans **after expiry of a bar on access previously approved by the Academic Standards & Quality Committee.**

Signed …… (candidate) Date ……

Acknowledgments

I would like to express my special thanks of gratitude to Prof. Jim Murray and Dr. Laurence Tisi for giving me this opportunity and for their supervision throughout the project. Their support and guidance has been invaluable during the last four years.

Within the Murray Lab, I would like to thank everyone for their continuous support and contribution through many insightful discussions and suggestions, particularly Dr Patrick Hardinge as his extensive expertise and support were invaluable. I would also like to direct my special thanks to Ms Angela Marchbank and Ms Jo Kilby for their invaluable technical support.

I am also very fortunate to have worked with ERBA Molecular during my Collaborative Award in Science and Engineering studentship scheme. I would like to express my special gratitude to Dr Laurence Tisi for giving me this one in a lifetime opportunity. I would also like to thank Dr Guy Kiddle for his tremendous support and guidance throughout the project and preparation of this thesis. I have gained not only highly valuable experience but also have grown as a scientist and an individual. I greatly enjoyed the time I spent with the ERBA Molecular team and I would like to thank everyone for their input. I am also most grateful to Rachel Blackwell and Eleonora Golfetto for providing me with all the essential samples and templates. I would also like to thank Mrs. Kirsty Thomson for her help with proofreading of this document.

I would like to thank BBSRC and ERBA Molecular for funding me through my degree. This opportunity would not have been available to me without their financial support.

I would also like to express my gratitude and love to all of my family and friends. I would not have done it without you. Mum and dad, thank you for the love and support you have given me. All I am and all I will ever be is because of you. Mum, you have been my closest friend, my strength. Thank you for all the sacrifices and your unconditional love. I hope I made you proud.

I would also like to direct my thanks to Eleonora Golfetto, Jamie Jenkins and Juan de Torez. Thank you for being true friends.

Finally, I would like to give my special thanks to Rob Bonemei. Thank you for believing in me.

Abstract

Real-time reverse transcription loop-mediated isothermal amplification (RT-LAMP) is becoming a widely accepted method for use in the field of molecular diagnostics. This method makes use of a highly robust core enzymology's that are tolerant to sample derived inhibitors, along with a priming mechanisms that permit impeccable amplification sensitivities and specificities. These are well documented attributes associated with LAMP, but little is known about factors that drive and interfere with the reverse transcription of RT-LAMP assays.

This study aims to address a number of factors that affect RNA amplification, including impedance of priming related to template structure, inhibition of polymerase activities by sample derived inhibitors and the general effect of assay chemistry and primer function with respect to reverse transcription. In addition to the chemistry optimisation and choice of polymerase (DNA / RT), the secondary structure innate within RNA, could significantly affect the efficiency of RT. Priming position and design would also need to be seriously considered with respect to the folding nature of these targets. Overtly, RT-LAMP showed an increased sensitivity to inhibition compared to its DNA counterpart.

Similar observations of impeded RNA transcription were made during the development of an internal amplification control (IAC), which was designed to determine the exact inhibitory nature of any tested samples, in tandem with the RT-LAMP. This report clearly discloses that RT amplification controls must be synthesised 'free of contaminating DNA', to avoid poor characterisation of first strand DNA synthesis.

Alternative 'non-enzymatic methods' of reporting amplification in real-time were compared to the bioluminescent assay real-time (BART) reporter; a well-established method of nucleic acid detection and quantification developed and patented by Lumora Ltd, Cambridgeshire (Fortes et al., 2013). Despite BARTs track record for detection of LAMP, its

indiscriminate reporting of amplification is of little use for duplexed assay characterisation, such as the IAC / RT-LAMP combined assay. Thus, methods of specific sequence detection were designed that could target single stranded elements of amplified products (STEMs and LOOP structures). It was demonstrated that the mechanism for RT-LAMP fluorescent probing 'presented here' was unique to this Thesis and does not fall under the guise of *Taq*man or other molecular beacon detection mechanisms. Together with BART, this new form of probing was successfully deployed to distinguish between true RT-LAMP and IAC afflicted amplifications.

The possibility of utilising the LAMP / BART technologies for microRNA (miRNA) detection was also explored. Even though it is well known that miRNAs have crucial roles in responding to and regulating a wide range of biological and cellular processes, no real headway has been made in developing highly sensitive, low resource methods for their detection. Here we develop novel methods of miRNA detection capable of sensing picomolar levels that also make use of the LAMP and BART chemistry.

Abbreviations

APS – Adenosine 5’ phosphosulfate

BART – Bioluminescent Assay in Real Time

DNA – Deoxyribonucleic acid

DTT – Dithiothreitol

dNTP – Deoxyribonucleotide

LAMP – Loop-mediated amplification

LH_2 – Luciferin

Luc – Luciferase

MGW – Molecular grade water

NLC – No ligation control

NTC – No template control

PCR – Polymerase chain reaction

PPi – Inorganic pyrophosphate

PVP – Polyvinylpyrrolidone

RLU – Relative luminescent unit

RFU – Relative fluorescent unit

RT – Reverse transcription

TTM – Time to max

Further abbreviations follow the guidelines described in the Nomenclature, Style and Conventions section in Biochemical Journal Instructions to Authors, The Biochemical Society, London 2014.

Table of Contents

Chapter 1

1 Introduction

1.1 Molecular diagnostics

The field of molecular diagnostics has undergone major developments in recent years, as the increasing need for highly accurate detection methods capable of screening a wide range of clinical and environmental samples has driven the development of these diagnostic tools (Opel et al., 2010, Craw and Balachandran, 2012). Most molecular diagnostics (MDx) platforms amplify and detect nucleic acid (NA) sequences, which are specific to a particular disease or phenotype. Increasingly, MDx has been adopted for a wide range of research and biomedical screening solutions that include pathogen testing, cancer diagnostics, GM / contaminant screening, DNA profiling, conservational biology and environmental monitoring (Young and Cotter, 1992, Fenton and Lowndes, 2004, Kiddle et al., 2012).

Molecular diagnostics have proven particularly useful for detection of infectious diseases, and as a consequence, have seen an explosion in advances over the last decade, as the need for quick and highly accurate detection methods have become more critical to our well-being (Euler et al., 2012, Scott and Gretch, 2007). The evolution and advances in MDx has been particularly useful, as the human population faces more acute challenges, caused by emerging and re-emerging infectious diseases. Research into molecular diagnosis of various diseases has provided scientists with a better understanding of all the molecular factors affecting human health, but has also offered solutions for treatment that can greatly improve a patient's prognosis and reduce the risk of new infections (Muldrew, 2009).

Serological-based diagnostics have been the methods of choice for decades, but many of these tests are stricken with problems that lead to poor performance, and significant variations in accuracy and reliability (Fierz, 2004). Serological diagnosis are surrogate tests that do not

qualify the presence of the disease causing agent or its cause directly, but rather the immune response of the host; which can lead to a misdiagnosis of positivity and negativity. Each patient's immunity is unique and large variabilities with respect to the amplitude and time to a response have been recorded (Kunisaki and Janoff, 2009, Simon et al., 2015). Accordingly, differences in immune response can not only result in a misdiagnosis, but also this variability greatly increases the risks of the disease spreading within a population. In addition, indirect measurements of one's antibodies gives a much less accurate prediction of disease outcome with respect to medical treatments (Zhang et al., 2011). Furthermore, during the acute phase of any infection (termed the eclipse), the immune response is undetectable, as these technologies have poor sensitivity and often the infected have not seroconverted (Kharsany et al., 2010).

Nucleic acid amplification technologies (NAAT) that directly measure the presence of a microorganism offer clinicians highly reliable alternative to serological tests and this type of diagnosis often leads to a much faster and more accurate diagnosis. These technologies are also far more sensitive than immunoassays, but are often expensive and require sophisticated machinery.

1.1.1 PCR-based platforms

Currently, quantitative, real-time polymerase chain reaction (PCR), is the method of choice used for MDx of infectious disease (Kurkela and Brown, 2009). Although, the PCR approaches have greatly improved the sensitivity and sample throughput of MDx assays, the technology still carries major limitations (Patel et al., 2006, Curtis et al., 2008, Yang and Rothman, 2004, Ding et al., 2011, Kiddle et al., 2012, Liolios et al., 2001). Firstly, the real time PCR-based NA detection techniques often employ expensive fluorescent probes, which require complex equipment that is capable of detecting the fluorescent signal but also complicated hardware

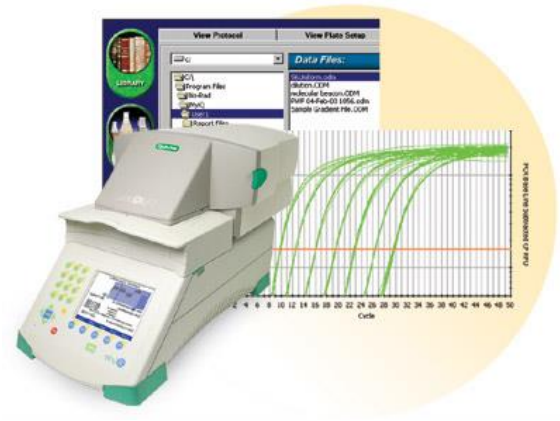

Figure 1. Typical real-time PCR equipment used in a wide range of biomedical research for detection and quantification of nucleic acids.

Source: http://www.gene-quantification.de/platform1.html

capable of driving thermal cycles (**Figure 1**). Secondly, depending on the source of the biological material tested (e.g. clinical samples such as blood, urea or faeces; processed foods or even environmental samples including soils and plan material), PCR amplification can suffer from severe inhibition resulting which may result in false negatives (Tebbe and Vahjen, 1993). Finally, due to the increased sensitivity of this technology, PCR assays have to be carried out in a nucleic acid-free laboratory, by experienced scientists in order to reduce potential for reagent contamination, which can often produce false positive results.

1.1.2 Isothermal amplification of nucleic acids

To prime any polymerised chain reaction requires the opening of the DNA or RNA structure to allow for a primed polymerisation. This is often performed using a thermal stable polymerase and denaturing conditions which melt the target polynucleotide prior to primer annealing and extension; this type of reaction requires sophisticated machinery capable of managing a thermal cycle. Alternative isothermal amplifications exist that make use of a unique property of certain DNA polymerases (e.g. Bst DNA polymerase from *Bacillus stearothermophilus*) that have helicase or strand displacement activity and unique primer design strategies enable nucleic acid synthesis to be carried out at a constant temperature eliminating the requirements for expensive thermocycling equipment.

Currently, there are over a dozen isothermal technologies that make use of displacement polymerases and priming mechanisms: Loop-mediated isothermal amplification (LAMP), rolling circle amplification (RCA), nucleic acid sequence based amplification (NASBA),

recombinase polymerase amplification (RPA), helicase-dependent amplification (HDA), transcription-mediated amplification (TMA), single primer isothermal amplification (SPIA) and strand displacement amplification (SDA(Gill and Ghaemi, 2008). However, among the techniques mentioned above, LAMP has been shown to be one of the most rapid and sensitive methods of nucleic acid amplification with an average assay time of 60 min or less (Gandelman et al., 2011, Walker et al., 1992, Compton, 1991).

1.1.2.1 Rolling circle amplification (RCA)

The rolling circle nucleic acid amplification employs a unique property of ϕ29 DNA polymerase with a strand displacement activity and circle-hybridized primers to generate multiple copies of a circular DNA/RNA probe via numerous rounds of isothermal amplification (Fire and Xu, 1995). More recent developments in the RCA technology has given rise to a much faster way of amplifying circular DNA directly from cells and plaques. Multiple-primed RCA involves addition of random primers, complementary to the sequences of interest, that target both the circular DNA template as well and the single-stranded (ss) DNA concatemers generated from replication of these targets (**Figure 2)**(Dean et al., 2001).

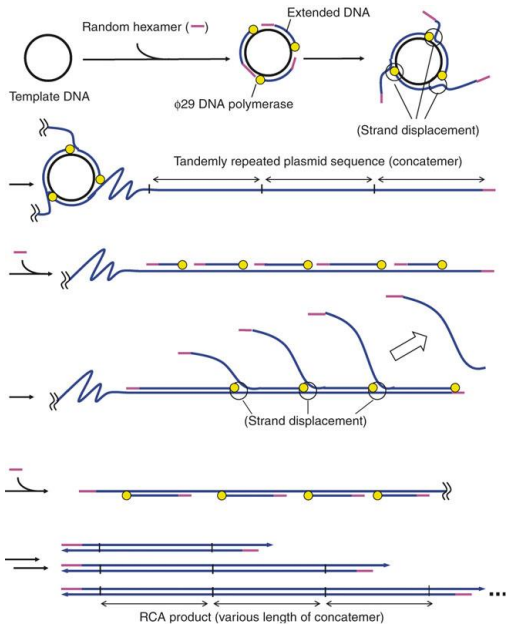

Figure 2. Graphic representation of multiply-primed RCA. Random oligonucleotides complementary to the target sequences hybridize to the circular template. Biding of the ϕ29 DNA polymerase initiate amplification. Multiple rounds of DNA synthesis results in generation of long single-stranded DNA concatemers with tandemly repeated target sequences.

Source:https://www.researchgate.net/publication/6416450_Error-prone_rolling_circle_amplification_The_simplest_random_mutagenesis_protocol

1.1.2.2 Nucleic acid sequence based amplification (NASBA)

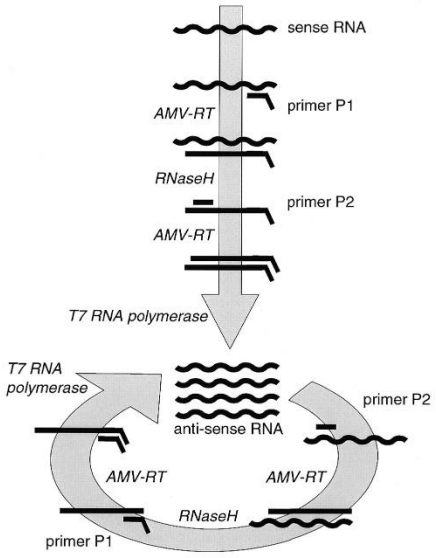

Figure 3. Schematic representation of the NASBA amplification technology. The straight arrow represents the initiation step of the amplification procedure required to start off the self-sustained phase (circular arrow) of the synthesis procedure by generating anti-sense RNA templates.

Source: https://www.researchgate.net/figure/259155941_fig2_Principles-of-nucleic-acid-sequence-based-amplification

Nucleic acid sequence-based amplification or self-sustained sequence replication (3SR) is another isothermal amplification method used in synthesis of nucleic acids (Compton, 1991). Unlike the previously mentioned RCA, NASBA uses RNA as the target for amplification. NASBA technology makes use of avian myeloblastosis virus reverse transcriptase (AMV-RT), RNase H and a T7 RNA polymerase to generate multiple copies of anti-sense RNA and single-stranded cDNA (sscDNA) molecules (**Figure 3**). The amplification reaction begins with hybridisation of specific primers containing T7 RNA polymerase-binding sites to the target RNA molecules. Once bound, reverse transcriptase begins the synthesis of a cDNA copy of the target RNA forming a RNA/DNA double-stranded hybrid molecule. Unique property of the RNase H enzyme to recognise such hybrids and degrade the RNA portion of the RNA/DNA complex results in generation of sscDNAs. A second set of primers binds to the sscDNA molecules initiating replication of the complementary strands. Once a double-stranded cDNA is formed the T7 RNA polymerase binding site becomes activated.

T7 RNA polymerase produces multiple copies of the anti-sense RNA template, which can be used in a self-sustained phase of the amplification procedure. Each anti-sense RNA, can be reverse transcribed into a double-stranded cDNA version of itself therefore carrying an active binding site for the RNA polymerase enzyme.

1.1.2.3 Recombinase polymerase amplification (RPA)

Recombinase polymerase amplification (RPA) utilizes three core enzymes including: a recombinase, a single-stranded DNA binding protein (SSB) and DNA polymerases with strand displacement activity (Euler et al., 2012).

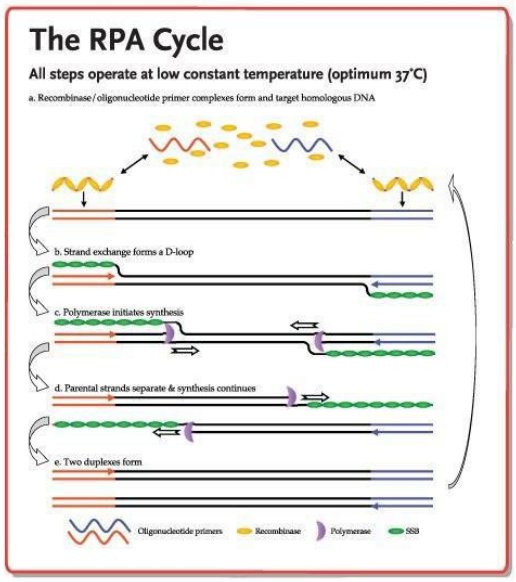

Figure 4. Schematics representation of the principle behind the RPA-based DNA amplification technology.

Source: https://www.researchgate.net/figure/264796231_fig1_The-three-core-proteins-recombinase-single-strand-DNA-binding-protein-SSB-and

In principle, the system relies on the ability of the recombinase to facilitate primer invasion which in turn allows the binding of DNA polymerases and initiation of the replication reaction (**Figure 4**). Once the DNA polymerase begins the amplification of new DNA strands, the parental strand (complementary to the strand used as the template for the DNA polymerase enzyme) is displaced and coated with the single-stranded DNA binding proteins to prevent re-hybridisation to its complement.

Recent developments in RPA have attracted the attention of diagnostic companies such as TwistDx^{TM} due to the efficiency and the simplicity of the assays with potential applications in rapid, near care diagnostics (Aebischer et al., 2014, Kersting et al., 2014).

1.1.2.4 Helicase-dependent amplification (HDA)

Helicase-dependent amplification is very similar mechanism to PCR amplification. Instead of the heat denaturation of the DNA double helix required in PCR, HDA uses helicase enzymes to unwind DNA molecules, thereby generating single-stranded DNA templates (Vincent et al., 2004).

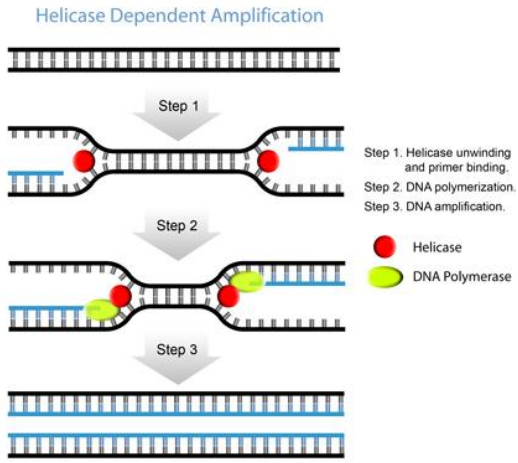

Figure 5. The figure shows HDA-based isothermal DNA amplification process.

Source: https://www.neb.com/products/h0110-isoamp-ii-universal-thda-kit

In general, the HDA-based DNA amplification is carried out in two main steps (**Figure 5**). Firstly, helicases unwind and separate both strands of the target DNA molecules allowing primers to anneal to their complementary sequences. Secondly, DNA polymerase binds and extends annealed primers until the entire complementary strand is fully synthesised. In addition, it has also been reported that the use of SSB proteins is crucial for the DNA replication step. SSB proteins prevent re-hybridization of the separated complementary strands which in turns indirectly facilitates the primer binding step of the amplification process (Cao et al., 2013, Chase and Williams, 1986). Recent studies have shown that the HDA-based assays have the potential of being developed into hand-held diagnostic devices suitable for the point-of-care or in-field diagnostics due to its simplicity and low energy requirements (Li et al., 2013).

1.1.2.5 Strand displacement amplification (SDA)

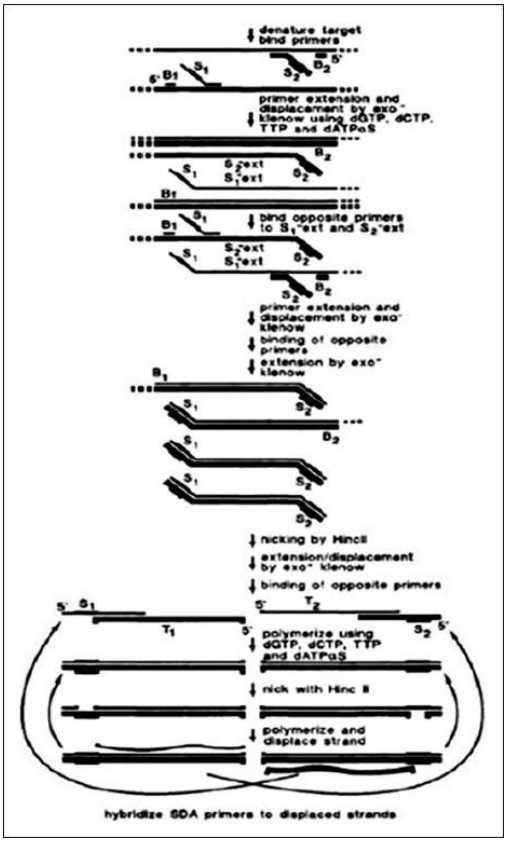

Figure 6. Graphic representation of the SDA-based DNA amplification technology. (A) This figure reflects the initial step of the SDA reaction which generates multiple copies of the target sequence flanked with HincII restriction sites. Primers S1 and S2 carries the HincII restriction sites targeting the sequence of interest. Primers B1 and B2 are displacement primers that anneal downstream of the S1/S2 primer binding sites. (B) The SDA reaction cycle.

Source: https://www.researchgate.net/figure/259155941_fig3_Target-generation-scheme-for-strand-displacement-amplification

Strand displacement amplification relies on restriction enzymes that introduce nicks to double-stranded DNA molecules and the action of DNA polymerases, lacking the exonuclease activity (e.g. klenow exo$^-$), to displace the complementary strand downstream from the nick. As a result, both the displaced and the complementary strands serve as templates for DNA replication generating multiple copies of the target sequence (**Figure 6**)(Walker et al., 1992).

In essence, the SDA amplification begins with a denaturation step, which is crucial for this technology. Four different primers (B1, B2, S1, S2) bind to the ssDNA templates, which initiate primer elongation and strand displacement events. The S1 and S2 primers are designed to target the sequence of interest as well as to introduce the HincII restriction sites to the target DNA which, the later stages of the SDA amplification, are required to sustain the isothermal amplified (**Figure 6**). Nick sites are then recognized by the klenow DNA polymerase, which initiates DNA replication and the displacement of the complementary, parental strand, which in turns acts as the template for further DNA replication reactions (**Figure 6**). The SDA technology has mainly been used in clinical diagnostics for infectious diseases such as chlamydia or gonorrhea. However, since the initial step of the SDA-based nucleic acid amplification involves a denaturation step, it is

unlikely that this technology will be used for rapid in-field diagnostics (Walker et al., 1992, Gill and Ghaemi, 2008, Chan et al., 2000).

1.1.2.6 Transcription-mediated amplification (TMA)

Transcription mediated amplification is a rapid method of nucleic acid amplification based on RNA transcription technology (**Figure 7**). In general, unlike most currently used isothermal methods, TMA produces RNA amplicons via T7 transcription using two core enzymes, T7 RNA polymerase and a reverse transcriptase (RT). Firstly, a specific primer containing a T7 promoter sequence at its 5' end binds to the target RNA molecule followed by a reverse transcription process carried out by the RT enzyme. During this step, a complementary cDNA strand is synthesized while the RNA template is being degraded by an RNase H activity of the chosen RT. Once a single-stranded cDNA is formed, a second primer anneals and triggers synthesis of the missing second strand of the cDNA, resulting in generation of a double stranded T7 promoter site.

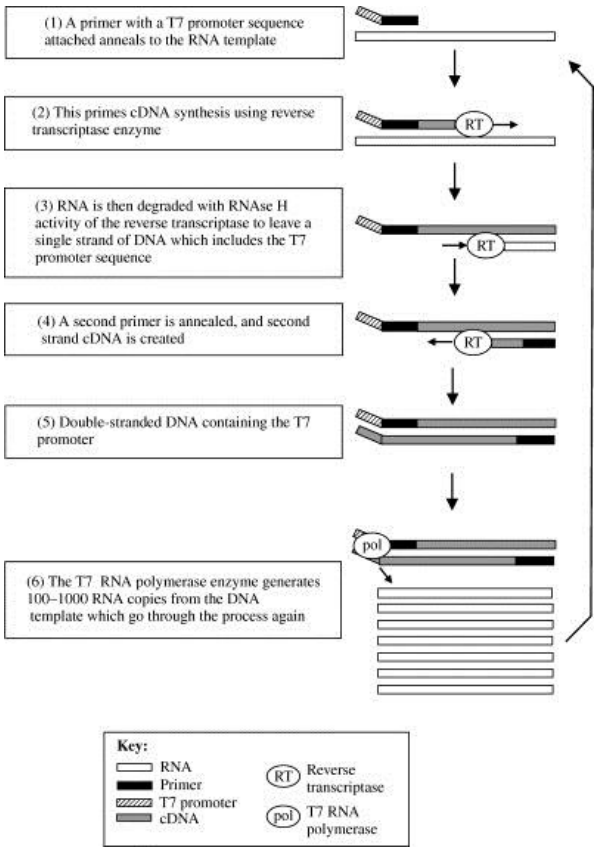

Figure 7. Graphic representation of the TMA NA amplification technology.

Source: https://www.researchgate.net/figure/11169695_fig3_Figure-2-Transcription-mediated-amplification-TMA

T7 RNA polymerase binds to the promoter site and begins transcription of the target RNA molecules, which in turns are again targeted by the T7 promoter site containing primer, repeating the described amplification cycle. TMA has been reported to be able to generate billions of amplicons in 60 min or less and has been successfully used in HIV or TB diagnostics.

1.1.2.7 Loop-mediated isothermal amplification (LAMP)

Loop-mediated isothermal amplification (LAMP) is a rapid and highly specific method of nucleic acid amplification, developed by the EIKEN Chemical Company, in-which the polymerization reactions proliferate at a constant temperature (Notomi et al., 2000, Nagamine et al., 2002). A typical LAMP mechanism can be sub divided into three main phases: **I** – the initiation**; II** – cycling amplification and **III** – recycling and elongation, which together amplify each original template molecule 10^9 times within 60 min (**Figure 8**).

Classical LAMP relies on at least two classes of primers that initiate and maintain amplification; known as inchworm and displacement primers. Two reciprocal inchworm primers (FIP and BIP) are utilized throughout all the phases of LAMP amplification, targeting the sense and antisense strands of each invaded DNA template. In contrast, the use of the displacement primers is only limited to the phase I.

Once amplification is initiated *via* the inchworm primers, the first order amplicon is chased from the original DNA template by dedicated displacement primers, releasing strands of DNA that contain self-replicating loops derived from the inchworm primer at the 5' terminus (**Figure 8 I4**). This molecule is then subjected to an amplification from the alternate inchworm generating a second order displaced molecule with two terminal self-hybridizing loop structures known as the dumbbell that has great potential for further rounds of amplification (**Figure 8 I6**). The terminal loop structures of the dumbbell are single-stranded and contain engineered sites originating from the inchworm primer that readily hybridize additional inchworm primers (**Figure 8 II7)**.

Further to the described, other LAMP derivatives are engineered to include additional unique template-derived priming sites, within the single stranded portions of the replication loops or dumbbell stems; these are aptly named Loop or Stem primers. Both primers serve to increase the overall concentration of DNA that can be specifically polymerized from the initiated

reaction, and therefore increase the kinetics of amplification detected in real time or shorten the time to result for endpoint reactions (Gandelman et al., 2011, Nagamine et al., 2002).

The final phase III of the amplification relies on the activity of both the LAMP and loop primers where the overall amplification kinetics are significantly accelerated resulting in the formation of a mixture of a wealth of secondary cauliflower-like, stem-loop structures of various lengths, as well as branch chain concatemers (**Figure 8III**) (Notomi et al., 2000).

From the point at which the dumbbell is synthesized, all down-stream amplification processes are cyclical and propagating through phase III, until either the primer and amplification precursors are exhausted or until the products of the reaction become intoxicating.

Like all isothermal amplification methods, LAMP is a displacement technology that does not just rely on sophisticated priming mechanisms, but also on highly displacing polymerases that have the capacity to unwind the double helix. The helicase activity associated with these enzymes defines their function. Of the commercialized enzymes such as Bst large fragment, Bst 2.0, Bst 2.0 WarmStart, Bst 3.0 (NEB), GSP-SSD (OptiGene) or phi29 (NEB), many have big variations in their temperature optimum, which can range from 30 to 75^{o}C. Some enzymes also possess additional associated activities that are helpful to biotechnologists such as reverse transcription, which is particularly useful in diagnostic tests, which check RNA expression or retro-viral loads (GSP-SSD, Bst 3.0). In addition, some of these enzymes are also marketed for their tolerance to sample derived inhibitors that are known to affect PCR-based platforms, such as humic acid or various salts (Bst 2.0, NEB; GSP-SSD, OptiGene) (Kiddle et al., 2012, Opel et al., 2010).

Furthermore, in comparison to other nucleic acid amplification technologies, such as PCR or TMA, LAMP offers a higher specificity, since any successful propagation of polymerization is reliant on coordinated priming from at least six annealing positions, which reduces the

number of false positive results caused by non-specific priming (Gandelman et al., 2011, Buhlmann et al., 2013).

As a consequence of the above the LAMP technology is attractive to companies and it has been licensed for food and clinical testing, and continues to grow as the preferred method for molecular diagnosis (Mori and Notomi, 2009).

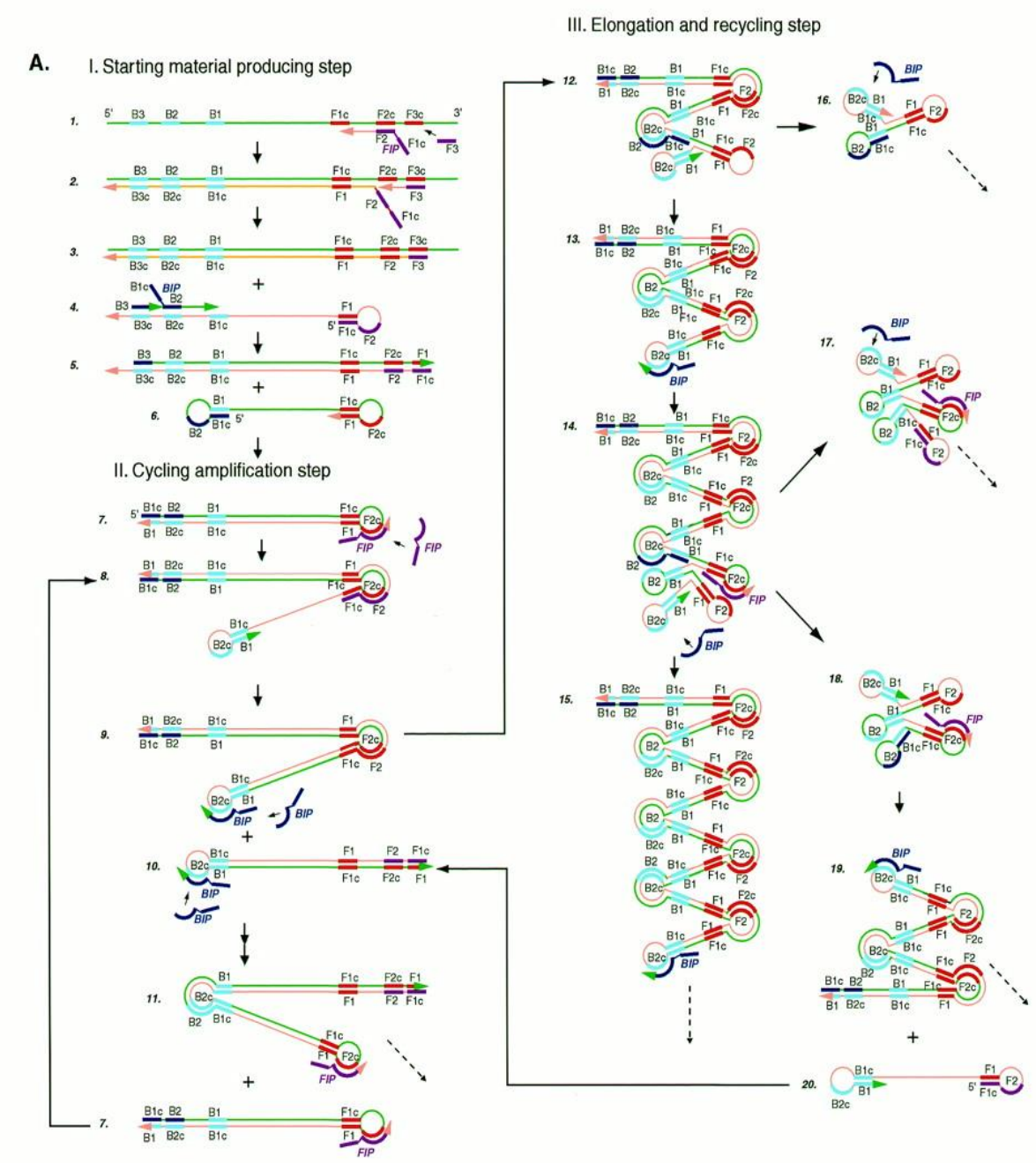

Figure 8. Schematic representation of the principle behind the LAMP-based DNA amplification technology. (I) The initiation of the LAMP amplification begins with a series of primer invasion, DNA replication and strand displacement events that result in generation of the starting LAMP material; dumbbell-like DNA structure (I6). This self-priming structure is a crucial element of the LAMP reaction enabling nucleic acid amplification without the need for heat-denaturation steps. (II) In the cycling amplification steps, DNA fragments of various length and stem structure are formed. (III) The elongation and recycling steps involve both, the LAMP and Loop primers targeting the previously formed dumbbell-like DNA fragments resulting in formation of cauliflower-like, multi-loop structures.

Source: https://www.researchgate.net/figure/260915985_fig5_Fig-10-Mechanism-of-Loop-mediated-amplification-LAMP-Four-probes-F1c-F2-F3-R1c-R2

Table 1. Characteristics of various isothermal nucleic acid amplification technologies and PCR.

Property	PCR	NASBA	SDA	RCA	LAMP	HDA	RPA
DNA amplification	+	+	+	+	+	+	+
RNA amplification	+	+	+	+	+	+	+
Temperature [°C]	95, 55-60,72	37-42	37	37	55-65	22-24, 37, 60-65	37-42
Primer design	simple	simple	complex	simple	complex	simple	simple
Multiplexing	+	+	-	+	-	+	+
Tolerance to inhibition	-	-	-	-	+	+	-
Need for template denaturation	+	+*	+	-	-	-	-
Denaturing agent	heat	RNase H	restriction enzymes	strand displacement	primer invasion	helicase	recombinase

*- denaturation step required when DNA template is used

1.1.3 Summary of isothermal amplification technologies

Isothermal amplification technologies are slowly becoming the method of choice and are used in a wide range of molecular applications, offering several advantages over the traditional PCR-based techniques. However, all of the currently available isothermal nucleic acid amplification methods, convey several advantages and disadvantages, which potentially limit their use (**Table 1**). Although, all of the isothermal amplification techniques mentioned previously can use both DNA and RNA, as the templates for replication reaction, some of them require additional steps to initiate self-sustained polymerisation. For example, SDA technology requires the use of four primers, an initial heat-denaturation step, as well as modified dNTPs in order to generate initial amplicons with strand-specific nicking (Walker et al., 1992). Furthermore, this technology is rather inefficient for amplifying of long sequences (Gill and Ghaemi, 2008).

LAMP requires four to six different primers to sustain nucleic acid amplification, which could be problematic if their design was poor. Despite the complexity of the LAMP primer design, the use of multiple primers to target the sequence greatly increase the specificity of detection. Furthermore, the final LAMP amplicons are a complex, they have cauliflower-like structures of different sizes that can limit their use in several downstream applications, such as sequencing and hybridization techniques (Gill and Ghaemi, 2008).

One of the most important advantages of the isothermal amplification technologies are their tolerance to inhibitory substances that are known to greatly affect PCR (e.g. haem, urea, humic acids). LAMP and HDA have been demonstrated to be least sensitive to inhibitory substances commonly encountered in molecular diagnostics (Niemz et al., 2011, Gill and Ghaemi, 2008, Vincent et al., 2004, Kiddle et al., 2012). According to those studies, LAMP was highly resistant to several components of various clinical samples where PCR was shown to fail.

Higher resistance to biological samples carries a huge advantage in terms of sample preparation where for some steps of the nucleic acid purification steps could potentially be omitted (e.g. HDA has been shown to be able to successfully amplify target DNA directly from human blood)(Vincent et al., 2004).

Isothermal amplification technologies eliminate the need for heat denaturation which reduce the costs of the equipment required to carry out such reactions. Since LAMP does not require initial DNA melting steps to facilitate primer binding and subsequent DNA replication events, this technology is much better suited for rapid and highly specific molecular diagnostic tests (Gill and Ghaemi, 2008, Gandelman et al., 2010).

In conclusion, current isothermal amplification technologies differ in their method of amplification, reaction volumes and sample preparation. There is no doubt that the simplicity and the isothermal nature of these technologies has huge implications for the development of hand-held molecular diagnostic devices suitable for near-care or in-field detection.

1.1.4 Bioluminescent Assay in Real Time

Currently, the most commonly used method of reporting nucleic acid amplification in real-time, for both the PCR- and isothermal- based technologies, is the use of fluorescent probing and inter chelating dyes (e.g. SYBR-green, molecular beacons or TaqMan probes)(**Figure 9**)(Freeman et al., 1999). Although, these methods of detection offer many advantages, such as the specificity of detection (TaqMan), or simplicity (SYBR-green) and the possibility of multiplexing (TaqMan / beacons) by combining probes derivatised with different colour dyes, fluorescence-based detection does have its limitations. These mainly include: complexed primer design, the expense of detectors capable of differentiating between fluorophores, and the inhibition of amplification by chelating dyes.

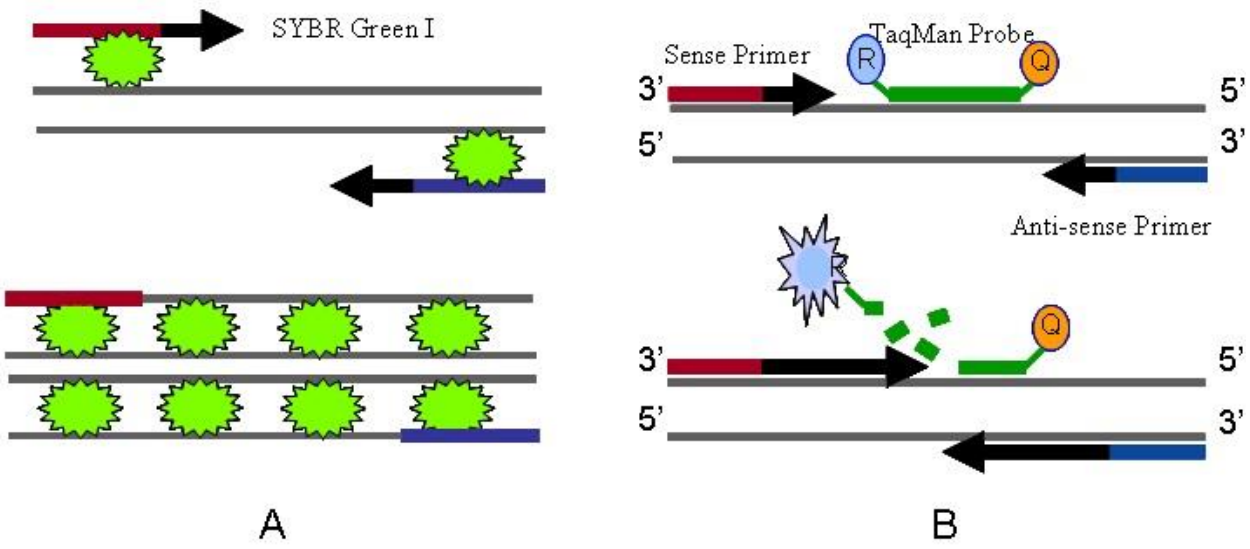

Figure 9. Current, commonly used, fluorescence-based DNA detection probes. (A) SYBR-green dye used for detection of double-stranded DNA molecules. In principle, the dye binds to any double-stranded DNA which results in emission of a fluorescent signal under blue light. The fundamental property of this dye is the fact that no signal emission occurs unless the dye molecules are bound to dsDNA. (B) TaqMan probes, unlike the SYBR-green, are designed to increase the specificity of DNA quantification (e.g. Quantifiler®DNA quantification kit uses probes specific only to human DNA). In general, the TaqMan probes are hydrolysis-based probes with covalently attached fluorophore (e.g. FAM) at the 5' end and a quencher (e.g. TAMRA) at the 3' end. The role of the quencher is to absorb any signal emitted by the fluorophore whilst both bound to the detection probe to prevent any false results. Once the probe binds to its target sequence and the DNA replication takes place, the exonuclease activity of *Taq* polymerase hydrolyse the probe releasing the fluorophore. Since the released fluorophore is no longer in close proximity to the quencher, emitted fluorescent signal can be detected.

As well as fluorescence technologies, bioluminescence approaches for detecting polymerisation were realised commercially at the turn of this century, but it was a while before these evolved to be mainstream detection of DNA amplification (Nyrén et al., 1993, Gandelman et al., 2010).

A method called enzymatic luminometric detection of inorganic pyrophosphate (ELIDA) was the first bioluminescent chemistry to detect the instantaneous production of pyrophosphate (PPi) generated as a biproduct of pyrosequencing (**Figure 10**)(Nyrén et al., 1993).

In this technology, the addition of one of the four deoxynucleotide triphosphates (dNTPs) during the sequencing reaction releases PPi that is converted into ATP *via* ATP sulphurylase in the presence of adenosine 5´ phosphosulfate. This ATP then acts as a substrate for the luciferase-

mediated conversion of luciferin to oxyluciferin resulting in generation of visible light, which can then simply be detected by a camera or photodiode.

However, DNA amplification reactions were never monitored in real-time using continuous ELIDA, because of the high temperatures essential for most nucleic acid polymerisation typically ranging from 60-74^{o}C. The temperatures of these reactions inhibit wild type luciferase enzymes but in 2002 a thermostable recombinant version of the firefly luciferase was developed by Cambridge University (Tisi et al., 2002). This engineered luciferase was demonstrated to be functional at temperatures exceeding 60^{o}C and this changed the prospects for measuring DNA polymerisation by bioluminescence in real-time and realised the potential for simple diagnostic platforms (Tisi et al., 2001, Kiddle et al., 2012).

Following on, BART (Bioluminescent assay real-time) emerged; a detection technology that capitalised on the ELIDA chemistry in conjunction with the thermostable firefly luciferase to monitor NAATs (patented by Lumora Ltd, Cambridgeshire) (Fortes et al., 2013).

BART is well suited to most isothermal methods as these produce copious amounts of PPi, and amplification technologies such as LAMP operate within a thermal window suited to the recombinant enzyme used for generating light.

BART, like ELIDA, relies on the detection of pyrophosphate ions (PP_i) released during DNA polymerisations. As the rate of amplification progresses and becomes exponential, the amount of released PPi ions and subsequently ATP molecules increases substantially, resulting in an increase in the intensity of the light signal emitted by the sample. Once the amount of PPi ions reaches a critical concentration, both the ATP sulphurylase and the luciferase enzymes become significantly inhibited leading to a complete switch off of BART. This results in a sharp-peak of light emission when monitored in real time, where the time to the highest emission is inversely proportional to

starting amount of target. In addition, this unique signature of the BART light signal greatly simplifies the detection of positive samples (**Figure 11**).

The BART-based assay offers a very sensitive and simple method of nucleic acid quantification that can be performed in a closed-tube, real-time format greatly reducing the contamination risks posed by this type of analysis due to the large amount of amplicon generated. In addition, similarly to the ELIDA technology, BART can be observed and detected by a CCD camera or photodiodes (Gandelman et al., 2010). Thus, offers the simplest and most cost effective, but yet sophisticated and highly sensitive, closed-tube format detection system available on the market.

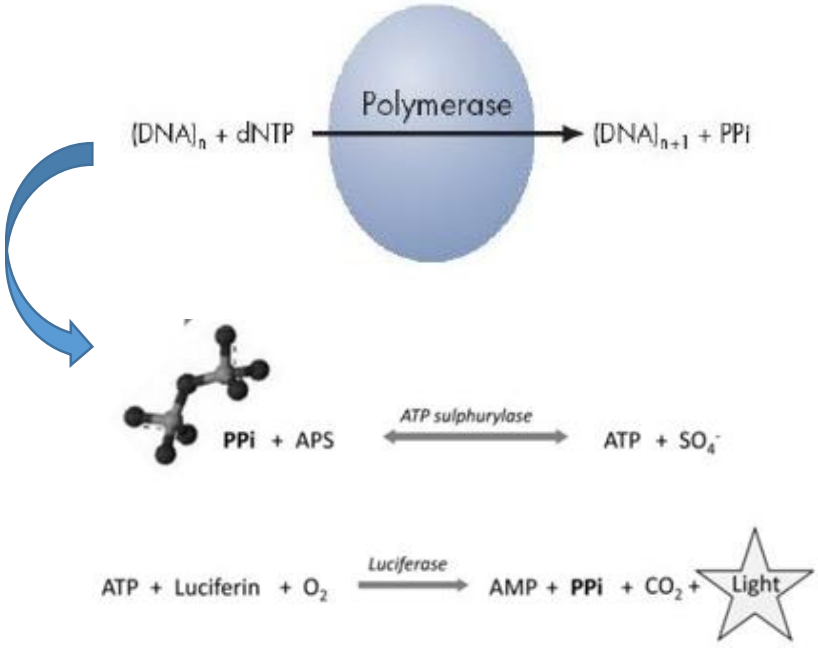

Figure 10. Enzymatic luminometric detection of inorganic pyrophosphate(ELIDA). PP_i realised during DNA synthesis react with APS in reaction catalysed by ATP sulphurylase, resulting in generation of ATP molecules. Formed ATPs together with luciferin under aerobic conditions undergo reduction reaction catalysed by a firefly luciferase enzyme resulting in emission of a light signal.

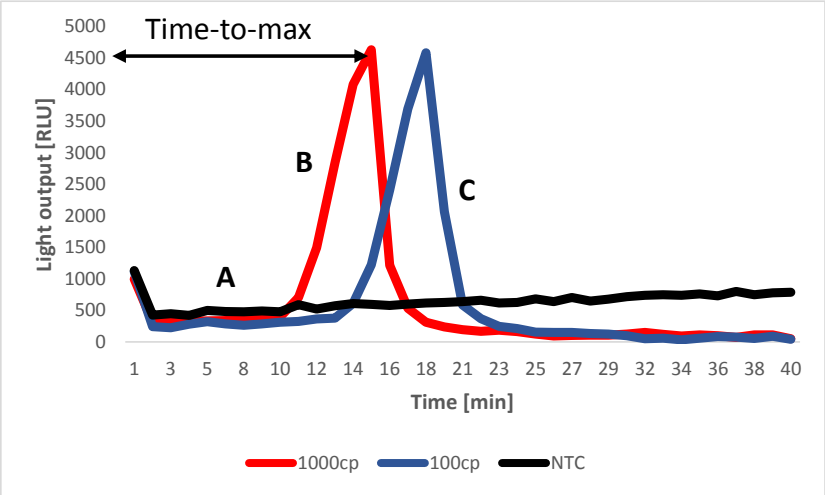

Figure 11. Graphic representation of a typical LAMP-BART amplification profile. Time-to-max (TTM) is a measure of time required for a LAMP-BART assay to reach its maximum light emission stage, which is inversely proportional to the initial amount of target DNA (red and blue curves represent reactions containing 1000 and 100 copies of DNA, respectively, whereas no template control (NTC) results in a flat baseline trace (black)). A typical LAMP-BART positive amplification signature is divided into three phases: initiation phase (A), exponential phase (B) and switch-off phase(C). Phase A represent the initiation stage of the LAMP amplification where the dumbbell structures are generated, whereas phases B and C corresponds to the elongation and recycling stages of DNA synthesis. Phase B represents the early exponential stage of DNA synthesis where the majority of PPi ions are converted into ATP. In contrast, the C phase corresponds to the later stage of the exponential amplification where the amounts of produced PPi ions becomes inhibitory to BART causing a complete switch off of light emission.

1.1.5 Fluorescence-based detection systems

Real-time PCR has been the method of choice for detection and quantification of both DNA and RNA targets. This technology combines the specificity and sensitivity of standard PCR with a fluorescence-based reporting system that enable monitoring of amplicon generation during each cycle of the PCR reaction. Thus, similarly to the BART technology, this eliminates the need for post-PCR amplicon analysis, which in turn can greatly reduce the contamination risks, as well as the hands-on time required to complete the analysis. Furthermore, real-time monitoring of amplification not only simplifies the detection but also can give some valuable insights to the quantities of the nucleic acid in the tested samples (Bashiardes et al., 2008, Chevaliez et al., 2007). Yet, fluorescent detection of amplification has not been exclusively confined to PCR amplification. Many isothermal methods, currently use fluorescent detection methods, such as TMA and LAMP that are reported using the standard assay chemistries. Three distinct fluorescence detection approaches for amplification detection are introduced below.

1.1.5.1 Intercalating dyes

SYBR green has been the most widely used intercalating dye for the detection of DNA amplification. In principle, these dye molecules bind to the minor grove of a double stranded (ds) DNA template, which in turns causes up to a 1000-fold increase in the fluorescent properties of the dye (Dragan et al., 2012) (**Figure 9A**). Upon excitation at wavelength of 480 nm, the dye emits a green fluorescent signal at 520 nm which is then detected by specrofluorometer detectors. The relative change in the emission of the fluorescent signal after each amplification cycle can therefore be associated with the amount of amplicon generated, and the initial target input.

The ability of the dye to bind to any dsDNA is a major advantage and disadvantage for monitoring polymerisation. SYBR green and other fluorescent inter-chelators offer quick and relatively cheap methods for monitoring DNA amplification where minor optimisations of the chemistry are required. However, the intercalating dyes do not allow discrimination between the amplification of the main target DNA template and any secondary targets including primer dimers in real-time. Nonetheless, the differentiation can be performed by including a dissociation analysis where different size amplicons are discriminated from one another based on their differences in melting temperatures (Tm) (Kochan et al., 2008). However, this step can significantly increase the overall time of an analysis which can be a significant limitation in a diagnostics setting. In addition, it has been reported that such dyes can reduce sensitivity of PCR assays (Gudnason et al., 2007).

1.1.5.2 *Taq*man probes

Unlike previously described intercalating dyes, *Taq*Man probes have been designed to increase the specificity of amplicon detection by employing dually labelled probes (Roche diagnostics). In principle, *Taq*Man probes consist of a single-stranded oligonucleotides labelled with a fluorophore at the 5’ and a quencher molecule at the 3’ end (Vermehren et al., 2008, Holland et al., 1991). The

probe is designed to anneal to a specific region of the template / amplified DNA target molecule that is flanked by typical PCR forward and reverse primers. The *Taq*Man probes rely on fluorescent resonance energy transfer (FRET) between the quencher and the fluorophore. In a free, un-bound state, the close proximity of the fluorophore to the quencher molecule, prevents any fluorescent signal emission. However, upon binding of the probe to its target, extension of the sense primer by the *Taq* DNA polymerase (**Figure 9B**) causes hydrolysis of the probe by the 5' -> 3' endonuclease activity of the DNA pol., releasing the fluorophore which in turns enables fluorescent signal emission upon excitation.

1.1.5.3 Molecular beacons

Similar, to *Taq*Man probes, the molecular beacons (MB) rely on the interactions between a oligonucleotide quencher and a fluorophore (Tyagi and Kramer, 2012). MBs do not require degradation of the probe in order to release fluorescence, this occurs when the probe sequence hybridises to is complementary amplified sequence. The MBs are hairpin shaped structures consisting of a fluorophore and a quencher covalently bound to the 5' and 3' ends respectively, a double-stranded stem region and a bigger single-stranded, open loop with at least 15 nt complementary to the target of interest (**Figure 12**). The double-stranded part of the probe is designed to maintain a sufficient proximity between the quencher and the chosen fluorophore, preventing any fluorescence release, in an un-bound state. Once, the target molecule is amplified, the MBs hybridise to the complementary region of its amplicon *via* the single-stranded loop, forcing stem region to disassociate and resulting in the separation of the fluorophore from the quencher that in turn enables fluorescence signal detection upon excitation.

MB have been widely used in a wide range of commercial diagnostic tests with an increased popularity amongst isothermal technologies. Since most of the DNA polymerases used in isothermal tests do not possess 5'→ 3' endonuclease activity, the *Taq*Man technology was found to be unsuitable for this type of analysis, making the MB probing the method of choice for specific amplicon detection.

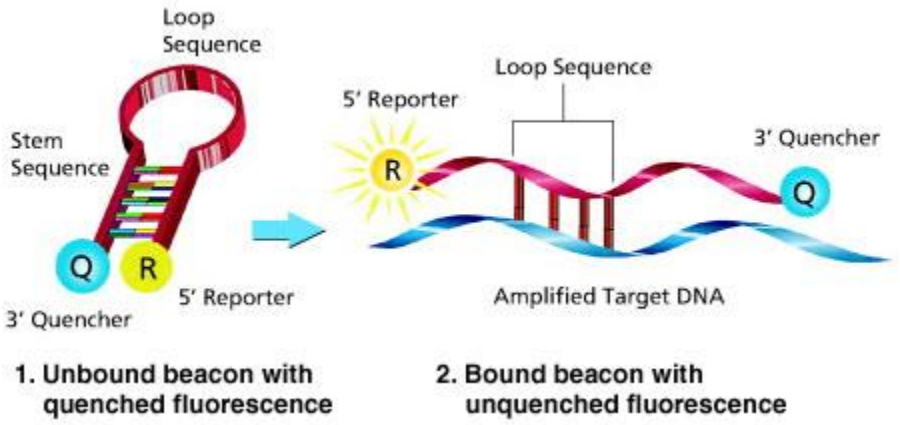

Figure 12. Graphic representation of molecular beacons technology. 1 – showing a secondary structure of a unbound probe consisting of a double-stranded stem with fluorophore and quencher at 5' and 3' ends, respectively, and a single-stranded loop region complementary to the target of interest; 2 – Bound beacon with an open structure caused by loop hybridisation to its target.

Source: http://www.sigmaaldrich.com/technical-documents/articles/biology/molecular-beacons.html

1.1.6 Summary

Probe-based detections systems offer real-time monitoring and quantification of amplification but also offer a significantly increase the sensitivity of molecular assays. *Taq*Man probes have been the most widely used in PCR-based detection systems. However due to their requirements for probe hydrolysis, are incompatible with most isothermal amplification technologies. Molecular beacons, on the other hand, offer the specificity of *Taq*Man probes without the need for probe digestion thus their use in isothermal platforms has significantly grown over the past 20 years (Yan et al., 2014). Although, fluorescent based detection systems have been widely used by PCR and isothermal technologies and offer some advantages over BART, such as the ability to simultaneously detect multiple targets (multiplexing), they require expensive optical components capable of detecting such signals, resulting in a significantly increased cost of both, assays and equipment.

Chapter 2

2 Material and methods

2.1 Materials

2.1.1 Samples

a) Freeze-dried Hepatitis C 5'UTR RNA and DNA fragments (RNA: LGC (ATCC), USA; DNA: ERBAM, UK)
b) Freeze-dried *Mycobacterium bovis* genomic DNA and rRNA (ERBAM, UK)
c) Freeze-dried *Hepatitis B* genomic DNA (ERBAM,UK)

2.1.2 Consumables

a) 2.0 mL ultra-non-stick screw-cap tubes (BioLabs, UK)
b) 96-well plates, White (ThermoFisher Scientific, UK)
c) 96-well plate adhesive seals (Sigma, Aldrich, UK)
d) Ultra-non-stick tips (10,100 and 1000) uL and Nishi/Gilson pipettes
e) Gloves

2.1.3 Reagents

a) 10x Isothermal buffer (NEB, UK)
b) 10x Thermopol buffer (NEB, UK)
c) 1M DTT (Sigma, Aldrich, UK)
d) 1x TAE buffer
e) 4x 50 mM Bicene Buffer (ERBAM, UK)
f) 4x 500 mM Bicene Buffer (ERBAM,UK)
g) Acrylamide (30%) (Sigma, Aldrich, UK)
h) APS (Biolog Institue, UK)
i) ATP sulphurylase (NEB, UK)
j) Bst 1.0 Large fragment (NEB, UK)
k) Bst 2.0 (NEB, UK)
l) Bst 2.0 Warm Start Large fragment (NEB, UK)
m) carrier tRNA (ThermoFisher Scientific, UK)
n) Collagen from calf skin (Sigma, Aldrich, UK)
o) dNTPs (Sigma, Aldrich, UK)
p) GSP-SSD (Optigene, UK)
q) Humic Acid (Sigma, Aldrich, UK)

r) Luciferase (NEB, UK)
s) Luciferin (Sigma, Aldrich, UK)
t) Maxima RNaseH- (ThermoFisher Scientific, UK)
u) Maxima RNaseH+ (ThermoFisher Scientific, UK)
v) Mineral oil (ThermoFisher Scientific, UK)
w) Molecular biology grade water (Sigma, Aldrich, UK)
x) Polyvinylpyrrolidone (PVP) (Sigma, Aldrich, UK)
y) Potassium Acetate (KAc) (Sigma, Aldrich, UK)
z) Potassium Chloride (KCl) (Sigma, Aldrich, UK)
aa) Salmon sperm DNA (NEB, UK)
bb) Sodium Chloride (NaCl)(Sigma, Aldrich, UK)
cc) SuperScript IV (ThermoFisher Scientific, UK)
dd) TEMED 10x (Sigma, Aldrich, UK)
ee) Trehalose (Sigma, Aldrich, UK)

2.1.4 Equipment

a) "BISON" LAMP-BART instrument (Lumora Ltd., UK)
b) "Lucy" LAMP-BART instrument (Lumora Ltd, UK)
c) Centrifuge (Technico mini, Thermo Scientific, UK)
d) CX-2000 UV crosslinker (Fisher Scientific UK Ltd., UK)
e) Freezer
f) Fridge
g) Gel electrophoresis tanks (BioRad, UK)
h) Laminar flow hood (BioQuell, UK)
i) UV-transilluminator (Syngene, Cambridge, UK)
j) Vortex

2.2 Methods

All samples used in this study, including HCV 5' UTR DNA and RNA, TB *M. bovis* gDNA and 23s rRNA as well as the IAC RNA, were prepared by ERBAM, UK. Samples were stored as a single-use aliquots at -80 °C.

2.2.1 Contamination control

Every precaution was taken throughout the study to minimize the risks of sample contamination. Preparation of the DNA and RNA templates and reaction mixes were carried out in a laminar flow hood crosslinked for 10 mins prior to each experiment. In addition, no-template controls (NTCs) were run each time new aliquots of the LAMP-BART reaction were prepared. Each aliquot was used only once per assay to minimize contamination events caused by sample handling.

2.2.2 DNA quantity and purity

All DNA and RNA templates were quantified by measuring its absorbance between 230 and 300 nm on a NanoDrop 2000 spectrophotometer. 1 ul of each aliquot of the linearized plasmid was analysed to check its purity and quantity. In addition, the samples were also quantified using the Agilent 2100 Bioanalyzer (Agilent Technologies Inc., UK).

Note that the HCV RNA template was quantified by a certified reference materials supplier that guaranties the highest accuracy quantifications. Thus, the concentration determined by the supplier was used to generate the working stock aliquots.

2.2.3 Reagents preparation for LAMP-BART assays

Reagents used for the development of isothermal miRNA detection systems were prepared according to the **Protocol 26**: Reagents preparation for miRNA assays (see **Appendix 26**).

All other reagents were supplied by ERBAM, UK and stored at -20 ℃.

2.2.4 Reconstitution of primers

Oligonucleotides used for HCV, TB and HBV LAMP assays were purchased from Eurofins MWG-BioTech, Germany. Oligonucleotides, including primers and probes, used for the development of isothermal miRNA detection systems were purchased from Sigma, UK.

All primers and probes used in this study were reconstituted with the required volume of 1x TE buffer (pH=8.0), as indicated on the company's technical datasheet, to 100 μM. The primers were then labelled and stored at -20 ℃.

2.2.5 Amplicon visualisation

Analysis of ligation and endonuclease digestion of the target oligonucleotides was performed using polyacrylamide gel electrophoresis (SDS-PAGE) according to the **Protocol 34**: SDS-PAGE protocol (see **Appendix 34**).

Gels were stained using 5 uL of 10000x GelRed per every 50 mL of the gel solution.

Electrophoresis was performed at 45 V for 60-85 min. Nucleic acid bands were visualised with a UV transilluminator.

2.2.6 Preparation of the internal amplification control RNA

IAC RNA template was *in vitro* transcribed using MEGAscript T7 transcription kit (ThermoFisher Scientific, UK) according to the protocol provided by the manufacturer [see MEGAscript T7 transcription kit manual: URL: https://www.thermofisher.com/order/catalog/product/AM1334].

pEX DNA plasmid containing the IAC insert and the T7 promoter sequence was purchased from Eurofins Genomics.

Full preparation of the final IAC RNA product was performed by ERBAM, UK.

2.2.7 Secondary structure analysis

Vienna RNAfold online software was used to determine the secondary structures of the 5'UTR HCV RNA [URL: http://rna.tbi.univie.ac.at/cgi-bin/RNAWebSuite/RNAfold.cgi]. The analysis was performed using the minimum free energy and partition function at 60 °C.

2.2.8 Data analysis and statistics

Microsoft EXCEL 2013 was used for analysis of the experimental data including ANOVA and t-test statistical analysis. Note that standard deviation was calculated from technical replicates, and was used as a measure of the reproducibility of an assay preformed on a given day.

Sequence alignments were visualised using GeneDoc free software [URL: http://genedoc.software.informer.com/]

2.2.9 LAMP primer design

2.2.9.1 HCV LAMP primers

HCV LAMP primers were designed to target the 5'UTR region of the *Hepatitis C* virus RNA genome. The sequence alignments were retrieved from HCV database [URL: https://hcv.lanl.gov/content/sequence/HCV/ToolsOutline.html]. Melting temperatures of all of the

HCV LAMP primers were assessed using IDT oligo analyser [URL: https://www.idtdna.com/calc/analyzer] under 50 mM sodium, 2 mM magnesium ions and 0.3 mM dNTPs. Self- and cross-priming interactions were assessed using multiple primer analyser provided by ThermoFisher [URL: https://www.thermofisher.com/uk/en/home/brands/thermo-scientific/molecular-biology/molecular-biology-learning-center/molecular-biology-resource-library/thermo-scientific-web-tools/multiple-primer-analyzer.html] under sensitivity setting 1.

Primer sequences were adjusted accordingly in order to minimise 3' interactions and thus reduce the NTC formation.

2.2.9.2 HBV LAMP primers

HBV LAMP primers were designed by ERBAM, UK (see **Appendix 39**).

2.2.9.3 TB LAMP primers

TB LAMP primers were designed by ERBAM, UK (see **Appendix 39**).

2.2.9.4 miRNA primers and probes

LAMP primers were designed to target the cauliflower mosaic virus 35S promoter sequence (GeneBank accession number X79465) by Dr Patrick Hardinge.

Ligation probes were designed based on the dumbbell sequence generated by the 35S LAMP primers where 22 nt of its stem sequence was substituted with the target miRNA complementary binding site. Each probe (P1 and P2) contained 11 nt of the miRNA binding site (refer to the ligation-based miRNA detection design, **Appendix 37**).

Note that a phosphate group at the 5' end of the P2 probe was introduced in order to enable ligation.

Endonuclease probes were designed based on the dumbbell sequence generated by the 35S LAMP primers where the loop F and FIP primer binding sites were substituted with an artificial stem loop sequence. miRNA binding site was introduced at the 3' end of the probe (see **Appendix 38**).

The sequence of the target miRNA lin-4 was retrieved from: Lee RC, Feinbaum RL, Ambros V (1993). "The C. elegans heterochronic gene *lin-4*encodes small RNAs with antisense complementarity to *lin-14*.". *Cell*. **75** (5): 843–854.

2.2.10 LAMP BART assays

All LAMP BART amplification reactions were performed on dedicated instruments that simultaneously control temperature and record bioluminescence ("BISON" and "Lucy", ERBAM., UK). Each LAMP-BART assay was performed in nuclease free 96-well plates (white) under molecular grade mineral oil, at 60 °C for 90-120 min. In addition, all LAMP-BART reactions were performed in a total volume of 20 uL, unless otherwise stated.

2.2.10.1 HCV LAMP BART assays

2.2.10.1.1 Primer screening assay

Initial master mix was prepared according to the reaction mix set up shown in **Appendix 2**. 1388 uL of the initial reaction mix was then split into four aliquots of 347 uL each. Final master mix was prepared by adding 2 uL of F3 and B3, 4 uL of Loop B and F and 8 uL of FIP and BIP of the appropriate LAMP primer sets to the aliquots containing 347 uL of the initial master mix. 15 uL of the final master mix was then mixed with 5 uL of the HCV 5' UTR RNA template [10^4 cp/5uL] in a 96-well plate (white) followed by an addition of two drops of mineral oil. Samples were sealed using a clear adhesive film and loaded onto BISON set at 60 °C and ran for 90 min.

2.2.10.1.2 DNA polymerase screening assay

Initial master mixes (2x) were prepared according to the reaction mix set up shown **Appendix 3**. 1498 uL of each of the prepared initial reaction mixes were then split into two aliquots of 749 uL. Final master mixes were prepared by adding 1 uL of either GSP-SSD [100 U/uL], Bst 2.0 [200 U/uL] or Bst 2.0WS [200 U/uL], or 1.3 uL of Bst large fragment [160 U/uL] to separate aliquots containing 749 uL of the initial master mix. 15 uL of the final master mix was then mixed with 5 uL of the appropriate HCV template in a 96-well plate (white) followed by an addition of two drops of mineral oil. Samples were sealed using a clear adhesive film and loaded onto BISON set at 60 ℃ and ran for 90 min.

HCV RNA at concentrations 10^4, 10^3, 100, 50 and 10 cps/5uL were used in this study.

2.2.10.1.3 Reverse transcriptase screening assay

Initial master mixes (2x) were prepared according to the reaction mix set up shown in **Appendix 4**. 1498 uL of each of the prepared initial reaction mixes were then split into two aliquots of 749 uL. Final master mixes were prepared by adding 1 uL of either Maxima RNaseH+ [200 U/uL], Maxima RNaseH+ [200 U/uL] or SuperScriptIV [200 U/uL] to separate aliquots containing 749 uL of the initial master mix. 15 uL of the final master mix was then mixed with 5 uL of the appropriate HCV template in a 96-well plate (white) followed by an addition of two drops of mineral oil. Samples were sealed using a clear adhesive film and loaded onto BISON set at 60 °C and ran for 90 min.

HCV RNA at concentrations 10^4, 10^3, 100, 50, 10 and 1 cps/5uL were used in this study.

2.2.10.1.4 Reaction buffers screening assay

Initial master mix was prepared according to the reaction mix set up shown in **Appendix 5**. 1300 uL of the prepared initial reaction mixes was then split into two aliquots of 650 uL each. Final master mix was prepared by adding 100 uL of either Isothermal [10x] or Thermopol [10x] buffers to separate aliquots containing 650 uL of the initial master mix. 15 uL of the final master mix was then mixed with 5 uL of the appropriate HCV template in a 96-well plate (white) followed by an addition of two drops of mineral oil. Samples were sealed using a clear adhesive film and loaded onto BISON set at 60 °C and ran for 90 min.

HCV RNA at concentrations 10^4, 10^3, 100, 50, 10 and 1 cps/5uL were used in this study.

2.2.10.1.5 Inhibitory substances screening assay: KCl, KAc and NaCl

Initial master mix was prepared according to the reaction mix set up shown in **Appendix 6**. 1498 uL of the initial reaction mixes was then split into two aliquots of 749 uL each. Final master mix was prepared by adding 1 uL of either GSP-SSD [100 U/uL] or Bst 2.0 [200 U/uL] to separate aliquots containing 749 uL of the initial master mix. 15 uL of the final master mix was then mixed with 5 uL of the appropriate inhibitory substance in a 96-well plate (white) followed by an addition of two drops of mineral oil. Samples were sealed using a clear adhesive film and loaded onto BISON set at 60 °C and ran for 90 min.

Potassium and sodium chloride and Potassium acetate at concentrations 0 to 50 mM, were tested in this study.

2.2.10.2 TB LAMP BART assays

All TB LAMP BART assays used GSP-SSD DNA polymerase and 500 mM Bicine buffer [4x], unless otherwise stated.

2.2.10.2.1 DNA polymerase screening assay

Initial master mixes (2x) were prepared according to the reaction mix set up shown in **Appendix 8**. 1498 uL of each of the prepared initial reaction mixes were then split into two aliquots of 749 uL. Final master mixes were prepared by adding 1 uL of either GSP-SSD [100 U/uL], Bst 2.0 [200 U/uL] or Bst 2.0WS [200 U/uL], or 1.3 uL Bst large fragment [160 U/uL] to separate aliquots containing 749 uL of the initial master mix. 15 uL of the final master mix was then mixed with 5 uL of the appropriate TB *M. bovis* template in a 96-well plate (white) followed by an addition of two drops of mineral oil. Samples were sealed using a clear adhesive film and loaded onto BISON set at 60 °C and ran for 90 min.

M. bovis nucleic acids concentrations of 1000 and 100 cps/5uL were used in this study.

Both genomic DNA and 23s rRNA were used.

2.2.10.2.2 Inhibitory substances screening assay: LDS (no IAC)

Master mix was prepared according to the reaction mix set up shown in **Appendix 9**. 15 uL of the master mix was then mixed with 5 uL of the appropriate *M. bovis* template* in a 96-well plate (white) followed by an addition of two drops of mineral oil. Samples were sealed using a clear adhesive film and loaded onto BISON set at 60 °C and ran for 90 min.

*- dilutions of the templates were performed using the appropriate concentrations of the tested inhibitors as diluents.

M. bovis 23s rRNA at concentration 1000 and 100 cps/5uL was used in this study.

Serial dilutions (20 uL sample + 180 uL diluent) of the 23s rRNA top stock [10^6 cps/5uL] were carried out in order to obtain the appropriate template concentrations.

For the inhibitory samples, 0.01 and 0.05% LDS was used as diluents.

2.2.10.2.3 Inhibitory substances screening assay: Bicine buffers

Initial master mix was prepared according to the reaction mix set up shown in **Appendix 10**. 1000 uL of the initial reaction mix was then split into two aliquots of 500 uL each. Final master mix was prepared by adding 250 uL of either 500 mM [4x] or 50 mM [4x] Bicine buffers to separate aliquots containing 500 uL of the initial master mix. 15 uL of the final master mix was then mixed with 5 uL of the appropriate *M. bovis* template* in a 96-well plate (white) followed by an addition of two drops of mineral oil. Samples were sealed using a clear adhesive film and loaded onto BISON set at 60 °C and ran for 90 min.

*- dilutions of the templates were performed using the appropriate concentrations of the tested inhibitors as diluents.

M. bovis 23s rRNA at concentration 10000 and 1000 cps/5uL was used in this study.

Serial dilutions (20 uL sample + 180 uL diluent) of the 23s rRNA top stock [10^6 cps/5uL] were carried out in order to obtain the appropriate template concentrations.

For the inhibitory samples, 0.05% LDS was used as diluent.

2.2.10.2.4 Inhibitory substances screening assay: carrier DNA (no IAC)

Master mix was prepared according to the reaction mix set up shown in the **Appendix 11**. 15 uL of the master mix was then mixed with 5 uL of the appropriate *M. bovis* template* in a 96-well plate (white) followed by an addition of two drops of mineral oil. Samples were sealed using a clear adhesive film and loaded onto BISON set at 60 °C and ran for 90 min.

*- dilutions of the templates were performed using the appropriate concentrations of the tested inhibitors as diluents.

M. bovis 23s rRNA at concentration 1000 and 100 cps/5uL was used in this study.

Serial dilutions (20 uL sample + 180 uL diluent) of the 23s rRNA top stock [10^6 cps/5uL] were carried out in order to obtain the appropriate template concentrations.

For the inhibitory samples, 1000 ng/5uL of salmon sperm DNA was used as diluent.

2.2.10.2.5 Inhibitory substances screening assay: carrier DNA (incl. IAC) (50 vs 10 uL reactions)

Initial master mix was prepared according to the reaction mix set up shown in **Appendix 19**. 1470 uL of the initial reaction mixes was then split into two aliquots of 735 uL each followed by an addition of 7.5 uL either MGW or TB *M. bovis* RNA. The two prepared initial master mixes (after additions) were then split into two smaller aliquots of 371.25 uL each. Final master mix was prepared by adding 3.75 uL of either MGW or carrier DNA [1000 ng/uL] to separate aliquots containing 371.25 uL of the initial master mix with either added TB RNA or MGW. 50 uL and 10 uL of the final reaction mix (including templates) were then dispensed across a 96-well plate (white) covered with 2 drops of mineral oil and sealed using adhesive clear film. Samples were run at 60 °C for 90 min on BISON.

2.2.10.2.6 Inhibitory substances screening assay (incl. IAC)

Initial master mix was prepared according to the reaction mix set up shown in **Appendix 16**. 1480 uL of the initial reaction mix was then split into two aliquots of 740 uL each. Final master mix was prepared by adding 5 uL of both MGW and IAC RNA or 5 uL of IAC and TB RNA to the separate aliquots containing 740 uL of the initial master mix. 15 uL of the final master mix was then mixed with 5 uL of the appropriate inhibitory substance in a 96-well plate (white) followed by an addition

of two drops of mineral oil. Samples were sealed using a clear adhesive film and loaded onto BISON set at 60 °C and ran for 90 min.

Inhibitory substances used in this study:

Sodium chloride at concentrations 20, 30 and 40 mM;

Salmon sperm DNA at concentrations 50, 500 and 1000 ng/5uL;

tRNA at concentrations 50, 500 and 1000 ng/5uL;

Mucin solution at concentrations 400, 500 and 700 ng/rxn;

NaOH at concentrations 1333, 1667 and 2326 µM;

2.2.10.2.7 Inhibitory substances screening assay: Mucin

Master mix was prepared according to the reaction mix set up shown in **Appendix 9**. 15 uL of the master mix was then mixed with 5 uL of the appropriate *M. bovis* [100 cps/5uL] or IAC RNA [10^6 cps/uL] template* in a 96-well plate (white) followed by an addition of two drops of mineral oil. Samples were sealed using a clear adhesive film and loaded onto BISON set at 60 °C and ran for 90 min.

*- dilutions of the templates were performed using the appropriate concentrations of the tested inhibitors as diluents.

Serial dilutions (20 uL sample + 180 uL diluent) of the 23s rRNA top stock [10^6 cps/5uL] were carried out in order to obtain the appropriate template concentrations.

For the inhibitory samples, 50, 200 and 400 ng/uL Mucin solution and 1333 mM NaOH were used as diluents.

2.2.10.2.8 Primer mutations screening assay

Initial master mix was prepared according to the reaction mix set up shown in **Appendix 12**. 1468 uL of the initial reaction mix was then split into four aliquots of 367 uL each. Final master mix was prepared by adding 8 uL of the appropriate version of the LAMP F primer to separate aliquots containing 367 uL of the initial master mix. 15 uL of the final master mix was then mixed with 5 uL of the appropriate *M. bovis* template [10^4 cps/5uL] in a 96-well plate (white) followed by an addition of two drops of mineral oil. Samples were sealed using a clear adhesive film and loaded onto BISON set at 60 °C and ran for 90 min.

Note that the loop primers were not added.

2.2.10.2.9 Standard TB assay (50 µL reactions)

Initial master mix was prepared according to the reaction mix set up shown in **Appendix 18**. 1470 uL of the initial reaction mixes was then split into two aliquots of 735 uL each. Final master mix was prepared by adding 7.5 uL of MGW and 7.5 uL of either *M. bovis* TB template [10^4 cps/5uL] or IAC RNA [10^7 cps/5uL] to separate aliquots containing 735 uL of the initial master mix. 50 uL of the final reaction mix (including templates) was then dispensed across 30 wells of a 96-well plate (white) covered with 2 drops of mineral oil and sealed using adhesive clear film. Samples were run at 60 °C for 90 min on BISON.

2.2.10.2.10 Assessment of DNA contamination in the IAC RNA samples

Initial master mix was prepared according to the reaction mix set up shown in **Appendix 7**. However, Maxima RNaseH+ was not added to the initial master mix. 1498 uL of the initial master mix was then split into two aliquots of 749 uL each followed by an addition of 1 uL of either Maxima RNaseH+ [200 U/uL] or MGW. 15 uL of the final master mix was then mixed with 5 uL of the appropriate *IAC* template in a 96-well plate (white) followed by an addition of two drops of

mineral oil. Samples were sealed using a clear adhesive film and loaded onto BISON set at 60 °C and ran for 90 min.

IAC RNA and DNA concentrations of 10^8, 10^7, 10^6 and 10^5 cps/5uL, were used in this study.

2.2.10.2.11 IAC interference study

Master mix was prepared according to the reaction mix set up shown in **Appendix 14**. 15 uL of the master [10^6 cp/rxn IAC RNA] mix was then mixed with 5 uL of the appropriate *M. bovis* template in a 96-well plate (white) followed by an addition of two drops of mineral oil. Samples were sealed using a clear adhesive film and loaded onto BISON set at 60 °C and ran for 90 min.

M. bovis 23s rRNA at concentrations 10^4, 10^3 and 100 cps/5uL were used in this study.

2.2.10.2.12 Effects of HIV ROX-loop probes on IAC RNA amplification

Initial master mix was prepared according to the reaction mix set up shown **Appendix 15**. 1482 uL of the initial reaction mix was then split into two aliquots of 741 uL each, followed by an addition of either 1 uL GSP-SSD or 1.3 uL Bst large fragment. Each of the two prepared aliquots was then split into two smaller aliquots of 370.5 uL each. Final master mix was prepared by adding 4 uL of either HIV probe or MGW to the separate aliquots containing 370.5 uL of the initial master mix with either GSP-SSD or Bst large fragment. 15 uL of the final master mix was then mixed with 5 uL of the IAC RNA template [10^6 cps/5uL] in a 96-well plate (white) followed by an addition of two drops of mineral oil. Samples were sealed using a clear adhesive film and loaded onto BISON set at 60 °C and ran for 90 min.

Note: 50 mM Bicine buffer was used in this study

2.2.10.2.13 Effects of DNA polymerases on the performance of HIV ROX loop probe-based detection

Initial master mix was prepared according to the reaction mix set up shown in **Appendix 23**. 1498 uL of the initial reaction mixes was then split into two aliquots of 749 uL each. Final master mix was prepared by adding 1 uL of GSP-SSD [100 U/uL] or 1.3 uL Bst large fragment [160 U/uL] to separate aliquots containing 749 uL of the initial master mix. 15 uL of the final reaction mix was then mixed with 5 uL of the appropriate IAC template in a 96-well plate (white) covered with 2 drops of mineral oil and sealed using adhesive clear film. Samples were run at 60 °C for 90 cycles on Strategene. Note: each cycle was set to run for 1 min.

2.2.10.3 HBV LAMP BART assays

All HBV LAMP BART assays were performed using 10x Isothermal buffer and Bst 2.0 WS.

2.2.10.3.1 Effects of BART on HBV ROX loop probe-based detection

Initial master mix was prepared according to the reaction mix set up shown in **Appendix 21-22**. 742 uL of the initial reaction mixes was then split into two aliquots of 371 uL each. Final master mix was prepared by adding 4 uL of either MGW or ROX-labelled loopF probe [100 uM] to separate aliquots containing 371 uL of the initial master mix. 15 uL of the final reaction mix was then mixed with 5 uL of the appropriate HBV template in a 96-well plate (white) covered with 2 drops of mineral oil and sealed using adhesive clear film. Samples were run at 60 °C for 90 cycles on Strategene. Note: each cycle was set to run for 1 min.

2.2.10.3.2 Effects of labelled loop probes on amplification of HBV DNA

Master mix was prepared according to the reaction mix set up shown in **Appendix 20**. Note that Loop F primer was not added during reaction mix preparation. 1484 uL of the intial master mix was split into four aliquots of 470 uL each followed by an addition of 5 uL of the appropriate loop probe/primer.

15 uL of the final master mix was then mixed with 5 uL of the appropriate *HBV* template in a 96-well plate (white) followed by an addition of two drops of mineral oil. Samples were sealed using a clear adhesive film and loaded onto BISON set at 60 °C and ran for 90 min.

2.2.10.4 miRNA LAMP BART assays

2.2.10.4.1 Ligation-based miRNA detection assay

Master mix was prepared according to the reaction mix set up shown in **Appendix 24**. 15 uL of the master mix was then mixed with 5 uL of the appropriate *miRNA* template in a 96-well plate (white) followed by an addition of two drops of mineral oil. Samples were sealed using a clear adhesive film and loaded onto "Lucy" set at 60 °C and ran for 90 min.

2.2.10.4.2 Endonuclease-based miRNA detection assay

Master mix was prepared according to the reaction mix set up shown in **Appendix 35**. 15 uL of the master mix was then mixed with 5 uL of the appropriate *miRNA* template in a 96-well plate (white) followed by an addition of two drops of mineral oil. Samples were sealed using a clear adhesive film and loaded onto "Lucy" set at 60 °C and ran for 90 min.

2.2.11 Ligation reactions

Ligation reactions were performed at room temperature according to the protocols 27-30 (see **Appendix 27-30**), unless otherwise stated. All ligation reactions underwent an inactivation step performed at 95 °C for 20 min.

2.2.11.1 Standard miRNA detection asay using SplintR ligase

Initial SplintR reaction mix was prepared according to the protocol 27 (see **Appendix 27**). Note that P1, P2 and the target miRNA were not added to the initial reaction mix. 340 uL of the initial reactions mix (set up for 20 rxn) was split into four aliquots of 85 uL each. Final reaction mix was prepared by adding 1 – 5 uL P1 [1 uM] and 10 uL MGW; 2 – 5 uL P2 [1 uM] and 10 uL MGW; 3 – 5 uL of both P1 and P2 [1 uM] and 5 uL MGW; 4 – 5 uL of both P1 and P2 [1 uM] and 5 uL miRNA lin-4 [100 uM].

Reactions were incubated for 30 min followed by an inactivation step. 100x dilution of each ligation sample was then performed using MGW. 5 uL of the diluted ligation sample was then mixed with the standard LAMP BART reaction mix (see **Appendix 24**).

2.2.11.2 Ligases screening assay

Separate reaction mixes were prepared according to the appropriate ligation protocol (see **Appendix 27-30**).

Note that 100x dilution [1 uM] of each probe was used in this study.

Reactions were incubated for 30 min followed by an inactivation step. 100x dilution of each ligation sample was then performed using MGW. 5 uL of the diluted ligation sample was then mixed with the standard LAMP BART reaction mix (see **Appendix 24**).

2.2.11.3 Time course study

SplintR reaction mix was prepared according to the protocol 27 (see **Appendix 27**). Note that 100x dilution [1 uM] of each probe was used in this study.

Samples were initially incubated for 5 min followed by transferring 100 uL of the ligation mix to a separate tube and placed on ice. The remaining volume was left at room temperature for additional 25 min. Both aliquots were then transfer onto a heating block for inactivation. 100x dilution of each inactivated sample was performed using MGW. 5 uL of the diluted ligation sample was then mixed with the standard LAMP BART reaction mix (see **Appendix 24**).

2.2.11.4 Probe optimisation study

Initial SplintR reaction mix was prepared according to the protocol 27 (see **Appendix 27**). Note that probes P1 and P2 were not added to the initial reaction mix. 540 uL of the initial reaction mix (set up for 30 rxn) was then split into six aliquots of 90 uL each. Final reaction mix was prepared by adding of 5 uL of both P1 and P2 probes.

Dilutions tested: 10, 1, 0.1, 0.05, 0.02 and 0.01 uM. Note that the final concentrations of the probes in the reaction mixture was 20x lower.

2.2.12 Restriction digest

Restriction digest was performed according to the protocols 31-32 (see **Appendix 31-32**).

Templates were prepared according to the PCR protocol 33 (see **Appendix 33**).

10 uL of each restriction digest reaction was then loaded onto a SDS-PAGE and run for 85 min at 45 V.

2.2.13 Endonuclease heat inactivation

Heat inactivation was performed at 95 ℃ for 30 min in the appropriate reaction buffer provided by the supplier.

2.2.14 Pre-incubation procedure

Nb.bsmI was pre-incubated in a modified LAMP BART reaction mix at 60 ℃ for 60 min followed by the standard endonuclease heat inactivation step.

LAMP BART reaction mix was prepared according to the protocol 24 (see **Appendix 24**). Note that enzymes were not added.

Chapter 3

3 Development of RT-LAMP assay for diagnosis of *Hepatitis C* infections

3.1 Introduction

Hepatitis C is a highly infectious disease caused by the *Hepatitis C virus* (HCV) that mainly infects the liver (Choo et al., 1989, Seeff and Hoofnagle, 2003). Initial infection usually results in very mild or no symptoms, which makes an early diagnosis very problematic (Zhang et al., 2016, Seeff and Hoofnagle, 2003). It has been estimated that an approximately 130–200 million people are infected with hepatitis C, worldwide (Modi and Liang, 2008, Zhang et al., 2016, Cloherty et al., 2016). In 2013, the vast majority of the 11 million new reported cases of HCV infections, occurred in Africa and Central and East Asia. In addition, that year alone, almost 800,000 deaths related to the chronic HCV infections, were reported (Petruzziello et al., 2016, Karoney and Siika, 2013).

HCV can primarily be transmitted *via* blood-to-blood route, and is mainly associated with intravenous drug users, poorly sterilised medical equipment, transfusions or needle stick injuries amongst healthcare personnel. However, HCV can also be transmitted from mother to child during birth (Tibbs, 1995, WHO, 2017, Maheshwari and Thuluvath, 2010, Pondé, 2011).

The HCV virus persists in up to 80 % of the infected individuals and the vast majority do not develop any symptoms during the early stages of the disease. However, during prolonged infection, HCV infection leads to liver disease and in some cases cirrhosis. In addition, patients with cirrhosis have an increased risk of developing liver failure, liver cancer or oesophageal and gastric varices (Kim, 2016, Alter, 2007, Xu et al., 2013).

Currently, there is no vaccine available against HCV infections. Prevention strategies involve harm reduction methods, amongst drugs abusing individuals, as well as extensive blood product screening prior to transfusions (Alter, 2007, Abdelwahab and Ahmed Said, 2016, Hagan et al., 2011). HCV treatment involving sofosbuvir and simeprevir, have been shown to be capable of curing up to 90 % of the chronic infections if diagnosed in the earlier stages of the disease (Panel, 2015, WHO, 2017, Abergel et al., 2016).

3.1.1 *The Hepatitis C* virus

Hepatitis C is an enveloped RNA virus with a diameter of approximately 50 nm and it belongs to the *flaviviridae* family. The HCV viron consists of a single-stranded, positive sense RNA ((+) RNA) molecule encapsulated by an icosahedral capsid composed of the core protein and an outer lipid layer of host's origin. Two key viral glycoproteins, E1 and E2, are embedded within the outer lipid layer and facilitate the viral attachment and entry to the host's cell (Ashfaq et al., 2011) (**Figure 13**).

It has been reported that the HCV virus can circulate in three main forms within the serum of infected individuals: a) as a free viron; b) virons bound to lipoproteins and c) non-enveloped nucleocapsid (Maillard et al., 2001, André et al., 2005). It has been suggested that the core protein functions not only as a structural protein, but it also has an effect on the host cells gene expression and in the regulation of apoptosis (one of the host's defence mechanisms against viral infections) (Okuda et al., 2002, Su et al., 2002, Song et al., 2016, Kwak et al., 2016).

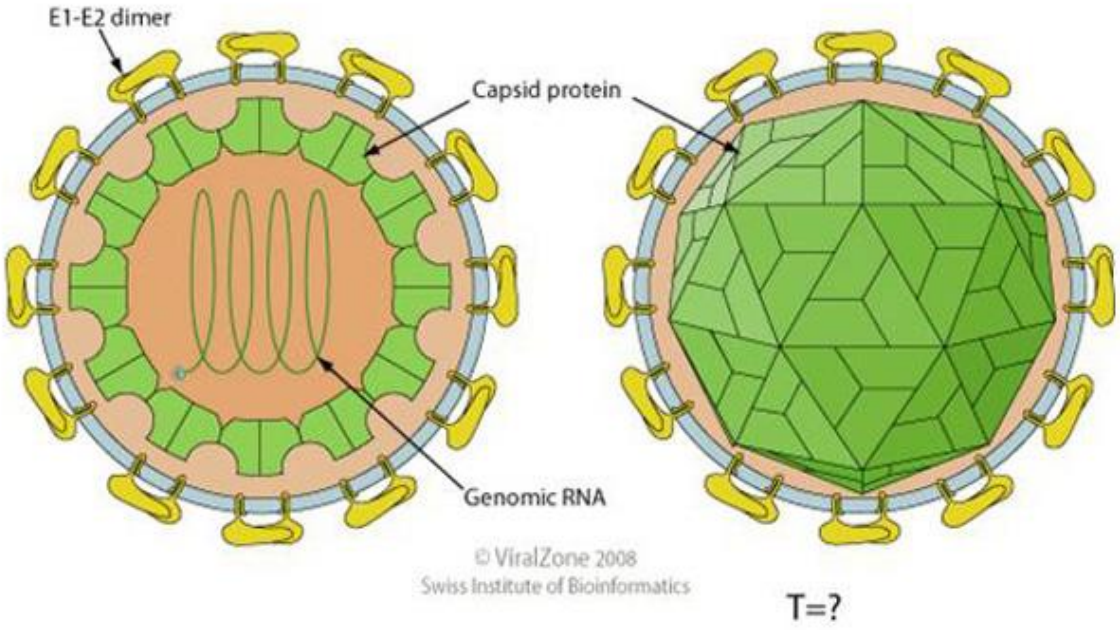

Figure 13. Graphic representation of the Hepatitis C viral particle structure.

Source: http://www.abcam.com/index.html?pageconfig=resource&rid=13135

3.1.2 *Hepatitis C* genomics

The genome of HCV is made of a positive-sense, single-stranded RNA of 9400 nt (Kato, 2000). It contains a single open reading frame (ORF) encoding a polyprotein of approximately 3000 amino acids. The ORF is flanked by 5' and 3' untranslated regions (UTR or NTR) of approximately 341 and 230 nucleotides, respectively. However, the length of the 3'UTR can vary significantly between different subtypes of the HCV virus, but it normally consists of a short poorly conserved region of approximately 28-42 nucleotides, poly-(U) / polypyrimidine (T/C) track and a highly conserved base element of 98 nucleotides (known as a 3'X region). The 3'X region together with the 52 upstream nt of the poly(U/C) domain have been reported to play a crucial role in the viral RNA replication (Jubin, 2001, Berry et al., 2011).

Of the two UTRs, the 5'UTR exhibits the highest degree of conservation for all the known HCV genotypes. It consists of four heavily structured domains (I-IV) made of many stem-loops and pseudoknots. It has been reported that the domain II-IV together with the first 30 nucleotides of the coding region make up the internal ribosome entry sequence (IRES). IRES is responsible for binding to the host's 40s ribosomal subunits and initiating the translation of the viral polyprotein in a cap-independent manner (Berry et al., 2011, Lukavsky, 2009). The translated polyprotein is subsequently co-translationally and post-translationally modified by the viral and host's proteases to produce 10 mature proteins (**Figure 14**). The N terminal part of the viral genome encodes for structural proteins: a) non-glycosylated nucleic acid-binding nucleocapsid protein, known as the core protein (approx. 190 aa/21kDa); b) two membrane-associated glycoproteins E1 and E2 of 190 and 370 aa, respectively (Moradpour and Penin, 2013).

The non-structural viral proteins include: a) NS1 (p7) thought to be involved in generation of the viroporin in the host's ER membrane; b) NS2 to NS5B are involved in the modification and processing of the viral polyprotein as well as viral genome replication. The post-translational processing of the viral polyprotein is carried out by two proteinases NS2-NS3 Zinc-dependent metalloproteinase and NS3 serine proteinase located at the N-terminal region of the NS3 protein. The NS2-NS3 proteinase is responsible for cleavage of the NS2/NS3 region of the viral polyprotein only. In contrast, the NS3 serine proteinase together with its cofactor NS4a releases the remaining proteins from the viral polyprotein complex (Moradpour and Penin, 2013, Penin et al., 2004, Moradpour et al., 2005).

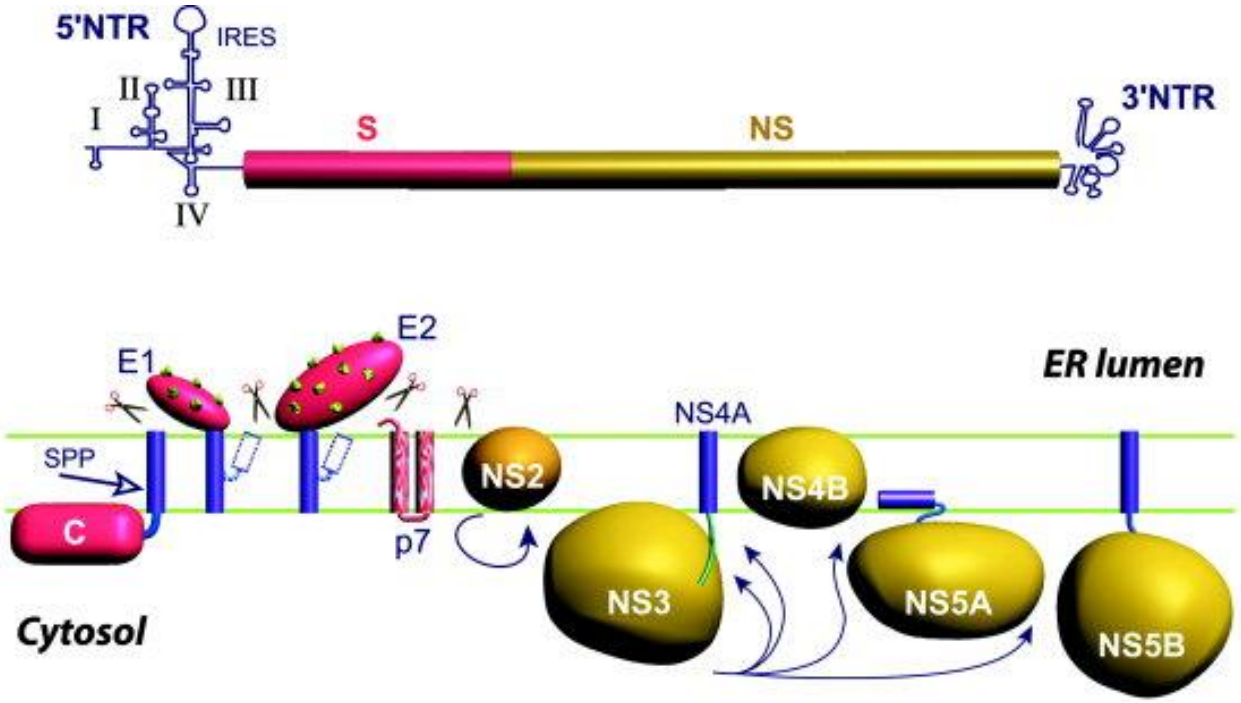

Figure 14. Graphic representation of the Hepatitis C viral genome structure. The HCV genome consists of two non-translated regions (5' and 3' NTR and a single polyprotein encoding for structural (red) and non-structural (yellow) proteins. During the co- and post-translational processing, the polyprotein is cleaved to generate ten proteins. C- structural core protein, E1 and E2 – viral glycoproteins responsible for attachment and entry, NS1 (p7) – viroporin, NS2-3 – viral proteinases, NS4a- NS3 cofactor, NS5b – RNA-dependant RNA polymerase.

Source: http://stanford.edu/~ncho/AR_2.html

3.1.3 The lifecycle of *Hepatitis C*

HCV enters the target cell through interactions with specific membrane receptors such as CD81 or SR-BI that are suggested to play crucial roles in viral binding (**Figure 15**). Upon attaching itself to the host's receptors, the viral lipid envelope is fused with the target cell's membrane and this is followed by release of the viral nucleocapsid into the cell cytoplasm. Attachment and fusion is mediated by viral surface glycoproteins (E1-E2) and can take place at either the host's plasma membrane or inside the endosomes followed endocytosis (Kim, 2016, Kato, 2000, Barth et al., 2006).

As previously mentioned, Hepatitis C virus stores its genetic material in a form of single-stranded, positive sense RNA molecule. The HCV genome can be used as a direct template for translation into viral proteins. Once the viral protein synthesis is complete, the NS4b protein stimulates

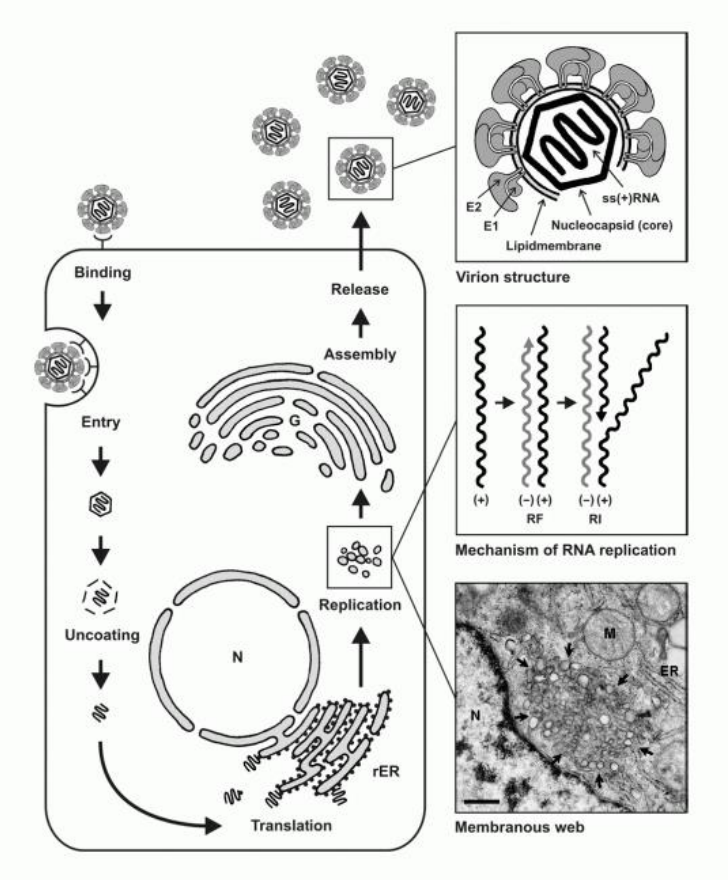

Figure 15. Graphic representation of the Hepatitis C life cycle.

Source: http://www.abcam.com/index.html?pageconfig=resource&rid=13135

formation of membrane vesicles, known as membranous web, which acts as a viral RNA replication machinery (Behrens et al., 1996, Elazar et al., 2003). The NS5b is then employed for the synthesis of the complementary to the viral genome, anti-sense strand ((-) RNA) which in turns serves as a template for synthesis of the viral ssRNA genome. Subsequently, upon synthesis of all the viral protein and its genetic material, assembly of new virons is carried out followed by their excretion from the host's cell via exocytosis (Ashfaq et al., 2011).

3.1.4 *Hepatitis C* diversity and classification

The HCV virus has recently been divided into seven distinct genotypes (1-7) based on the variation in the nucleotide sequence of all the known HCV genomes (**Figure 16**) (Kato, 2000, Alter, 2007). On average, each of these genotypes differ in 30-35% in their nucleotide sequence when the entire genomes where taken into consideration. It has been reported that the vast majority of the variation seen between different HCV genotypes are concentrated in the regions encoding for the E1 and E2 glycoproteins (Simmonds, 1995, Simmonds et al., 1993, Cuypers et al., 2015).

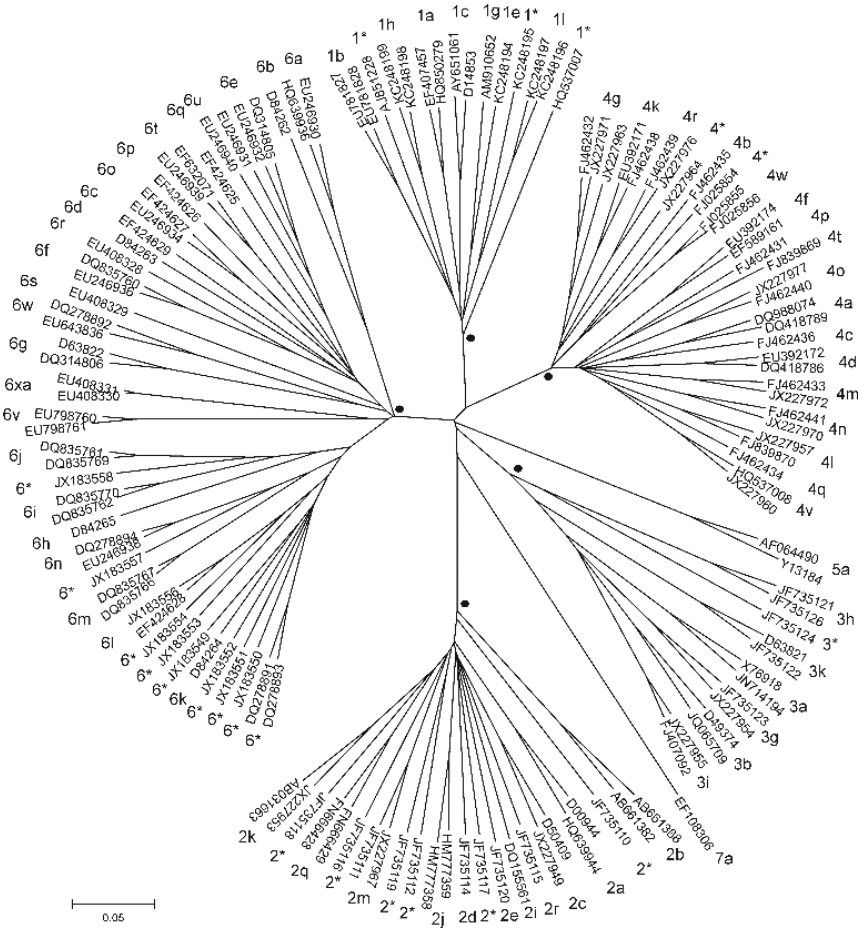

Figure 16. Graphic representation of the Hepatitis C phylogenetic tree showing all the currently known genotypes and the corresponding subtypes.

Source: http://www.abcam.com/index.html?pageconfig=resource&rid=13135

Furthermore, according to the more recent reviews of the HCV genotype / subtype classification, approximately 67 subtypes of the virus were identified (genotype number followed by a letter a,

b, c, etc.). Each identified subtype differs in at least 15 % in their coding region (or 20-25 % in their entire genome sequence) – variability is particularly dominant in the regions coding for the core, E1 and NS5B proteins. In addition, several strains of the same subtype have also been identified and reported to differ at less than 15 % in their genomic sequence (Timm and Roggendorf, 2007, Cuypers et al., 2015).

3.1.5 *Hepatitis C* geographical distribution

The geographical distribution of the HCV infections is complex. It has already been reported that certain subtypes including 1a, 1b, 2a and 3a are distributed globally and account for over 60 % of all HCV infections (**Figure 17**) (Timm and Roggendorf, 2007, Kato, 2000). Such a wide spread dispersal of these particular subtypes could potentially be explained by the adoption of blood transfusions that occurred in the 20th century (Simmonds, 2004, Kato, 2000). In addition, the use of unsterilized needles for injections and vaccinations (a practice that continues in many developing countries to-date), as well as needle sharing within drug user groups of industrialised countries. Many of the remaining subtypes are considered to be endemic strains, which are rather rare and have circulated for a much longer period of time in more restricted regions of the globe: 1 and 2 – West Africa; 3 - South Asia; 4 – Central Africa and Middle East; 5 – Southern Africa; 6 – South-east Asia. According to the most recent reports, only genotype 7 infection was reported in Canada where the strain was isolated form a Central African immigrant (Simmonds, 2004).

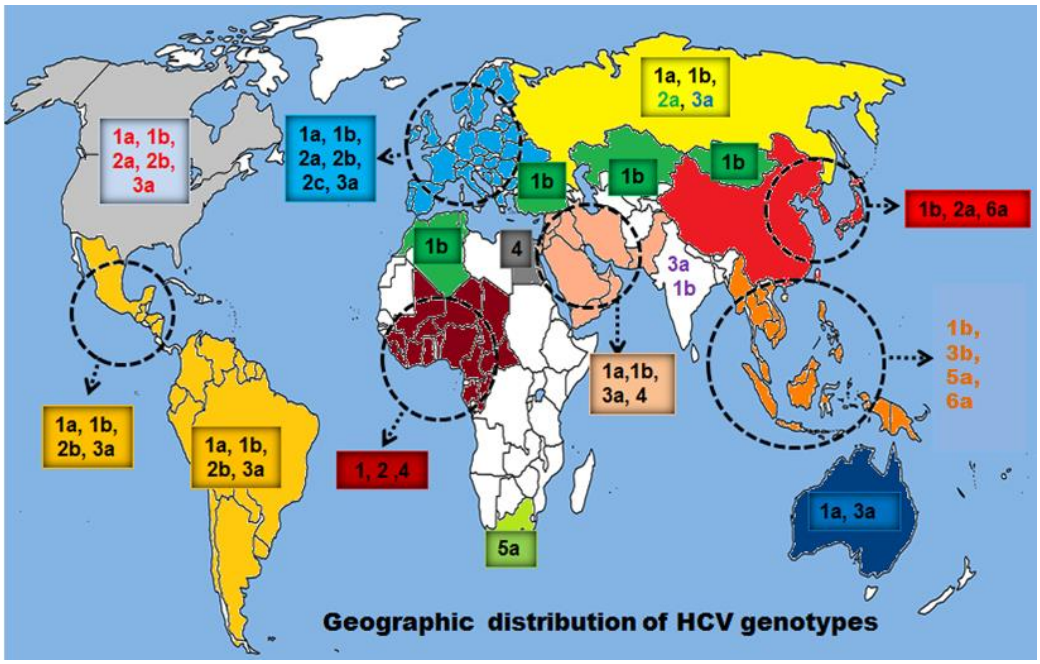

Figure 17. Graphic representation of the Hepatitis C geographical distribution with an emphasis on the most prevalent genotypes for each region.

Source: (Hussain, 2013) https://www.intechopen.com/books/practical-management-of-chronic-viral-hepatitis/genomic-heterogeneity-of-hepatitis-viruses-a-e-role-in-clinical-implications-and-treatment

Globally, genotype 1 has been estimated to contribute to over 46 % (83.4 million) of all HCV infections with one-third cases located in East Asia followed by the HCV genotype 3 which contributed to over 30 % (54.3 million) of HCV incidents most of which occurred in South Asia. Genotypes 2, 4 and 6 are responsible for most of the remaining HCV infections and account for 9.1 % (16.5 million), 8.3 % (15 million) and 5.4 % (9.8 million) cases worldwide, respectively (Simmonds, 2004). Recent reports have shown that the genotype 5 contributed to less than 1 % of all the HCV infections where the vast majority occurred in Southern and sub-Saharan Africa. No apparent differences in the HCV structure, replication, transmission and the ability to establish a persistent infection have been observed between all the known genotypes. In addition, the wide spread of HCV infections in the human population suggests that each genotype is equally capable

of maintaining infections. However, despite the phenotypic similarities between the genotypes, there is a growing evidence of genotype-specific differences in persistence and interactions with the innate cell defences and resistance to antiviral therapies. It has been shown that only 10-20 % and 40-50% of individuals infected with the genotype 1 HCV fully recovered when either IFN monotherapy or IFN (interferon-α)/ribavirin combination therapy, respectively, was used. In contrast, 50 % and 70-80 % of individuals infected with genotypes 2 or 3 were cured upon implementation of the exact same antiviral therapy (Hussain, 2013, Kato, 2000, Timm and Roggendorf, 2007). Furthermore, it is becoming more apparent that the variation in the coding regions, particularly within the E2 and NS5A, can have a significant effect in host's immune responses and the resistance to the antiviral drug therapies.

3.1.6 Molecular diagnostics of *Hepatitis C*

Enzyme immunoassays (EIA / ELISA) and chemiluminescence immunoassays (CIA) have been the most widely used methods for screening of HCV infections in both developed and developing countries (Cloherty et al., 2016, Pawlotsky, 1999). Both technologies rely on detection of patient's antibodies against chosen core antigens such as the core and / or NS3-5 proteins. The latest 3rd generation EIA/CIA, such as OraQuickHCV®, have not only been FDA-approved, but also recommended by the WHO to be used as the gold standard test in developing countries (Gupta et al., 2014). They exhibit a very high, over 95 %, accuracy and in most cases are able to detect antibodies within the first 2-3 weeks after the exposure (WHO, 2017). However, the success of the 3rd generation ELI-based tests lies not only in their high sensitivity and accuracy but also can be contributed to their relatively low cost and simplicity in use (Abdel-Hamid et al., 2002, Marwaha and Sachdev, 2014). Nonetheless, due to the initial window period required for the seroconversion

of the infected blood prior to testing, immunoassays should not be solely relied on for blood screening purposes (**Figure 18**).

HCV core antigen testing is yet another example of highly effective diagnostic tools for HCV infections. Unlike the EIA-based technologies, the diagnosis of HCV infections is performed *via* direct detection of the pathogen rather than the host's response to infection (Freiman et al., 2016). In this approach, a specific matrix (either a membrane or microparticles) is coated with monoclonal antibodies, which are specific to the core protein that makes up the HCV nucleocapsid. Since, the core protein has been shown to be the most conserved protein amongst all of the HCV genotypes and is one of the first protein synthesised during HCV life cycle, it became the target of choice for the direct detection. The Architect HCV Ag assay developed by Abbott, was one of the first commercially available platforms in Europe that utilised this technology (Ghany et al., 2009). However, despite its extremely high specificity, of nearly 100%, and simplicity, it did not become the method of choice due to its much lower sensitivity compared to many RNA or EIA-based platforms. It has however, widely used as a method for confirmation of positive EIA results.

Despite the great success of immunoassays in HCV diagnosis, nucleic acid amplification technologies (NAAT) have become the preferred method of choice in diagnosis of early infections, as well as monitoring of anti-viral therapies and been playing a crucial part in the fight against the spread of the disease (Ghany et al., 2009, Gupta et al., 2014).

NAAT-based technologies rely on the detection of the circulating viral RNA and make use of either RT-PCR or other technologies, such as TMR or bDNA assays (Morishima et al., 2006, Chan et al., 2000). As previously described, the HCV genome divides into two non-translated UTR regions (5' and 3' UTRs) and a single coding open reading frame encoding for the viral polyprotein. The unique function of the 5' UTR in HCV translation reflects its high conservation,

with nearly 90% sequence identity amongst all of the HCV genotypes (Simmonds et al., 1993, Kato, 2000). Thus, it is the most targeted part of the vial genome for almost all of the currently available commercial and in-house developed kits. Direct detection of the viral genome, very much like in case of the core antigen detection technologies, enables diagnosis of pre-seroconverted individuals.

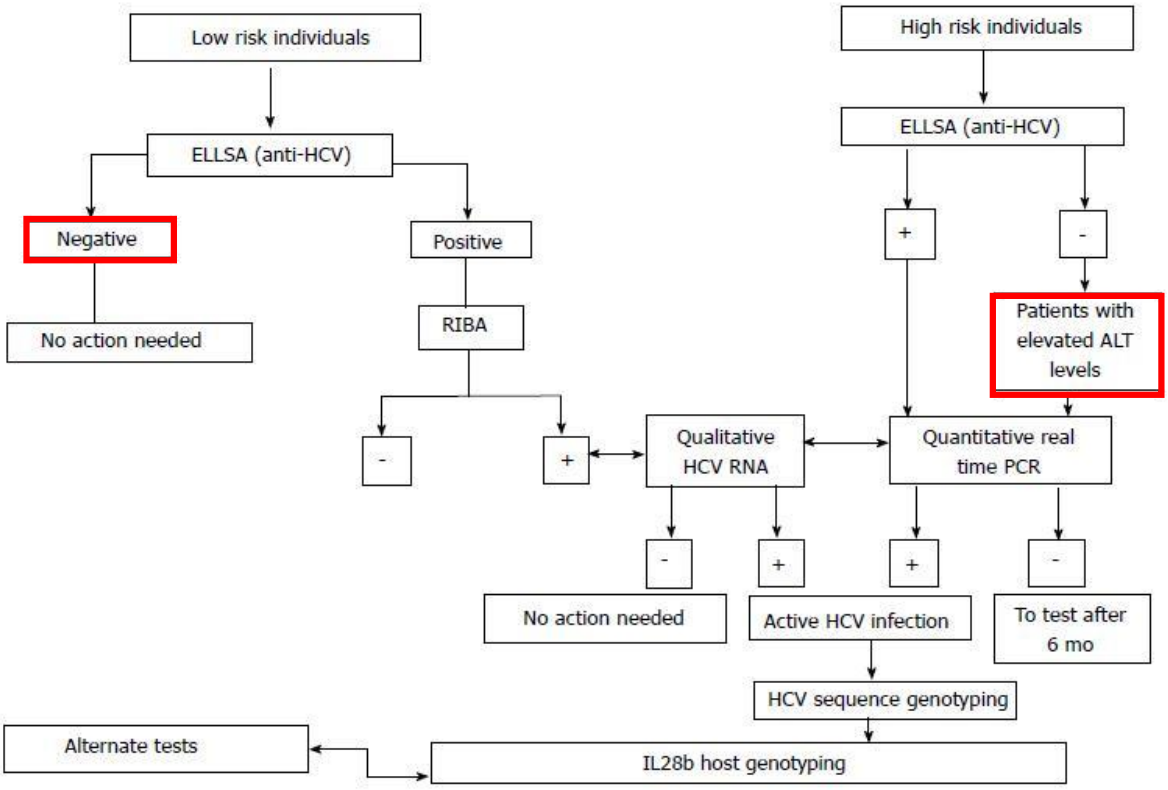

Figure 18. Graphic representation of the Hepatitis C screening steps. Highlighted in red are stages of the screening process where false negative diagnosis based on serological testing may contribute to further spread of the disease.

Source: https://www.health.ny.gov/publications/1852/diagnosis.htm

Thus, greatly limiting the risks of new infections. However, unlike the direct immunoassay platforms, the NAAT-based detection is more accurate and highly sensitive (Firdaus et al., 2015, Kargar et al., 2012, Wang et al., 2011, Yang et al., 2011).

Nonetheless, most currently available NAAT-based kits cannot fully replace the immunoassay screening but should rather be used in conjunction. During the development of the disease, particularly in the first 10 weeks of the infection, the level of HCV RNA can not only vary significantly, but also fall below the limit of detection of many currently available tests (**Figure 19**). Thus, increasing the risks of misdiagnosis (Ghany et al., 2009, Cacopardo et al., 2009).

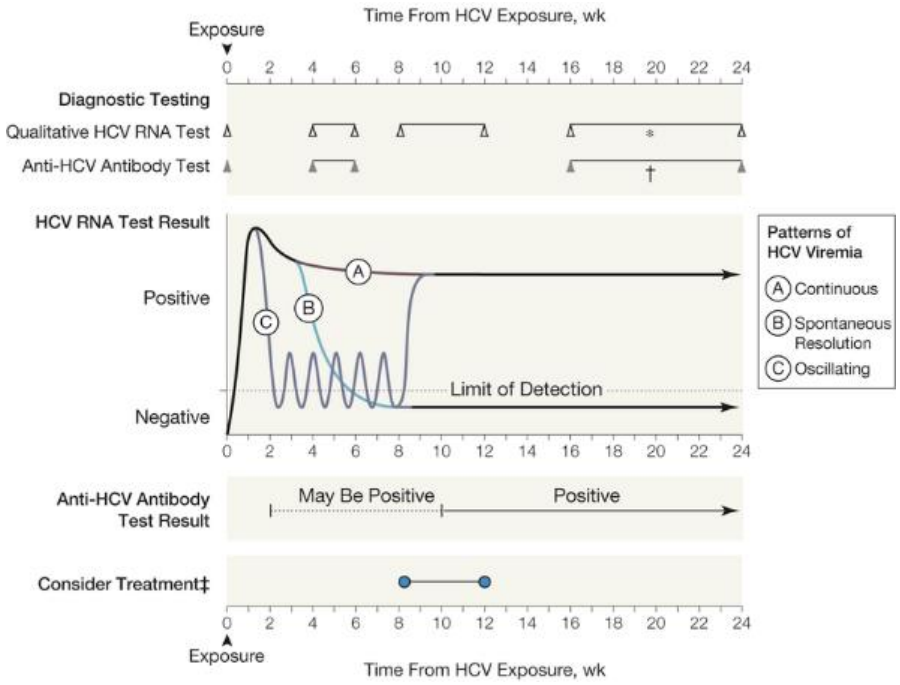

Figure 19. Graphic representation of 3 main patterns of HCV viremia. A – continuous high level of detectible HCV RNA; B – spontaneous resolution of the disease; C – Oscillating levels of HCV RNA usually falling below the limit of detection.

Source: http://jamanetwork.com/journals/jama/fullarticle/205592

In summary, HCV diagnosis begins with testing for anti-HCV markers (**Figure 18**) and depending on the result of such a test, the NAAT-based confirmation assay will be performed.

Since even the most sensitive immunoassays available on the market, have a minimum of 2 weeks prior to seroconversion of the infected blood, the risks of misdiagnosis and false negative results, as well as asymptomatic course of the disease development, increase the risks of new infections and make the eradication of the disease impossible (**Figure 18, red boxes**)(Cacopardo et al., 2009, Ghany et al., 2009, Scott and Gretch, 2007). Even more so, in developing countries, such as India, where immunoassays are not routinely accompanied by NAAT-based tests (WHO, 2017). The NAAT-based platforms, could potentially generate false positive results, due to viral RNA load oscillations during the acute phase of the Hepatitis infection (Scott and Gretch, 2007). Thus, it is becoming clear that the NAAT-based platforms should be used in conjunction with immunoassays in order to avoid misdiagnosis and reduce the risk of new exposures.

Several highly sensitive platforms for HCV testing have been developed with a limit of detection ranging between 5 to 50 IU/mL of plasma. The AMPLICOR 2.0 and Ampliscreen 2.0, both by Roche Diagnostics, Indianapolis, Ind as well as The VERSANT HCV RNA Qualitative Assay (Bayer Diagnostics, Emeryville, Calif) have been shown to reach the highest sensitivity levels in clinical diagnosis with over 98% accuracy. Nonetheless, due to the cost of their equipment, this technology cannot be utilised in most developing countries, such as India, where the HCV burden increases every year. Thus, despite all of the advances in HCV diagnostics, the lack of a quick, sensitive and affordable test continuous to be the major obstacle in the fight against HCV in the developing world (Suthar and Harries, 2015).

3.1.7 Implications of RNA structure on the efficiency of RNA assays

3.1.7.1 Reverse transcription technology

Reverse transcription (RT) assay, is a two-step reaction, in which RNA template is converted into its complementary DNA (cDNA) strand by reverse transcriptases. Subsequently, the reverse complimented RNA (1st strand cDNA) is then amplified by a standard LAMP reaction or other amplification technologies including PCR (Freeman et al., 1999, Lee et al., 2011). In addition, depending on the chosen RT enzyme, the initial RNA strand can either be digested during the cDNA synthesis by RNaseH activity (e.g. Maxima RNaseH+, ThermoFisher UK), to improve the yields, or remain in the assay in a form of a cDNA:RNA heteroduplex (e.g. Maxima RNaseH minus, Superscrip IV, THermoFisher, UK). While both methods can increase the yield of cDNA synthesis, they also carry disadvantages depending on the type of template and amplification technology used. For instance, RT enzymes with intrinsic RNaseH activity have been reported to reduce the overall efficiency of cDNA synthesis, when reverse transcribing longer amplicons, since many of those enzymes can cut RNA templates during pausing (Kotewicz et al., 1988). Thus resulting in premature termination and synthesis of shorter products. In contrast, enzymes lacking this activity have been shown to have an increased processivity and therefore the capability of transcribing longer, up to 20 kb, templates (Maxima RNase H minus, ThermoFisher, UK). However, since the initial RNA target forms highly stable cDNA: RNA hetero duplex, these structures can potentially impair primer invasion and thus reduce the efficiency of initiation and consequently the overall amplification reaction, particularly in LAMP-based assays (Lesnik and Freier, 1995, Chien and Davidson, 1978). PCR-based technologies are less likely to be affected by those structures, since each amplification cycle involves a 95 °C denaturation step.

Although the RT assays are two-step reactions, many of the currently available RT kits carry out those reactions in a single-tube format (One-*Taq* RT-PCR kit, NEB, UK; SuperScript III RT-PCR system, ThermoFisher, UK). However, despite the single-tube format, most of the RT-PCR reactions involve a pre-PCR isothermal reverse transcription step carried out isothermally at a lower, more suitable for the enzyme, temperature, followed by RT inactivation and template denaturation. In contrast, RT-LAMP utilises a highly stable RT enzymes capable of withstanding up to 65 ℃ thus allowing maintaining constant assay temperature throughout (Maxima RNaseH +/minus, SuperScript IV, ThermoFisher, UK). In addition, several dual-function enzymes have also been developed to further optimise and simplify the RT process. For instance Bst 3.0 recently developed by NEB have been shown to exhibit not only an increased displacement activity but also the capacity to use RNA and DNA as templates for DNA synthesis.

3.1.7.2 RNA structures can affect the efficiency of oligonucleotide hybridisation

The biological function of many RNA molecules, including the HCV RNA genome, relies on their substantial folding into secondary or even tertiary structures such as hairpins and pseudoknots as well as interaction between them (Smith et al., 2002, Smith and Wu, 2004). In fact, replication and translation of the HCV genomic RNA relies solely on the conformation of the 5' and 3' UTR regions (Smith et al., 2002, Jubin, 2001, Berry et al., 2011). While this structural function ensures a high degree of conservation between different genotypes and subtypes, it also simplifies the primer design for inclusivity, it can pose a significant barrier for primers and probes hybridisation greatly reducing the efficiency of amplification and detection.

Anato et al. reported how sequence variations between different RNA hairpin structures can have direct effects on their thermostability (Antao et al., 1991). For instance, he demonstrated that loop structures containing UUCG motifs neighbouring with cytosine and guanine at the 5' and 3'end,

respectively exhibited an increased thermostability with an average Tm of over 70 °C. In contrast, the same motif neighbouring with guanine at the 5' end reduced the stability of this hairpin by over 10 °C. However, Anato and co-workers not only concluded that RNA hairpin structures varied in their thermal stability depending on the loop sequence but also showed that RNA hairpins are significantly more stable than corresponding DNA hairpins. He showed that the difference between thermal stability of certain RNA and DNA secondary structures could be as much as 20 °C.

Although, several factors can affect amplification performance including template integrity, chemistry or efficiency of chosen enzymes, primer binding is crucial for successful target detection (Forsell et al., 2015, Stadhouders et al., 2010). Thus, due to such a great variations in thermostability observed between different hairpin motifs, careful consideration has to be taken while designing primers for RT assays.

Currently, a wide range of primer design tools are available on the market and online databases, but most of these tools utilise DNA template as the matrix for primer and as a consequence do not consider the conformational structure of the chosen target (PrimerQuest Tool, IDT, USA, GenScript Primer design tool). Similarly, in PCR-primer designs, the potency of secondary structures on the impairment of primer binding is often underestimated, as displacement is achieved by DNA template denaturation during the thermocycle. As most reverse transcription of RNA are performed between 45-60 °C the secondary and tertiary structures of the template may need to be negotiated in the RT primer design. This is true for PCR that goes through a denaturing step and isothermal amplification like LAMP that operates at assay temperatures ranging between 60-65 °C.

3.2 Aims and objectives

The main focus of this study was to develop a highly optimised RT-LAMP assay for diagnosis of Hepatitis C infections with a careful consideration of the target's secondary structures and their implications on the primer design and the efficiency of the target detection.

3.3 Results

3.3.1 HCV RT-LAMP primer design

HCV RT-LAMP primer sets were designed according to the specifications listed in the methods section. The HCV sequence data retrieved from the HCV sequence database [URL: https://hcv.lanl.gov/content/sequence/NEWALIGN/align.html] was aligned and the region with the highest degree of similarity across all of the known HCV genotypes was used (**Figure 20**). As described throughout the literature, the 5' UTR region of the HCV genome was the most conserved amongst all of the seven HCV genotypes and numerous subtypes characterised and deposited in GenBank [URL: https://www.ncbi.nlm.nih.gov/nuccore/?term=HCV] (**Figure 20 – red box**).

In-depth *in silico* analysis of the sequence and the characterisation candidate primer binding positions resulted in the generation of three HCV primer sets that were analysed in terms of, potential primer interactions and orientation with respect to RNA template secondary structure.

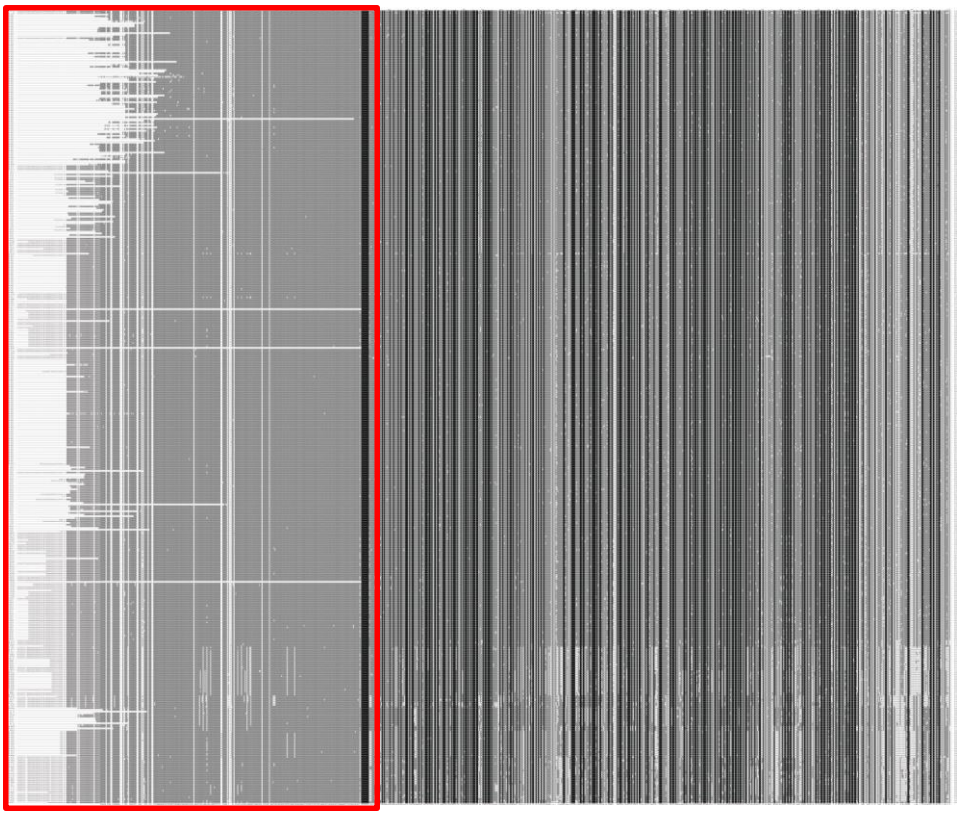

Figure 20. Graphic representation of a HCV genome alignment containing representative sequences from all 7 genotypes and several subtypes. The most conserved region of the HCV genome across all of the retrieved sequences is highlighted in red.

Source: https://hcv.lanl.gov/content/sequence/NEWALIGN/align.html

Table 2 lists the HCV primer sets designed according to the parameters described in the methods section, along with two published sets (Nyan and Swinson, 2016, Young et al., 1993). Primer sets 13-40 were designed in-house. For LAMP primers, two Tm were calculated, where each corresponds to the F/B1 and F/B2 respectively.

primer identifier	Sequence (5'->3')	Tm [°C]
PCR-LGC-F	GCAGAAAGCGTCTAGCCATGGCGT	70.5
PCR-LGC-R	ctcgcaagcaccctatcaggcagt	69.8
HCV001-DN3-F3	GGCGACACTCCACCATGAAT	64.6
HCV002-DN3-R3	ctatcaggcagtaccacaaggc	64.4
HCV003- DN3-FIP	cactatggctctcccgggagTTTTCGTCTAGCCATGGCGTTAG	65.4/62.1
HCV004-DN3-BIP	GGAACCGGTGAGTACACCGGTTTTcccaaatctccaggcattga	66.1/62.5
HCV005- DN3-LF	aggctgcacgacactcata	63.3
HCV006- DN3-LB	GACCGGGTCCTTTCTTGGA	63.5
HCV013-LF	CCTTGTGGTACTGCCTGATA	61.2
HCV014-FIP	CCGAGTAGTGTTGGGTCGggtctacgagacctccc	61.4/59.6
HCV015-F3	aggtttaggattcgtgct	58.4
HCV016-BIPv1	ggctgcacgacactcataACTACTGTCTTCACGC	61.7/55.2
HCV018-B3	GAATCACTCCCCTGTG	55.6
HCV019-BIP	caccggttccgcagaCGGGAGAGCCATAGTG	61.0/57.9
HCV013-LF	CCTTGTGGTACTGCCTGATA	61.2
HCV014-FIP	CCGAGTAGTGTTGGGTCGggtctacgagacctccc	61.4/59.6
HCV015-F3	aggtttaggattcgtgct	58.4
HCV020-B3	AGTATGAGTGTCGTGC	55.3
HCV-034 FIP	TGCCTGGAGATTTGGGCccctatcaggcagtacca	62.0/60.0
HCV-035 BIP	aaaggacccggtcgtTGGTCTGCGGAACCGGTGAG	59.6/68.0
HCV-036 LoopF	GAGTAGTGTTGGGTCG	55.1
HCV-038 F3	gtgcacggtctacgaga	60.6
HCV-039 LoopB	cctggcaattccggtgta	61.8
HCV-040 B3	TCCCGGGAGAGCCAT	61.6

3.3.2 HCV 5'UTR secondary structure analysis

Since, the *Hepatitis C* virus genome is a single-stranded RNA, most of the currently available nucleic acid amplification technologies, involve a reverse transcription step that results in the production of cDNA that is subsequently re-amplified by a DNA polymerase. It is well known that single-stranded nucleic acid molecules, particularly RNAs, have an extremely high tendency to fold into various stable motifs, such as hairpins or pseudoknots.

The secondary structure of the 5'UTR sequence, typical of HCV genotype 1 was assessed *in silico*, to understand any imposition that could interfere with primer annealing, particularly the proposed FIP and reverse displacement priming positions necessary for the initiation of reverse transcription.

Figure 21 shows a graphic representation of the secondary structure of the first 400 nucleotides of the 5'UTR region. An online software was applied in order to generate the most probable secondary structure output of the chosen fragment at the assay temperature (60 °C). The data was displayed in a form of a graphical model and a colour-coded sequence alignment.

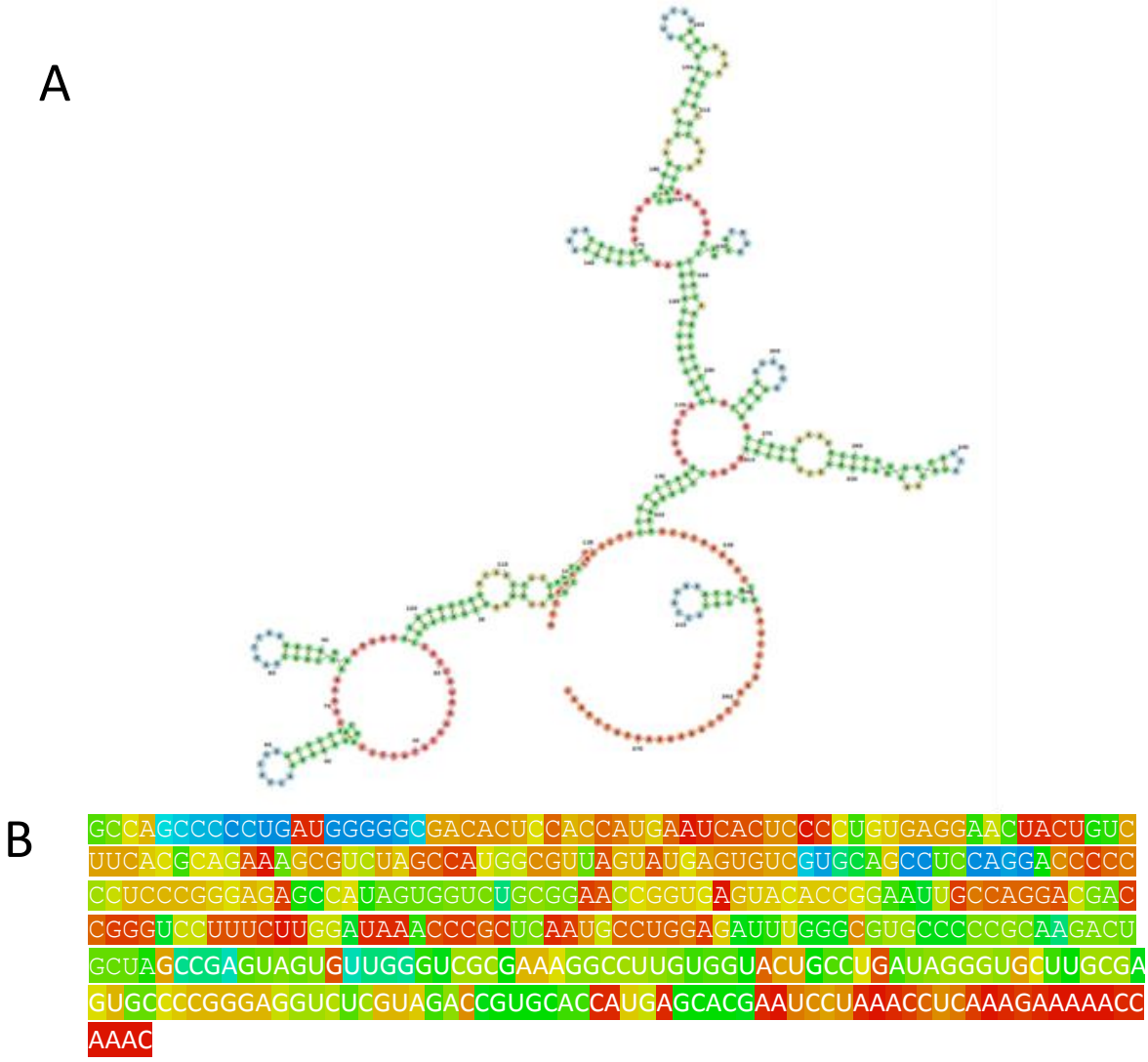

Figure 21. Graphic representation of the HCV 5'UTR folding prediction performed by Vienna online RNA folding tool. A – 2-D RNA folding structure with double-stranded stems and open loops highlighted in green and blue/orange, respectively. B – HCV 5' UTR sequence output (5' → 3') with highlighted probabilities of forming secondary structures. Red, orange and yellow represent highly structured regions whereas green, and blue indicate the likelihood of open loop formation.

Source: http://rna.tbi.univie.ac.at/cgi-bin/RNAWebSuite/RNAfold.cgi

The 5'UTR region of the HCV genome is highly structured with numerous hairpins and pseudoknots exhibiting various levels of stability. According to the colour-coded sequence, highly stable secondary structures are dispersed throughout the UTR region. Each colour represents the probability of a stable base pairing with the warmer (Red, orange and yellow) colours being the

most stable. The position of red and orange bases are indicative of structures extremely difficult to melt and invade by primers that rely solely on the displacement activity of the polymerase. A substantial amount of open and weak secondary structures indicated by the green and blue bases were also be detected. This analysis is rarely afforded by primer design tools, and was enabling allowing for RT primer designs that would not only account for inclusivity, but also consider the efficiency of primer binding with respect to target structure.

3.3.3 Effects of secondary structures on HCV 5'UTR RT-LAMP-BART

Three in-house designed HCV RT-LAMP primers sets (**Table 2** – Set 13-18; 13-20 and 34-40) were designed to be highly inclusive for all of the known HCV genotypes with a particular emphasis on the genotypes 1-3 due to their high clinical relevance. Prior to experimental assessment, each primer set was analysed *in silico* in order to determine potential primer interactions that could result in mis-amplification.

Despite the fact that the *in silico* analysis of the primer interactions did not predict any significant primer-dimers, only the HCV 34-40 primers amplified the target RNA sequence specifically (**Figure 22A-B**). Consequently, the binding positions of each primer set was analysed with respect to the RNA secondary structure of the UTR template, in order to determine the possible cause of amplification failures. Similar analysis was then performed on two published primer set for reference purposes.

Figures 23-24 show a colour-coded output of the *in silico* sequence analysis using the Vienna software for the first 400 nt of the 5'UTR region. Primer binding positions were underlined for visual clarity.

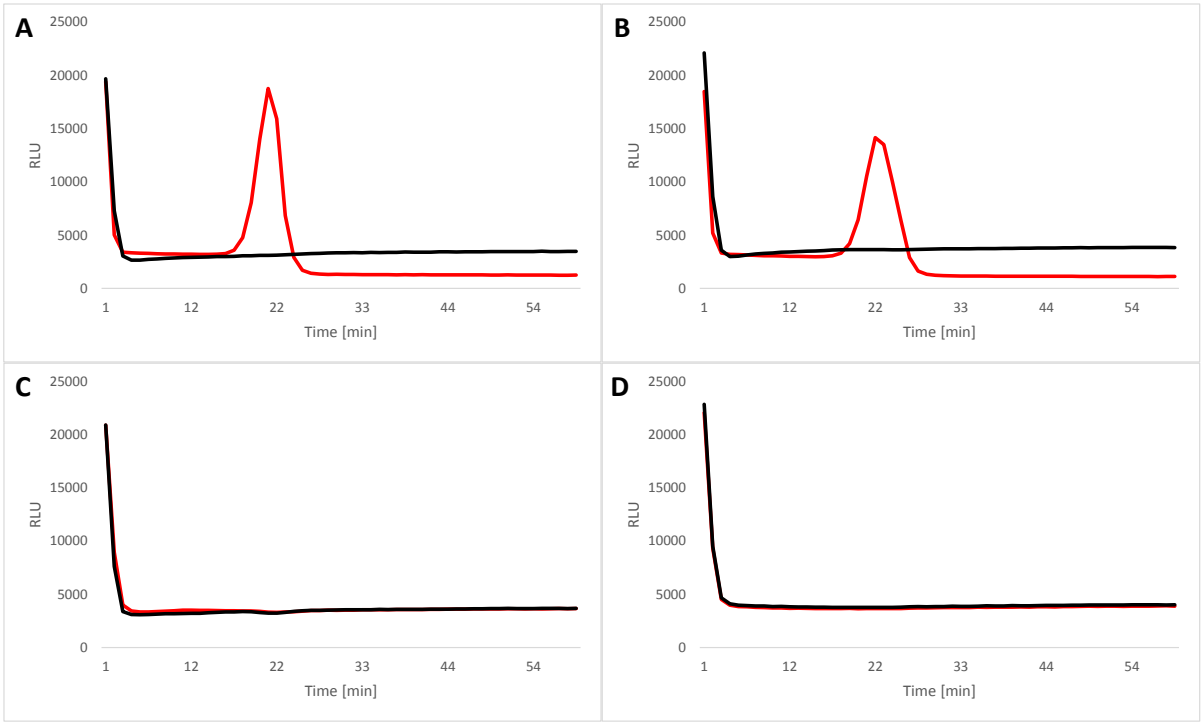

Figure 22. LAMP-BART profiles generated using in-house designed HCV LAMP primers. A – HCV assay using 10^4 cps of synthetic 5'UTR DNA and the 34-40 primer set; B – HCV assay using 10^4 cps HCV 5'UTR RNA fragments and the 34-40 primer set; C – HCV assay using 10^4 cps HCV 5'UTR RNA fragments and the 13-18 primer set; D – HCV assay using 10^4 cps HCV 5'UTR RNA fragments and the 13-20 primer set.

Note that red curves represent the reactions containing the target template. Black profiles were generated from the NTC control reactions (no Template)

Refer to protocol 2

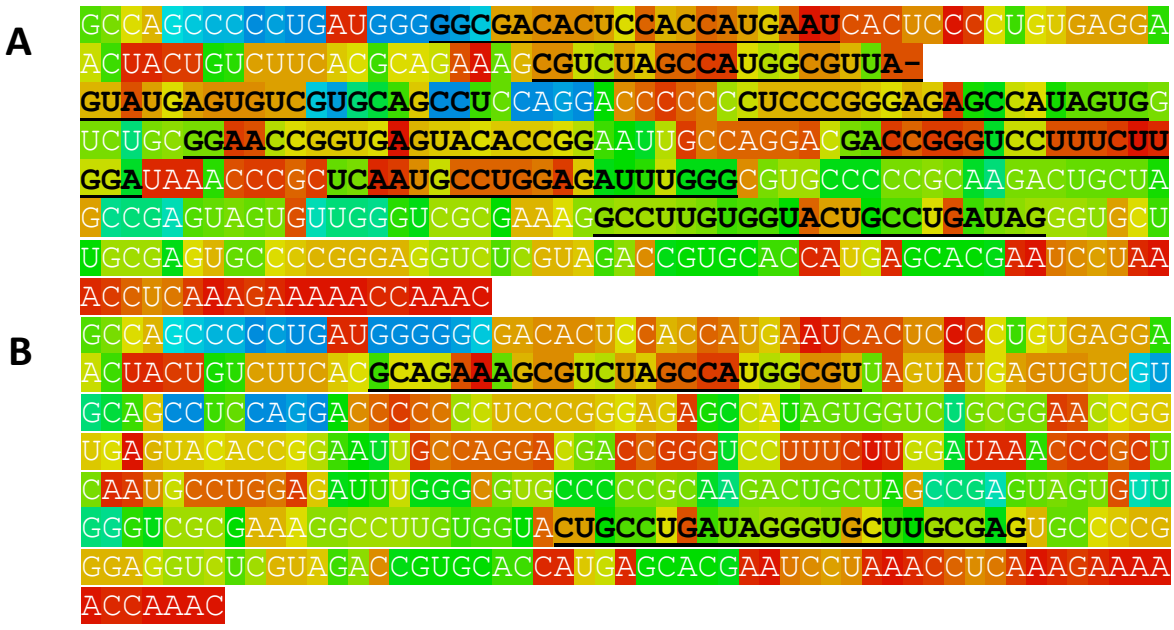

Figure 23. HCV 5′ UTR sequence output (5′ → 3′) generated by the Vienna RNA fold software with highlighted probabilities of forming secondary structures. Red, orange and yellow represent highly structured regions whereas green, and blue indicate the likelihood of open loop formation. A – HCV 5′ UTR sequence output with highlighted published DN3 primer binding sites. Each separate primer binding site was highlighted in bold and underlined in a specific order: 5′ – B3, B2, LoopB, B1, F1, LoopF, F2, F3 – 3′. Note that certain sites were separated by a "-" for visual clarity due to the proximity to the other recognition sites. B - HCV 5′ UTR sequence output with highlighted published LGC primer binding sites in a specific order : 5′ – Forward, Reverse primer – 3′

Source: http://rna.tbi.univie.ac.at/cgi-bin/RNAWebSuite/RNAfold.cgi

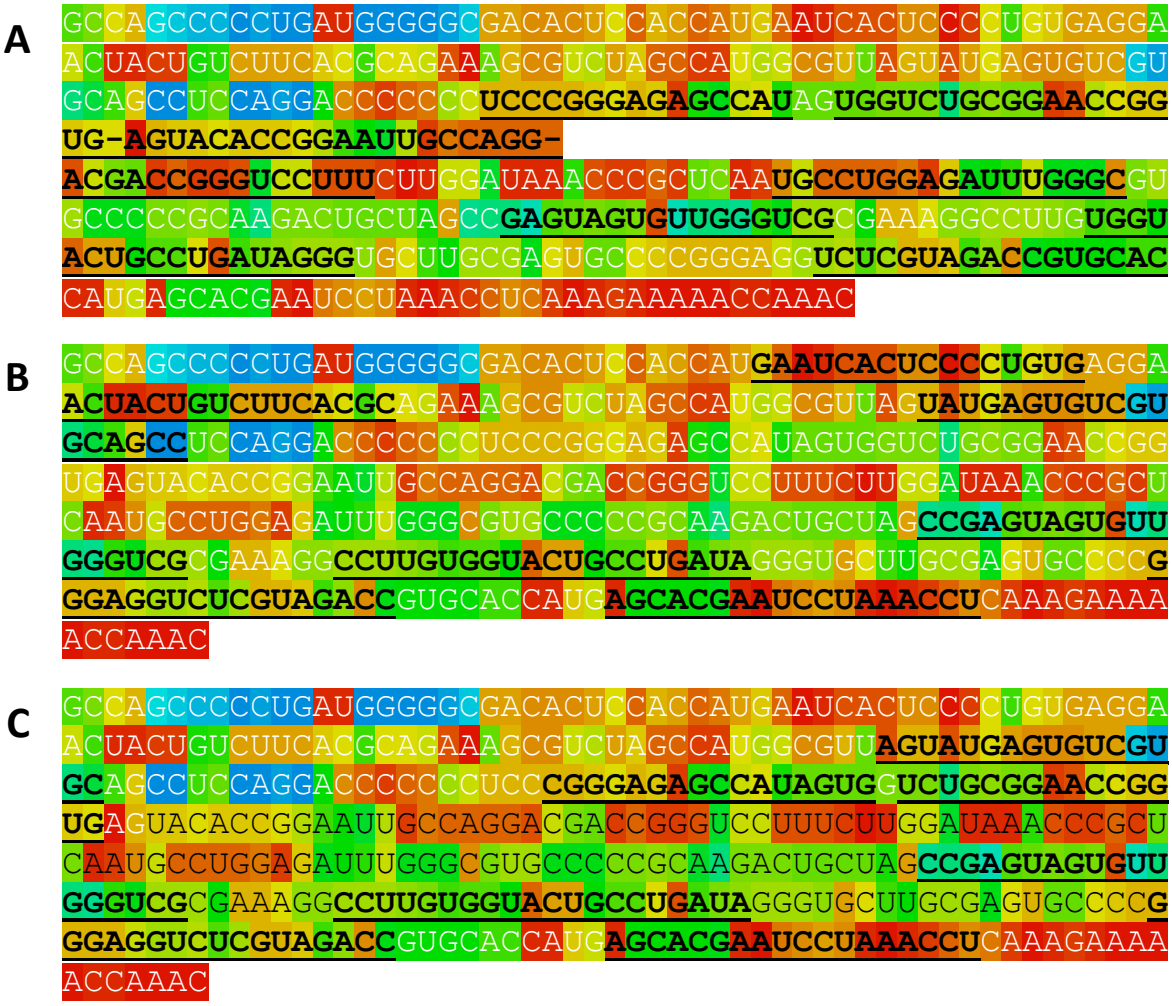

Figure 24. HCV 5' UTR sequence output (5' → 3') generated by the Vienna RNA fold software with highlighted probabilities of forming secondary structures. Red, orange and yellow represent highly structured regions whereas green, and blue indicate the likelihood of open loop formation. A – HCV 5' UTR sequence output with highlighted in-house designed 34-40 primer binding sites. Each separate primer binding site was highlighted in bold and underlined in a specific order: 5' – B3, B2, LoopB, B1, F1, LoopF, F2, F3 – 3'. Note that certain sites were separated by a "-" for visual clarity due to the proximity to the other recognition sites. B - HCV 5' UTR sequence output with highlighted in-house designed 13-18 primer binding sites. Each separate primer binding site was highlighted in bold and underlined in a specific order: 5' – B3, B2, LoopB, B1, F1, LoopF, F2, F3 – 3'. C - HCV 5' UTR sequence output with highlighted in-house designed 13-20 primer binding sites. Each separate primer binding site was highlighted in bold and underlined in a specific order: 5' – B3, B2, LoopB, B1, F1, LoopF, F2, F3 – 3'.

Source: http://rna.tbi.univie.ac.at/cgi-bin/RNAWebSuite/RNAfold.cgi

As expected, all of the publish RT-LAMP primer sets that were analysed here, known to target the least structured regions of the 5'UTR amplified very efficiently. Both, the F3 and FIP primers of the RT-LAMP DN3 primer set, as well as the reverse RT-PCR primer of the LGC set, landed

within either very mild secondary structures or open regions of the target (**Figure 23A-B**). Interestingly, the reciprocal priming positions for the RT-LAMP DN3 (BIP) and LGC RT-PCR forward primer, did show mild to heavy secondary structure. Similarly, the current HCV 34-40 RT-LAMP primer set, which showed satisfactory amplification efficiency, (**Figure 22A-B**), annealed to sequence devoid of secondary structure. In fact, it was shown that both key reverse transcribing LAMP primers avoided RNA secondary structure altogether (**Figure 24A**).

In contrast, primer sets 13-18 and 13-20, both landed within either mild or heavily structured regions of the 5' UTR (**Figure 24B-C**). In both cases, the sequences targeted by the FIP and BIP primers showed increased folding probability. Initial evaluation of these sets, under the same amplification chemistry as the HCV 34-40 primer set, showed no detection of the target RNA **(Figure 22C-D).**

3.3.4 HCV assay optimisation

Amongst all of the novel RT-LAMP primer sets designed for this study, only the HCV 34-40 set showed satisfactory performance during the initial evaluation, thus it was moved forward for further assay optimisation studies.

3.3.4.1 Effect of DNA polymerases on the RT-LAMP HCV assay performance

The performance of two different versions of the Bst DNA displacement polymerase (isolated from *Bacillus stearothermophilus*), 'Bst 2.0' and 'Bst 2.0 Warm Start' (from NEB), and GSP-SSD (isolated from *Geobacillus* sp.) (from Optigene) enzyme were compared in this study.

The results presented in the **Figure 25A-C** shows RT-LAMP-BART profiles generated using appropriate DNA polymerases and various amounts of the target 5'UTR HCV RNA template.

Among all the DNA polymerases tested, the assays containing the GSP-SSD enzyme performed noticeably better, regardless of the amount of the target RNA used. However, a significant reduction in the time-to-max (TTM) was observed with increasing copy number per reaction, when the GSP-SSD was compared with the other two enzymes assessed here (p value < 0.05, t-test). In contrast, at a lower copy numbers, no significant difference in TTM was detected between the GSP-SSD and Bst 2.0 (p *values* > 0.05, t-test; **table 3**). However, a slight increase in mis-primed amplifications was observed when utilising the Bst 2.0 enzyme.

Inclusion of Bst 2.0 WS had a detrimental effect on the performance of the HCV assay with a significant increase in TTM and a significant reduction in the overall RT-LAMP sensitivity, when compared to the other two displacement polymersaes at the same specific activity; only reactions containing higher copy numbers of the HCV template amplified (p *value* < 0.05; **figure 25C**). On

average, a 13 min increase in TTM was detected at the 10^4 copies (final copy number of IVT in the assay) when the Bst 2.0 WS enzyme was used (**Table 3**).

The sensitivity of the chosen DNA polymerases were also assessed by scoring amplification frequencies at various copy numbers and determining the number of false positive reactions detected during a pre-determined time-frame. The initial comparison of Bst 2.0 and the GSP-SSD polymerase did not show any significant effect on the amplification frequencies and the reproducibility of the HCV test, regardless of the copy number of the target RNA used (*p value* > 0.05, t-test; **table 3**). In contrast, when the reactions containing the Bst 2.0 WS were assessed, a dramatic reduction in both sensitivity and reproducibility of the test was observed with respect to the other enzymes tested. No detection below 1000 copies of the target was achieved and a significant deterioration in reproducibility was observed between the replicates analysed at both 10^ 4 and 10^3 copies of IVT per assay.

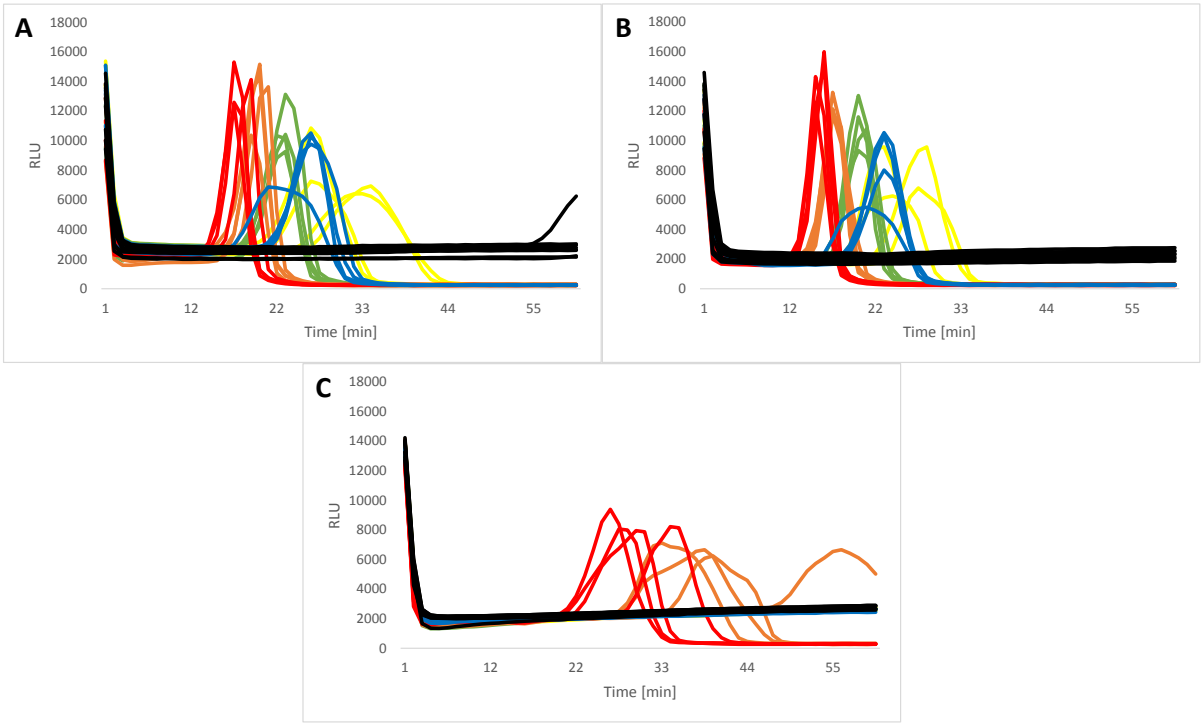

Figure 25. Comparison of LAMP-BART profiles generated using HCV 5'UTR RNA fragments, 34-40 primer set and three chosen DNA polymerases. A – HCV assay using Bst 2.0 DNA polymerase; B – HCV assay using GSP-SSD DNA polymerase; C – HCV assay using Bst 2.0 WarmStart DNA polymerase.

Note that each concentration of the HCV RNA used was colour coded as follows: Red – 10^4 cps; Orange – 10^3 cps; Green – 10^2 cps; Blue – 50 cps; Yellow – 10 cps; Black – NTC (No template)

Table 3 showing summary of the data presented in the **figure 25**. Each set of reactions was analysed using average TTM (Mean), reproducibility (STDev) and sensitivity (Amp.Freq).

DNA polymerase	RNA [cp/rxn]	Mean [min]	STDev	Amp. Freq. [%]
	10^4	16	0.6	100
	10^3	17	0.0	100
	10^2	21	0.5	100
	50	20	3.9	100
	10	26	2.5	100
GSP	NTC	90		100
	10^4	30	3.3	100
	10^3	42	9.7	100
	10^2			0
	50			0
	10			0
BST WS	NTC	117		100
	10^4	18	1.1	100
	10^3	20	0.9	100
	10^2	23	0.5	100
	50	25	2.7	100
	10	30	4.0	100
BST 2.0	NTC	88		100

Similar observations were made when the chosen DNA polymerases were tested on a TB assay developed by ERBA Molecular, targeting 23s ribosomal RNA (rRNA).

Figures 26-27 show LAMP-BART profiles generated using four different DNA polymerases according to the protocol 8 (see **Appendix 8**).

Note that the number of units of each of the tested DNA polymerases differed due to differences in unit's definition used by the manufacturer. For each comparison assay the most optimal amount of each DNA enzyme was used according to the previous optimisation studies performed by Lumora LTD (data not shown).

As expected, the reactions utilising the GSP-SSD DNA polymerase performed noticeably better than all the other assays tested, in terms of both the sensitivity and amplification speed (**Figure**

26A, C). Amplification of the *M. bovis* genomic DNA (gDNA) was significantly faster when GPS-SSD was used in comparison with the assays containing Bst Large fragment and Bst 2.0 WS (**Figure 27C**), regardless of the amount of the target present (*p value* < 0.05, t-test). On average, the GSP-SSD reactions amplified the target 2 min faster than those containing Bst 2.0WS and Bst Large fragment. However, no significant difference in the reaction speed was noticed when Bst 2.0 DNA polymerase was assessed (*p value* > 0.05, t-test). Nonetheless, the overall performance of the assays utilising the GSP-SSD enzyme was better when the sensitivity data was taken into consideration.

All of the tested assays achieved full detection of the target DNA when 1000 cp/rxn was added. However, at 100 cp the reactions utilising Bst 2.0 failed to detect 1 out of 6 replicates whereas all other assays reached 100 % detection (**Table 4**).

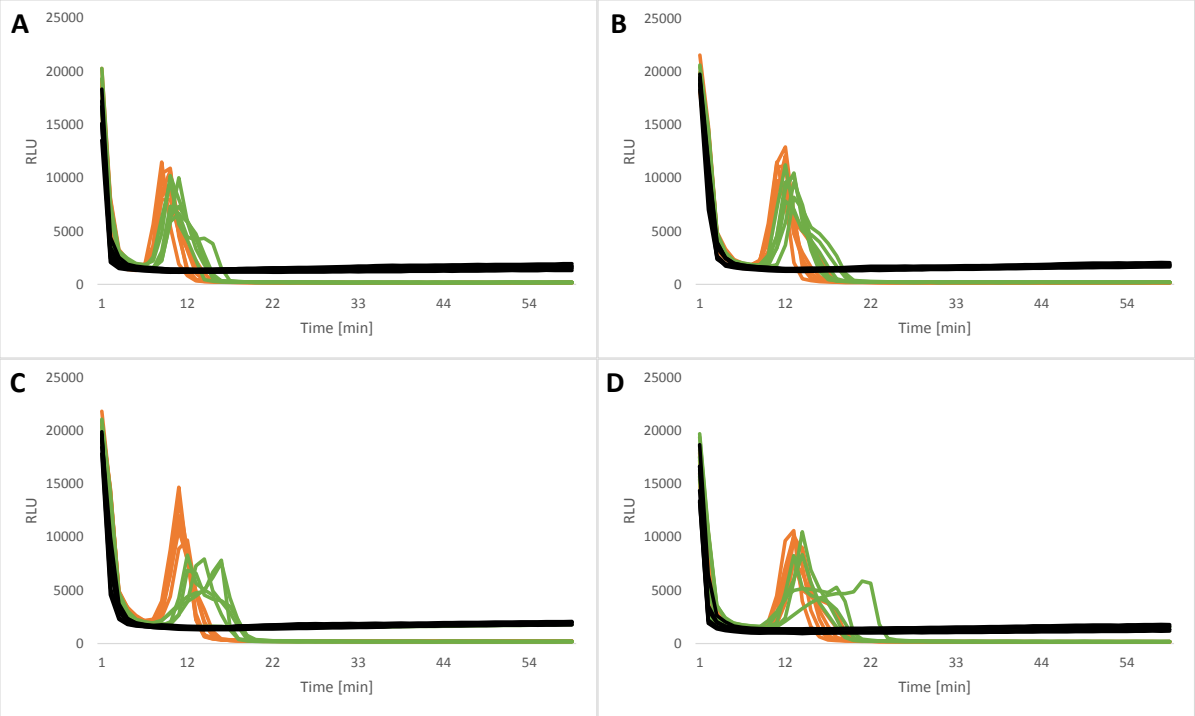

Figure 26. Comparison of LAMP-BART profiles generated using TB assay model system. A – TB assay using GSP-SSD DNA polymerase and *M. bovis* gDNA; B – TB assay using Bst Large fragment DNA polymerase and *M. bovis* gDNA; C – TB assay using GSP-SSD DNA polymerase and *M. bovis* 23s rRNA; D – TB assay using Bst Large fragment DNA polymerase and *M. bovis* 23s rRNA.

Note that each concentration of the *M. bovis* NA used was colour coded as follows: Orange – 10^3 cps; Green – 10^2 cps; Black – NTC (No template)

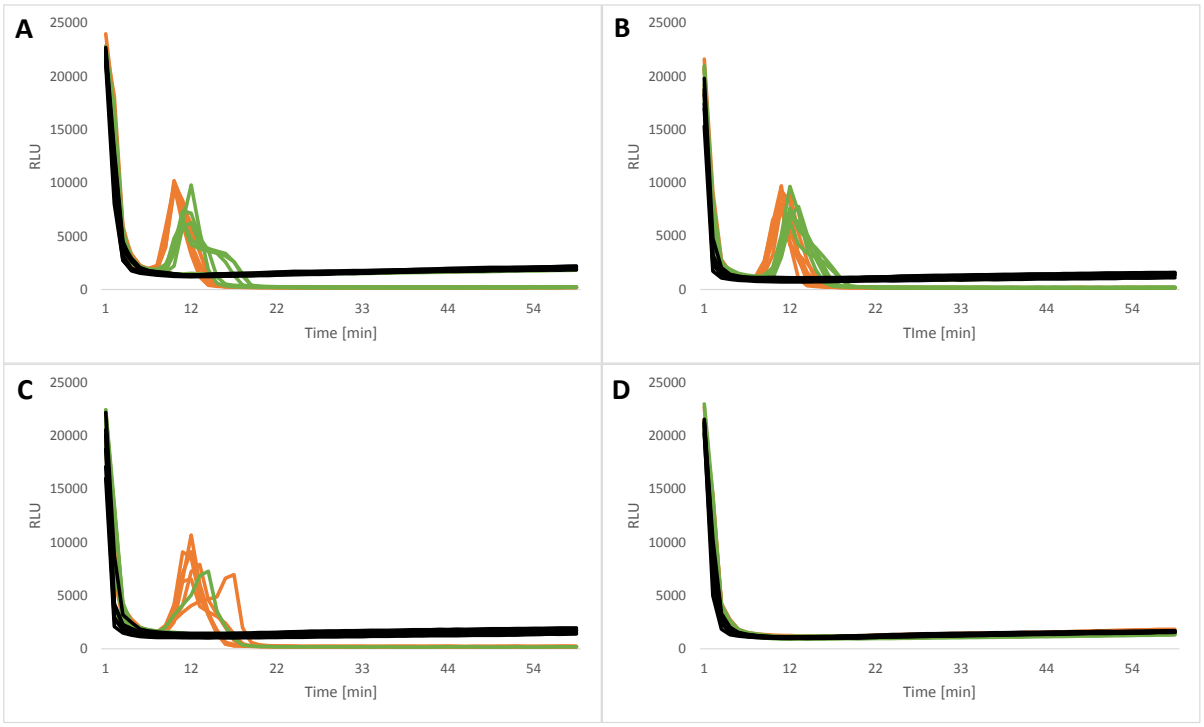

Figure 27. Comparison of LAMP-BART profiles generated using TB assay model system. A – TB assay using Bst 2.0 DNA polymerase and *M. bovis* gDNA; B – TB assay using Bst 2.0WS DNA polymerase and *M. bovis* gDNA; C – TB assay using Bst 2.0 DNA polymerase and *M. bovis* 23s rRNA; D – TB assay using Bst 2.0WS DNA polymerase and *M. bovis* 23s rRNA.

Note that each concentration of the *M. bovis* NA used was colour coded as follows: Orange – 10^3 cps; Green – 10^2 cps; Black – NTC (No template)

Similarly, when the RNA assays were assessed, the reactions utilising GSP-SSD enzyme performed noticeably better (**Figure 26C**). On average, the GSP-SSD assays detected the target 2 min faster than those using Bst LF and Bst 2.0 when 1000 cp of the RNA was added. However, GPS-SSD reactions performed significantly faster when compared to the Bst LF assays only (*p value* < 0.05, t-test, **table 4A**). In contrast, at 100 cp of the target RNA, no significant difference in the amplification speed was noticed when Bst LF, Bst 2.0 and GSP-SSD assays were assessed. However, the reactions utilising the GSP-SSD enzyme generated data with noticeably higher reproducibility than all the other DNA polymerases tested.

Furthermore, the assay sensitivity data showed that only the reactions utilising the Bst LF and the GSP-SSD enzymes reached satisfactory level of overall sensitivity. Both, GSP-SSD and Bst LF

assays managed to amplify 83 and 100 % of the target RNA when 100 and 1000 cps were added, respectively (**Table 4A**). In contrast, the reactions containing the Bst 2.0 detected 1 out of 6 replicates containing 100 cps and 6 out of 6 with 1000 cps of the target. In addition, the assays utilising the Bst 2.0 WS enzyme failed to detect any level of the target RNA (**Table 4B**).

Table 4 showing summary of the data presented in the **figure 26-27**. Each set of reactions was analysed using average TTM (Mean), reproducibility (STDev) and sensitivity (Amp.Freq).

A

DNA pol.	Template	NA conc. [cp/rxn]	TTM [min]	Stdev	Amp.Freq. [%]
GSP-SSD	DNA	1000cp	9	0.6	100
		100cp	10	0.6	100
	RNA	1000cp	11	0.4	100
		100cp	14	2.1	83
Bst LF	DNA	1000cp	11	0.6	100
		100cp	12	0.6	100
	RNA	1000cp	13	0.0	100
		100cp	16	3.6	83

B

DNA pol.	Template	NA conc. [cp/rxn]	TTM [min]	Stdev	Amp.Freq. [%]
Bst 2.0	DNA	1000cp	10	0	100
		100cp	11	0.6	83
	RNA	1000cp	13	2.3	100
		100cp	14		17
Bst2.0WS	DNA	1000cp	11	0.4	100
		100cp	12	0.4	100
	RNA	1000cp			0
		100cp			0

3.3.4.2 Effect of reverse transcriptases on the RT-HCV assay performance

In this evaluation, two versions of Maxima reverse transcriptase (Maxima RNaseH- and Maxima RNaseH+), as well as a new Superscript IV reverse transcriptase, were assessed for utility in the isothermal RT-LAMP reactions. The three scripts were assessed in terms of their impact on amplification speed, reproducibility and sensitivity.

Figure 28-29, shows RT-LAMP-BART profiles generated using GSP-SSD DNA polymerase and all three reverse transcriptases.

The overall performance of the assays containing Maxima RNaseH- were deemed to amplify more efficiently than the other enzymes tested. The speed and reproducibility was improved in Maxima lacking the RNaseH, resulting in a significant reduction in both the TTM and improved reproducibility at each of the RNA copy numbers tested (*p values* < 0.05, t-test; **figure 28B**). The overall difference in speed of each tested set up increased with reducing quantities of 5'UTR RNA was marked, demonstrating the importance in choice of enzyme on the amplification of HCV RNA. At lower copy numbers (10 copies RNA / assay), the sensitivity of detection with Maxima RNaseH (-) was greater than similar assays performed with Maxima H (+) (**Table 5**). This could be attributed to the overall amplification efficiency and speed that also resulted in greater numbers of mis-primed amplifications that were also associated with the use of Maxima RNaseH(+) enzyme (**Figure 28A**).

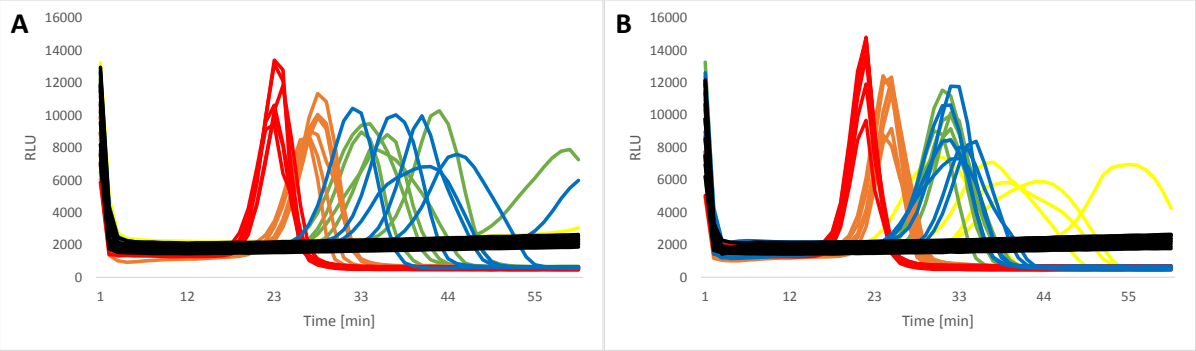

Figure 28. Comparison of LAMP-BART profiles generated using HCV 5'UTR RNA fragments, 34-40 primer set and two chosen Reverse transcriptases. A – HCV assay using Maxima RNase H +; B – HCV assay using Maxima RNase H -

Note that each concentration of the HCV RNA used was colour coded as follows: Red – 10^4 cps; Orange – 10^3 cps; Green – 10^2 cps; Blue – 50 cps; Yellow – 10 cps; Black – NTC (No template)

Refer to protocol 4

Table 5 showing summary of the data presented in the **figure 28**. Each set of reactions was analysed using average TTM (Mean), reproducibility (STDev) and sensitivity (Amp.Freq).

Maxima	RNA [cp/rxn]	Mean [min]	STDev	Amp. Freq. [%]
	10^4	23	0.4	100
	10^3	27	0.6	100
	10^2	40	9.9	100
	50	43	10.2	100
	10	77	5.7	50
RNaseH(+)	NTC	122		41.7
	10^4	21	0.0	100
	10^3	24	0.6	100
	10^2	32	0.9	100
	50	33	1.3	100
	10	41	8.7	83
RNaseH(-)	NTC	115		50

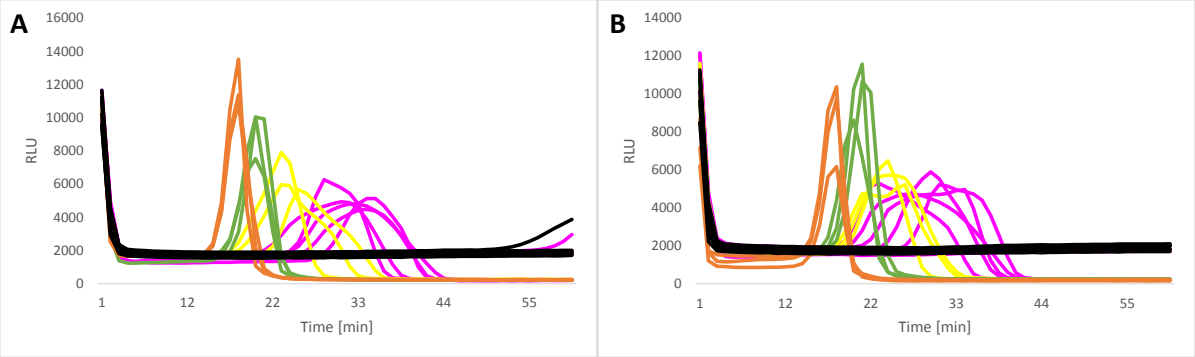

Figure 29. Comparison of LAMP-BART profiles generated using HCV 5'UTR RNA fragments, 34-40 primer set and two chosen Reverse transcriptases. A – HCV assay using Maxima RNase H -; B – HCV assay using SuperScript IV

Note that each concentration of the HCV RNA used was colour coded as follows: Orange – 10^3 cps; Green – 10^2 cps; Yellow – 10 cps; Pink – 1 cps; Black – NTC (No template)

Table 6 showing summary of the data presented in the **figure 29**. Each set of reactions was analysed using average TTM (Mean), reproducibility (STDev) and sensitivity (Amp.Freq).

RT enzyme	RNA [cp/rxn]	Mean [min]	STDev	Amp. Freq. [%]
	10^3	18	0.0	100
	10^2	20	0.0	100
	10^1	24	1.2	100
	10^0	32	2.3	55.6
Maxima	NTC	82		100
	10^3	18	0.0	100
	10^2	21	0.6	100
	10^1	25	1.2	100
	10^0	29	4.0	55.6
SuperScript	NTC	83		100

Since all experiments with Maxima reverse transcriptase demonstrated that the HCV RT-LAMP had a preference for the RNaseH deficient version of this reverse trascriptases, a new version of SuperScript RT enyme SuperScript IV also deficient in reverse transcriptase was tested. According to the supplier (Thermofisher), SuperScript IV was highly resistant to inhibition from various matrixes, and possessed a wider thermal range that may also be suited to this assay (45-60 °C).

Figure 29, shows the RT-LAMP-BART profiles generated using the chosen reverse transcriptases and GSP-SSD DNA polymerase. Assays performances were compared with respect to amplification sensitivities, speed, reproducibility and specificity.

No significant difference in the performance of the tested assays were observed (*p value* < 0.05, t-test; **figure 29**). Neither the sensitivity, reproducibility nor the speed of the assays using the SuperScript IV were affected when compared to amplifications benchmarked using the standard HCV LAMP protocol, which utilised the Maxima RNaseH- RT enzyme; both scripts achieved the same sensitivity of 10 copies / reaction with 100% amplification and single copy detection was achieved in 55% of the amplifications tested (**Table 6**).

3.3.4.3 Effects of different assay chemistries on the amplification performance.

In this study, two different reaction buffers (i.e. Thermopol and Isothermal buffer), suitable for isothermal amplification, were compared. **Figure 30** shows the LAMP-BART profiles generated using GSP-SSD DNA polymerase and both reaction buffers on HCV assay.

In this experiment, a range of HCV 5' UTR RNA dilutions was used to assess the performance of the HCV LAMP assay in terms of both the speed and sensitivity as well as NTCs formation, under different buffering conditions. Firstly, 100 % amplification frequency was achieved for all of the RNA titrations tested, regardless of the reaction buffed used. However, the reactions containing the Isothermal buffer showed a significant improvement in both the speed of amplification and the reproducibility (p values < 0.05, t-test). All of the reactions containing 10 cp of the template amplified under 30 min when the Isothermal buffer was used whereas nearly 40 min was required for the corresponding template concentration to be amplified under the Thermopol buffering conditions.

Moreover, on average, over 9 min difference in TTM was detected between the two assessed reaction set ups, regardless of the amount of the template used. However, the differences in TTM between the two tested reaction set ups was noticed to increase with reducing amount of the template used.

In addition, the STDev was noticeably lower, for the reactions utilising the Isothermal buffer, showing a much higher reproducibility. However, unlike the Isothermal buffer, the reactions under the Thermopol buffering conditions showed no NTCs throughout the run.

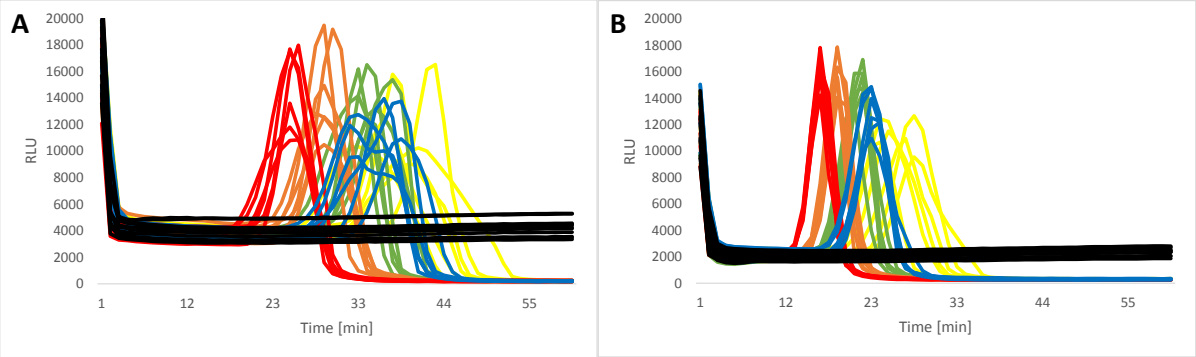

Figure 30. Comparison of LAMP-BART profiles generated using HCV 5'UTR RNA fragments, 34-40 primer set and two chosen reaction buffers. A – HCV assay using Thermopol buffer; B – HCV assay using Isothermal (ISO) buffer.

Note that each concentration of the HCV RNA used was colour coded as follows: Red – 10^4 cps; Orange – 10^3 cps; Green – 10^2 cps; Blue – 50 cps; Yellow – 10 cps; Black – NTC (No template)

Table 7 showing summary of the data presented in the **figure 30**. Each set of reactions was analysed using average TTM (Mean), reproducibility (STDev) and sensitivity (Amp.Freq).

	RNA [cp/rxn]	Mean [min]	STDev	Amp. Freq. [%]
	10^4	16	0.0	100
	10^3	18	0.0	100
	10^2	21	0.6	100
	50	23	0.4	100
	10	26	2.0	100
ISO buffer	NTC	93		100
	10^4	25	0.6	100
	10^3	29	0.7	100
	10^2	35	1.6	100
	50	35	2.9	100
	10	38	3.4	100
Thermo Buffer	NTC			0

3.4 Discussion

3.4.1 Impact of RNA structure on assay performance

Although, formation of secondary and tertiary structures by most RNA genomes and transcripts can often be attributed to biological function, very limited consideration is given to possible steric hindrance, in commercial software packages used to design, RT-PCR and RT-LAMP primers (Jubin, 2001, Lukavsky, 2009). Moreover, despite a wide range of bioinformatics tools available for RNA folding analysis, such as Vienna or RNAFold, secondary structure analysis prior to primer design for RNA amplifications is not yet common practice. Several publications have reported formation of highly stable RNA hairpins, with melting temperatures (Tm) of 70 °C or more (Antao et al., 1991, van der Werf et al., 2013, Chen and García, 2013). Despite the widespread understanding of the thermostability of such RNA structures, the impact of this on reverse transcribed priming is limited in the scientific press. Although, it is often assumed that RT-PCR assays are immune to this limitation in primer design, these assays must also undergo a low temperature RT step, therefore, cannot make the use of the denaturation step characteristic for this type of DNA amplification. cDNA synthesis by reverse transcription occurs isothermally, irrespective of the technology used and reverse transcription cannot make use of high melting temperatures to delineate RNA secondary structures. Since the RT step initiates all subsequent activity in RT-PCR amplifications it is of paramount importance to nurture this activity with respect to RNA secondary structure that can now be more reliably predicted with software as was observed.

In this study, we attempted to assess the effects of RNA structure on the performance of HCV RNA detection by using an online RNA folding software, Vienna. Our *in silico* analysis of 5' UTR RNA folding showed a high degree of secondary structures predicted by the software. This was to

be expected, since the initiation of the HCV RNA translation relies on formation of IRES. Nonetheless, certain regions of the sequence used also showed mild to no folding indicated by the green and blue colour code (see the Vienna alignment), thus these regions of the sequence were more suited for primer design. All of the designed RT-LAMP primer sets performed efficiently, where the RNA secondary structure with respect to primer design had been careful considered and negotiated (Set 34-40). Both, the F3 and FIP primers of the 34-40 primer set, landed in a highly open region of the HCV UTR sequence. Conversely, the B3 and BIP primer targeted fragments with mild folding. All primers of RT-LAMP designs 13-18 and 13-20, were annealed to RNA with a high level of complexity, and performance suffered as a consequence. In an RT- LAMP amplification, the FIP and F3 are crucial primers for initiating reverse transcription, since they bind to the target RNA directly. Both set primer sets 13-18 and 13-20 shared common F3 and FIP primers and since no amplification was observed in any of the reactions utilising those primers, one could conclude that the heavily structured region of the HCV 5'UTR RNA targeted by the F3 and FIP were simply inaccessible. The same RT primers of RT-LAMP set 13-20 utilised B3 and BIP primers targeting significantly more open regions of RNA than those used by the 13-18 primer set. However, since the B3 and BIP binding relied on the first strand cDNA synthesis, no difference in performance between those primer sets, was observed. Thus, we concluded that the FIP and F3 binding positions were crucial for the initiation and therefore fundamental to the success when amplifying from RNA.

Furthermore, we also assessed the role of B3 and BIP primers in the overall performance of RT-LAMP. Both, published DN3 and currently designed 34-40 primer sets, amplified the target HCV RNA with satisfactory performance. However, to our knowledge, the 34-40 set performed noticeably better and achieved a higher degree of sensitivity. We contributed this increased

performance to the role of B3 and BIP primers. We noticed that both B3 and B2 part of the published BIP primer (DN3) landed within highly structured region of the HCV 5'UTR, whereas our designed primer set targeted more open structures at these annealing positions. We concluded that the accessibility of the BIP and B3 primers to the template may affect the amplification performance but to a much lower extent and limited to DNA templates. We assume that once the first cDNA strand is synthesised from FIP and F3 extension, it can either be displaced or the original RNA template is digested resulting in formation of a single-stranded cDNA fragment. Thus, due to the single-stranded nature of the generated target, one could also conclude that folding of this structure would also occur; although the affinity of bases may not be quite the same as the original template RNA (Antao et al., 1991). DNA secondary structures are known to be less stable than their corresponding RNA hairpins, primer invasion by B3 and BIP may not be impaired by structure to the same extent as the FIP and F3 on the original RNA target (Chen and García, 2013).

Although, many factors affect performance of polymerisation, the *in silico* analysis does not always reflect the true primer interactions, on template and with each other; our study indicates that RNA folding must be considered in the RT-PCR / RT-LAMP design as it can significantly impair reverse transcribed polymerisations.

3.4.2 Optimisation of the HCV RT-LAMP amplification

Since changes in the chemistry of any amplification technology can have a dramatic effect on their performance and sensitivity, a lot of effort has been put into creating highly optimised methods for nucleic acid synthesis, a wide and growing range of enzymes and their buffers is constantly being developed and improved upon (Freeman et al., 1999, Godfrey and Kelly, 2005, Estes et al., 2012). It is often the case that different amplification mechanisms and reporter systems require completely different chemistries (Balmer, *2007*2007, Kramer and Coen, 2006). In this study, two versions of

the Bst large fragment DNA polymerase were compared to 'a new, highly displacing enzyme, GSP-SSD' to evaluate any differences in performance that could be attributed to displacement polymerases in an RT-LAMP amplification.

In general, the Bst DNA polymerases used (i.e. Bst 2.0 and 2.0 Warm Start) have been shown to be much more active and less sensitive to inhibitory substances such as potassium and sodium salts when compared to the Bst large fragment (NEB [URL: https://www.neb.com/products/m0537-bst-20-dna-polymerase]). The kinetics, as well as inhibitor sensitivity, were factors most likely changed, by either introducing alternate amino groups into the original version of the DNA polymerase or by coupling the enzyme with additional subunits (e.g. DNA binding proteins or nucleic acid aptamers) giving the new version of the enzyme additional or improved properties (Elshawadfy et al., 2014, Lahr and Katz, 2009, Bedford et al., 1997). For example, according to the supplier's specifications, the active site of the Bst 2.0 Warm Start was modified by a reversible binding of additional components in order to maintain the enzyme inactive at room temperature. Furthermore, improved performance of the Bst 2.0 have been shown to have a tremendous impact on the overall time of amplification reactions, where over 10 % decrease in TTM values between Bst 1.0 and 2.0 were recorded (data not shown). This work does not substantiate the supplier's claims; Rather than the improved assay performance promised by the supplier, the utilisation of Bst 2.0 Warm Start had a negative impact on the overall performance of both the HCV RT-LAMP-BART and TB RT-LAMP-BART assays. It was previously described that the warm start version of the Bst 2.0 could significantly increase the performance of DNA synthesis under isothermal conditions, as this version of the enzyme would help to control unwanted primer extensions (Tanner and Evans, 2014, Tang et al., 2016). Indeed, we saw an improvement in amplification kinetics of the reactions containing the WS version of Bst 2.0 when compared to the performance

of the Bst Large fragment (**Table 4**). However, the nucleic acid detection of both HCV and TB assays was significantly impaired by the addition of the modified DNA polymerase. It was assumed that the poor performance on RNA amplifications was attributed to the aptamer introduced into Bst 2.0 as this enzyme was demonstrated to amplify efficiently when used in its absence. It was very evident that the aptamer only inhibited the reverse transcription process as the TB DNA assay remained unaffected.

Of all of the DNA polymerases tested, GSP-SSD proved to be the most optimal for the current RT-LAMP HCV assay. This polymerase not only increased the kinetics of the amplification, but also generated far fewer NTCs compared to Bst 2.0. Primer dimerization, is a very well-known cause of such non-template amplification events and when combined with increased enzyme activity, increased rates of non-specific amplification are more likely to occur (Friedberg et al., 2000, Poritz and Ririe, 2014). Despite GSP-SSD higher polymerisation efficiency, priming specificity was maintained, which would tend to contradict Friedberg et al. However, the disparity between the polymerisation efficiency and the observed NTC formation could be contributed to the reduced activity of the GSP-SSD at lower temperatures. In contrast, the Bst 2.0 enzyme is well known to retain partial activity at room temperature which drove the development of Bst 2.0WS. Nonetheless, it is highly likely that an improved RT-LAMP for HCV diagnosis could be developed if the GSP-SSD polymerase is used. Most of polymerases used in isothermal nucleic acid amplifications, utilise enzyme that can either synthesise DNA from DNA templates (DNA polymerases) and enzymes that reverse transcribe RNA into a cDNA (RT enzymes). GSP-SSD as well as other recently developed dual-function enzymes including Bst 3.0 (NEB) or rtTh *Taq* (Cosmo Bio) are unique enzymes, possessing both polymerase activities, which allows initiation of amplification from RNA and recopying of cDNA and higher order amplification products

(Optigene [URL: http://www.optigene.co.uk/reagent_type/dna-polymerase-enzymes/]). GSP-SSD was the most optimal for the RT-LAMP-BART.

Evaluation of three reverse transcriptases was also performed to determine the most suitable enzyme for the RT-LAMP HCV chemistry. As shown in **Figure 28B**, the Maxima RNaseH- was proven to be the most optimal generating significantly faster and more reproducible amplification kinetics regardless of the RNA concentration tested. DNA synthesis via LAMP utilise a displacement polymerase to open up the DNA in preparation for synthesis, unlike PCR that uses denaturing temperatures to melt the double helix. We therefore hypothesised that RNaseH deficient reverse transcriptase's would preserve the original RNA molecule throughout the synthesis process, and increase in performance of the RT-LAMP amplification. Since the original RNA molecule would not be digested during the reverse transcription process, it would remain available for cDNA synthesis throughout the duration of the assay. Utilising these RNaseH negative enzymes could potentially result in an accumulation of cDNA, which would benefit the assay sensitivity. In addition, the inherited ability of LAMP to strand invade and displace, would then ensure production of single-stranded DNA molecules required for the cycling and elongation steps without compromising on the overall performance of the assay. Furthermore, it is well known that the reverse transcriptase enzymes with intrinsic RNAseH activity can prematurely terminate cDNA synthesis as a consequence of template restriction and polymerase pausing (Kotewicz et al., 1988). This could also be the cause of the observed differences in performance between the reverse transcriptases tested.

Comparisons of the Maxima RNaseH- and the Superscript IV showed no significant difference in performance. This was likely due to the fact that both enzymes were deficient in RNase H activity.

However, according to the supplier, the latter had the potential to be highly resistant to a wide range of inhibitory substance and perform better in a wider range of temperatures.

Furthermore, additional optimisation of the HCV LAMP-BART assay involved comparison of two commonly used reaction buffers: Thermopol and Isothermal buffer. As predicted, the reactions containing the isothermal buffer performed significantly faster, generating highly reproducible peaks. However, an increase in NTCs formation was observed when the isothermal buffer was used whereas no non-specific amplifications were detected with the thermopol buffer. The difference in performance could be contributed to the fact that isothermal buffer contains 40 mM more KCl than the thermopol buffer. It has previously been reported that the amount of salt can significantly affect the overall Tm of given primers, where a positive correlation between the concentration and the Tm was described. Since an increase in Tm of given primers, would result in a stronger binding their target, it could also result in a stronger non-specific binding of the primers either to the target DNA or the primers themselves which in turns could lead to an increase in NTCs formation.

3.5 Perspective

This research has demonstrated the importance of not only highly optimised chemistry and the right choice of enzymes but also showed the requirement for choosing RT primers that negotiate RNA secondary structure and polymerases which can adequately displace RNA and DNA molecules in isothermal reactions. This work resulted in a RT-LAMP assay that was highly sensitive and capable of detecting, as little as 40 copies of 5'UTR through the workflow with an analytical LoD of less than 5 cps. Despite this success further evaluations are needed to optimise this assays chemistry and to assess its performance when challenged with RNA extracted from clinical samples, and when challenged with classical polymerase chain inhibitors.

Chapter 4

4 Inhibition of RT-LAMP assays

4.1 Introduction

4.1.1 PCR inhibition

One of the major drawbacks of PCR amplification is its sensitivity to inhibitory substances which can result in either a reduction in the efficiency of amplification or a complete failure in detection (Bustin and Nolan, 2004, Schrader et al., 2012). Thus inhibitory substances pose a real risk, particularly in the field of molecular diagnostics, where an amplification failure can lead to a misdiagnosis and have a direct effect on patients' wellbeing (Huggett et al., 2008, Drosten et al., 2002).

PCR inhibitors' are highly heterogeneous substances that can originate from the tested sample itself or be introduced during sample processing and nucleic acid extraction procedure (Lim et al., 2016, Schrader et al., 2012). Matrixes such as faeces or soil samples, may contain a wide range of inhibitory substances from inorganic salts to more complex organic constituents, such as humic acid. Additionally, many of these inhibitors can be found in a variety of different matrices (Sidstedt et al., 2015, Braid et al., 2003, Bessetti, 2007).

The most well-known and encountered inhibitors are organic compounds such as bile salts, urea, phenol, sodium dodecyl sulphate, collagen, haem, polysaccharides and carrier nucleic acid (Opel et al., 2010, Wilson, 1997, Gieffers et al., 2000). However, commonly found inorganic inhibitors affecting PCR like inorganic salts or calcium ions also affect many isothermal amplification technologies (Gieffers et al., 2000, Bessetti, 2007).

The concentration of these inhibitory compounds play a crucial role in their inhibitory effect. For instance, potassium chloride is widely used for preparation of amplification buffers, however at concentrations exceeding 100 mM it is documented to be inhibitory to PCR and LAMP (Montgomery and Wittwer, 2014, Bessetti, 2007). In addition, collagen and calcium ions are components of connective tissue and bone and are often co-extracted from food samples but only significantly inhibits PCR amplification when their concentration is too great (>8 µg/rxn) to be overcome by the polymerases activity (Opel et al., 2010, Kim et al., 2000, Bickley et al., 1996a).

Isothermal amplification-based assay inhibition has not been as widely studied, although inhibitory effects similar to PCR have been reported. LAMP has been shown to exhibit an increased resistance in inhibition when compared to the standard PCR assays (Kiddle et al., 2012, Edwards et al., 2014).

4.1.1.1 Mechanism of inhibition

Inhibitory substances can interfere with several components of an amplification reaction including nucleic acids, enzymes or other constituents such as Mg ions or dNTPs (Bessetti, 2007). For instance, DNA can be absorbed onto the polymeric surfaces of the reaction tubes used during sample processing and nucleic acid extraction, resulting in a loss of sensitivity due to poorer yields (Butot et al., 2007, Fox et al., 2007). DNA or RNA templates can also be severely degraded by nucleases if the samples were not properly preserved and the extraction procedure failed to remove any such activity (Zhang et al., 2010b, Kreader, 1996a, Wiedbrauk et al., 1995). Thus, many nucleic acid extraction methods include a Proteinase K step in order to ensure the inactivation of any residual nuclease activity originating from the sample (Hilz et al., 1975, Rossen et al., 1992). However, if co-extracted into the final reaction mixture, it can inactivate any enzymatic activity

required to carry out successful amplification reaction (Rossen et al., 1992, Powell et al., 1994, Wilson, 1997, Mertens et al., 2014).

Several publications have reported that phenolic compounds can not only denature polymerases and other protein-based reaction components, but also can cross-link RNA under oxidising conditions and thus impair RNA isolation (Smart et al., 1999, Schrader et al., 2012). In addition, it has also been found that the presence of polysaccharides during purification of sample extracts can significantly reduce the efficiency of RNA re-suspension, affecting the final yield and subsequently reducing detection sensitivity (Sipahioglu et al., 2006, Schrader et al., 2012).

Annealing of the primers have also been reported to be affected by certain inhibitory substances, such as humic acid (HA), that are capable of binding to DNA, thus obstructing the binding sites (Opel et al., 2010). Opel *et al.* (2010) found that primers with higher melting temperatures were less affected by the inhibition, suggesting that the nucleic acid sequence may have a direct effect on inhibition and indicates the competitive nature of nucleic acid hybridisation.

Although amplification inhibition is thought to be the result of many factors, research has mainly focused on the inhibition of DNA polymerase function (Opel et al., 2010, Al-Soud and Rådström, 2001).

To date, a wider range of inhibitory substances affecting DNA polymerases have been characterized and include substance that either affect the enzymatic activity directly by interfering with the template or indirectly via other reaction components (Opel et al., 2010, Schrader et al., 2012, Bessetti, 2007). As mentioned previously, proteases (like proteinase K) and detergents can denature DNA polymerases, RT enzymes and BART components. For instance, urea and phenols have been shown to directly interfere with DNA polymerases by degrading the enzyme whereas

collagen, calcium or haematin inhibit its activity (Opel et al., 2010, Khan et al., 1991, Wilson, 1997). Melanin has been shown to bind to DNA polymerases and RT enzymes in a reversible manner causing competitive inhibition (Opel et al., 2010, Eckhart et al., 2000). Polysaccharides have been found to indirectly affect the activity of DNA polymerases by mimicking DNA structures thus resulting in sequestration of the enzymes (Kiddle et al., 2012, Opel et al., 2010, Schrader et al., 2012). Humic acids have been found to have a dual function as inhibitory compounds (Tebbe and Vahjen, 1993, Opel et al., 2010). Their phenolic structures have been shown to directly bind to the DNA polymerases causing denaturation of the protein. It has also been reported that HA can interact with the templates obstructing amplification reactions causing premature termination or initiation failure by competing for the primer binding sites (Opel et al., 2010, Zipper et al., 2003, Saeki et al., 2011).

Other substances have been found to react with co-factors of DNA polymerases or RT enzymes. High concentrations of calcium ions can compete with magnesium for the binding sites of both proteins, disrupting their ability to carry out their enzymatic reactions (Bickley et al., 1996a, Funes-Huacca et al., 2011). In contrast, tannic acids or bicine can act as a chelating agent and thus deplete the magnesium available (Nakon and Krishnamoorthy, 1983, L. Lawson et al., 2003). Nonetheless in both cases the amount of free magnesium binding to the enzyme is greatly impaired, resulting in a reduction of amplification efficiency or a complete failure.

Nucleic acids themselves can also act to inhibit the amplification of a target. High concentrations of nucleic acid can sequester polymerases and primers, thus inhibiting amplification. This puts an upper limit on the total amount of nucleic acid that can be added to an amplification reaction.

Table 8. Common inhibitory substances and their mode of inhibition encountered during DNA amplification as well as methods of overcoming PCR inhibition.

Substrate(s)	Inhibitor(s)	Mode of inhibition	Facilitator(s)	Reference
Faeces and plants	Bile salts and complex polysaccharides	Interaction with DNA template (sequestration of DNA)	BSA, gp32, sample dilution	(Rouhibakhsh et al., 2008) (Radstrom et al., 2004)
Bones and connective tissues	Collagen	Binds to DNA template	Sample purification, use of less sensitive *Taq* polymerases, addition of Mg^{2+}	(Burkhart et al., 2002) (Opel et al., 2010)
Bones	Calcium ions	Competitive inhibitor of Mg^{2+} required for *Taq* activity	Sample dilution, chelation, addition of Mg^{2+}	(Opel et al., 2010) (Bickley et al., 1996b)
Clothing dyes (e.g. indigo)	Dyes	Affects DNA template by incorporating into DNA structure.	Sample purification,	(Larkin and Harbison, 1999)
Lactoferrin and haemoglobin(Blood)	Iron ions (From lactoferrin and Heamoglobin)	Competitive inhibitor of Mg^{2+} required for *Taq* activity	Sample dilution, chelation, addition of Mg^{2+}	(Radstrom et al., 2004)
Blood	Haem	Binds to *Taq* polymerases causing dissociation of the DNA-polymerase complex	BSA, gp32	(Kreader, 1996b) (Akane et al., 1994)
Hair and skin	Melanin	Binds to DNA	Sample purification, sample dilution	(Opel et al., 2010) (Eckhart et al., 2000)
Soils and bones	Millard Products	DNA trapped in complex polysaccharide-rich matrix (inaccessible to *Taq* polymerases)	Sample purification (repeated silica extraction)	(Alaeddini, 2012)
Environmental samples containing soil	Phenolic compounds (e.g. humic, fulvic and tannic acids)	Chelating with Mg^{2+}, Humic acids have also been reported to directly affect *Taq* polymerases and DNA through sequence specific binding of DNA, reducing the amount of amplifiable template	Retardation of phenolic migration in PVP-containing agarose gel electrophoresis, sample dilution, addition of Mg^{2+}, ion-exchange chromatography,	(Mayer and Palmer, 1996) (Herrick et al., 1993) (Tebbe and Vahjen, 1993) (Tsai and Olson, 1992)
Semen swabs from sexual assaults, microorganisms found in environmental samples	Vaginal microorganisms, non-target DNA	DNA sequestration, reduction of primer concentration by non-specific binding to non-target DNA molecules	Sample dilution, gel filtration,	(Lienert and Fowler, 1992)
Urine	Urea	Denaturation of *Taq* polymerases	Sample dilution, addition of *Taq*	(Abu Al-Soud and Radstrom, 1998)

4.1.2 Current methods of nucleic acid purification for molecular diagnostics assays

Currently most molecular diagnostic kits rely on the quality and purity of extracted DNA or RNA for successful diagnosis of disease (Wink, 2011). Due to the wide range of potentially inhibitory substances present nucleic acid purification has become one of the most routinely used procedures in molecular biology and the diagnostic field (Rudi and Jakobsen, 2006, Niemz et al., 2011). In general, every nucleic acid extraction procedure known to date, can be divided into four main steps: 1) cell disruption; 2) removal of protein and lipid membranes, other cell components and non-target nucleic acid; 3) binding/purification of the target nucleic acid and 4) nucleic acid release and concentration (Tan and Yiap, 2009).

Cell disruption is the break down the membranes and cell walls enabling release of the cell content and can be achieved via either physical or chemical means (Tan and Yiap, 2009, Brown and Audet, 2008). Disruption procedures vary and are often dependent on the type of sample used where physical methods might be more suited than chemical means, and *vice versa*. For instance, many nucleic acid extraction kits from plant tissue involve physical cell disruption step such as grinding, due to the highly resistant cellulose-based cell wall (Tsugama et al., 2011). In contrast, most purification methods used for nucleic acid extraction from blood or cell cultures involve chemical lysis to prevent shearing of the target (Robe et al., 2003). Those methods often combine chemical lysis using detergents such as sodium dodecyl sulphate (SDS), chaotropic agents like salts and enzymes as well as elevated temperatures to facilitate the process (Tan and Yiap, 2009, Krsek and Wellington, 1999).

In most cases, cell disruption and the break down of cellular debris and protein occurs simultaneously, where one reaction component might be suitable for both steps. Proteinases have been widely used to facilitate not only disintegration of the cell membranes by disrupting protein components, but also to liberate nucleic acids from their protective protein coating such as histones (Goldenberger et al., 1995). Lithium dodecyl sulphate (LDS) has also been used

commercially to improve cell lysis as well as inactivate cellular nucleases ensuring the integrity of the extracted nucleic acids (Cook, 1984)(ERBA Molecular, UK).

The Phenol/chloroform method is one of the oldest techniques in molecular biology for the purification of nucleic acids (Chomczynski and Sacchi, 1987, Sambrook and Russell, 2006). The technique/methodology takes advantage of the differences in the solubility of DNA, RNA, protein and other cellular components. In principle, due to the organic hydrophobic nature of phenol-chloroform mixture, once mixed with aqueous solution containing cellular lysates, two distinct phases are formed upon centrifugation. The upper aqueous phase contains the cellular nucleic acids and other soluble components, whereas the bottom organic phase consists mostly of hydrophobic lipids and precipitated proteins (**Figure 31**). Furthermore, by modulating the pH of the aqueous phase, either a total pool of nucleic acid can be extracted or a preferential purification of RNA can be performed in acidic conditions.

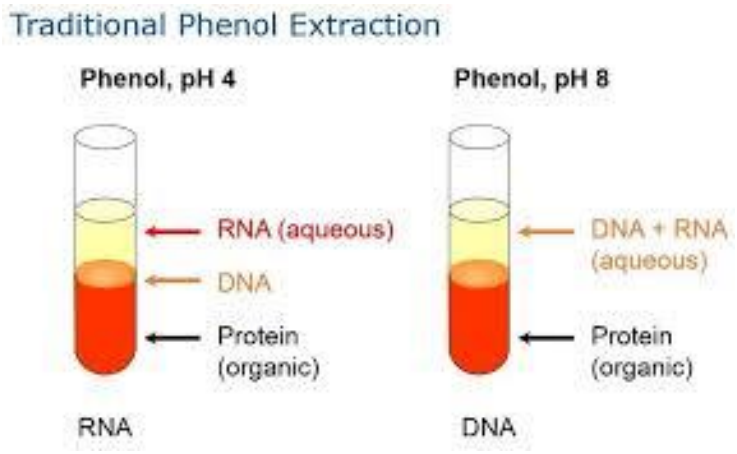

Figure 31. Graphic representation of phenol:chloroform nucleic acid purification procedure.

Source: https://www.genetargetsolutions.com.au/product/5prime-phase-lock-gel/

However, due to the time consuming and toxic nature of this technique, phenol/chloroform extraction is no longer the method of choice in molecular diagnostics (Lahiri and Nurnberger Jr, 1991, Tan and Yiap, 2009).

Most of the currently used purification kits rely on binding of DNA or RNA to a solid matrix, such as silica membranes, followed by various wash steps introduced to remove protein, cellular debris and inhibitory substances (Vandeventer et al., 2012). Many industry standard kits (Qiagen) utilise spin columns with a silica based sieve to capture nucleic acids of certain size during the centrifugation process followed by nucleic acid release using various reconstitution buffers (**Figure 32**). Other methods employ magnetic beads coated with silica matrix enabling automation of the entire sample preparation procedure, greatly reducing the risks of sample contamination as well as increase productivity and throughput (MagJET, ThermoFisher; MagAttract, Qiagen) (Berensmeier, 2006).

Although such methods have been proven to be extremely useful, depending on a sample type used, they might pose severe disadvantages. For instance, extraction of total nucleic acid carried out by either spin columns of silica based magnetic beads, from sputum samples may cause severe inhibition of RNA detection due to significant content of non-target DNA or RNA (He et al., 2017, Adams et al., 2015).

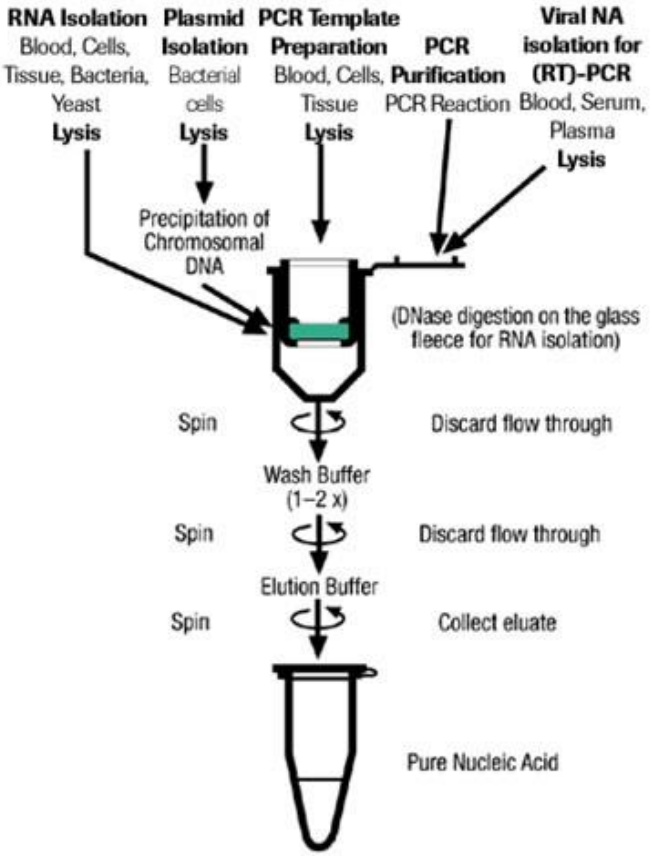

Figure 32. Graphic representation of a typical spin-column based nucleic acid purification technique.

Source: https://shop.roche.com/wcsstore/RASCatalogAssetStore/Articles/HTML%20Articles/High-Pure-Technology.html

Thus, some researchers prefer a more selective method of nucleic acid purification offered by capture probes. In general, a capture method involves labelling of a solid phase with an oligonucleotide probe that is complementary to the target of interest. Thus the vast majority of extracted nucleic acid consists of the target of interest by ensuring conditions favouring hybridisation **(Figure 33).** While this method generates lower yields, the specificity of the target extraction have been reported to significantly increase the overall sensitivity of a diagnostic assay, particularly in the samples containing large amounts of non-target nucleic acids.

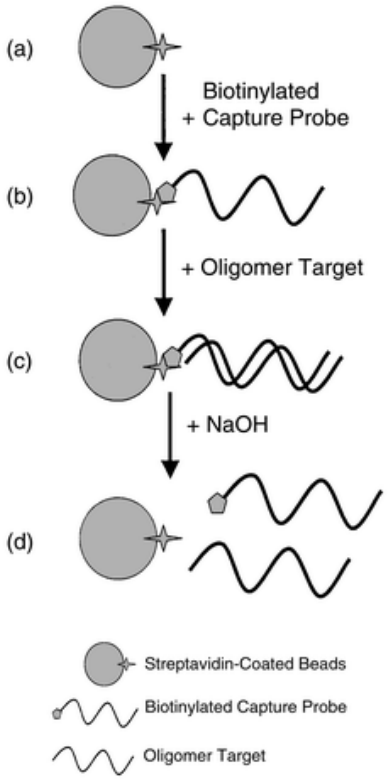

Figure 33. Graphic representation of a magnetic bead with capture probes- based nucleic acid purification methods.

Source: http://pubs.rsc.org/en/content/articlelanding/2001/an/b106343j/unauth#!divAbstract

4.1.3 Summary

Although co-extraction of inhibitory substances and their mode of DNA polymerisation inhibition have been widely studied and reported throughout the literature, little is known about the effects of those substances on the reverse transcription, a key step in most RNA detection kits.

Furthermore, nucleic acid extraction procedures have been reported to significantly improve the quality and purity of isolated nucleic acid. However, since different types of samples such as faeces, blood or sputum can significantly differ in their biochemical composition, a careful consideration should be taken as to what nucleic acid extraction procedure is most suitable.

4.2 Aims and objectives

The main focus of this study was to determine the inhibitory effects of key components of sample preparation chemistries associated with the extraction of DNA or RNA from samples. In particular, the work focused on in-house technologies for the extraction of TB, HIV, HBV and HCV where the associated buffers had potassium and sodium salts and LDS as key components. Further, the nature of the clinical samples means that significant amounts of non-target nucleic acids could be present. The aim was to quantify the effects of these substances on the RT-LAMP assay using HCV and TB model assays.

4.3 Results

4.3.1 Effects of inhibitory substances on the performance of nucleic acid amplification

Co-extraction of inhibitory substances during nucleic acid purification is the most common cause of amplification failure when a sufficient amount of the target template is present. However, the choice of DNA polymerase and RT enzyme or the nature of the target and the detection method can react to inhibitory substances differently.

4.3.1.1 Effects of sample-prep derived inhibitors on the performance of NAAT assays.

In this study, the effects of various components of the in-house developed nucleic acid purification method(s), on the performance of TB detections, was assessed.

Figure 34 shows LAMP-BART profiles generated using a standard TB assay challenged with various amounts of LDS detergent according to the protocol 9 (see **Appendix 9**).

As expected, the TB assay was inhibited by the presence of LDS detergent (**Figure 34B-C**). However, unlike most inhibitory substances, LDS affected the amount of light emitted to a much higher extent than the amplification itself, and is reflected by a reduction in peak heights. At 0.05 % LDS, the amount of emitted light was reduced by over 50 %, in comparison with the non-inhibited samples, without significantly affecting the average TTM for the reactions containing 1000 copies of the TB target RNA (*p value* > 0.05, t-test) (**Figure 34A and C**) (**Table 9**). In addition, an apparent decline in the base line was observed at 0.05 % LDS, suggesting that BART was affected/ inhibited irrespective of the DNA polymerase and RT performance.

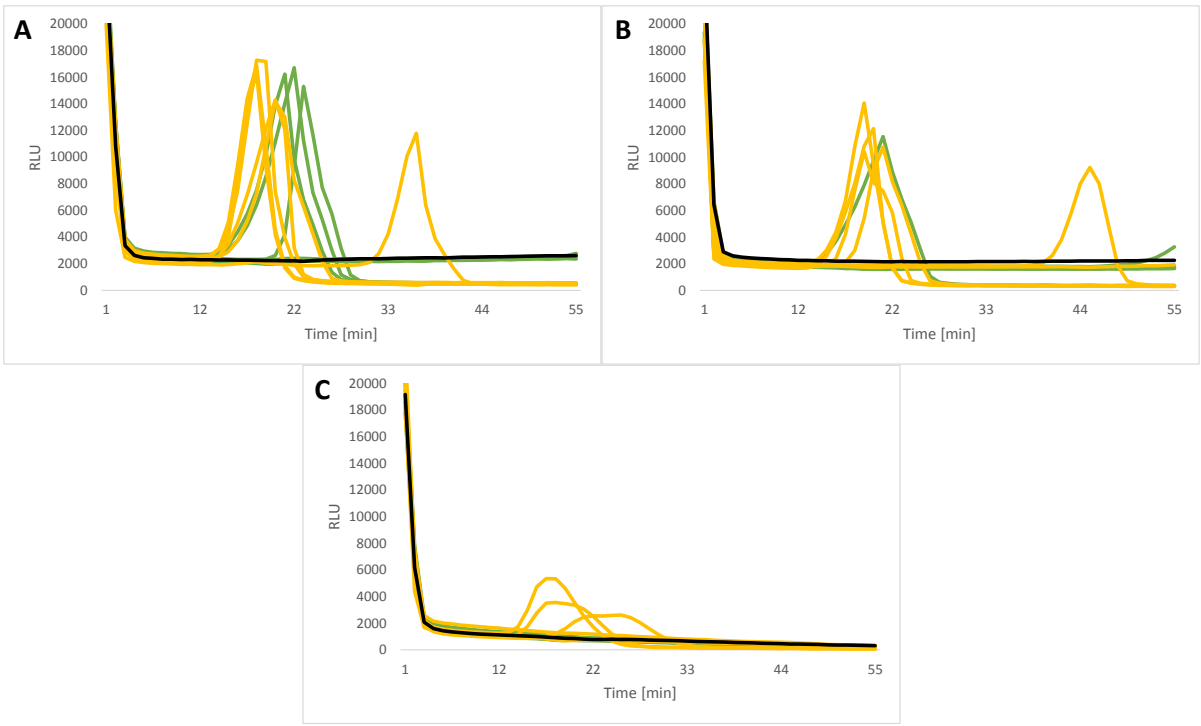

Figure 34. LAMP-BART profiles generated using the TB assay model system and various amounts of *M. bovis* positive control 23s rRNA. A – amplification profiles generated with non-inhibited reactions; B – amplification profiles generated with reactions containing 0.01 % LDS; C – amplification profiles generated with reactions containing 0.05 % LDS.

Note: orange curves correspond to the reactions containing 1000 cps of the target; green curves show reactions containing 100 cps of the target; black curves represent NTC (No template control)

Table 9 showing summary of the data presented in the **figure 34**. Each set of reactions was analysed using average TTM (Mean), reproducibility (STDev) and sensitivity (Amp.Freq).

LDS [%]	TB RNA [cp/rxn]	TTM [min]	Stdev	Amp.Freq. [%]
0%	1000cp	22	7	100
	100cp	22	1	50
0.01%	1000cp	25	11	83
	100cp	21		17
0.05%	1000cp	20	5	50
	100cp			0

As previously shown in this study, buffers can affect amplification kinetics (p. 94) and different amplification chemistries can significantly affect the performance of nucleic acid synthesis or NTC formation. However, the choice of reaction buffer can modulate the inhibitory effect of LDS on assay kinetics.

Figure 35 shows LAMP-BART profiles generated using a modified TB protocol where either 12.5 or 125 mM bicine buffer was used in the absence of both loop primers.

Similarly to the previous LDS inhibition data (p. 115), the addition of 0.05 % LDS to the TB reactions caused a significant reduction in light emission without affecting the average TTM, regardless of the buffer used (*p value* > 0.05, t-test) (**Figure 35E**). The characteristic decline of the base line was also observed in the challenged samples confirming the previous findings. Nonetheless, when the average peak heights of the challenged and un-challenged samples were compared, the inhibitory effect of LDS was more apparent in the reactions utilising the 12.5 mM bicine buffer. However, it was also observed that the non-inhibited reactions containing the 12.5 mM bicine buffer generated less light than those with the higher concentration of bicine thus a direct comparison between the two buffers could not be performed. Nevertheless, the relative difference in light emission, between the two buffers with either presence or absence of inhibition, revealed interesting effects of buffering on the impact of LDS on BART (**Table 10**).

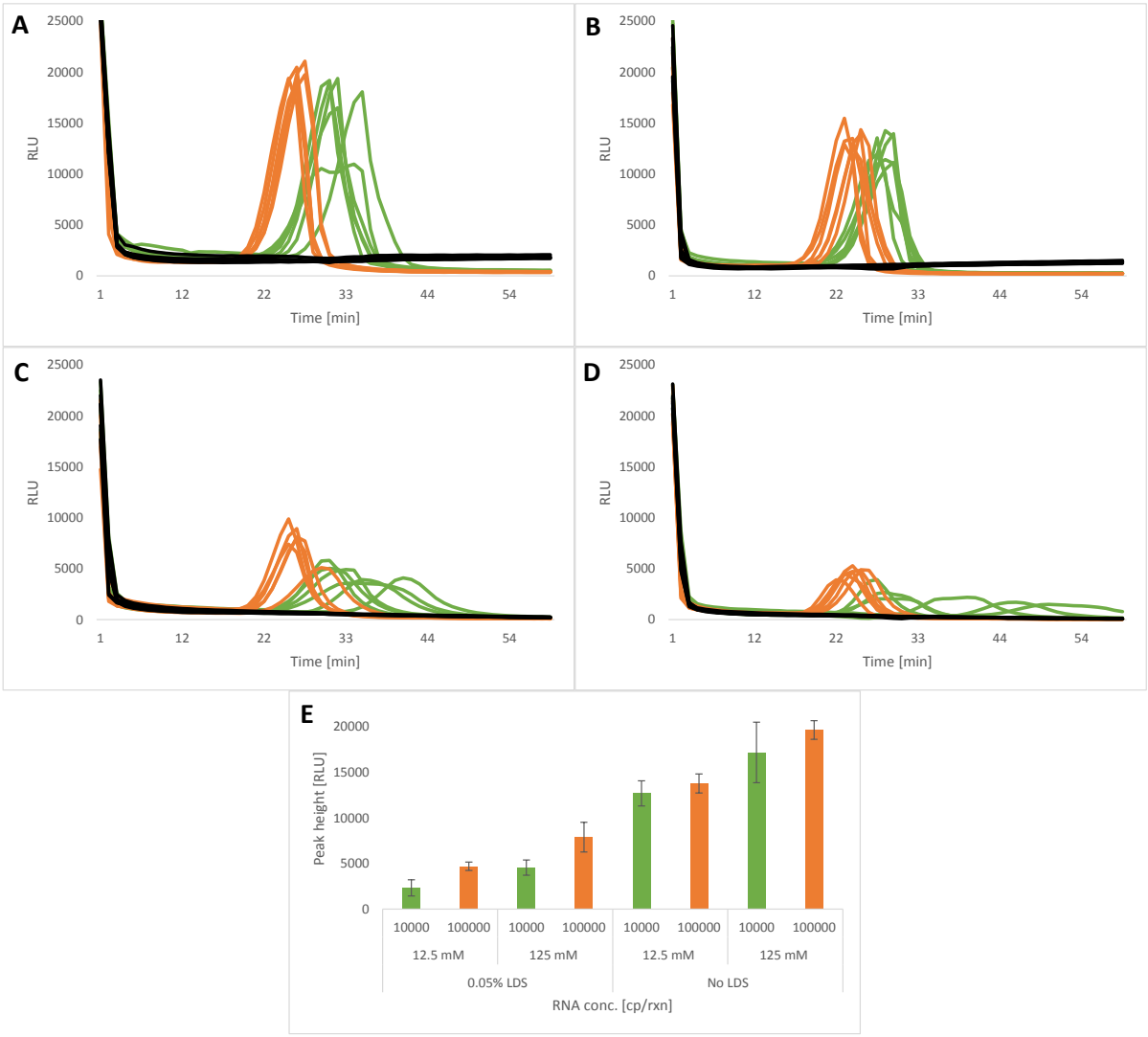

Figure 35. LAMP-BART profiles and summary bar charts generated using the TB assay model system various amounts of *M. bovis* positive control 23s rRNA under two different buffering chemistries.

A – amplification profiles generated with non-inhibited reactions and 125 mM 1x Bicine buffer; B – amplification profiles generated with non-inhibited reactions and 12.5 mM 1x Bicine buffer; C – amplification profiles generated with reactions containing 0.05 % LDS and 125 mM 1x Bicine buffer; D – amplification profiles generated with reactions containing 0.05 % LDS and 12.5 mM 1x Bicine buffer; E – bar chart showing the effects of LDS and chosen reaction buffers on the average peak height.

Note: orange curves correspond to the reactions containing 100000 cps of the target; green curves show reactions containing 10000 cps of the target; black curves represent NTC (No template control)

Table 10 showing summary of the data presented in the **figure 35**. Each set of reactions was analysed using average TTM (Mean), reproducibility (STDev) and sensitivity (Amp.Freq) (**A**) as well as light emission (RLU) (**B**).

A

Inhibitor	Bicine Buffer	RNA conc. [cp/rxn]	Mean [min]	Stdev	Amp.Freq.[%]
0.05% LDS	12.5 mM	10000	39	9.7	83
		100000	24	1.2	100
	125 mM	10000	34	3.6	100
		100000	27	1.6	100
No LDS	12.5 mM	10000	29	1.0	100
		100000	25	1.0	100
	125 mM	10000	33	1.8	100
		100000	27	0.8	100

B

Inhibitor	Bicine Buffer	RNA conc. [cp/rxn]	Mean [RLU]	Stdev
0.05% LDS	12.5 mM	10000	2335	882.4
		100000	4700	461.7
	125 mM	10000	4561	840.9
		100000	7897	1622.6
No LDS	12.5 mM	10000	12703	1371.8
		100000	13785	1045.5
	125 mM	10000	17190	3323.5
		100000	19653	1018.9

In the non-inhibited samples utilising 100,000 copies of the target TB RNA, the average peak height generated by 125 mM bicine was 1.4 x higher than those with the low bicine. Similarly, when the reactions containing 10,000 copies of the target were assessed, in the absence of the inhibitor, the reactions utilising the 125 mM bicine produced peaks 1.35 x brighter. However, when the challenged samples were evaluated, the reactions containing 125 mM bicine buffer generated 1.7 and 1.95 x brighter peaks than those utilising lower bicine for 100,000 and 10,000 copies of the target RNA, respectively.

In this study, the effects of three inorganic salts; sodium chloride, potassium chloride and potassium acetate, were assessed on the performance of nucleic acid amplification. **Figure 36** shows LAMP-BART profiles generated using HCV RNA assay challenged with various amounts of potassium chloride and potassium acetate, in addition to salts already present in the assay. The assays were prepared according to the protocol 6 (see **Appendix 6**).

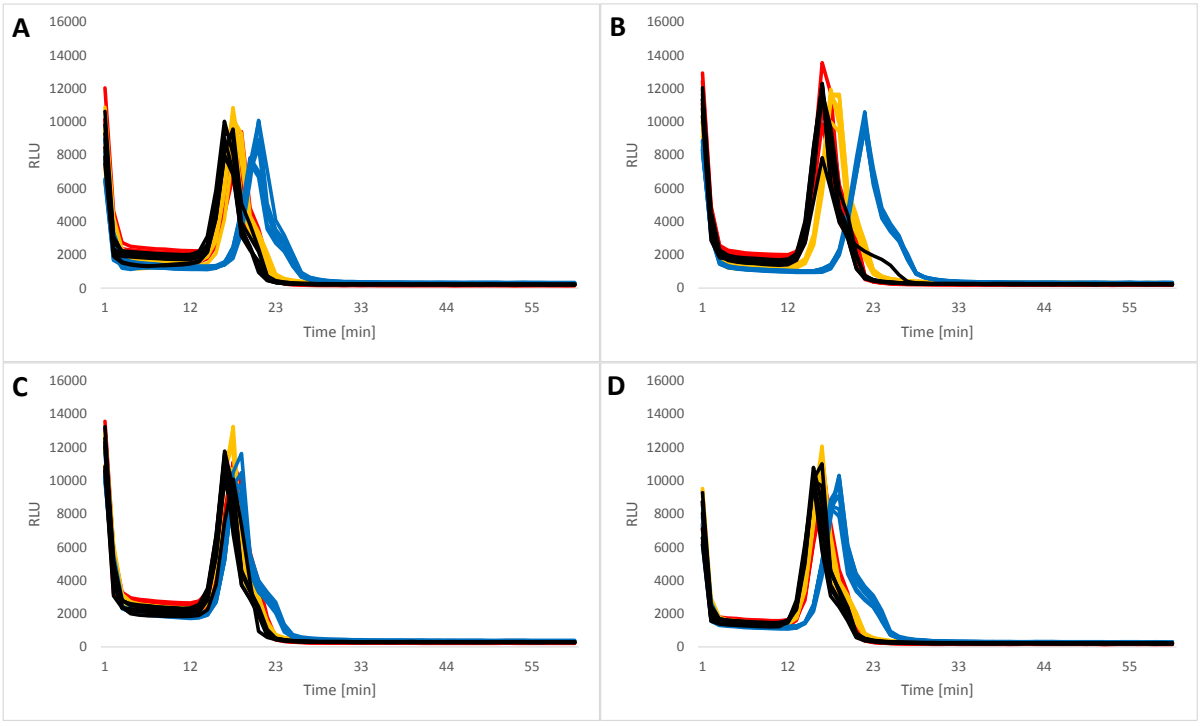

Figure 36. LAMP-BART profiles generated using the HCV assay model system, 2000 cps of HCV 5'UTR RNA fragments and two chosen DNA polymerases challenged with various amounts of KCl and KAc.

A – amplification profiles generated with reactions containing Bst 2.0 and various amounts of KCl; B – amplification profiles generated with reactions containing GSP-SSD and various amounts of KCl; C – amplification profiles generated with reactions containing Bst 2.0 and various amounts of KAc; D – amplification profiles generated with reactions containing GSP-SSD and various amounts of KAc.

Note: red curves correspond to the non-inhibited reactions; black curves show reactions containing 10 mM additional potassium salt; orange curves represent reactions containing 31.25 mM additional potassium salt; blue curves shows reactions challenged with 50 mM additional potassium salt.

Inhibition of the nucleic acid synthesis was observed for both assays regardless of the inhibitor used. The reactions utilising the DNA polymerase GSP-SSD were more sensitive to higher concentrations of the salts tested (**Table 11**). However, the inhibition coming from potassium chloride (KCl) affected these assays to a much higher extent when compared to the reactions containing potassium acetate (KAc). A 5 minute increase in TTM was observed when 50 mM of KCl was added whereas only 2 minute difference was detected in the reactions containing 50 mM of the KAc salt. In contrast, only 3 and 2 minute increases in TTM was detected in the reactions containing the Bst 2.0 DNA polymerase, when challenged with the same amounts of the KCl and KAc salts, respectively (**Table 11**).

Interestingly, the addition of 10 mM of either salt improved the speed of the assay, when utilising the Bst 2.0 DNA polymerase, by at least one minute. However, a similar improvement on the amplification speed of the assay containing the GSP-SSD DNA polymerase was only seen upon the addition of 10 mM KAc.

Table 11 showing summary of the data presented in the **figure 6**. Each set of reactions was analysed using average TTM (Mean), reproducibility (STDev) and sensitivity (Amp.Freq). Note that the concentrations of the tested potassium salts shown, correspond to the amounts of additional salt added, not the final concentration used in the assay (Isothermal buffer used contained 50 mM KCl at 1x concentration).

DNA pol	Salt conc. [mM]	Mean [min]	STDev	Amp. Freq. [%]	Inhibitor
Bst2.0	0	17	0.44	100	KCl
	10	16	0.44	100	
	31.25	17	0.44	100	
	50	20	0.55	100	
GSP-SSD	0	16	0.00	100	
	10	16	0.00	100	
	31.25	17	0.44	100	
	50	21	0.00	100	
Bst2.0	0	17	0.00	100	KAc
	10	16	0.44	100	
	31.25	17	0.44	100	
	50	18	0.59	100	
GSP-SSD	0	16	0.00	100	
	10	15	0.44	100	
	31.25	16	0.00	100	
	50	18	0.56	100	

Furthermore, the initial assessment of the effects of sodium chloride on the HCV assay performance revealed similar responses to inhibition when GSP-SSD and Bst 2.0 DNA polymerases were tested.

Figure 37 shows LAMP-BART profiles generated using HCV assay utilising either Bst 2.0 or GSP-SSD DNA polymerases, challenged with various amounts of sodium chloride, again in addition to the salt already present within the assay.

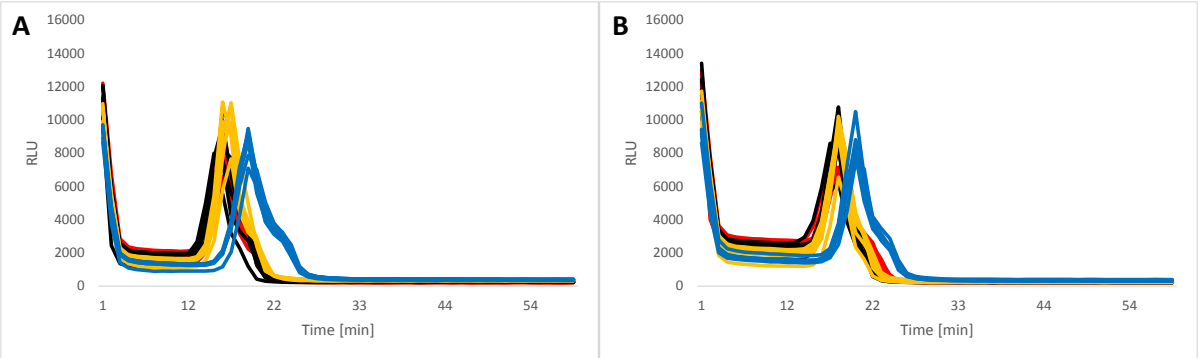

Figure 37. LAMP-BART profiles generated using the HCV assay model system, 2000 cps of HCV 5'UTR RNA fragments and two chosen DNA polymerases challenged with various amounts of NaCl.

A – amplification profiles generated with reactions containing GSP-SSD and various amounts of NaCl; B – amplification profiles generated with reactions containing Bst 2.0 and various amounts of NaCl;

Note: red curves correspond to the non-inhibited reactions; black curves show reactions containing 10 mM additional potassium salt; orange curves represent reactions containing 30 mM additional potassium salt; blue curves shows reactions challenged with 50 mM additional potassium salt.

The assay when utilising the DNA polymerase GSP-SSD was more sensitive to the tested salt, as the addition of 30 mM NaCl resulted in an increase in TTM by at least 1 minute. In contrast, no sign of inhibition was observed for the reactions using Bst 2.0 when 10-30 mM of sodium chloride (NaCl) was added. In addition, a 3 minute increase in TTM was observed when 50 mM of NaCl was added to the reactions containing the GSP-SSD enzyme, whereas only 2 minute difference was detected in the reactions utilising Bst2.0 when compared to the non-inhibited samples (p *value* < 0.05, t-test)(**Table 12**).

In contrast to the previous experiment, addition of 10 mM NaCl did not result in improvement in the assay kinetics, regardless of the DNA polymerase used.

Table 12 showing summary of the data presented in the **figure 37**. Each set of reactions was analysed using average TTM (Mean), reproducibility (STDev) and sensitivity (Amp.Freq). Note that the concentrations of the tested NaCl shown, correspond to the final concentration used in the assay.

DNA pol.	Salt conc. [mM]	Mean [min]	STDev	Amp. Freq. [%]	Inhibitor
Bst2.0	0	18	0.55	100	NaCl
	10	18	0.00	100	
	30	18	0.00	100	
	50	20	0.00	100	
GSP-SSD	0	16	0.00	100	
	10	16	0.57	100	
	30	17	0.55	100	
	50	19	0.00	100	

4.3.1.2 Effects of sample-derived inhibitors on the performance of NAAT assays.

In this study the effect of variety of different inhibitory substances, found in blood and sputum, on the performance of NAAT assays, was assessed. In particular we looked at non target nucleic acids commonly abundant in most samples.

Figures 38 show LAMP-BART profiles generated using the TB RNA and DNA assays challenged with various amounts of carrier DNA (salmon sperm DNA).

As expected, all assays managed to detect the target, regardless of the type of nucleic acid tested. However, full detection was seen only when *M. bovis* gDNA was used at 1000 and 100 copies. In the non-inhibited samples, a slight reduction in sensitivity was detected when RNA was used for amplification. At 100 copies of the target RNA only 5 out of 6 replicates showed positive amplification profiles whereas full detection was observed when DNA template was used. Moreover, similarly to our previous data, an increase of 2-3 minute in TTM was observed in the assays containing the positive control RNA when compared with the same reactions utilising gDNA target.

Furthermore, addition of 1000 ng of carrier DNA caused severe inhibition of the TB assay regardless of the type of template used. However, the RNA assay was observed to be far more sensitive to inhibition than the reactions utilising gDNA as the template for amplification.

Firstly, the presence of carrier DNA significantly impeded the amplification of gDNA (*p value* < 0.05, t-test). On average, a 3 and 7 minute delay in detection was observed in the challenged reactions containing 1000 and 100 copies of the DNA target, respectively (**Table 13**). However, no effects on the assay sensitivity was observed, even at limit of detection of 100 copies of the gDNA.

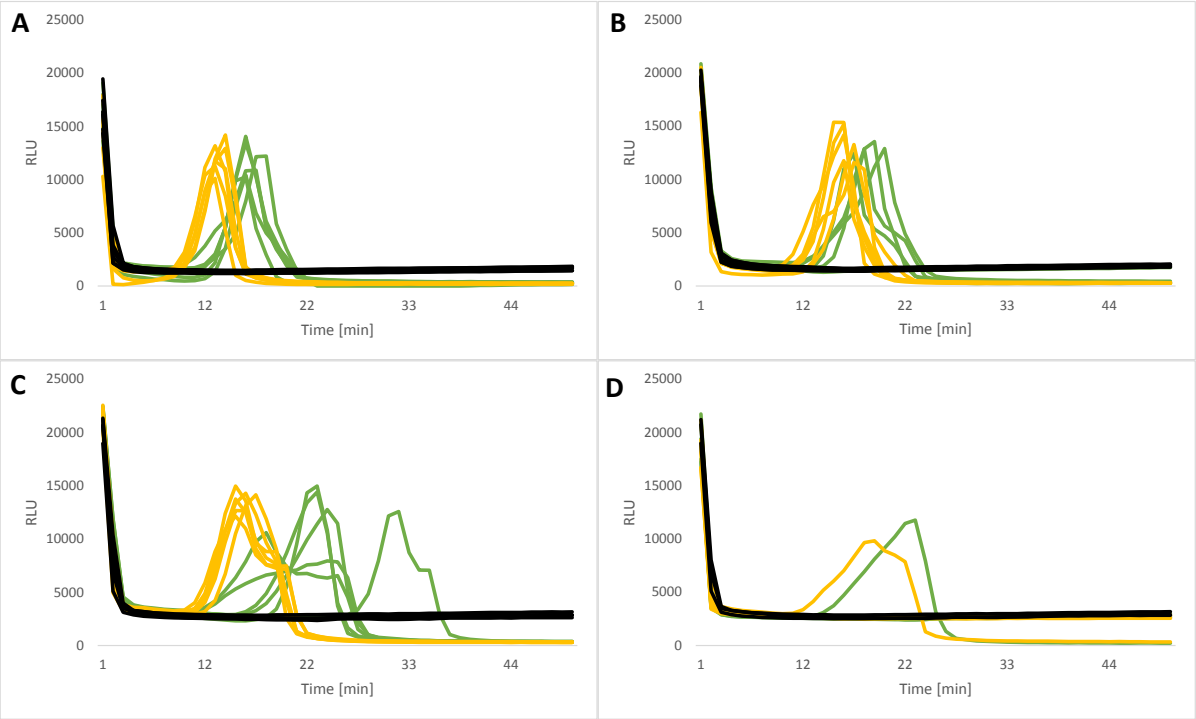

Figure 38. LAMP-BART profiles generated using the TB assay model system and various amounts of *M. bovis* positive control 23s rRNA or genomic DNA (gDNA). A – amplification profiles generated with non-inhibited reactions containing gDNA template; B – amplification profiles generated with non-inhibited reactions containing 23s rRNA template; C – amplification profiles generated with reactions containing gDNA template and 1000 ng of salmon sperm carrier DNA; D – amplification profiles generated with reactions containing 23s rRNA template and 1000 ng of salmon sperm carrier DNA.

Note: orange curves correspond to the reactions containing 1000 cps of the target; green curves show reactions containing 100 cps of the target; black curves represent NTC (No template control)

Table 13 showing summary of the data presented in the **figure 38**. Each set of reactions was analysed using average TTM (Mean), reproducibility (STDev) and sensitivity (Amp.Freq).

Template	Carrier DNA [ng/rxn]	NA conc. [cp/rxn]	TTM [min]	Stdev	Amp. Freq. [%]
gDNA	0 ng	1000 cps	13	0.6	100
	1000 ng	1000 cps	16	0.9	100
	0 ng	100 cps	17	0.9	100
	1000 ng	100 cps	24	4.5	100
rRNA	0 ng	1000 cps	16	0.8	100
	1000 ng	1000 cps	19		17
	0 ng	100 cps	19	1.4	67
	1000 ng	100 cps	24		17

Nonetheless, the overall performance of the DNA assay was noticeably impaired due to both, reduction in amplification speed and reproducibility at 100 copies.

Secondly, carrier DNA had similar effects on amplification speed and sensitivity when the target nucleic acid was RNA rather than gDNA. However, the observed inhibition was far more severe than that of the previously showed DNA assays.

Similarly to the DNA assays, addition of the carrier DNA caused significant amplification delays, regardless of the amount of target TB RNA used ($p\ value < 0.05$, t-test). On average, 3 and 7 minute delays in detection were observed when 1000 and 100 copies of the target RNA was used. However, unlike the inhibition of the TB DNA assays, the sensitivity of RNA detection in the presence of the carrier DNA was greatly reduced, regardless of the amount of template used. At both 1000 and 100 copies of the target, only 1 out of 6 replicates showed positive amplification profiles when challenged with the inhibitor.

Note that full detection of 100 copies of the target RNA, in the non-inhibited conditions, was not achieved. Nonetheless, clear reduction in the assay sensitivity was still observed when compared to the non-inhibited reactions.

4.4 Discussion

Amplification inhibitors are highly heterogeneous substances that can act on different components of a diagnostic test leading to either reduction in the sensitivity of the assay or a complete amplification failure (Bessetti, 2007, Zhang et al., 2010b, Schrader et al., 2012, Huggett et al., 2008, Speers, 2006). For instance, we showed that both the carrier DNA and LDS could reduce the overall sensitivity of the TB assay leading to a number of false negative results. However, the observed inhibitory mechanism differed significantly between the two tested substances. LDS showed to have no effect on the speed of amplification, regardless of the amount of template and inhibitor used. We suggest LDS interferes with the BART components rather than the polymerisation reaction, since a significant reduction in the light output was detected in the inhibited samples. It is likely that the observed inhibition of light was a direct result of the sensitivity of the Luciferase enzyme to either LDS or pH changes caused by the detergent (Kitayama et al., 2003, Gabriel and Viviani, 2014, Imani et al., 2010).

In contrast, carrier DNA caused significant delays in amplification of the target *M. bovis* RNA without affecting the light emission. Although, the presence of high amounts of non-target DNA is unlikely to directly interfere with the enzymatic properties of the polymerases or RT enzymes, it has been reported that sequestration of enzymes and primers onto non-target templates can significantly reduce assay performance (Kiddle et al., 2012, Morata et al., 1998, Rohrman and Richards-Kortum, 2015). In addition, several researchers have shown that DNA molecules can bind magnesium ions in order to stabilise their own structure, therefore resulting in a reduction of the amount of free magnesium available for DNA polymerase and RT enzyme activity (Robinson et al., 2000, Serec et al., 2016).

Furthermore, we have also demonstrated that the assay chemistry and the type of target nucleic acid can impact the inhibitory effects of certain substances such as LDS or carrier DNA. LDS was showed to reduce the overall light emission by 60 % in the reactions utilising the 125 mM

1x bicine buffer. In contrast almost 70 % reduction in the light intensities was observed in the samples containing the 12.5 mM 1x bicine buffer. Since LDS is a highly potent acidic detergent, the most likely explanation for the observed behaviour of BART could be simply associated with a lower buffering capacity of the 12.5 mM bicine buffer. Nonetheless, our data indicates that the choice of reaction chemistries can play a key part in the extent of inhibition.

Furthermore, our analysis on the effects of carrier DNA on amplification of both DNA and RNA templates, revealed interesting correlations between the type of nucleic acid and the degree of inhibition coming from non-target nucleic acids. Although, carrier DNA inhibition has been widely reported across the literature, limited consideration have been made in regards to the effects of such contaminants on RNA assays. We demonstrated that despite a significant increase in the TTM of the reactions containing genomic *M. bovis* DNA, the presence of carrier DNA had no effect on the overall assay sensitivity, regardless of the amount of template used for each reaction. In contrast, almost 90 % reduction in detection was observed when the *M. bovis* rRNA target was being amplified in the presence of the same inhibitor and inhibitor load.

Reverse transcription, a crucial step in most RNA detection systems, has been reported to be a less efficient process when compared to the DNA synthesis step (Bustin and Nolan, 2004, Sanders et al., 2013). Thus, one can conclude that inhibitory substances can further impact this process. As mentioned previously non-target DNAs can sequester primers and enzymes including RTs thus further reduce the efficiency of reverse transcription. In addition, RT steps have been reported to have an increased requirement for magnesium ions, thus can be highly sensitive to changes in the amounts of available free magnesium (Goldschmidt et al., 2006). Consequently, the choice of nucleic acid purification method can have a significant effect on the performance of the downstream detection. As mentioned previously, more a selective purification using target capture technology, could prevent RT inhibition by favouring

extraction of the target RNA over other carrier nucleic acids (Chandler et al., 2000, Wu et al., 2015).

Furthermore, we showed that not only the type of inhibitory substances present but also its concentration are key elements of the overall potency of the inhibitory effect. As an example, we showed different responses of our model HCV assay to certain salts such as NaCl, KCl or KAc. We showed that all assays containing greater than 100 mM of total salt were significantly inhibited, regardless of the type of salt tested. However, when 10 mM additional salt (total 60 mM) of either KCl or KAc was added to the assays, a noticeable improvement of the amplification speed was observed. Since KCl and similarly KAc, have been reported to stabilise the primer-template interaction by reducing the repulsion of negatively charged DNA backbones, one could conclude that the observed improvement was caused by optimisation of this effect through increasing of the salt concentration. However, whilst optimal salt concentration can facilitate primer binding and therefore improve the initiation step of amplification reactions, greater salt amounts have also been shown to significantly increase the Tm of longer DNA molecules. Although, higher salt concentrations have been shown to be beneficial when very short sequences are targeted, it can also impede primer invasion due to increased stability of DNA helixes and secondary structure of RNA molecules (de Vega et al., 2010). Moreover, the counter ion chlorine has also been suggested to negatively affect DNA polymerases by binding to their active sites, leading to temporary inactivation and thus resulting in impaired binding to the target templates.

4.5 Perspective

Although, we demonstrated different nature of chosen inhibitory substances and their effects on detection of DNA and RNA templates, our amplification models have not been challenged with some key inhibitory substances commonly found in biological samples such as haem or heparin, due to time limitations. Moreover, since RT assays rely on the performance of both DNA polymerases and RT enzymes, the observed inhibitory effects were most likely a combined inhibitory effect of the two enzymes rather than solely contributed to the RT efficiency.

In addition, since very little is known about the direct effects of inhibitory substances on reverse transcriptases, it would be of great benefit to screen a wider range of inhibitors in regards to their effects on different RTs.

Moreover, it has been reported in this study, that assay chemistry could potentially affect the potency of certain inhibitors, thus it is recommended to further test this hypothesis using a wider range of buffers including Thermopol and Isothermal buffers (NEB, UK).

Chapter 5

5 Development of internal amplification controls for RT-LAMP assays

5.1 Introduction

During the last 20 years, nucleic acid purification technologies have advanced dramatically, resulting in significant improvements that affect the reliability of down-stream applications that are dependent upon quality preparations (Tan and Yiap, 2009). Despite these improvements. co-extraction of inhibitory substances affecting nucleic acid amplifications (NAAT) and reporter chemistries can still occur (Bessetti, 2007, Bickley et al., 1996a, Funes-Huacca et al., 2011, Opel et al., 2010). Thus, it has becoming more common to control polymerised chain reactions by qualifying the inhibitory nature of the extracted samples in order to eliminate the risks of misdiagnosing false negative amplifications (Hoorfar et al., 2004b, Hoffmann et al., 2006).

In any NAAT-based diagnostic approach, a negative result could be unreliable if such an inhibitor control is not included in the test; as this result could be due to amplification failure caused by inhibitory substances, sub-optimal amplification efficiency, problematic detection chemistries, or faulty equipment (Rådström et al., 2008). In general, amplification controls (IACs) should consist of a pre-defined input copy number of nucleic acid or microorganism, and the amplification should run in parallel with the true positive (Rosenstraus et al., 1998, Hoorfar et al., 2004b, Malorny et al., 2003). By comparing the detection parameters of these controlled amplifications, with those performed under non-challenged conditions, an estimation of the inhibitory nature of the samples can be made. In practice, two main types of controls can are used – external and internal amplification controls (Lion, 2001).

The external control is added at the very start of the sample preparation and purification process. Thus, controlling the extraction processes such as cell lysis, nucleic acid binding and recovery, as well as the amplification (Kalle et al., 2013). External controls for microorganisms can be 'synthetic mimics' comprising of encapsulated nucleic acid (such as Armoured RNA or DNA), that resemble the true target organism, and are extracted from the same matrix (Meng and Li, 2010, Yu et al., 2008, Pasloske et al., 1998). These controls are used to simplify a single-tube assay design and reduce the complexity of primer design (often a problem encountered for IAC) and the risks of potential, unwanted interactions (Hoorfar et al., 2004b). The external controls can be extremely beneficial for evaluating integrated workflows of diagnostic assays, where sample preparation, nucleic acid purification and detection are performed in a single module / device or consumable (Hata et al., 2011). However, these controls provide no information with respect to the cause of potential detection failure.

In contrast, internal amplification controls (IACs), are added to the amplification chemistry, and control for the amplification and its detection. The IAC, therefore gives meaningful information about the cause of amplification failure and can be used to effectively judge the nature of inhibition with respect to the sample and its effect on the polymerase activity. There are currently two main strategies adopted for use of IACs in molecular diagnostic assays, and each depends on the level of competition between the target diagnostic chemistry and the detection of IAC targets.

5.1.1 Competitive vs. non-competitive IAC systems

Generally, a non-competitive IAC system relies on separate primer sets targeting the IAC template and the target of interests, and can be performed together with the target amplification or in a separate tube (Selvey et al., 2001). Some commercial platforms, such as Illumigene, adopted this approach, where each tested sample is ran as a set of two reactions; one for detection of the potential disease and one IAC (Lucchi et al., 2016). However, this approach increases the overall cost of an assay as well as require an increased amount of the biological sample to accommodate the IAC reactions.

In contrast, the competitive IAC involves the utilisation of a single primer set that can amplify the true target and IAC template simultaneously in the same tube. Both strategies are somewhat similar, and competitive inhibition of the true amplification can occur if a single tube is used for both true and IAC reactions. There is always a risk that the IAC amplification will compete for the amplification precursors, (dNTPs / primers) and enzymes required for the true amplification (Hoorfar et al., 2004b, Dingle et al., 2004). This competition would be reported regardless of the detection system used. As many isothermal amplifications require the use of multiple and long primers (such as LAMP) that span large template regions, the use of additional primer sets for IACs may be necessary to reduce competitive inhibition, but this poses challenges related to non-specific priming (Kiddle et al., 2012, Lee et al., 2015). All IAC strategies require precise optimisations that favour the detection of the true target without compromising the overall sensitivity of the control assay (Abdulmawjood et al., 2002, Cubero et al., 2002, Kleiboeker, 2003).

5.2 Aims and objectives

The main focus of this study was to develop a reverse transcribed internal amplification control for RT-LAMP assays that used delayed competitive IACs. We aimed to reduce the level of competition for primers, enzymes and precursors by impeding the amplification of the IAC with respect to limiting copy numbers of true target nucleic acid. This would be achieved by using a synthetic template, akin to the target of interest, albeit with eliminated and altered primers annealing positions designed to hinder amplification. Manifestations of this IAC would be reportable by BART and a specific probe that would allow differentiation between positive amplifications and those initiated from the IAC.

5.3 Results

5.3.1 Development of Internal Amplification Control for monitoring assay inhibition

In this section, a step-by-step approach for generating a single-tube IAC will be realised. It has been demonstrated that certain primers and modifications can perturb amplification kinetics. These primer modifications were exploited as a way of impeding the initiation and propagation of IAC amplifications, thereby reducing the competition with the core RT-LAMP.

5.3.1.1 Impeded RT-LAMP assay as a model for IAC generation

As shown in a different study, loop primer elimination and LAMP primer mutations with respect to the true target, could cause severe delays in amplification without affecting the sensitivity of the assay (see **Appendix 39**). Thus, it was decided to explore similar approaches in this study.

Figure 39 shows LAMP-BART profiles generated using the standard TB assay as a model.

Since it is well established that loop primers significantly improve the amplification speed, they were removed from the RT-AMP TB 23S primer set used in this study (Nagamine et al., 2002).

In addition, the number of introduced mismatches differed depending on the LAMP primer used. It was necessary to maintain similar melting temperatures for complementary regions, to enable direct comparison of the effects of mutated primer melting temperatures and priming positions on the performance the TB assay.

Table 14 shows all of the tested versions of the TB LAMP primers with introduced mismatched bases highlighted in red. The shown Tm values represent the melting temperatures of the mutated priming regions that maintained complementarity with the target, unless otherwise stated.

Primer	5'→3' sequence	Tm [°C]
WT BIP	ACTCGCAGGCTCATTCTTTTTTCCGGAGGAGGGTGG	B1-60.2 B2-61.4
WT FIP	AAGGTTAACCCGTGTGGTTTTCGCGTGTGGGTCGCC	F1-58.6 F2-65.2
MutFIPv2	AAGGTTAACCCGacaccTTTTCGCGTGTGGGTCGCC	F1-44.0 F2-65.2
MutFIPv3	AAGGTTAACCCcacaccTTTTCGCGTGTGGGTCGCC	F1-37.3 F2-65.2
MutFIPv4	AAGGTTAACCgcacaccTTTTCGCGTGTGGGTCGCC	F1-30.2 F2-65.2
MutFIPv5	AAGGTTAACCCGTGTGGTTTTgcCGTGTGGGTCGCC	F1-58.6 F2-58.0
MutFIPv6	AAGGTTAACCCGTGTGGTTTTgcgcaGTGGGTCGCC	F1-58.6 F2-46.8
MutFIPv7	AAGGTTAACCCGTGTGGTTTTgcgcacaGGGTCGCC	F1-58.6 F2-37.7
MutBIPv2	ACTCGCAGGCagtaagaTTTTTCCGGAGGAGGGTGG	B1-45.5 B2-61.4
MutBIPv3	ACTCGCAGGgagtaagaTTTTTCCGGAGGAGGGTGG	B1-37.3 B2-61.4
MutBIPv4	ACTCGCAGcgagtaagaTTTTTCCGGAGGAGGGTGG	B1-29.0 B2-61.4
MutBIPv5	ACTCGCAGGCTCATTCTTTTTaggGGAGGAGGGTGG	B1-60.2 B2-50.6
MutBIPv6	ACTCGCAGGCTCATTCTTTTTaggcGAGGAGGGTGG	B1-60.2 B2-45.4
MutBIPv7	ACTCGCAGGCTCATTCTTTTTaggcctGGAGGGTGG	B1-60.2 B2-36.9

The introduced mismatches significantly affected the amplification of the *M. bovis* positive control rRNA (*p value* < 0.05, t-test) (**Figure 39**). In general, the lower Tm's of the mutated LAMP primers impeded the amplification from target RNA; the more bases mutated the greater the observable impact. However, the biggest impact on amplification kinetics was seen when using the MutFIPv2-4 and MutBIPv2-4 (**Table 14-15**). These primers generated both highly delayed and reproducible amplifications. Over a 15 to 30 min delay in time-to-peak was achieved with the MutFIPv2 and MutBIPv2 primers. Interestingly, despite the differences to which the amplification times were delayed, the Tm of these primers are calculated to be highly similar (separated by 1 °C). Furthermore, the reactions containing the MutFIPv3-4 and MutBIPv3-4 produced peaks at 82-64 min and 70-74 min, respectively (**Figure 39A, C**). However, the reproducibility of those reactions suffered a noticeable loss in amplification efficiency when compared to either the assays utilising the WT primers or version 2 of the RT-LAMP primers tested (**Table 15**). The standard deviation in time to maximum varied between

5 to 10 min, whereas only 2 min difference was observed in the average TTM of reactions performed with version 2 primers. LAMP primer, variants 5-7 also caused significant delays in amplification (*p value* < 0.05, t-test) (**Table 15**). Together with the overall delay in amplification caused by LAMP primers, there were also noticeable differences in the assays performance between the affected BIP and FIP primers.

Mutagenesis resulting in the reduction in Tm of the B2 position within the back inchworm primer (BIP; MutBIPv5-7) caused mild delays in amplification speed, compared with all the other reactions tested (**Figure 39D**). Surprisingly, only a 7 min difference in the time to maximum light output (TTM) was detected between reactions containing the WT and the mutant versions (v5-7) of the BIP (**Table 15**). MutBIPv5 and v7 generated BART curves with similar TTM although reactions utilising the MutBIPv7, suffered a noticeable reduction in reproducibility. The overall reproducibility of the TB amplification, was highly comparable between the above BIP variants. The MutBIPv6 and the MutBIPv2 designs resulted in almost identical calculated Tm but showed a prominent difference in amplification performance. When mismatches were introduced to the B1 site of the BIP primer a 30+ min delay in amplification was achieved, whereas only a 4 min difference in TTM was observed when the B2 side was mutated by the same temperature difference (**Figure 39C**).

Similar reductions in the Tm on the F2 region of the forward inchworm primer (FIP), had a completely different impact on the assay (**Figure 39B**). On average, these reactions amplified

10 min slower than those containing similar mutations within the BIP. The amplification reproducibility was affected to a much greater extent than any of the mutated variants tested.

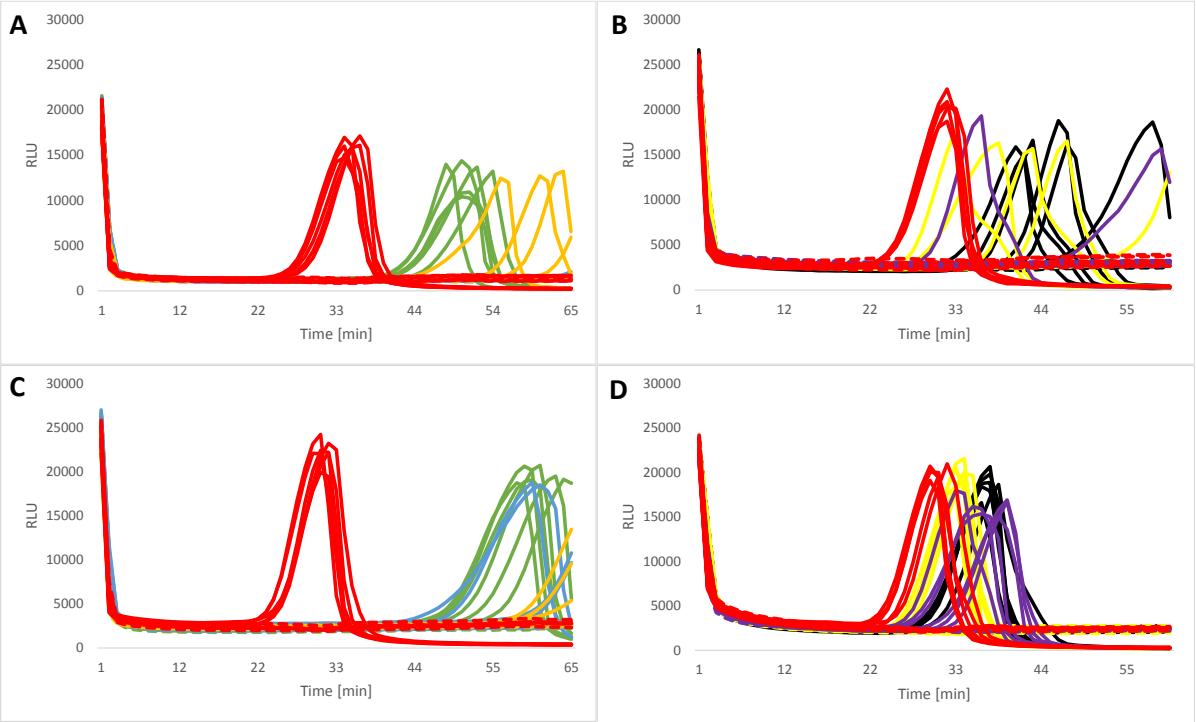

Figure 39. Comparison of LAMP-BART profiles generated using mutated versions of TB LAMP primers. A – amplification profiles generated suing FIP primer with altered F1 site; B – amplification profiles generated using FIP primer with altered F2 site; C – amplification profiles generated using BIP primer with altered B1 site; D – amplification profiles generated using BIP primer with altered B2 site

Each version of LAMP primers was colour-coded as follows: red – WT primer; Green – version 2; Blue – version 3; Orange – version 4; Black – version 5; Yellow – version 6; Purple – version 7

Primer	Mean [min]	Stdev	Amp.Freq.[%]
TB mutFIPv2	51	2.2	100
TB mutFIPv3	82	6.9	100
TB mutFIPv4	64	6.5	83
WT FIP	35	1.1	100
TB mutFIPv5	46	6.3	100
TB mutFIPv6	45	11.0	83
TB mutFIPv7	48	15.9	33
WT FIP	32	0.5	100
TB mutBIPv2	61	2	100
TB mutBIPv3	70	10	83
TB mutBIPv4	74	5	50
WT BIP	31	1	100
TB mutBIPv5	37	0.8	100
TB mutBIPv6	34	0.6	100
TB mutBIPv7	37	2.6	100
WT BIP	30	0.9	100

Table 15 showing summary of the data presented in the **figure 39**. Each set of reactions was analysed using average TTM (Mean), reproducibility (STDev) and sensitivity (Amp.Freq).

5.3.1.2 Internal amplification control template design

In order to maintain similarity between the IAC template and true amplifications the 23s rRNA targeted by the RT-LAMP, was used as a template for the IAC design. **Figure 40B** shows the consensus region targeted by the 23s *Mycobacterium bovis* rRNA with highlighted RT-LAMP primers and the capture probe binding sites used for its extraction.

Table 16 contains colour-coded primer sites corresponding to each binding position shown in the **Figure 40.**

Primer	sequence 5' -> 3'
LAMP B (BIP)	ACTCGCAGGCTCATTCT-TTTT-TCCGGAGGAGGGTGG
LAMP F (FIP)	AAGGTTAACCCGTGTGG-TTTT-CGCGTGTGGGTCGCC
Loop B	CAAAAGGCACGCCATCA
Loop F	CGAAAGCGAGTCTGAATAG
Displacement B (DispB)	AGAGTACCTGAAACCGTG
Displacement F (DispF)	ATTCACACGCGCGTAT
Capture probe	CGGGTCCAGAACACGCCAC

Figure 40A shows the IAC template design generated from the 23S rRNA sequence along with the mutated and altered primer annealing positions that were introduced (black box).

To accommodate the proposed IAC design and reduce the cost of synthesis, the entire sequence was truncated to remove unnecessary bases. The loop priming positions were substituted for probe sites; this would serve to decelerate the amplification significantly and allow for alternative specific fluorescent detection of the IAC. The substitution of the loop primer annealing position did not affect the overall length of the target sequence. Finally, to further impede the IAC amplification, base substitutions were introduced to the B2 binding site, mimicking the alterations within the MutBIPv2.

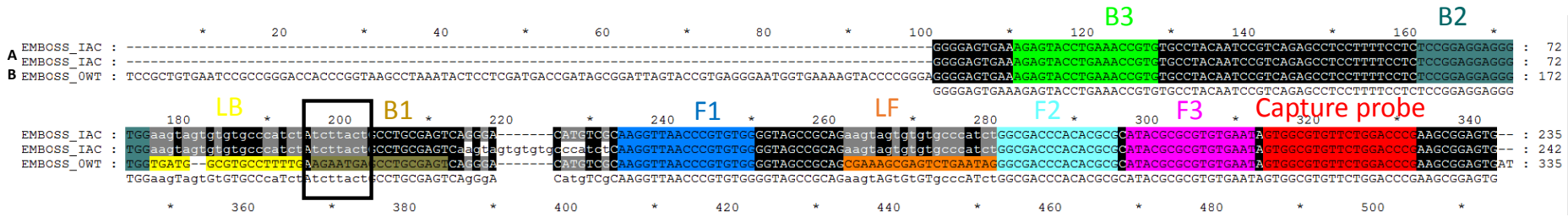

Figure 40. showing a sequence alignment using the consensus region targeted by the TB primers and the IAC design. Each corresponding primer binding site was colour-coded as follows: Green – B3; Teal – B2; Yellow – Loop B; Dark yellow – B1; Dark blue – F1; Orange – Loop F; Light blue – F2; Pink – F3; Red – capture probe binding position. Each highlighted sequence corresponds to a fully complementary region of the TB primers.

Black box showing the mutated region of the IAC template. Note: A – consists of two identical IAC sequence alignments; B – WT region of the TB consensus sequence.

5.3.2 Detecting assay inhibition using the RT-LAMP IAC

In this section, the parameters affecting the performance of the standard TB assay, including the IAC interference study as well as inhibition, were assessed.

5.3.2.1 Assessing the performance of the in-house developed IAC assay

In the first instance, the performance of the newly designed IAC template was evaluated using the in-house freeze-dried 50 uL RT-LAMP 23S TB assay, which contained all the chemistry and primers required for true positive and IAC amplifications.

Figure 41 shows LAMP-BART profiles (**A**) and summary bar charts (**B**) generated using the 50 uL standard TB assay.

The positive control 23s rRNA and the IAC *in vitro* transcribed (IVT) RNA successfully amplified under the RT-LAMP conditions used. However, the amplification of the IAC RNA was significantly delayed compared to the target 23s RNA (*p value* < 0.05, t-test) (**Figure 41B**). Over a 20 min difference in TTM was achieved between the two amplification mechanisms, good reproducibility was observed for both amplifications at the copy numbers tested.

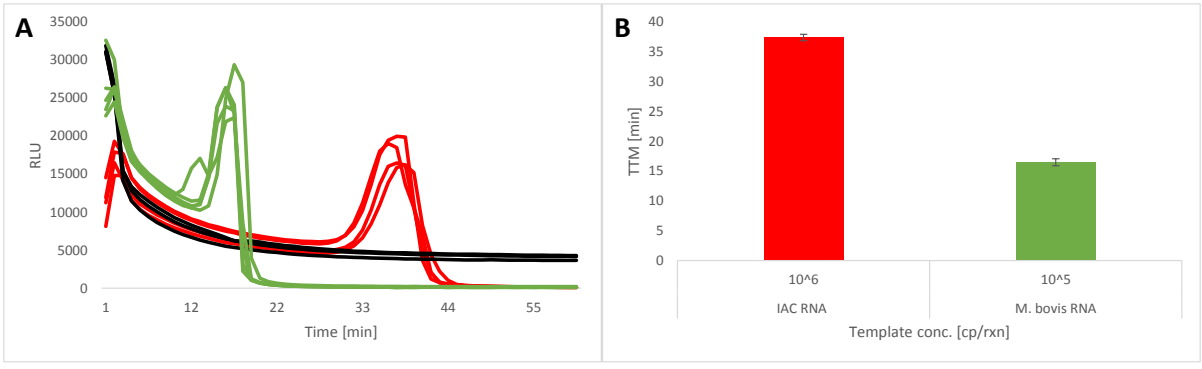

Figure 41. Comparison of LAMP-BART profiles (**A**) and summary bar chart (**B**) generated using standard TB 50 uL reactions containing full primer set. Each tested template was colour-coded as follows: Green – 10^5 cps of 23s *M. bovis* rRNA; Red – 10^6 cps of the in-house IAC RNA; Black - NTC

5.3.2.2 DNA contamination in the IAC IVT RNA.

As the IAC IVT RNA was synthesised from a DNA template it was important to account for any contaminating DNA that may affect our interpretation of DNA and RNA polymerised events later in this chapter.

Figure 42 RT-LAMP and LAMP-BART profiles generated using in the presence and absence of reverse transcriptase.

All reactions conducted with Maxima RNaseH+ amplified, the reproducibility and speed was comparable to the previously generated data for 10^6 cp of the IAC (data not shown). Surprisingly, the reactions deficient in Maxima RNaseH+ also exhibited exceptionally good amplification efficiency, and reproducible detection at all copy numbers tested (**Figure 42B**). Reactions with RT amplified slightly faster than those deficient in this activity. In fact, reactions performed at 10^8 copies of IVT RNA without the RT enzyme amplified at the same time as RT dependent amplifications containing 10^7 copies of the target IVT (**Table 17**). This suggested the IVT RNA was contaminated with 10 % of its parental DNA template.

In order to further confirm the DNA contamination levels, the amplification performance of the IAC RNA assay lacking the RT enzyme was compared with a sample standard generated from an IAC DNA PCR product quantified using qPCR and Agilent by ERBA Molecular (data not shown).

Figure 43 shows LAMP-BART profiles generated using a standard TB assay (no MaximaRH+) and various amount of either IAC RNA or positive control DNA. The average TTM for each sample dilution was then used to estimate the contamination levels in the RNA samples.

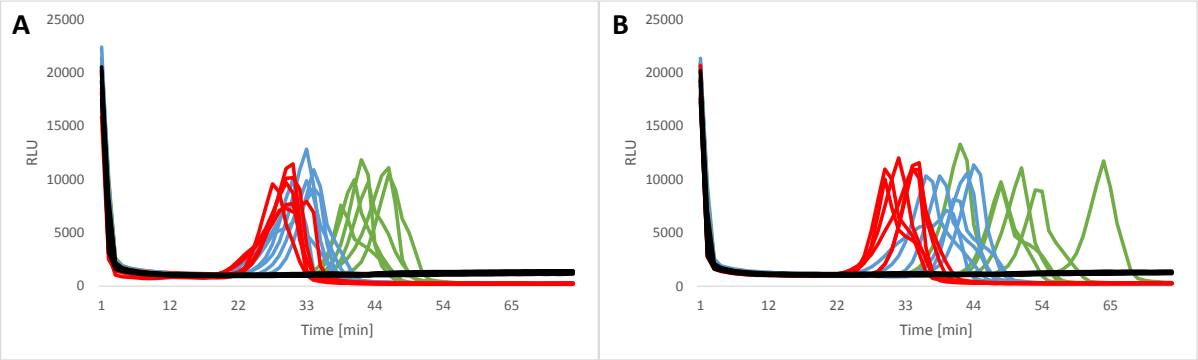

Figure 42. Comparison of LAMP-BART profiles generated using standard TB 20 uL reactions containing full primer set and various amounts of IAC RNA. A – represents reactions containing the reverse transcriptase (MaximaRNaseH+); B – showing amplification profiles generated in the absence of RT.

Concentrations of the IAC RNA used were colour-coded as follows: Red – 10^8 cps; Blue – 10^7 cps; Green – 10^6 cps; Black - NTC

Table 17 showing summary of the data presented in the **figure 42**. Each set of reactions was analysed using average TTM (Mean), reproducibility (STDev) and sensitivity (Amp.Freq).

Assay	IAC RNA [cp/rxn]	TTM [min]	Stdev	Amp.Freq. [%]
+MaximaRH	10^6	43	3.0	100
	10^7	33	1.5	100
	10^8	31	1.7	100
-MaximaRH	10^6	51	7.5	100
	10^7	40	2.8	100
	10^8	33	2.5	100

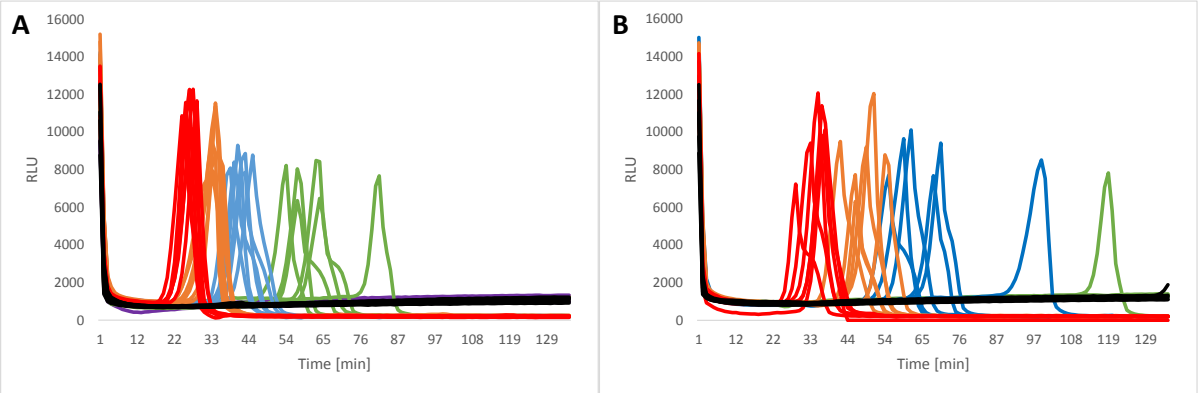

Figure 43. Comparison of LAMP-BART profiles generated using standard TB 20 uL reactions containing full primer set and various amounts of IAC targets. A – represents reactions amplifying the positive control IAC DNA; B – showing amplification profiles generated using the ivt IAC RNA. Note that none of these reactions contained RT enzyme. Bst Large fragment was also used.

Concentrations of the IAC templates used were colour-coded as follows: Red – 10^8 cps; Orange – 10^7 cps; Blue – 10^6 cps; Green – 10^5; Black - NTC

Table 18 showing summary of the data presented in the **figure 43**. Each set of reactions was analysed using average TTM (Mean), reproducibility (STDev) and sensitivity (Amp.Freq).

Template	NA conc. [cp/rxn]	Mean [min]	Stdev	Amp.Freq. [%]
IAC DNA	10^5	63	9.6	100
	10^6	41	2.4	100
	10^7	34	0.6	100
	10^8	27	1.6	100
IAC RNA	10^5	119		17
	10^6	69	15.7	100
	10^7	48	4.5	100
	10^8	35	3.1	100

As expected, successful amplification of the target was achieved on both the DNA and RNA templates without the standard RT enzyme, confirming the presence DNA contamination (**Figure 43A-B**). Similarly to our previous findings, the contaminations levels were estimated to be approximately 10 %. **Table 18**, shows TTM values for each DNA and RNA titration used. In general, the amplification of IAC DNA was observed to be significantly faster than of corresponding RNA amount (*p value* < 0.05, t-test). However, the comparison of TTM between the samples containing the IAC DNA and a corresponding 10-fold dilution of the RNA target showed no significant difference in amplification speed (*p value* > 0.05, t-test). On average, the reactions containing 10^5 cps of the IAC DNA amplified in 63 min whereas 69 min was required to detect 10^6 cps of IAC RNA. Similarly, when the reactions utilising 10^6 cps of the IAC DNA were compared to the assays containing 10^7 cps of the IAC RNA, highly comparable amplification times were detected (**Table 18**). In fact, the same pattern was noticed across all of the DNA and RNA titrations tested.

5.3.2.3 RT-LAMP - IAC interference study

Due to the single-tube format of the 23S rRNA RT-LAMP / IAC amplification and knowledge that the true and control reactions utilise the same primer set and substrate, it was crucial to determine any potential effects that the IAC amplification may have on the RT-LAMP-BART. **Figure 44** 23S rRNA RT-LAMP-BART profiles generated using the standard reaction conditions protocol 14 (**see Appendix 14**), spiked with a final load of 10^6 copies of the *IVT* IAC RNA

No significant differences in amplification speed were perceived between those reactions containing purely the 23S rRNA and reactions spiked with the IAC RNA (*p value* > 0.05, t-test; **Table 19**). Amplifications containing various titrations of 23S RNA and IAC IVT all amplified faster than those containing the IAC RNA alone (**Figure 44A NTC+IAC**). All of the reactions containing 100 cp of the 23S rRNA target, amplified prior to the IAC IVT RNA **Figure 19**. Interestingly, a slight improvement in true target amplification sensitivities were detected when the IAC IVT RNA was present in the reaction. In the spiked samples containing 100 cps of the 23S rRNA target, 5 out of 6 replicates showed positive amplification profiles, whereas only 3 out of 6 reactions were detected in the absence of the IAC IVT RNA (**Figure 44B**).

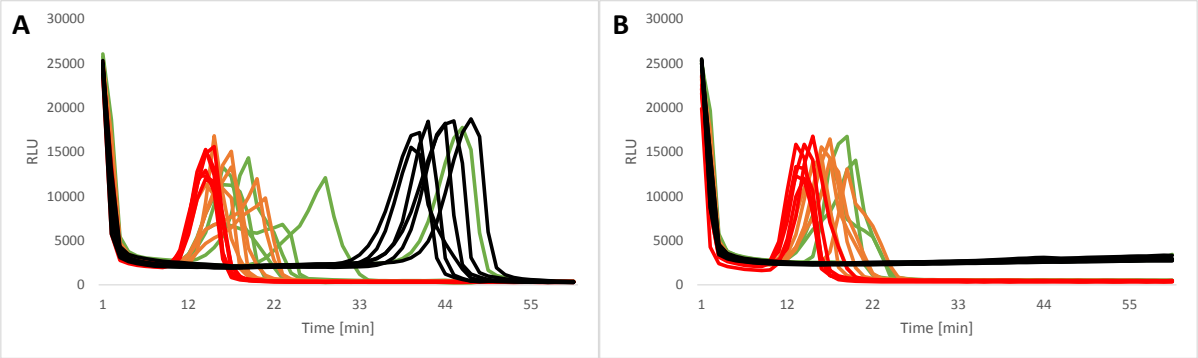

Figure 44. Comparison of LAMP-BART profiles generated using standard TB 20 uL reactions containing full primer set and various amounts of TB target. A – represents reactions spiked with 10^6 cps of IAC RNA; B – showing amplification profiles generated in the absence of IAC template.

Concentrations of the TB target 23s rRNA used were colour-coded as follows: Red – 10^4 cps; Orange – 10^3 cps; Green – 10^2; Black – NTC.

Table 19 showing summary of the data presented in the **figure 44**. Each set of reactions was analysed using average TTM (Mean), reproducibility (STDev) and sensitivity (Amp.Freq).

Sample	RNA conc. [cp/rxn]	MeanTTM [min]	Stdev	Amp.Freq. [%]
***M. bovis* RNA**	10000cp	14	0.9	100
	1000cp	17	1.5	100
	100cp	19	1.6	50
***M. bovis* + IAC RNA**	10000cp + 10^6 IAC	14	0.7	100
	1000cp + 10^6 IAC	17	2.9	100
	100cp + 10^6 IAC	19	5.6	83
IAC RNA	10^6	43	2.8	100

5.3.2.4 The effects of probing on the performance of IAC and 23S RT-LAMP-BART

As already described earlier in this chapter the TB loop priming positions were forsaken for non-TB probe sequences that may be used as an alternative reporter for the detection of IAC IVT amplification. The effect of ROX-labelled loop probes on the performance of IAC RNA amplification were therefore assessed.

Figure 45 23S RT-LAMP-BART profiles and summary bar charts generated using a modified TB assay conditions according to the protocol 15 (**see Appendix 15**). Amplifications were tested in the presence of probe designed to target the recombinant loop position of the IAC IVT RNA and either BstLF (**B**) or GSP-SSD (**A**)

A significant difference in amplification performance was detected between reactions containing GSP-SSD and Bst LF polymerase, irrespective of the presence of the ROX loop probes (*p value* < 0.05, t-test). On average, reactions utilising the GSP-SSD amplified over 10 min faster than those containing the Bst LF (**Table 20**). In addition, over a 30 min difference in TTM was observed between those containing the ROX probes compared to those without. The presence of the ROX probes had a detrimental effect on amplification kinetics, regardless of the DNA polymerase used. However, the degree of inhibition realised was greater in reactions containing the Bst LF compared to similar reactions with GSP-SSD. On average, only an 11 min difference in amplification of the IAC target was observed between reactions containing the ROX probes and the controls (**Figure 45** dotted red curves) when the GSP enzyme was used. In contrast, this difference increased to over 30 min when the Bst LF enzyme was added (**Table 20**). Furthermore, the presence of the ROX-probes seemed to reduce the level of non-specific amplification. In general 50% NTC's amplified in reactions containing the GSP-SSD and no probe compared to 15% in its presence. The same improvement was true for reactions with BstLF.

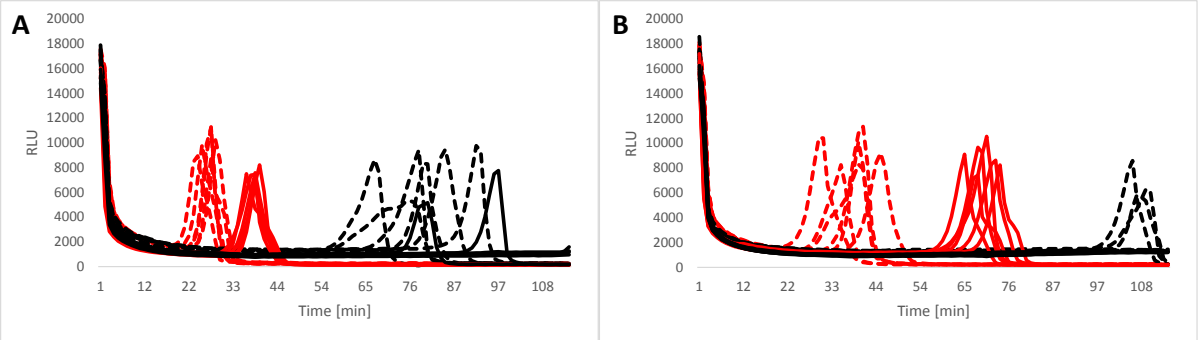

Figure 45. Comparison of LAMP-BART profiles generated in a presence or absence of ROX loop probe using a modified TB 20 uL reactions containing full primer set. A – represents reactions utilising GSP-SSD enzyme ; B – showing amplification profiles generated using Bst LF.

Note that dotted lines represent the samples lacking the ROX probe (P), whereas solid curves show amplification profiles generated in the presence of the ROX probe. Red – samples containing 10^6 cps of IAC RNA; Black – NTC

Table 20 showing summary of the data presented in the **figure 45**. Each set of reactions was analysed using average TTM (Mean), reproducibility (STDev) and sensitivity (Amp.Freq). Addition or ROX loop probe was indicated with "P".

DNA pol.	Sample [cp/rxn]	TTM [min]	Stdev	Amp.Freq. [%]
Gsp-SSD	10^6 IAC RNA	27	1.6	100
	10^6 IAC RNA +P	38	1.1	100
	NTC	79	8.3	100
	NTC +P	89		33
Bst LF	10^6 IAC RNA	38	5.1	100
	10^6 IAC RNA +P	70	3.1	100
	NTC	107	1.6	50
	NTC +P			0

5.3.2.5 Assessing the effects of inhibitory substances on the performance on 23S RT-LAMP and IAC RNA amplification.

The inhibitory effect of sodium chloride, carrier DNA and RNA, humic acid and sodium hydroxide/mucin would be assessed on the 23S RT-LAMP / IAC.

Figure 46 RT- LAMP-BART profiles generated using a modified assay according to the protocol 16 **(see Appendix 16)** challenged with various amounts of sodium chloride. Each reaction contained both the target 23S rRNA and the IAC RNA at a concentration of 10^6 cps per reaction, unless otherwise stated and a titration of NaCl (Ranging from 0 to 40 mM additional salt)

The NaCl showed an inhibitory effect on the performance of the integrated IAC IVT RNA amplification and the RT-LAMP-BART designed to detect the *M. bovis* 23s rRNA. Overall, the TTM of the true positive samples (*M. bovis* 23S rRNA) and the IAC IVT RNA differed noticeably between the amounts of inhibitor used. A 5 min difference in TTM was observed between the uninhibited samples containing 100 copies of the target 23S rRNA (and an additional 10^6 copies of IAC IVT RNA) and the corresponding reactions spiked with 40 mM NaCl. Similarly, for the reactions containing 1000 copies of the 23S rRNA, a significant increase in TTM was observed between the uninhibited reactions and the samples containing 40 mM NaCl, where over a 5min difference in amplification speed was detected (*p value*< 0.05, t-test). Interestingly, the salt did not cause reduction in the sensitivity of the 23s rRNA assay.

A significant shift in TTM was also observed when the performance of IAC amplification was considered across all of the tested amounts of inhibitor (*p value* < 0.05, t-test) (**Table 21**). Within the time frame of the assay (60 min), full detection of IAC target was lost when assays were challenged with 30 and 40 mM of the NaCl (**Figure 46C**).

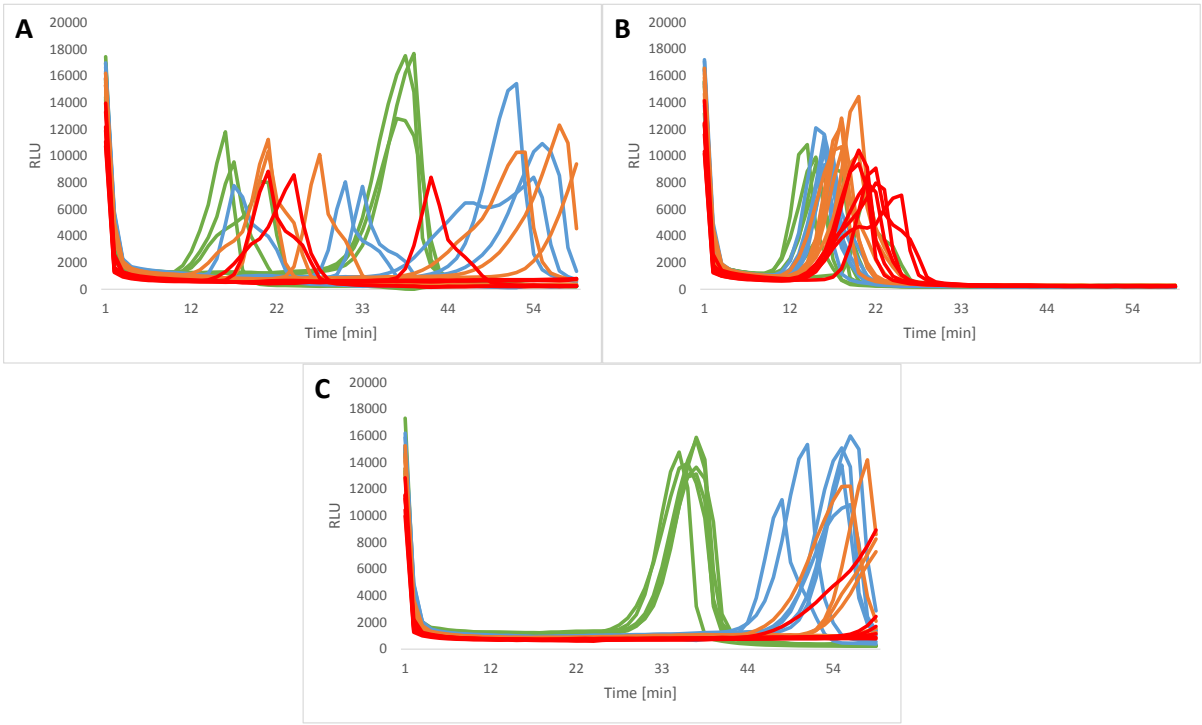

Figure 46. Comparison of LAMP-BART profiles generated using a modified TB 20 uL reactions containing full primer set challenged with various amounts of NaCl. A – represents reactions containing 100 cp of the 23s rRNA spiked with 10^6 cps IAC RNA; B – showing amplification profiles generated using 1000 cps of the 23s rRNA spiked with 10^6 cps IAC RNA; C – amplification profiles generated using 10^6 cps of the IAC RNA.

Amounts of NaCl added to each reaction were colour-coded as follows: Green – 0 mM; Blue – 20 mM; Orange – 30 mM; Red – 40 mM.

Table 21 showing summary of the data presented in the **figure 46**. Each set of reactions was analysed using average TTM (Mean), reproducibility (STDev) and sensitivity (Amp.Freq).

Sample	*M. bovis* RNA conc. [cp/rxn]	NaCl conc. [mM]	Mean [min]	Stdev	Amp.Freq. [%]
M. bovis RNA + IAC RNA	100	0	18	2.2	50
		20	27	8.7	50
		30	24	3.7	50
		40	23	2.3	33
	1000	0	16	2.7	100
		20	16	0.7	100
		30	19	1.1	100
		40	22	2.0	100
IAC RNA	0	0	37	0.9	100
		20	54	3.5	100
		30	63	5.7	100
		40			0

Figure 47 RT- LAMP-BART profiles generated using a modified reaction chemistry according to the protocol 17 (see **Appendix 17**) Amplification reactions were challenged with various amounts of salmon sperm DNA (ranging from 0 to 1000 ng). Each reaction contained both the target 23S rRNA and the IAC IVT RNA at a concentration of 10^6 cps per reaction, unless otherwise stated.

The salmon sperm DNA caused inhibition of the 23S RT-LAMP amplification which was very apparent at the lowest copy number tested here (100 copies per assay). Over 50% reduction in amplification detections at 100 copies per reactions were observed in the presence of 1000 ng salmon sperm DNA, compared to the control (**Table 22**). When 1000 cps of the target 23S rRNA, were challenged with 500 and 1000 ng of the salmon sperm DNA a significant deterioration in amplification kinetics was realised. The amplification profiles of the IAC IVT RNA were also affected by the presence of the carrier DNA. Mirroring the RT-LAMP, a significant decrease in amplification speed of almost 10 min was observed, between reactions containing 1000 ng ssDNA and the control reactions (*p value* < 0.05, t-test) (**Figure 47C**). As little as 500 ng of the carrier DNA was potent enough to negatively impact upon amplification kinetics. Contrasting with NaCl inhibition, where no effect on the assay sensitivity was detected, carrier DNA caused a significant reduction in detection at the lowest copy number tested here. On average, every 10-fold increase in the concentration of the salmon sperm DNA, resulted in a 15% loss of sensitivity at 100 copies. Furthermore, concentrations of carrier DNA that caused a failure to detect 100 copies of 23S rRNA were not reflected by a failure full detect the IAC IVT RNA, just a reduction in the overall amplification efficiency.

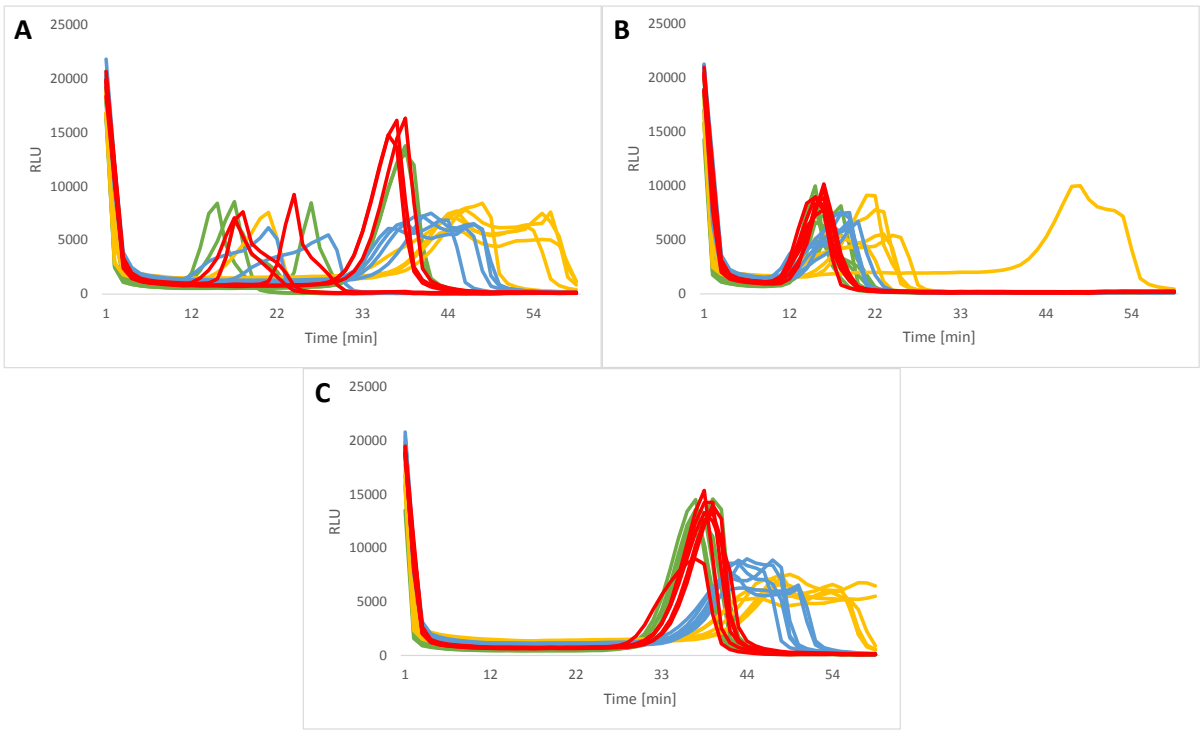

Figure 47. Comparison of LAMP-BART profiles generated using a modified TB 20 uL reactions containing full primer set challenged with various amounts of salmon sperm DNA. A – represents reactions containing 100 cp of the 23s rRNA spiked with 10^6 cps IAC RNA; B – showing amplification profiles generated using 1000 cps of the 23s rRNA spiked with 10^6 cps IAC RNA; C – amplification profiles generated using 10^6 cps of the IAC RNA.

Amounts of salmon sperm DNA added to each reaction were colour-coded as follows: Red – 0 ng; Green – 50 ng; Blue – 500 ng; Orange – 1000 ng.

Table 22 showing summary of the data presented in the **figure 47**. Each set of reactions was analysed using average TTM (Mean), reproducibility (STDev) and sensitivity (Amp.Freq).

Sample	*M. bovis* RNA [cp/rxn]	carrier DNA conc. [ng/rxn]	Mean [min]	Stdev	Amp.Freq. [%]
TB + IAC RNA*	100	0	19	5.3	67
		50	20	4.0	50
		500	25		33
		1000	21		17
	1000	0	16	1.7	100
		50	16	0.6	100
		500	19	1.1	100
		1000	22	2.9	83
IAC RNA*	0	0	38	0.9	100
		50	39	0.9	100
		500	44	3.4	100
		1000	49	3.2	100

Figure 48 23S RT-LAMP-BART profiles and bar charts generated using a modified reaction chemistry challenged with various amounts of tRNA.

In this experiment, the target 23S RNA and the IAC RNA were amplified separately under the same inhibitory conditions.

The 23S RT-LAMP and IAC IVT RNA amplification suffered from a reduction in performance when assays were challenged with 500 to 1000ng of tRNA, causing significant delays in amplification compared to the non-inhibited reactions (p *value* < 0.05, t-test) (**Figure 48A-B**). However, as was previously seen, the effects of carrier DNA, affected the 23s rRNA amplification to a much higher extent.

A dramatic reduction in the sensitivity of the 23S RT-LAMP was detected when challenged with 1000 ng of the tRNA, yet none of the carrier RNA concentrations affected the sensitivity of the IAC IVT RNA amplifications. Furthermore, the reproducibility of the 23S-RT-LAMP containing 500 ng of carrier tRNA was compromised compared to the control reactions, whereas the IAC IVT RNA amplifications were unperturbed. At 50 ng of carrier tRNA, the amplification speed and reproducibility of 23S RT-LAMP was noticeably improved (**Table 23**).

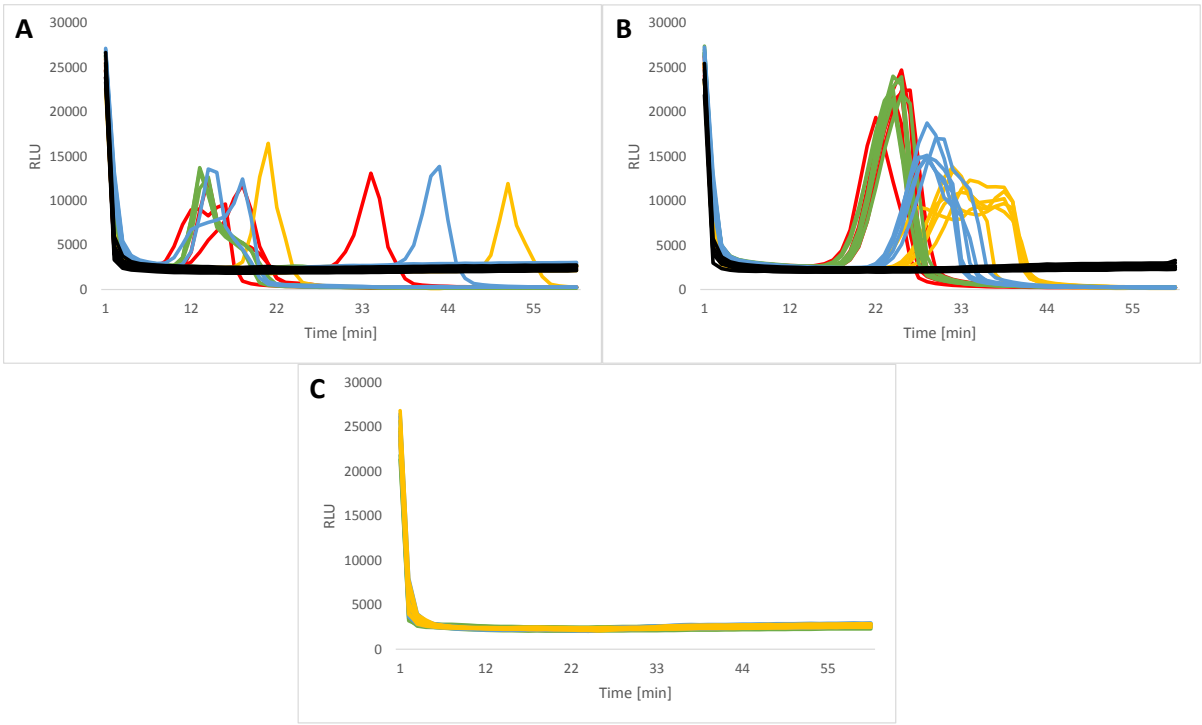

Figure 48. Comparison of LAMP-BART profiles generated using a modified TB 20 uL reactions challenged with various amounts of carrier tRNA. A – represents reactions containing 100 cp of the 23s rRNA; B – showing amplification profiles generated using 10^6 cps IAC RNA; C – amplification profiles generated in the absence of both the 23s rRNA and IAC template.

Amounts of the carrier RNA added to each reaction were colour-coded as follows: Red – 0 ng; Green – 50 ng; Blue – 500 ng; Orange – 1000 ng.

Table 23 showing summary of the data presented in the **figure 48**. Each set of reactions was analysed using average TTM (Mean), reproducibility (STDev) and sensitivity (Amp.Freq).

Template	Carrier tRNA [ng/rxn]	TTM [min]	Stdev	Amp.Freq. [%]
IAC RNA	0ng	25	1.5	100
	50ng	25	0.6	100
	500ng	29	0.7	100
	1000ng	33	1.6	100
M. bovis RNA	0ng	21	9.3	67
	50ng	13	0.6	50
	500ng	25	15.6	50
	1000ng	36		33

Figures 49 23S-RT-LAMP-BART profiles and bar charts generated using various amounts of mucin / sodium hydroxide. A mucin stock was prepared according to the protocol 40 (**Appendix 40**), the mucin therefore contained contaminating levels of sodium hydroxide. Each template titration was prepared using the corresponding inhibitory solution as diluent.

Tables 24 show the amounts of mucin used to challenge both, the TB and IAC assay and the concentrations of sodium hydroxide expected in each mucin titration.

An inhibitory effect of the mucin / sodium hydroxide solution on the IAC IVT RNA amplification performance was detected (**Figure 49A, C**). At the 400ng mucin containing approximately 1.3 mM NaOH, reduced the amplification speed by 3 min (*p value* < 0.05, t-test) (**Table 24**). Once more, the RT-LAMP assays were more prone to inhibition by the inhibitor. The mucin / sodium hydroxide caused a 40% reduction in amplification sensitivity without affecting the amplification speed. Both the 400ng mucin and 1.3 mM sodium hydroxide affected the amplifications equally suggesting the latter to be the main cause of inhibition.

Further investigation of mucin inhibition showed no apparent effect on neither the TB IAC nor the target TB 23s rRNA amplification (**Figure 50**).

In that experiment, both the target TB 23s rRNA and the IAC RNA were amplified in a single-tube format, where the two templates were spiked directly into the reaction mix followed by an addition of the appropriate inhibitory solution, unlike previously described in the **Figure 49**.

When challenged with as much as 700 ng of mucin solution, which contained approximately 2.3 mM NaOH, no significant change to either assay sensitivity or kinetics was detected when compared to the non-inhibited samples (*p value* > 0.05, t-test). Both reactions generated highly reproducible peaks with a TTM of 13 min and reaching over 80 % detection. In fact, similar effects were seen across all of the mucin and NaOH amounts used.

Note that in this set up 20 min threshold was chosen as a cut off point for true positive amplification. Thus, any profiles generated after that time were scored as IAC amplification.

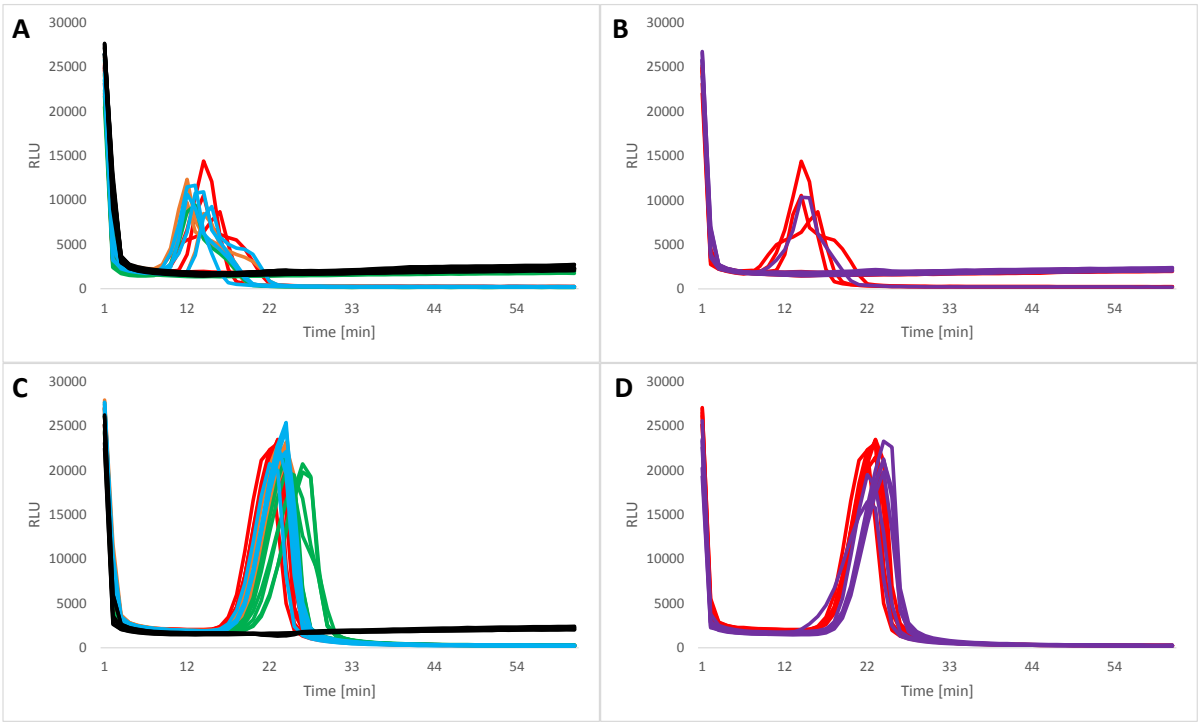

Figure 49. Comparison of LAMP-BART profiles generated using a modified TB 20 uL reactions challenged with various amounts of mucin / NaOH. A – represents reactions containing 100 cp of the 23s rRNA challenged with mucin solution; B – showing amplification profiles generated using 100 cps of the 23s rRNA challenged with NaOH only; C – amplification profiles generated using 10^6 cps of the IAC template challenged with mucin solution; D – amplification profiles generated using 10^6 cps of the IAC template challenged with NaOH only.

Amounts of mucin added to each reaction were colour-coded as follows: Red – 0 ng; Blue – 50 ng; Orange – 200 ng; Green – 400 ng; Black - NTC.

The reactions containing 1.3 mM NaOH only are shown in red.

Table 24 showing summary of the data presented in the **figure 49**. Each set of reactions was analysed using average TTM (Mean), reproducibility (STDev) and sensitivity (Amp.Freq).

Target	Mucin [ng/rxn]	NaOH [uM]	TTM [min]	Stdev	Amp.Freq. [%]
IAC RNA	0ng	0uM	23	0.4	100
	50ng	175uM	24	0.9	100
	200ng	675uM	24	0.4	100
	400ng	1333uM	26	1.0	100
	0ng	1333uM	24	1.1	100
M. bovis r RNA	0ng	0uM	15	1.2	50
	50ng	175uM	13	1.4	67
	200ng	675uM	12	1.2	50
	400ng	1333uM	13		17
	0ng	1333uM	14		17

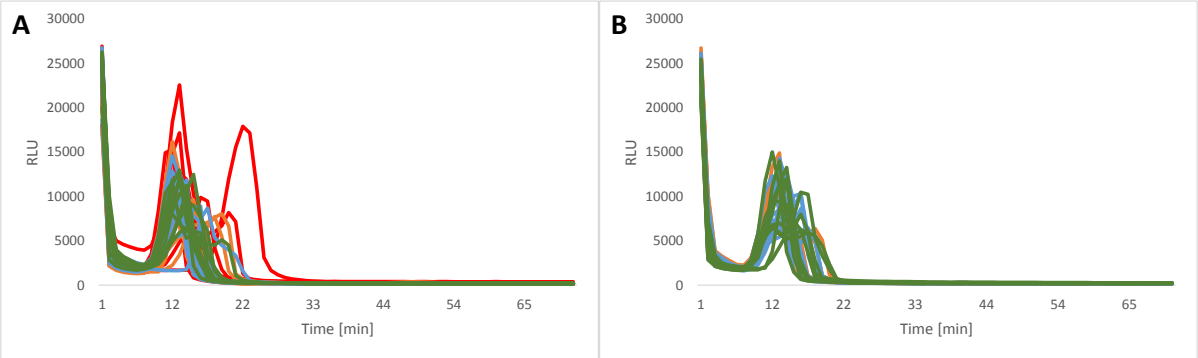

Figure 50. Comparison of LAMP-BART profiles generated using a modified TB 20 uL reactions challenged with various amounts of mucin / NaOH. A – represents reactions containing 100 cp of the 23s rRNA challenged with mucin solution; B – showing amplification profiles generated using 100 cps of the 23s rRNA challenged with NaOH only.

Amounts of mucin added to each reaction were colour-coded as follows: Red – 0 ng; Orange – 400 ng; Blue – 500 ng; Green – 700 ng.

Amounts of NaOH added were colour-coded as follows: Orange – 1.3 mM; Blue – 1.7 mM; Green – 2.3 mM.

Table 25 showing summary of the data presented in the **figure 50**. Each set of reactions was analysed using average TTM (Mean), reproducibility (STDev) and sensitivity (Amp.Freq).

Inhibitor	Conc.	TTM [min]	Stdev	Amp.Freq. [%]
Mucin	0ng	13	1.5	80
	400ng	13	1.2	80
	500ng	13	1.8	100
	700ng	13	1.2	100
NaOH	1333 uM	12	0.6	90
	1667 uM	14	1.7	100
	2326 uM	13	1.7	100

5.3.3 IAC detection

In the current RT-LAMP / IAC amplifications that utilise BART, differential detection of multiple amplifications in the same tube is not possible. Thus, two strategies were developed to enable differentiation between the RT-LAMP amplification and the IAC IVT RNA amplification. To this end the suitability of BART or fluorescent probing, would be assessed.

5.3.3.1 Bioluminescent Assay Real-time (BART) as a method of IAC detection

Although, the current BART reporter cannot distinguish between two simultaneous amplifications, the TTM, amplification frequency or peak shape could hypothetically enable this differentiation.

Figure 51 23S-LAMP-BART profiles generated using a modified chemistry according to the protocol 18 (see **Appendix 18**). In this experiment, the effects of reaction volume on both amplification speed and reproducibility, were tested. A single reaction mix was made which contained 10^7 copies of the IAC IVT RNA per 50 ul. Two sets of reactions containing either 50 or 10 uL of that reaction mix were then tested in order to determine the effects of concentration and reaction volume on the amplification performance.

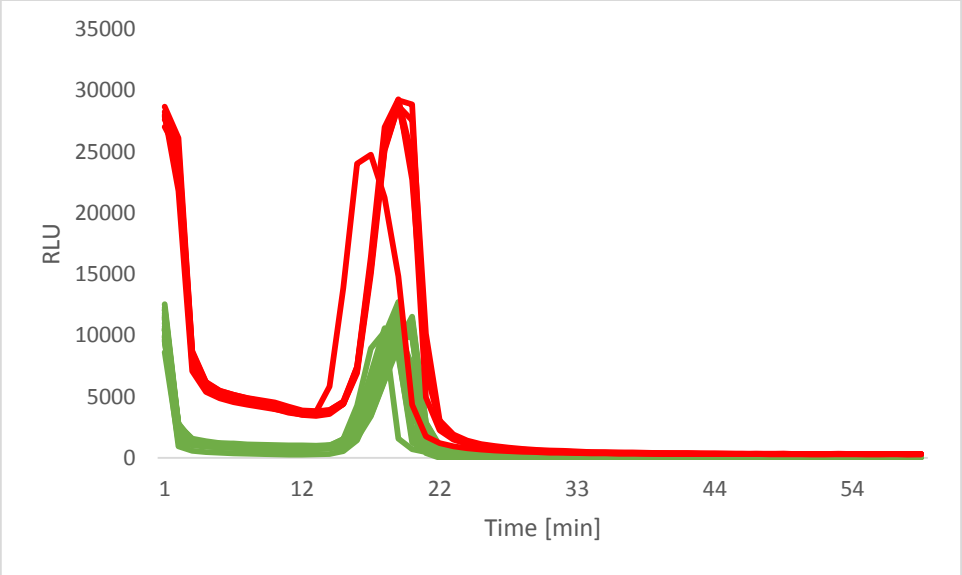

Figure 51. Comparison of LAMP-BART profiles generated using a modified TB assay and 10^7 cps/50 uL of the IAC RNA. Red curves represent the reactions carried out in 50 uL volume, whereas the green lines shows amplification profiles generated in 20 uL reaction volume. Note that both sets of reactions contained equal concentration of the target IAC RNA (2 x 10^5 cps/uL).

The reaction volume had little effect on the speed, sensitivity or reproducibility of the IAC amplification. Both reaction volumes amplified in less than 20min, achieving comparable reproducibility and identical sensitivity. Peak height was the only parameter tested that differed significantly between the two sets of reactions (*p value* < 0.05, t-test) (**Figure 51**).

When the reactions containing a challenging amount of the 23S rRNA were assessed, a significant effect of the reaction volume on the sensitivity and reproducibility, was observed.

Figure 52 23S-LAMP-BART profiles and bar charts generated using a modified reaction chemistry according to the protocol 18 (see **Appendix 18**). Each reaction mix was prepared with 100 copies of the 23S RNA target per 50 uL. Two sets of reactions containing either 50 or 10 uL of that reaction mix were then tested.

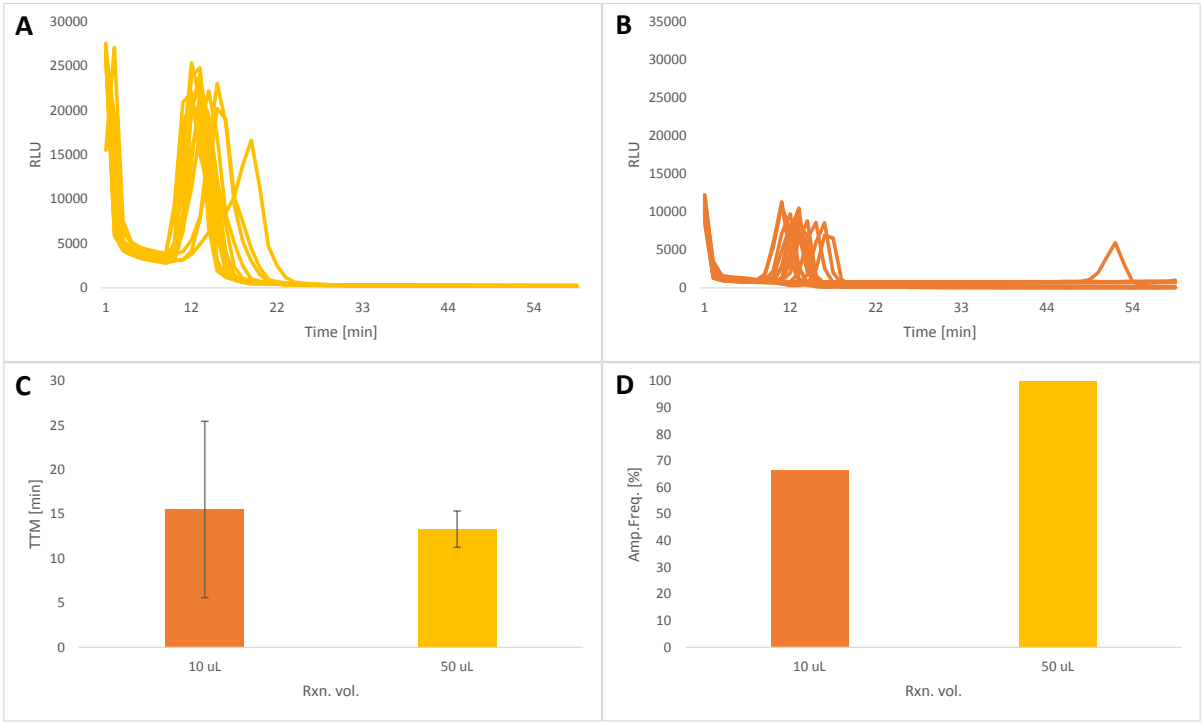

Figure 52. Comparison of LAMP-BART profiles and summary bar chats generated using a modified TB assay and 100 cps/50uL of the 23s rRNA. A – profiles generated using 50 uL reactions; B – amplification curves generated from 10 uL reactions; C – summary data using average TTM; D – summary data using amplification frequencies. Note that both sets of reactions contained equal concentration of the target RNA (2 cps/uL).

Almost 40 % reduction in the RT-LAMP detection of 23S rRNA was observed when 10 uL reaction volumes were compared to 50ul reaction volumes, and although no significant change to TTM was seen, the reproducibility was noticeably altered by the choice of reaction volume tested (**Figure 52D**). Moreover, the variability in amplification time decreased with increased reaction volumes (**Figure 52C**).

Since significant differences in the performance of RT-LAMP and IAC amplifications were observed when the 10 ul volumes were used, the effects of carrier DNA inhibition on the performance of a combined RT-LAMP / IAC amplification would be assessed using two different reaction volumes. This analysis was needed to establish whether or not the BART had the capacity to distinguish between the IAC and RT-LAMP amplification times and

frequencies, under both controlled and inhibited reaction conditions, when using a lower reaction volume.

Figure 53 23S-LAMP-BART profiles and bar charts generated using a modified reaction chemistry according to the protocol 19 (see **Appendix 19**). Samples containing either the 100 cps of the 23s rRNA spiked with 10^6 cps IAC RNA or 10^6 cps IAC only, were challenged with 500 ng carrier DNA (salmon sperm DNA) and run at 50 anf 10 uL volumes.

Full detection of the IAC IVT RNA was achieved under both, inhibited and uninhibited conditions, regardless of the reaction volume. In addition, no significant change in TTM was noticed between the two tested volumes (+ or – inhibitor; *p-value* > 0.05, t-test; **Table 26**). In contrast, the presence of 500 ng of carrier DNA, affected the IAC RNA significantly, compared to the uninhibited controls (*p-value* < 0.05, t-test) (**Figure 53A-B**), where over a 30 min increase in TTM was detected. The opposite effect was seen when a challenging amount of the 23s rRNA template was spiked with 10^6 copies of the IAC RNA. Firstly, a significant reduction in sensitivity was observed between the 50 and 10 uL reactions with the lower volumes amplifying less frequently under the uninhibited chemistry – over a 40 % decrease in sensitivity was detected (**Figure 53C**). Secondly, unlike the IAC RNA amplification, the presence of carrier DNA greatly impacted upon the sensitivity of the 23s rRNA assay, where over a 40 % and 25 % drop in amplification frequency was observed for the 50 uL and 10 uL reactions, respectively (**Figure 53D, F**).

However, similarly to the IAC RNA data, no effect of reaction volume on the average TTM was detected in the mixed samples, regardless of the presence of carrier DNA. In addition, similar response to the inhibitor was observed, where a significant 10 min increase in TTM of the reactions amplifying the 23s rRNA was detected when compared to the mixed uninhibited samples.

Note that overall full detection was observed across all of the tested assays. However, in the mixed samples, the profiles generated after 50 min were scored as IAC RNA amplification (IAC RNA[3]). Both the 50 and 10 uL reactions amplifying after that time generated identical profiles as those observed from the samples containing the IAC RNA only.

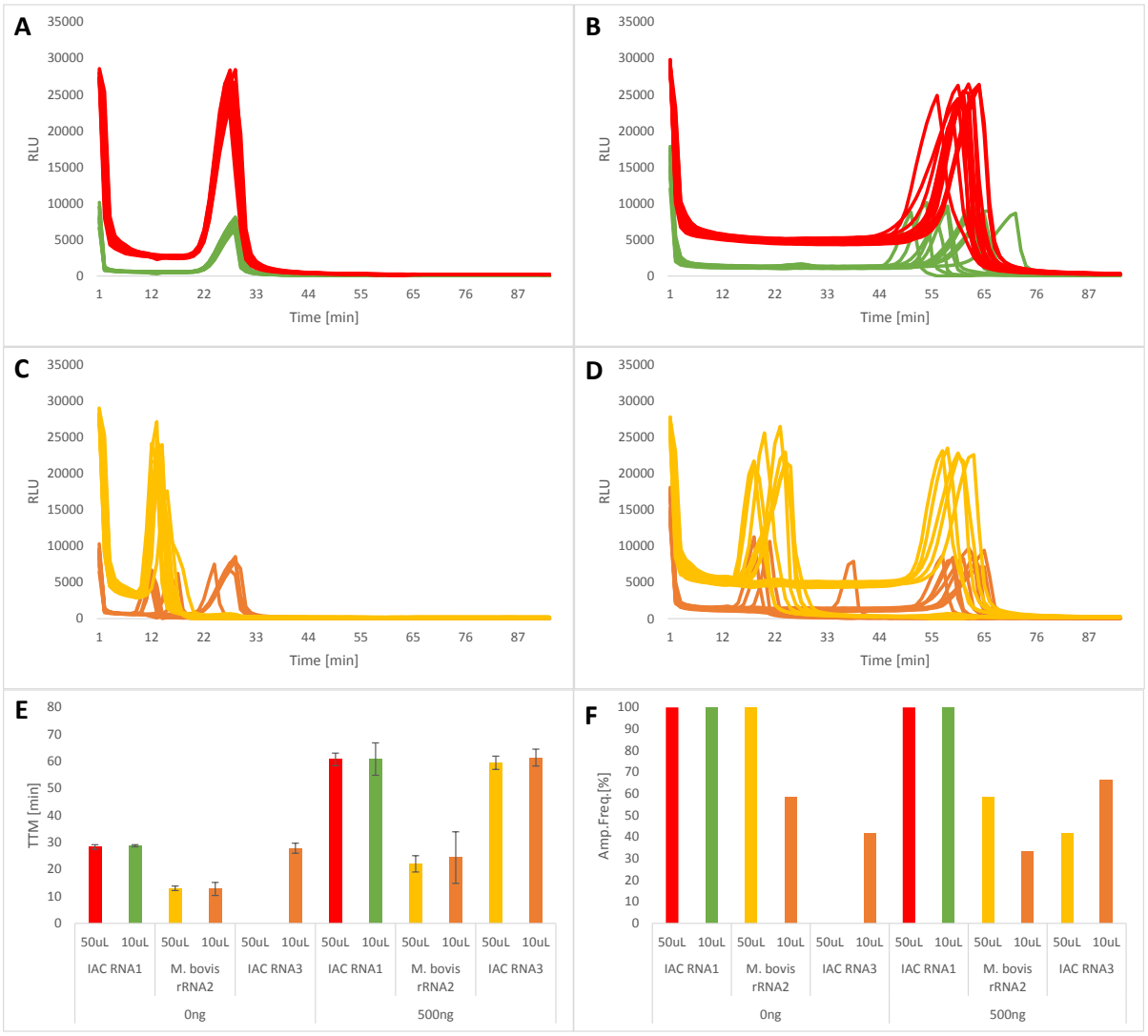

Figure 53. Comparison of LAMP-BART profiles and summary bar chats generated using a modified TB assay and 100 cps/50uL of the 23s rRNA and/or 10^6 cps IAC RNA. A – profiles generated using 10^6 cps IAC RNA amplified at 50 (red) and 10 (green) uL volumes; B – profiles generated using 10^6 cps IAC RNA amplified at 50 (red) and 10 (green) uL volumes, challenged with 500 ng salmon sperm DNA; C – profiles generated using 100 cps of the 23s rRNA spiked with 10^6 cps of the IAC RNA and amplified at 50 (yellow) or 10 (orange) uL volumes; D – profiles generated using 100 cps of the 23s rRNA spiked with 10^6 cps IAC RNA and amplified at 50 (yellow) and 10 (orange) uL volumes, challenged with 500 ng salmon sper DNA; E – summary data using average TTM; F – summary data using amplification frequencies.

Table 26 showing summary of the data presented in the **figure 53**. Each set of reactions was analysed using average TTM (Mean), reproducibility (STDev) and sensitivity (Amp.Freq). Samples 1-2 represent the mixed reactions whereas sample 3 was amplified in the presence of IAC RNA only.

Carrier DNA	Template	Rxn. Vol.	TTM [min]	Stdev	Amp.Freq. [%]
0ng	IAC RNA[1]	50uL	28	0.9	100
		10uL	29	0.4	100
	M. bovis rRNA[2]	50uL	13	0.8	100
		10uL	13	2.4	58
	IAC RNA[3]	50uL			0
		10uL	28	1.9	42
500ng	IAC RNA[1]	50uL	61	2.3	100
		10uL	61	6.0	100
	M. bovis rRNA[2]	50uL	22	3.0	58
		10uL	24	9.5	33
	IAC RNA[3]	50uL	59	2.5	42
		10uL	61	3.1	67

5.3.3.2 Fluorescent probing as a method of IAC detection

Molecular probes were assessed as novel tools for the differential detection of RT-LAMP and IAC. As described in the introduction to this chapter (**section 1.1.5**), most of the methods used to detect nucleic acid amplifications rely on the 5'->3' endonuclease activity of DNA polymerases, which liberate digested fluorescent tag from a specific oligonucleotide (*Taq*Man probes). Hairpin loop structures are also commonly used that ensure the close proximity of fluorophores to the quencher (beacons). Here we describe an original method for LAMP detection, whereby a loop primer is labelled with rhodamine X (ROX) and the black hole quencher 2 (BHQ2) at the 5' and 3' ends, respectively. It is believed that proximity of the fluorophore and the quencher is maintained on the loop oligonucleotide *via* static interactions between the functional groups, which keep the ROX fluorescence low when unbound; while the binding of the loop probe to amplified LAMP or IAC complimentary sequences results in an increased distance between the functional groups, that causes a liberation of ROX fluorescence. The more single stranded loop amplified the greater the fluorescence signal achieved. This mechanism relies on the probing of single stranded amplified product such as the suggested loop or even stem regions of LAMP. This method can report the amplification in real time and is quantifiable. The following section of this Thesis explores the possibility of using Loop probing to detect the IAC when duplexed with the RT-LAMP-BART. The mechanism makes use of a specific loop sequence that can only be probed as a consequence of the IAC and not the RT-LAMP amplification.

Figure 54 shows the folding predicted of the chosen loop B probe, under typical RT-LAMP salt (50mM) and temperatures (60^{o}C), performed using the IDT oligo analyser tool [URL: https://www.idtdna.com/calc/analyzer].

No secondary structure was detected in the chosen probe design. Only a small hairpin was predicted by the software that was thermal labile. No strong interactions were observed between the 5 and 3' of this sequence. No specific design was engineered that would generate a highly complementary region at the 5' and 3' ends, which would ensure quenching of the probe, as is the case for molecular beacons.

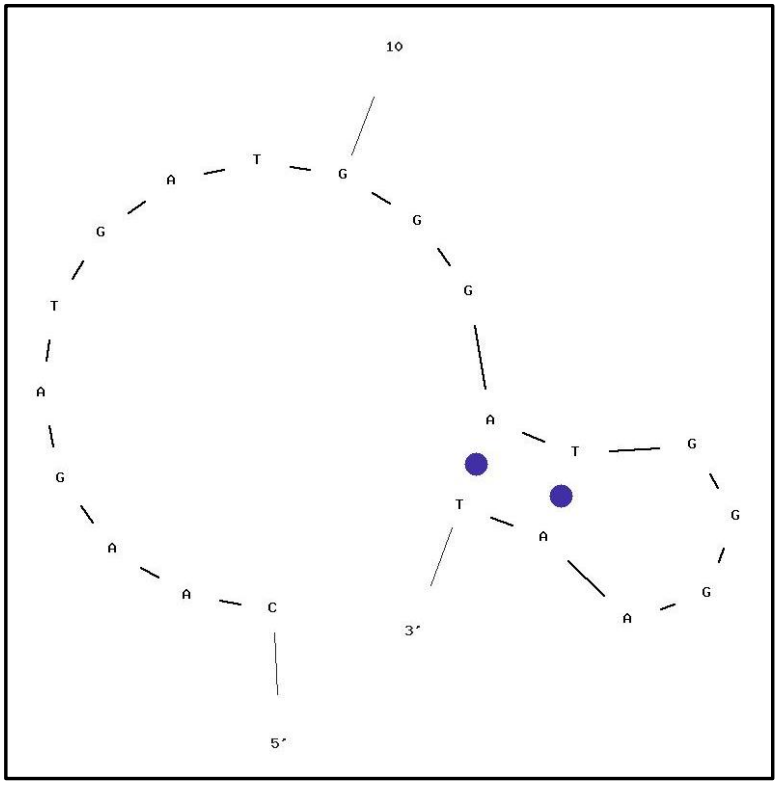

Figure 54. showing a typical sequence analysis output generated using the IDT oligo analyser. The tested oligo probe showed very mild folding with only 2 bp stem.

Figure 55 shows LAMP-ROX profiles generated using the proposed fluorescence-based approach, according to the protocol 21-22 (see **Appendix 21-22**).

No detection of RT-LAMP amplification occurred when ROX-loop probes were eliminated from the amplification. BART did not cause any significant shift in the background fluorescence observed in the absence of the ROX-loop probes. In contrast, full detection of the target was achieved in all RT-LAMP amplifications that contained the ROX-loop probe, and

target DNA irrespective of BART. Furthermore, BART did have an effect on the probe chemistry, elevating the fluorescence signal in the presence and absence of target DNA (**Figure 55D**).

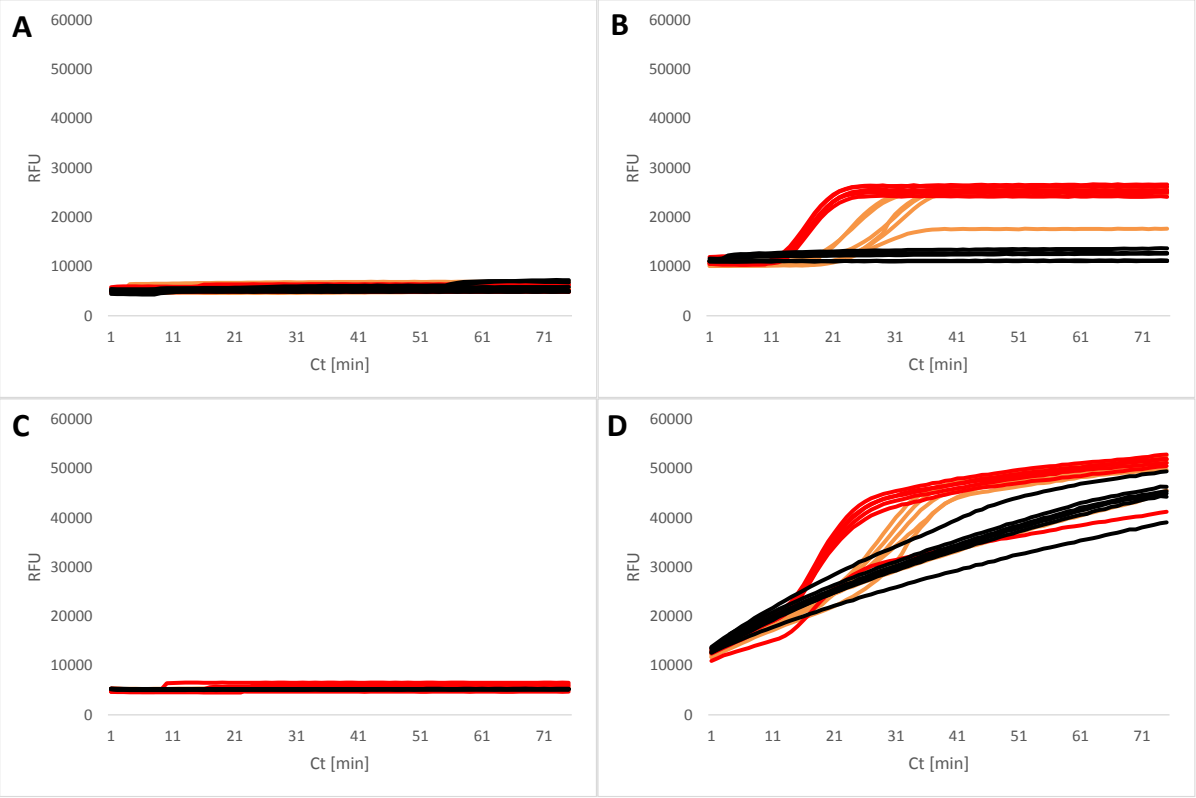

Figure 55. showing a typical LAMP-ROX profiles generated using the HBV assay model. Each reaction was amplified in either presence or absence of BART components. A – amplification profiles generated in the absence of both the BART and ROX loop probes; B – amplification profiles generated in the presence of 0.8 uM ROX loop probe; C – amplification profiles generated in the presence of BART only; D – amplification profiles generated using 0.8 uM of the ROX loop probes in the presence of BART.

Different concentrations of the HBV dsDNA used in this study were colour-coded as follows: Red – 10^4 cps; Orange – 10^3 cps; Black - NTC

Figure 56 LAMP-BART profiles and bar charts generated using the standard HBV protocol 20 (**Appendix 20**). The effect of FAM and ROX labelled probes on the LAMP-BART performance was assessed.

The addition of unlabelled loop primers (**Figure 56 orange curves**) resulted in a significant acceleration of amplification when compared to the reactions lacking these primers (**Figure 56 green curves**). On average, a significant 4 min reduction in TTM was observed in the presence of unlabelled loop primers (*p value* < 0.05, t-test; **Table 27**). In contrast, a significant 5 and 6 min increase in TTM was detected when the forward loop primer was substituted by either the FAM- or ROX-labelled probe, respectively (*p value* < 0.05, t-test). Furthermore, when compared to the reactions lacking both loop primers, the addition of labelled loop probes did not cause acceleration of amplification, but rather slowed it down, as seen previously with the probes tested under BART chemistry (**see p.144**).

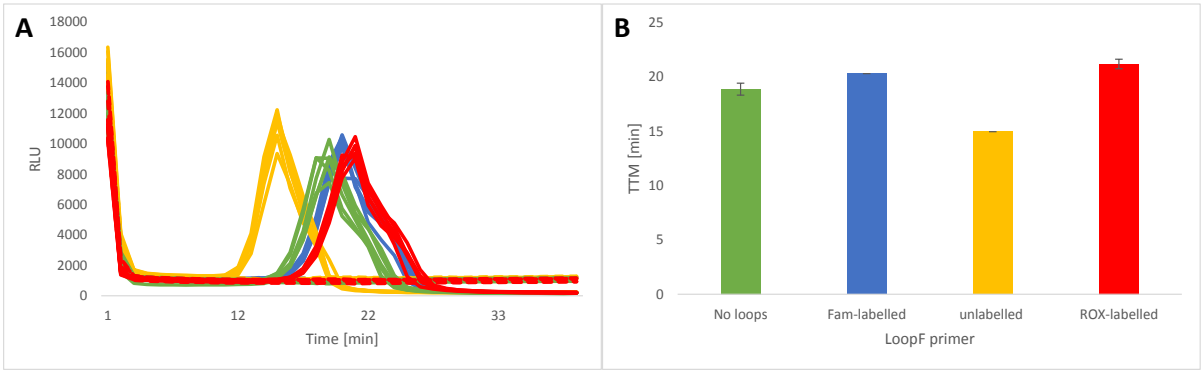

Figure 56. showing LAMP-BART profiles (**A**) and summary bar chart (**B**) generated using the HBV model assay in a presence of functional Loop B and various other loop probes. Each type of loop F probes used was colour-coded as follows: Red – 5'ROX and 3'BHQ2 labelled loop F; Blue - 5'FAM and 3'BHQ2 labelled loop F; Yellow – unlabelled loop F; Green – absence of both loop primers.

Note that each reaction contained equal amount of the target HBV dsDNA (5 x 10^5 cps).

Table 27 showing summary of the data presented in the **figure 56**. Each set of reactions was analysed using average TTM (Mean), reproducibility (STDev) and sensitivity (Amp.Freq).

LoopF primer	Mean [min]	Stdev	Amp.Freq.[%]
No loops	19	0.6	100
Fam-labelled	20	0.0	100
unlabelled	15	0.0	100
ROX-labelled	21	0.4	100

Figure 57 IAC ROX and SYBR green detection using GSP-SSD or BstLF. The HIV ROX-loop probe and SYBR green chemistry were used to detect 10^5, 10^6 and 10^7 copies of IAC RNA.

The reactions performed with GSP-SSD performed noticeably better with SYBR green and ROX-labelled probe detection systems compared to those performed with BstLF. When GSP-SSD was used full detection of 10^7 and 10^6 copies of the IAC was achieved using both reporters; 80% of the reactions containing the lowest copy number (10^5) were detected using both methods (**Figure 57A, C**). In contrast, reactions utilising the BstLF managed to fully detect the highest copy number only when the SYBR detection system was used, the sensitivity was compromised when using the ROX probe and only limited detection occurred in reactions that contained lower amounts of the IAC RNA (**Figure 57B, D**).

The overall performance of the HIV probing was a lot lower than that observed in the HBV probed IAC (reported earlier; **Figure 55**), regardless of the DNA polymerase used. Both, the reproducibility and light output was noticeably higher when HBV loop probe was used (**Figure 56**). The IAC makes use of two loop probe annealing positions, whereas in the HBV design, only one loop probe is used, which could account for the performance differences.

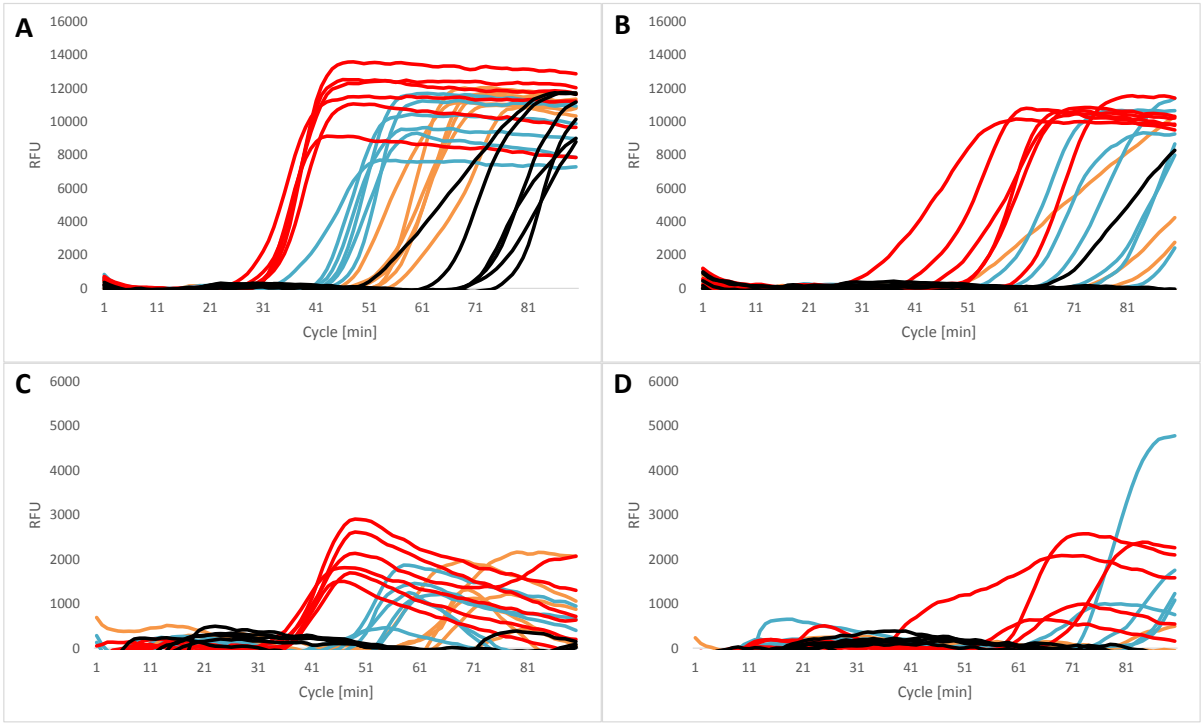

Figure 57. showing a typical LAMP-ROX/SYBR profiles generated using the IAC assay model. Each reaction was amplified in absence of BART components. A – amplification profiles generated using GSP-SSD and SYBR dye; B – amplification profiles generated using Bst LF and SYBR dye; C – amplification profiles generated using GSP-SSD and 0.8 uM of the ROX HIV stem probe; D – amplification profiles generated using Bst LF and 0.8 uM of the ROX HIV stem probe.

Different concentrations of the IAC RNA used in this study were colour-coded as follows: Red – 10^7 cps; Blue – 10^6 cps; Orange – 10^5 cps; Black - NTC

5.4 Discussion

One of the major limitations of NAAT diagnostic platforms, is the lack of amplification controls, which ensure the integrity of the detection system, and the inhibitory effects carried forward by the sample preparation procedures (Hoorfar et al., 2004a, Malorny et al., 2003). Without such controls, negative results can be highly misleading, as they are often attributed to faulty chemistry or inhibition of amplification and detection. Characterisation of false negatives is particularly important in the field of infectious disease diagnostics, where failings can affect patients well-being and prognosis, but also allow the increased spread of a disease (Chua and Gubler, 2013). Thus, in this study, we aimed to develop a non- or low-competitive IAC, to further our understanding of sample inhibition and to empathise the need for such controls in the diagnostic field.

5.4.1 Development of the IAC model system

Although, the loop mediated isothermal amplification (LAMP) technology has been shown to be an extremely useful and sensitive tool for nucleic acid amplification, one of the major limitations of this technology is the primer design (Kiddle et al., 2012, Lee et al., 2011). In order to achieve a high degree of specificity and sensitivity, LAMP employs up to six primers and 8 priming positions, but this causes increased complexity for primer design for singleplex assays, and severely limit the use of this technology for duplex or multiplexed amplifications. As a consequence of these limitations, we decided to adopt a competitive model for the development of internal amplification controls. This approach would not only limit the number of primers required for each assay, but also enable us to maintain a high level of similarity between the IAC and true targets sequence. Hence, factors such as GC-rich regions that can cause RT and DNA polymerase pausing or even secondary structure that are potentially limiting for primer and / or capture probe hybridisation, would have a similar effect on the two targets (Smith and Wu, 2004, Viguera et al., 2001).

Since LAMP is an extremely rapid amplification, several alterations were introduced into the IAC template that would ensure an impeded amplification, which in turn would avoid significant competition with the true positive amplification. Moreover, impediment of IAC amplification with respect to the core target was crucial for drawing a clear distinction with BART curves generated from late true positive amplifications.

Since loop primers significantly accelerate LAMP, both annealing sites were substituted with alternative sequences for oligonucleotide probing of our IAC template design. This alteration to the IAC template served to confine the loop primed acceleration to the true LAMP amplification, but it also permitted fluorescent detection of the IAC amplification. Furthermore, as described earlier, the introduction of mismatches between a given LAMP inchworm primer (BIP or FIP) and its template resulted in amplification delays, which did not affect the overall reproducibility of the amplification time.

All of the mismatches introduced into the BIP and FIP primers affected the performance of *M*ycobacterium complex 23s rRNA RT-LAMP amplification, regardless of the extent and the location of the mutations. Mutation introduced into specific poles of the inchworm primers (B1 and F1) had a much greater impact on the amplification speed than corresponding alterations in F2 and B2. This difference could be correlated with distinct roles governed by each pole of the LAMP inchworm primers within the initiation and propagation of target sequence amplification. For example, the F2 site is crucial for the initiation of cDNA synthesis and the entire resultant amplification and therefore impacts upon the function of the BIP primers. Any alterations to the F2 region would therefore be expected to cause a severe reduction in amplification performance (sensitivity / kinetics). We did indeed observe significant amplification delays, along with a deterioration in the reproducibility of the RT-LAMP RNA amplification that utilised FIP primers, which had the F2 site mutated. In contrast, we did not see such severe effects of similar F2 mutations on DNA amplifications via LAMP (data not

shown). It is likely that the F2, has a more fundamental role in reverse transcribing the RNA in RT-LAMP, while, both the B2 and F2 sites have more equal roles in the initiation of amplification from DNA. Thus, we concluded that the increased variability in RT performance caused by impairment of the initiation step was responsible for this disparity.

Mutations in the B2 sites of the BIP primer caused significant amplification delays, but these did not show the same potential to impede LAMP compared to corresponding F2 mismatches within the FIP, suggesting that primers involved in reverse transcribing RNA have a greater role in the initiation of LAMP from RNA than DNA. It could therefore be argued that first strand synthesis and displacement from RNA, are similar in nature to the second strand synthesised from cDNA and that amplification of the cDNA solely relies on the B2 site of BIP. Since it has been demonstrated that DNA hairpins are less stable than RNA, the effect of cDNA structure B2 primer hybridisation be mild compared to the effects of similar RNA structures on the F2 mutations (Antao et al., 1991). When primer carrying mismatches within the F2 or B2 sites are extended, newly formed amplicon will also contain sites exactly complementary to the introduced mutations, making the impact of these alterations less than those introduced into the other pole of the inchworms (B1 and F2), as is discussed.

The B1 and F1 mutated sites caused significant amplification delays compared to their B2 and F2 counterparts without affecting the reproducibility of amplification time. The impact of these mutations is associated with their stabilising effect on the LAMP dumbbell intermediate, a molecule pivotal for propagation of these isothermal reactions. Mismatches introduced within the B1 and F1 persist throughout the amplification reaction, since they are incorporated into the freshly synthesised target amplicon (refer to LAMP **figure 8**). Thus, this mechanism guarantees the continued impaired interaction between these sites and their compliments on the dumbbell and extended concatemers. Furthermore, the impediment of amplification continues

throughout the course of the amplification, resulting in a greater impact upon the kinetics of amplification than mutations with the 3’ of the inchworm primers.

After taking all experimental data and bioinformatics analysis into consideration, the IAC RNA template was designed, and this impacted upon loop primer binding sites, and alterations to the BIP B1 position, since this alteration to the BIP caused amplification impediment without affecting the reproducibility of amplification time.

5.4.2 Performance of the IAC for monitoring inhibition of RT-LAMP.

Our initial assessment of the designed IAC RNA assay demonstrated a significant delay in amplification time using our impeded LAMP mechanism, and also proved the potential of a test to report on the inhibitory nature of sample and sample preparation derived substances such as sodium chloride and carrier DNA, without affecting the core RT-LAMP amplification. It was noted that the 23S RT-LAMP assay could tolerate 10^6 copies of the IAC template without exhibiting any untoward effects. This proves that alterations to the LAMP priming mechanism, used to drive the impeded the amplification also served to sufficiently reduce the competition between the RT-LAMP and IAC. When challenged with sodium chloride or carrier nucleic acid, substantial delays in amplification times for the IAC were observed, proving these mechanisms responsiveness to inhibition. However, we did note that the inhibitor often affected the RT-LAMP amplification to a greater extent than the IAC when challenged with limiting amounts of RNA.

Carrier DNA is a known inhibitor of PCR and isothermal assays that not only delayed the RT-LAMP amplification, but also caused a significant reduction in the overall assay sensitivity and generation of detectable false negative results (Rohrman and Richards-Kortum, 2015, Kiddle et al., 2012). This effect was not observed when the IAC template was challenged by the same inhibitor, as all replicates of the target were detected even at the highest concentration of carrier

DNA used. Similar differences in the responsiveness of the RT-LAMP and IAC were observed for mucin, sodium hydroxide and carrier RNA.

It is very likely that differences in inhibitor tolerance exhibited by both amplifications are associated with differences in the manifestation of the target nucleotide. The RT-LAMP assays are solely dependent on reverse transcriptase, as the template is known to be a highly pure 23S RNA preparation, while the IAC IVT RNA template is known to contain a mixture of RNA and DNA. To be certain of accurate scores of reverse transcribed inhibition the IAC template would have to be presented in a purer form, as it is likely that the susceptibility of different polymerases to all of the tested inhibitors has been inadvertently scored in these experiments.

The nature of *in vitro* generated RNA templates showed to have a great impact on the performance and accuracy of IAC assays. We showed that using highly pure RNA IAC controls is required not only for controlling RT step, but also inhibitory substances that affect amplification of RNA compared to DNA. This work also shows that the reverse transcriptase is likely to be more rate limiting in our RT-LAMP amplifications that the DNA polymerase, and the tolerance of reverse transcriptase to classical PCR inhibitors may be a factor that significantly influences clinical sensitivity.

5.4.3 IAC detection systems

The simplicity and affordability of the bioluminescent amplification reporter (BART) makes this detection highly competitive and very useful in low resource settings. It was however undefined whether BART could be used to differentiate between the impeded IAC and RT-LAMP; the potential for this was assessed in this investigation.

Reactions that contained limiting amounts of the target rRNA amplified significantly slower under inhibitory conditions than uncompromised RT-LAMP amplifications. Thus, a molecular diagnostic in the field, should be able to discriminate between RT-LAMP inhibition, false positive amplifications and true positive amplifications that amplify inefficiently due to low inputs of target nucleotide. An efficient method of differentiating between the IAC and inhibited and non-challenged true target amplification was crucial to avoid mis diagnosing samples. The major limitation of the BART reporter, is inability to discriminate between amplifications, as it responds to amplification per se and is not sequence dependent like probe based strategies for detection. Accordingly, a different approach had to be considered.

The high concentration of IAC template used to control each amplification, were taken advantage of, to differentiate between this amplification and the RT-LAMP mechanism. It was envisaged that the two forms of amplification could be resolved by assessing amplification kinetics and frequency.

A method was developed that made use of limiting amplification volumes and a greater number of analytical replicates to assess the impact of inhibitors. The standard 50 ul reaction volume used for the RT-LAMP (which included the IAC target) was analysed and compared to the exact same reaction tested as 5x 10ul reactions. An assessment of BART timings (TTM) and amplification frequencies was then conducted in the presence and absence of inhibitor.

Thus, in the proposed approach, if all 5 of the 10ul reactions amplified within an early time frame, such a result would be deemed as truly positive and likely to contain large amounts of the target rRNA. Following on, if a smaller proportion of the 10ul reactions amplified with reduced kinetics, but still within a time frame known to be associated with RT-LAMP the overall result would still be scored as a positive diagnosis, but at the limit of detection. In contrast, where none of the reactions amplified in a time frame typical of LAMP, but corresponding to the IAC amplification times, such result would be deemed as a true negative. Thus using this approach, reactions containing limited copy numbers of the RT-LAMP or those compromised by inhibition are less likely to fully amplify within all 5 partitions. The Tmax as well as amplification frequencies generated by such partitioned reactions are less likely to be mistaken for the IAC detection profiles.

In this chapter it was demonstrated that no difference in IAC amplification speed or amplification frequencies were detected when the volume of the reaction partition was reduced. It is thought that this result reflected the constant IAC concentration, despite varying copy numbers. Consequently, the likelihood of template-primer interactions remained constant for both sized reaction partitions. In contrast, when limited amounts of the RT-LAMP template RNA was used, a deterioration in amplification frequency was observed with the reduced reaction volume. This change in reaction volume did not affected the RT-LAMP amplification kinetics. It was concluded that the impeded nature of the RT-LAMP was caused by a limited amount of target available in the smaller reaction partition. Furthermore, when observing RT-LAMP at its limit of detection performed with the IAC, similar observations were made. When RT-LAMP amplifications were conducted in 10 ul reactions, two populations of peaks were generated, indicating that the reduced volume affected sensitivity without impacting upon the detection of the IAC. It was also confirmed that the IAC amplification did not mask the effect that volume contributed to the RT-LAMP sensitivity.

5.4.3.1 Fluorescent detection system

One of the major advantages of probe-based fluorescent detection technologies over BART is their sequence specificity that lends itself well to multiplexed PCR of two or more targets (Sint et al., 2012). Thus, we decided to explore this type of technology for detection of the IAC targets described above. We demonstrated that dually labelled loop primers (using fluorophores and quenchers) could be used for detection of LAMP products. We also proved that such probes cannot prime amplification and do not require hydrolysis *via* exonuclease activities to release fluorescent signal. This was an interesting finding which suggested that the *Taq*Man probes also do not require hydrolysis to release fluorescence, as suggested by the Roche patent, but could simply rely on the probe binding to its target.

Secondary structure analysis of the loop probes demonstrated that the chosen loop primers did not form any significant 5' to 3' structure that would explain detection *via* a mechanism, similar to that described for molecular beacons. Several reports have suggested the potential static interactions between fluorophores and quenchers which could explain our finding.

The Loop-probes were shown to work well in conjunction with BART and these could detect both DNA and RNA LAMP amplifications. The loop-probes could also discriminate between isothermal amplifications that had complementary loops in their target compared those targets deficient in the sequence. This made the loop-probed approach particularly well suited for the specific detection of the IAC. The loop-probes did not contribute to the amplification and delayed amplification times were observed from targets hybridising such probes; the probes therefore contribute to the impeded amplification required for the IAC.

Together with functionality in the IAC, It is envisaged that this type of LAMP probing could allow for further multiplexing of true positivity and SNP detection.

5.5 Perspective

It was demonstrated that the current IAC amplifies with a significant delay, compared to all copy numbers amplified by the RT-LAMP, this control also exhibits sensitivity to various inhibitory substances such as LDS, NaCl or carrier DNA. Nonetheless, despite the fact the current system works as an internal positive control, further optimisations are still required to improve upon its performance:

a) Fluorescent probe binding site – a HIV sequence was used as a probing site in the current IAC TB RNA design. The use of non-human or -pathogen related sequence might be more suitable to avoid false positive detection from samples containing an abundance of this genome.
b) IAC RNA purity – As already discussed it is important to have an IAC template specific for the target nucleotide of interest. Further purification of the IAC IVT is required to remove all DNA template, so that the full inhibitory effect on reverse transcription can be assessed.
c) Further screening of inhibitory substances should be performed, including a wider range of substances found in clinical samples such as blood or sputum. The effect of these substances on reverse transcribed and DNA polymerised reactions should be ascertained.
d) Although BART detection showed huge potential for differentiating between the IAC and RT-LAMP, further work needs to be performed, to assess this techniques limitation with respect to sensitivity.

Chapter 6

6 Development of isothermal mechanisms of miRNA detection

6.1 Introduction

Micro RNA's (miRNAs) are small, non-coding RNA molecules found in eukaryotic cells that average around 22 nucleotides in length (He and Hannon, 2004). These small miRNAs play a crucial role in regulating gene expression, in plants, animals and humans by controlling translation (Ambros, 2004, Bartel, 2004, Bartel, 2009). The mode of action of miRNAs as post-transcriptional regulators involves the repression of translation, by interfering with the binding, promotion or the degradation of messenger RNA (mRNA) (Fabian et al., 2010, Jones-Rhoades et al., 2006).

It has been reported that the human genome encodes over 1500 different miRNAs, which can target the translation of approximately 60% of the expressed genes (Kontomanolis and Koukourakis, 2015, Holland et al., 2013). miRNAs can be found in many different cell types and are known to regulate multiple genes associated with human cancer, neurological diseases and viral infections (He et al., 2012, Musilova and Mraz, 2015, Mraz and Pospisilova, 2012, Radhakrishnan and Alwin Prem Anand, 2016, Weber et al., 2010). Abnormal expression of miRNAs is commonly associated with the initiation of cancer, oncogenesis, and even tumour responses to treatments (Giza et al., 2014, Ardekani and Naeini, 2010, Li et al., 2016).

6.1.1 Function and biogenesis of miRNAs

miRNAs are encoded in the genome in a form of long primary transcripts called pri-miRNA, which are mainly localised within the intron sequences of regulated genes (Rodriguez et al., 2004, Cai et al., 2004, Weber, 2005). Although, little is known about the mechanisms of regulation of miRNA transcription, their localisation within the coding and non-coding regions of genes may indicate the host gene promotors involved in the regulation process (Rodriguez et al., 2004, Kim and Kim, 2007, Baskerville and Bartel, 2005).

In animals, formation of mature miRNAs is normally carried out in two stages. Firstly, pri-miRNAs consisting of a 5' cap, a stem loop and a 3' polyA tail that is transcribed by RNA polymerase II (**Figure 58**); this is then followed by cleavage events that result in the formation of approximately 70 bp long precursor miRNAs (called pre-miRNA), where each pri-miRNA may contain as much as six pre-miRNAs molecules (Lee et al., 2004, Zhou et al., 2007, Faller and Guo, 2008).

The first stage of miRNA maturation occurs in the nucleus and is mediated by two core enzymes, Drosha and Pasha (Lee et al., 2003, Gregory et al., 2006). Pasha recognises the double-stranded regions of hairpin loop structures and together with an RNA restriction enzyme 'Drosha', several fragments of pre-miRNAs are formed. Each of the pre-miRNAs consists of a stem loop and a 2 nt long 3' overhang, which is recognised by the Exportin-5 and a Ran-GTP dependent nucleo-cytoplasmic cargo transporter and translocated into the cytosol for further processing (Conrad et al., 2014, Auyeung et al., 2013, Ali et al., 2012, Murchison and Hannon, 2004).

In the second stage of miRNA maturation, the pre-miRNA is cleaved into 20-25 nt products by an RNase III Dicer enzyme (Lund and Dahlberg, 2006, Park et al., 2011). The Dicer removes the loop structure of the pre-miRNA hairpin generating an imperfect miRNA: miRNA duplex

that consists of both the mature miRNA and its complementary strand. Separation of the two compliments is then carried out by the Dicer's helicase domain DUF283 resulting in formation of single-stranded mature miRNA fragments (Mirihana Arachchilage et al., 2015, Kurzynska-Kokorniak et al., 2016).

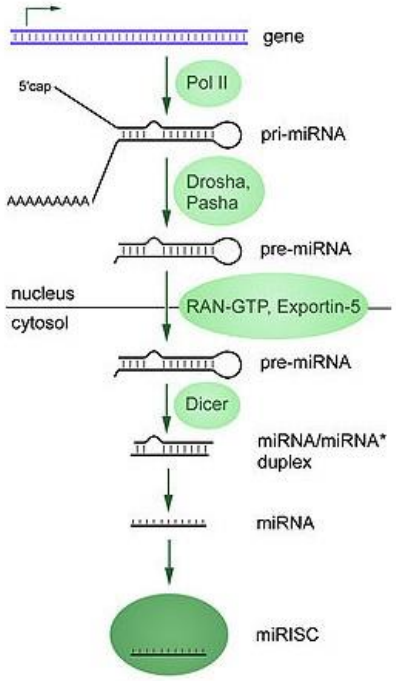

Figure 58. Graphic representation of a typical miRNA synthesis pathway.

Source: http://www.biosyn.com/tew/gene-silencing-by-micro-rnas.aspx

The miRNAs main cellular function is to regulate expression of proteins *via* inhibition of translation or degradation of the target mRNAs. The exact contribution of each mechanism remains unclear. It is thought that post-transcriptional inhibition of translation is the most common mode of gene silencing found in the animal kingdom (Williams, 2008, Bazzini et al., 2012, Maroney et al., 2006). Some reports have suggested that binding of miRNA to the 3'UTR regions of mRNAs affects the protein translation/release form the mRNA/ribosome complex, whereas others claim the disruption of translation to be the main factor (Nottrott et al., 2006, Petersen et al., 2006, Gu et al., 2009, Mathonnet et al., 2007).

In plants, translational inhibition is very rare and the mode of gene silencing occurs through the RNA-induced silencing complex of proteins (RISC) containing Dicer and other activities

that facilitate the cleavage of the mRNA **(Figure 59)** (Zhang, 2013, Jones-Rhoades et al., 2006)**.** In this model, Argonaute (Ago) proteins containing PAZ and PIWI domains responsible for binding to the mature miRNA, help to orient the guide RNA within the RISC complex, which in turn binds to the target mRNA and initiates degradation (Yan et al., 2003, Schwarz and Zamore, 2002, Pratt and MacRae, 2009).

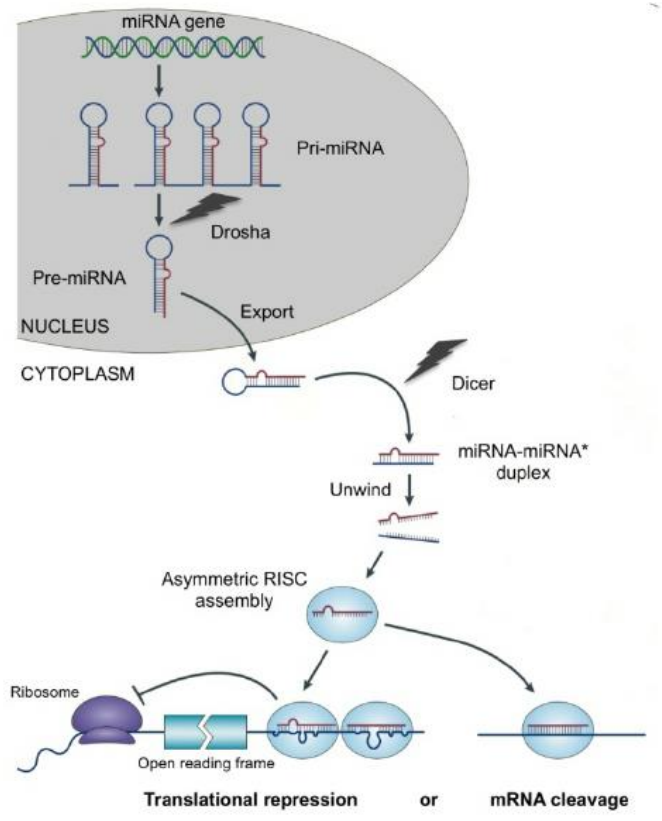

Figure 59. Graphic representation of regulation of gene expression using RISC complex.

Source: https://www.researchgate.net/figure/miRNA-based-post-transcriptional-gene-silencing-Briefly-endogenous-miRNA-genes-are_fig3_235768533

It has also been suggested that the RISC complex plays a role in post-transcriptional inhibition *via* either deadenylation of the 3' polyA tail, thereby affecting the mRNA functionality, preventing translation factors from binding to the 5' cap, and impairing the binding of the 60s ribosomal subunit or by encouraging the premature termination of translation **(Figure 59)** (Pratt and MacRae, 2009, Filipowicz et al., 2008, Wakiyama et al., 2007). Although, miRNA-mediated mRNA degradation is well documented, it is still unknown whether translational repression is caused by mRNA degradation or inhibition of translation.

It has recently been shown that inhibition of the translation events where the levels of mRNA remained unaffected, had a very modest impact on protein synthesis. In contrast, modulation

of the mRNA stability in a miRNA-dependant manner showed a much higher reduction in the overall protein concentrations suggesting this mechanism to be the main contributor in gene silencing (Guo et al., 2010).

In a different study, it was found that lin-4 miRNA negatively regulated the translation of its lin-14 transcript without affecting its cellular concentration (Bagga et al., 2005). It was reported that although the lin-4 miRNA inhibited the translation of the lin-14 protein, it failed to affect the synthesis, polyadenylation or abundance of the lin-14 transcript. Moreover, it has also been proposed that depending on the level of complementarity between the miRNA and its target transcript, gene silencing can be achieved *via* translational inhibition of mRNA degradation. In animals, miRNAs match imperfectly with their target sequence, where typically only 2-7 nucleotides must be conserved, to effect translational inhibition (Lewis et al., 2005, Lewis et al., 2003). In contrast, plants require perfect matching between the miRNA and message, in order to initiate degradation of the transcript (Mazière and Enright, 2007). Some miRNAs showed a dual function. For example, miR16 with an AU-rich element commonly found in unstable mRNAs, such as TMF α or GM-CSF, can either stimulate translational inhibition or mRNA degradation (Jing et al., 2005). It has been demonstrated that full complementarity between the miR16 and its target lead to mRNA degradation *via* Ago2 protein complex. However, when only partial complementarity was maintained, gene regulation was carried out *via* translational inhibition (Jing et al., 2005, Lim et al., 2003, Lim et al., 2005).

6.1.2 miRNAs as disease biomarkers

Many clinically relevant human miRNAs are located within the regions associated with cancer or at fragile sites and control a wide range of important processes, such as cell proliferation, apoptosis or angiogenesis, where dysregulation of these regulatory mechanisms play a key role in the onset and progression of cancer (Wang et al., 2016). Numerous studies have shown altered miRNA profiles in a wide range of cancer types, such as breast cancer, leukaemia or liver cancer (Calin et al., 2004, Tam, 2008, Qi et al., 2013). In 2004, Takamizawa and co-workers associated the levels of miRNA expression with the disease progression (Takamizawa et al., 2004). They found that expression of the let-7 miRNA was greatly reduced in all lung cancers tested and the patients exhibiting lower expression profiles had a significantly lower survival rate, after potentially curative resection.

In 2005, Calin et al. showed the importance of miRNAs in diagnosing chronic lymphocytic leukaemia (CLL) (Calin et al., 2005). It was reported that miRNA expression profiles could directly discriminate between normal B cells and the malignant disease, in patients with CLL. Since then, the interest in miRNA as biomarkers has grown exponentially. Although, miRNA biomarkers have been most widely characterised in cancer diagnostics, several reports have suggested the potential of miRNAs for the diagnosis of viral infections, neurological disorders and even diabetes (Wang et al., 2016).

It has been shown that miR-199a and miR-210 can reduce replication of HBV virus by binding to the S protein coding region (Zhang et al., 2010a). In a different study, an association between miR-122 and facilitation of HCV RNA replication was reported, where a knock down of miR-122 gene caused almost complete inhibition of viral replication (Jopling et al., 2005, Scaria et al., 2006). Furthermore, it has been reported that over 70 % of miRNA are localised in the brain and frequently mutations in the miRNA processing machinery has been associated with numerous neurological disorders, such as amyotrophic lateral sclerosis or fragile X syndrome

(Cao et al., 2006). miR-9 and miR-134 have been characterised as key players regulating neural development (Zhao et al., 2009, Bavamian et al., 2015). It has been reported that aberrant expression of those miRNA significantly impaired neural differentiation and was associated with numerous neuro-developmental diseases such as Alzheimer's or Parkinson's disease, even schizophrenia (Perkins et al., 2007, Liu et al., 2014a).

Upregulation of 12 miRNAs found in serum, has been linked with type 1 diabetes (Chen et al., 2014). Similarly, miR-23a and miR-126 were reported as potential biomarkers for early detection of type 2 diabetes (Nielsen et al., 2012). Another three serum miRNAs, (miR-132, miR-29a, and miR-222), were found to be associated with gestational diabetes mellitus. miR-278 and miR-375 were reported to regulate insulin secretion, thus these could potentially act as targets for pharmacological treatments of diabetes (Liu et al., 2014b, Wang et al., 2016).

6.1.3 miRNA detection

Since disruption in miRNA expression profiles have been associated with a wide range of different diseases, efficient detection methods could provide valuable insights into disease progression and allow for early diagnosis.

Northern blotting, quantitative real-time PCR and microarrays are currently the standard methods used for the detection of miRNAs (Válóczi et al., 2004, Chen et al., 2005, Li and Ruan, 2009). Most of these technologies have limitations, such as low sensitivity, poor reproducibility questionable specificities, and most are time consuming and require large numbers of samples.

6.1.3.1 miRNA detection using Northern blotting

Before the implementation of PCR or microarray hybridisations, northern blotting had been the most widely used method for analysis of RNA expression (Kevil et al., 1997). In principle, the technology relies on the separation of RNA molecules by electrophoresis. Following RNA separation, capillary transfer of the RNA bands to a nitrocellulose membrane is proceeded by a probe hybridisation and detection steps (**Figure 60**). Probes used in northern blot analysis can be either single-stranded DNA or RNA molecules that are complementary to the RNA of interest. Usually detection of the bound probes occurs through radioactive labelling (^{32}P) or *via* a chemiluminescence reaction, in which alkaline phosphatase or horseradish peroxidase metabolise their substrates to generate a weak light signal that can be detected digitally or by using X-ray films.

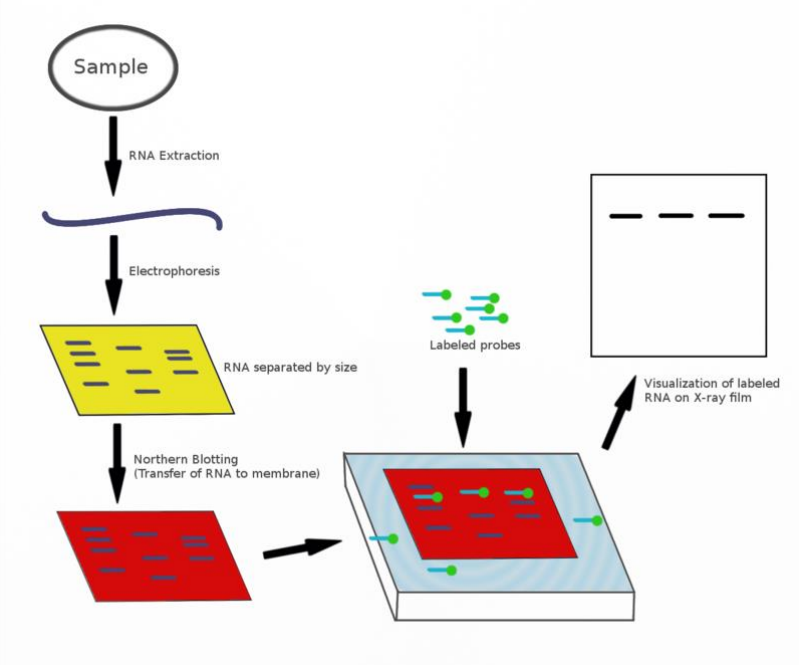

Figure 60. Graphic representation of a typical Northern blot workflow.

Source:
https://en.wikipedia.org/wiki/Northern_blot#/media/File:Northern_blot_diagram.png

A major drawback of the northern blot technique is its low sensitivity to low abundance RNAs. Consequently, large amounts of total RNA are required, which might be problematic when the cells or the source of tested tissue are limited (Streit et al., 2009, Koscianska et al., 2011).

6.1.3.2 qPCR microRNA detection

Ever since its discovery, PCR has become one of the most widely used molecular techniques for studying nucleic acids, including miRNAs (Chen et al., 2005). Current PCR-based methods target the mature miRNA or their precursors and most commonly involves the detection of amplified product using *Taq*man probes (Benes and Castoldi, 2010, Mitchell et al., 2008). In principle, the miRNA molecules are targeted by stem loop primers containing a 3'-overhang complementary to the 5' end of the target miRNA (**Figure 61**). Reverse transcription results in the formation of a cDNA-stem loop structure that can be detected by *Taq*man probing. *Taq*man probes are designed to complement the stem loop and the miRNA of interest. In the second step, a forward primer binds to the cDNA molecule, which initiates synthesis of the complementary strand and amplification results in the hydrolysis of the Taqman probe and emission of the fluorescent signal.

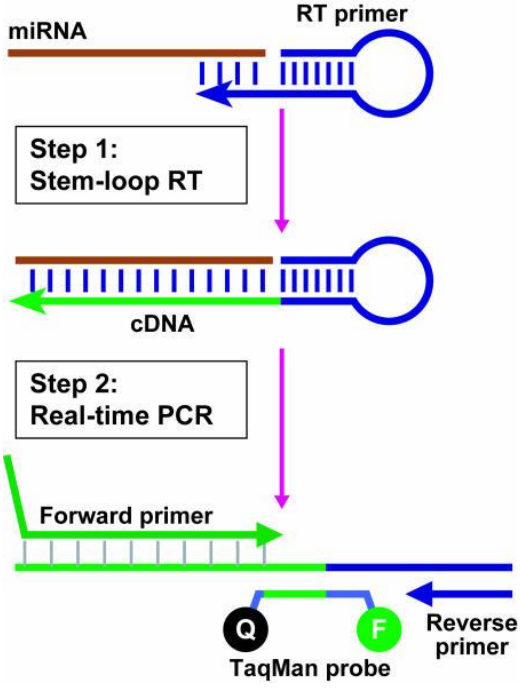

The use of fluorescence-based systems and expensive thermocyclers for miRNA detection can significantly increase the overall cost of analysis.

Figure 61. Graphic representation of a typical real-time PCR for detection of miRNAs using *Taq*man probes and stem-loop primer.

Source: https://www.researchgate.net/figure/7455286_fig1_Schematic-description-of-TaqMan-miRNA-assays-TaqMan-based-real-time-quantification-of

6.1.3.3 miRNA detection using isothermal amplification methods

Several isothermal miRNA amplification methods have been developed over the years since PCR was invented, such as RCA-, SDA- or the duplex-specific nuclease-based techniques (Jonstrup et al., 2006, Zheng et al., 2016, Zhang et al., 2015). Due to LAMPs complicated priming mechanism, the use of this technology has been greatly limited to the amplification of larger DNA and RNA molecules and it has not been exploited for miRNA detection, with the exception of Li et al, who reported a successful use of the LAMP amplification for the detection of miRNA (**Figure 62**). Li et al used the miRNA to replace a displacement primer on one amplification symmetry and claimed the miRNA was necessary to initiate the amplification within this mechanism, it was also claimed the published method was capable of discriminating between different miRNAs and that it could even detect SNPs (Li et al., 2011). This result is quite surprising, as it is well documented that LAMP FIP and BIP primers are predominating primers required for a successful amplification. The Loop and displacement primers only accessorise the LAMP amplification serving to accelerate or increase the overall sensitivity of these assays. Thus, it remains unclear whether the presented method was selective and would be able to detect low abundance miRNAs.

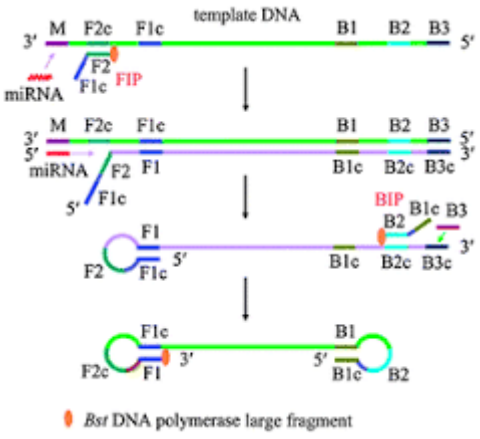

Figure 62. Graphic representation of a LAMP-based miRNA detection approach.

Source: http://pubs.rsc.org/en/content/articlelanding/2011/cc/c0cc03957h/unauth#!divAbstract

6.2 Aims and objectives

Main focus of this study was to develop an isothermal BART assay for more affordable and accessible detection of miRNAs.

In this section, three alternative in-house designed methods of miRNA detection have been explored using loop-mediated isothermal amplification approach.

6.3 Results

In this study, three in-house developed miRNA detection methods utilising the LAMP technology were assessed.

6.3.1 Ligation-mediated miRNA detection

As shown in **Figure 63**, the probe ligation-based miRNA detection technology involves two separate single-stranded probes - each containing a sequence complementary to the target miRNA molecules. Binding of the miRNAs to the probe results in the generation of RNA-DNA heteroduplex with the annealed DNA stem loop probes being separated by a single nucleotide. The DNA stem loops can then be ligated to one another using SplintR ligase, which exhibits increased affinity for heteroduplex templates. Once ligated, the probes take on a dumbbell-like confirmation, which is an intermediate product generated during LAMP. Upon addition of the LAMP primers, the dumbbell can be propagated further generating pyrophosphate (PPi), which is subsequently detected by BART.

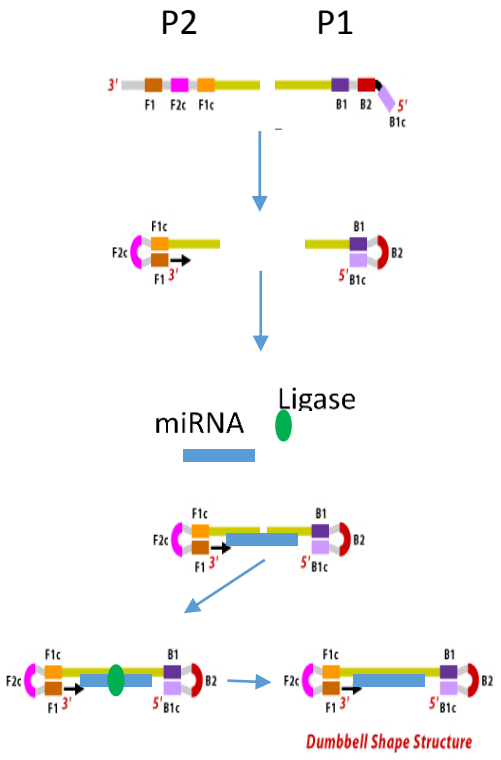

Figure 63. Graphic representation of a in-house designed ligation-based miRNA detection method utilising LAMP technology.

In this design, two probes (P1 and P2) containing the target miRNA recognition sites in the stem regions (yellow) are linked together using a heteroduplex bridge formed between the RNA and the probes. The generated nick is then sealed by a ligase resulting in formation of a complete dumbbell structure.

6.3.1.1 Assessment of the performance of the in-house developed ligation-mediated miRNA detection system

Figure 64 shows LAMP-BART amplification curves generated using the detection probes and CAMV 35Sp LAMP primers. Each reaction component was tested in the presence or absence of the SPLINT R ligase (**Appendix 26**).

The initial analysis showed no amplification of product in the absence of ligation (no ligation control (NLC)), regardless of the reaction component tested (**Figure 64A**). In contrast, positive amplifications were achieved by reactions that were successfully ligated (**Figure 64B**). No peaks were detected in the P1 and P2 reactions where only one type of the probe was used for each assay (**Figure 64B**). Samples containing both probes gave positive peaks regardless of the presence of the target miRNA, where a 10 min delay was observed between the true and the false positives samples.

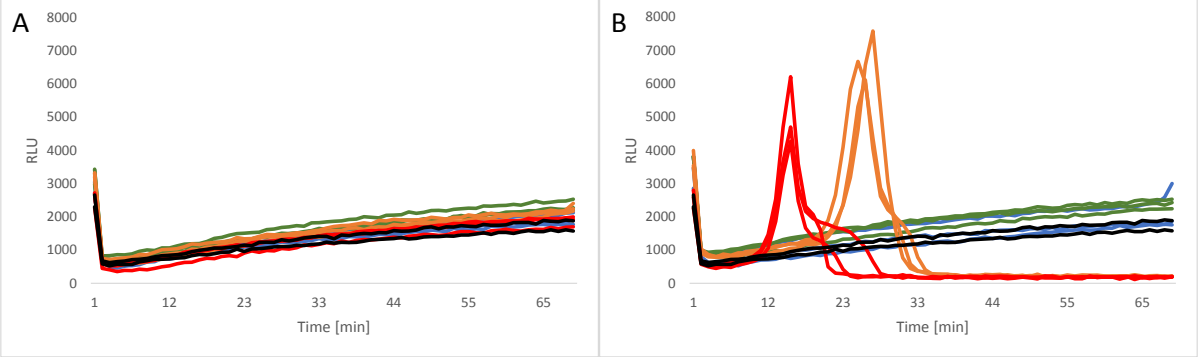

Figure 64. LAMP-BART profiles generated using the ligation-based miRNA approach. A – amplification profiles produced by the reactions lacking SPLINTR ligation step; B – amplification profiles produced by the reaction that undergone ligation in the presence of SPLINTR ligase.

Note: blue peaks – reactions containing P1 template probe; green – reactions containing P2 template probe; orange – reactions containing P1 and P2 template probe; red – reactions containing P1 and P2 template probe as well as the target miRNA; black - NTC

Despite New England Biolabs clear product specification, stating that SplintR ligase, cannot perform ligation of single-stranded DNA molecules, it was evident that ligation of both P1 and P2 probes occurred in a miRNA independent manner. Nonetheless, SDS-PAGE analysis did

not show any ligation products in the samples lacking miRNA (see **Appendix 35**). However, the amount of the ligation product generated in a miRNA-independent manner might have not been sufficient enough to visualise on the PAGE gels.

6.3.1.2 Optimisation of the ligation-mediated miRNA detection system

The initial analysis of the ligase-mediated miRNA detection system showed that non-specific ligation of the probes occurred in a miRNA independent manner. Thus, several ligases were tested in an attempt to improve the specificity of this reaction.

Figure 65 shows the LAMP-BART profiles generated using the ligation-mediated miRNA method under different chemistries. Once more, no amplification profiles were generated in reactions deficient in ligase, proving that no prior contamination of the probes had occurred with the post-ligation products (**Figure 65E**). Only the reactions utilising Ampligase did not generate false positive amplifications (**Figure 65D**) in the absence of miRNA, within the time frame of analysis. The amplification observed with ampligase was significantly delayed compared to reactions performed with either T4 or SplintR ligase (**Figure 65A-B**; *p values* < 0.05, t-test). The reactions containing T7 ligase showed no significant difference in observed polymerisation rates, whether the miRNA was included or excluded from the reaction. The T4 and SplintR-mediated ligations worked most efficiently in the presence of the target miRNA, generating positive results within 17 min (**Figure 65A-B**). The assays utilising the SplintR ligase generated the quickest rates of true amplification, but also a greater delay in non-specific amplification (**Figure 65B**). In contrast, a slight difference in amplification times were noted between miRNA dependent and independent controls, when the T4 ligase was used (**Figure 65A**).

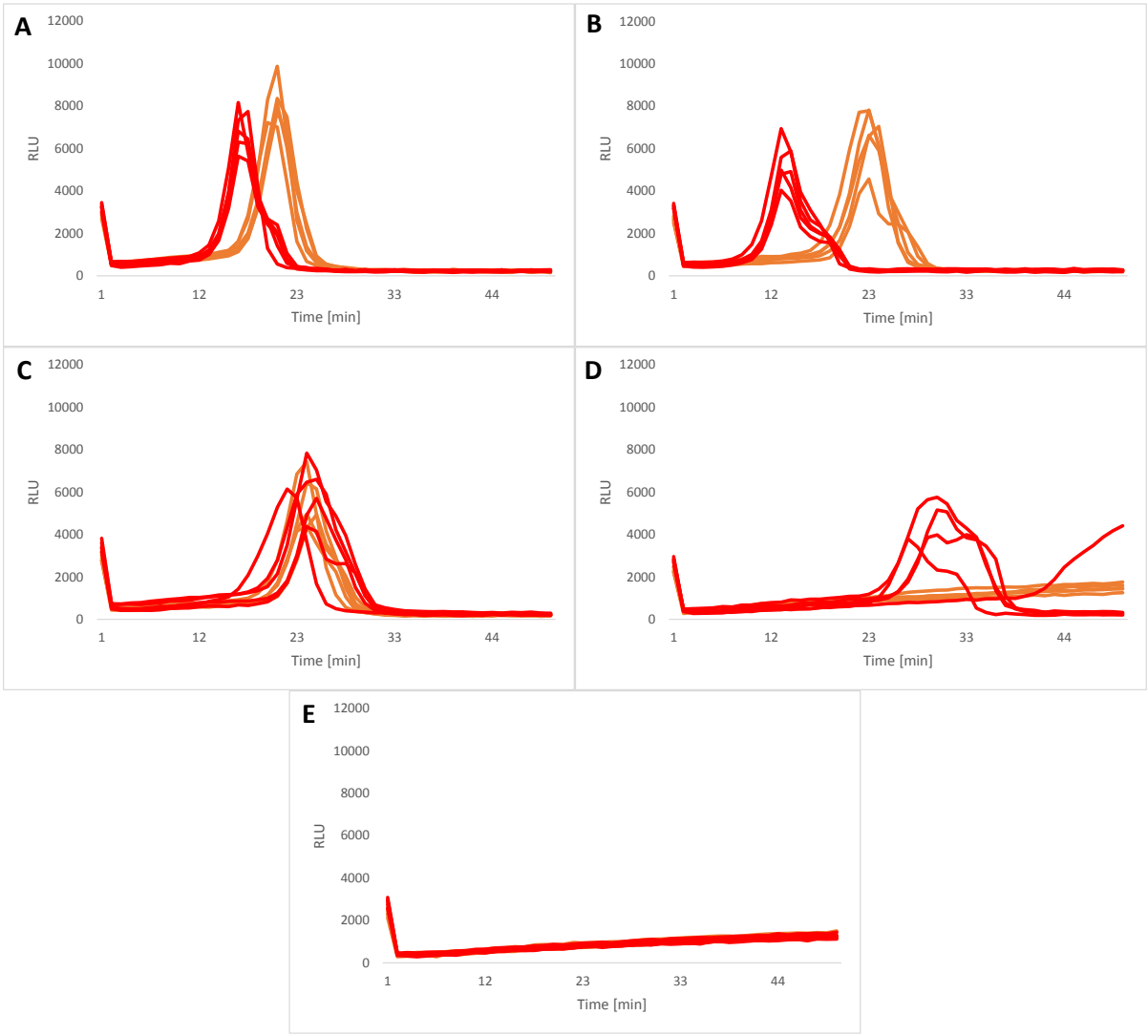

Figure 65. LAMP-BART profiles generated using the ligation-based miRNA approach comparing performance of four chosen ligase enzymes.

A – T4 ligase; B – SplintR ligase; C – T7 ligase; D – Ampligase; E – No ligation control (NLC)

Note: red curves represent reactions containing the target miRNA; orange curves shows amplification profiles generated in the absence of the miRNA target.

In this section, various attempts were made to further improve the ligation of probes, in a manner that was dependent on miRNA.

Figure 66 shows BART reported LAMP amplifications during a time course study. In this study, the reactions have undergone ligation (using the SplintR ligase) at room temperature for 5 or 30 min.

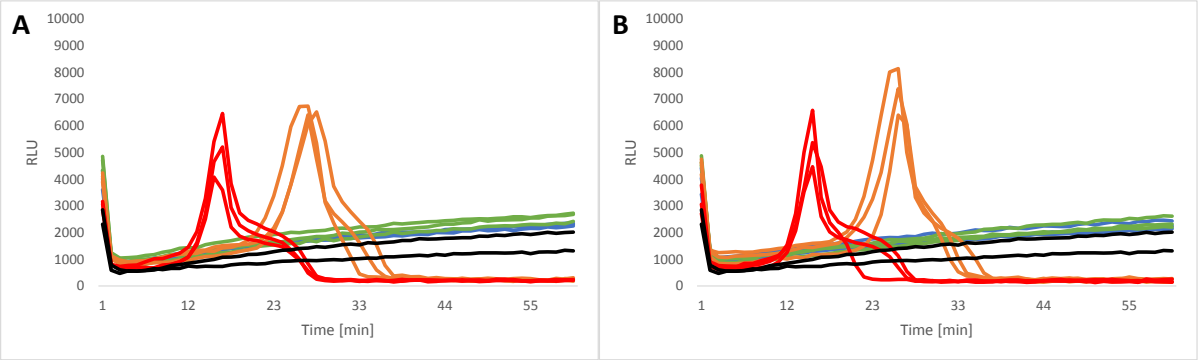

Figure 66. LAMP-BART profiles generated using the ligation-based miRNA approach. A – amplification profiles produced by the reactions containing samples that undergone 5 min ligation using SplintR; B – amplification profiles produced by the reaction containing samples that undergone 30 min ligation using SplintR.

Note: blue peaks – reactions containing P1 template probe; green – reactions containing P2 template probe; orange – reactions containing P1 and P2 template probe; red – reactions containing P1 and P2 template probe as well as the target miRNA; black - NLC

The no ligation control (NLC) reactions and the samples containing separate P1 and P2 probes did not generate any BART reported amplification, regardless of the duration of ligation. When a mixture of P1 and P2 underwent a ligation, positive BART profiles were observed, indicating amplification, and presumably successful ligation, although this was not dependent on the presence of the miRNA template (**Figure 66A-B**). Moreover, when the miRNA was added to the ligation reactions, a 10 min reduction in the amplification time was observed, compared to reactions lacking the target miRNA template (p *value* < 0.05, t-test), suggesting an increase in efficiency of ligation. The duration of the ligation step did not affect the amplification kinetics when the probes and miRNA were present together in the reaction chemistry (p *value* > 0.05, t-test). However, a 2 min increase in the rates of positive amplification was observed between

the 5 and 30 min ligation time (*p value* < 0.05, t-test); the increased ligation time therefore improves the rate of amplification (**Table 28**). To further increase the time differential in amplification kinetics observed between true and false positive polymerisations, the concentration of probe used in the reaction was optimised.

Table 28 showing summary data presented in the **figure 66**. Each set of reactions was analysed using average TTM (Mean), reproducibility (STDev) and sensitivity (Amp.Freq).

Ligation time [min]	Sample	TTM [min]	Stdev	Amp.Freq. [%]
5	P1	N/A	N/A	0
	P2	N/A	N/A	0
	P1+P2	27.2	0.6	100
	P1+P2+microRNA	15.8	0.6	100
30	P1	N/A	N/A	0
	P2	N/A	N/A	0
	P1+P2	25.8	0.0	100
	P1+P2+microRNA	15.0	0.0	100

Figure 67 shows a summary bar chart of the probe concentrations used in this study.

It may be of interest to note that the probe concentrations shown, represent the final concentration of each probe in the ligation reactions.

The probe concentration did have an effect on the amplification kinetics, but this was independent of the template miRNA. False positive reactions were also affected by probe concentrations to a much greater extent than true positive reactions (**Figure 67**).

A significant reduction in amplification speed of 3 min was observed for the true positive amplifications, between 500 nM and all the other concentrations tested (*p value* < 0.05, t-test) (**Table 29**). Reactions containing 1 to 50 nM of each probe did not show any significant difference in amplification kinetics for the miRNA dependent reaction (*p value* > 0.05, ANOVA). A further reduction in probe concentrations to 0.5 nM, did reduce the miRNA

dependent amplification speed by 8 min compared to all other concentrations tested (*p value* < 0.05, t-test).

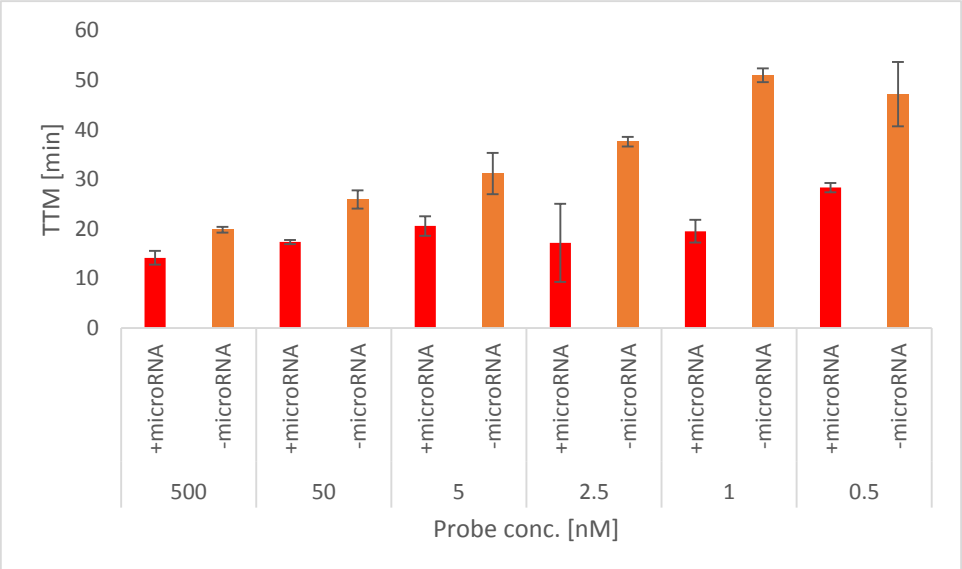

Figure 67. Summary bar chart generated using the ligation-based miRNA approach with various amounts of the P1 and P2 probes added during the ligation stage.

Table 29 showing summary data presented in the **figure 67**. Each set of reactions was analysed using average TTM (Mean), reproducibility (STDev) and sensitivity (Amp.Freq).

Probes conc. [nM]	Sample	TTM [min]	Stdev	Amp.Freq. [%]
500	+microRNA	14.18	1.40	100
	-microRNA	19.86	0.59	100
50	+microRNA	17.36	0.44	100
	-microRNA	25.93	1.85	100
5	+microRNA	20.61	1.97	100
	-microRNA	31.16	4.18	100
2.5	+microRNA	17.20	7.86	100
	-microRNA	37.60	0.96	100
1	+microRNA	19.53	2.30	100
	-microRNA	51.02	1.39	67
0.5	+microRNA	28.34	0.96	100
	-microRNA	47.21	6.49	80

Similarly, when the probe concentration was reduced below 500 nM, false positive reaction rates reduced. Unlike the miRNA dependent amplifications, which did not show any significant reduction in assay kinetics between 1 and 50nM, the false positive reaction was slowed-down by decreasing the concentration of probe used.

Additional reductions in probe concentration did not show any further improvements with respect to amplification kinetics or specificity. The probe concentration therefore significantly affects the rate of positive and negative amplification and reducing the amount of probe serves to reduce positive amplification rates, but also improves the ability to differentiate between BART timings resulting from true positive and nonspecific reactions.

In summary, amongst all of the probe concentrations tested, the biggest time difference between the true and false amplification of over 30 min was observed in the reactions containing 1 nM of each probe, whereas, on average, only 5, 8, 11 and 19 min difference was detected in the reactions utilising 500, 50, 5, 2.5 and 0.5 nM of each of the probes, respectively.

The sensitivity of the ligation-mediated miRNA detection system was assessed on a range of miRNA template concentrations (**Figure 68**). This experiment successfully detected as little as 125 fM of the target miRNA; a clear difference in amplification time (of 8 min) was observed between the lowest copy number of miRNA tested and the template independent amplification time. The amplification time also decreased with increasing copies of miRNA tested, and all amplifications times were very reproducible at each respective concentration tested. It is also interesting to note that the given sensitivity represents detectible concentrations of the miRNA in the final LAMP-BART assay. The true analytical LoD of the ligation reaction was 50 pM (125 fM in the assay).

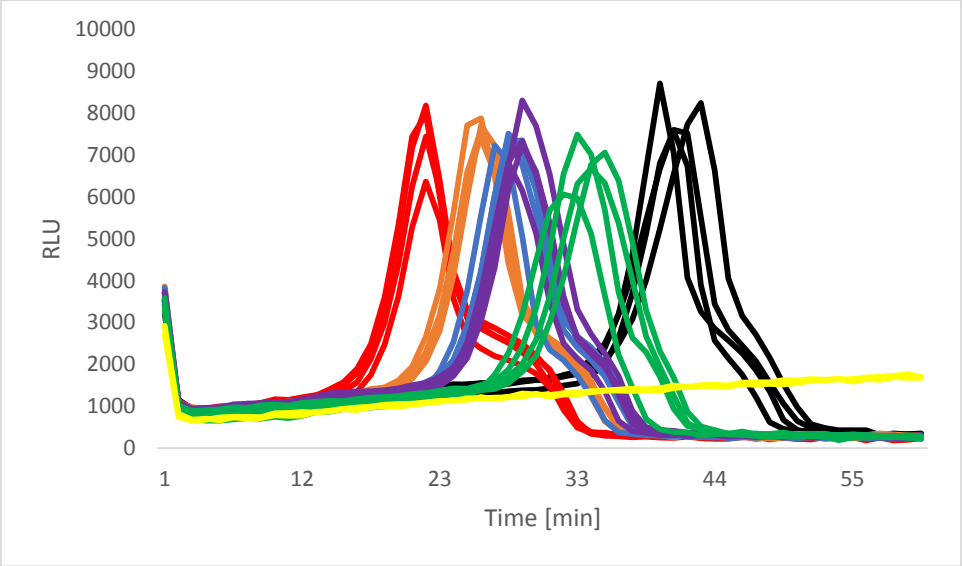

Figure 68. LAMP-BART profiles generated using the ligation-based miRNA approach and various amounts of the target miRNA.

Note: red curves – 500 nM miRNA; orange – 50 nm miRNA; blue – 5 nM miRNA; purple – 500 pM miRNA; green – 50 pM miRNA; black – no miRNA control.

The concentrations of target miRNA shown represent the amounts of target added to each ligation reaction not the final assay concentration. Analytical (assay) sensitivity is 400 x higher taking into account 100 and 4 fold dilutions of ligation mix and sample

6.3.2 Endonuclease-mediated miRNA detection

Figure 69 shows the restriction enzyme mechanism of miRNA detection in a closed-tube format, which involves binding of the target miRNA to a single-stranded dumbbell probe with the target recognition site at the 3' end, followed by its extension by the Bst DNA polymerase. Synthesis of the complementary strand then generates a restriction site (between the miRNA and the F2 site of the forward loop; black striped rectangle), LAMP primer binding site (green striped rectangle); as well as the displacement primer binding site (brown striped rectangle). Restriction of DNA using BstUI ensures that the product of strand invasion by the LAMP primer will terminate at an exact predefined position, in-order to prevent miss-folding of the generated dumbbell structure.

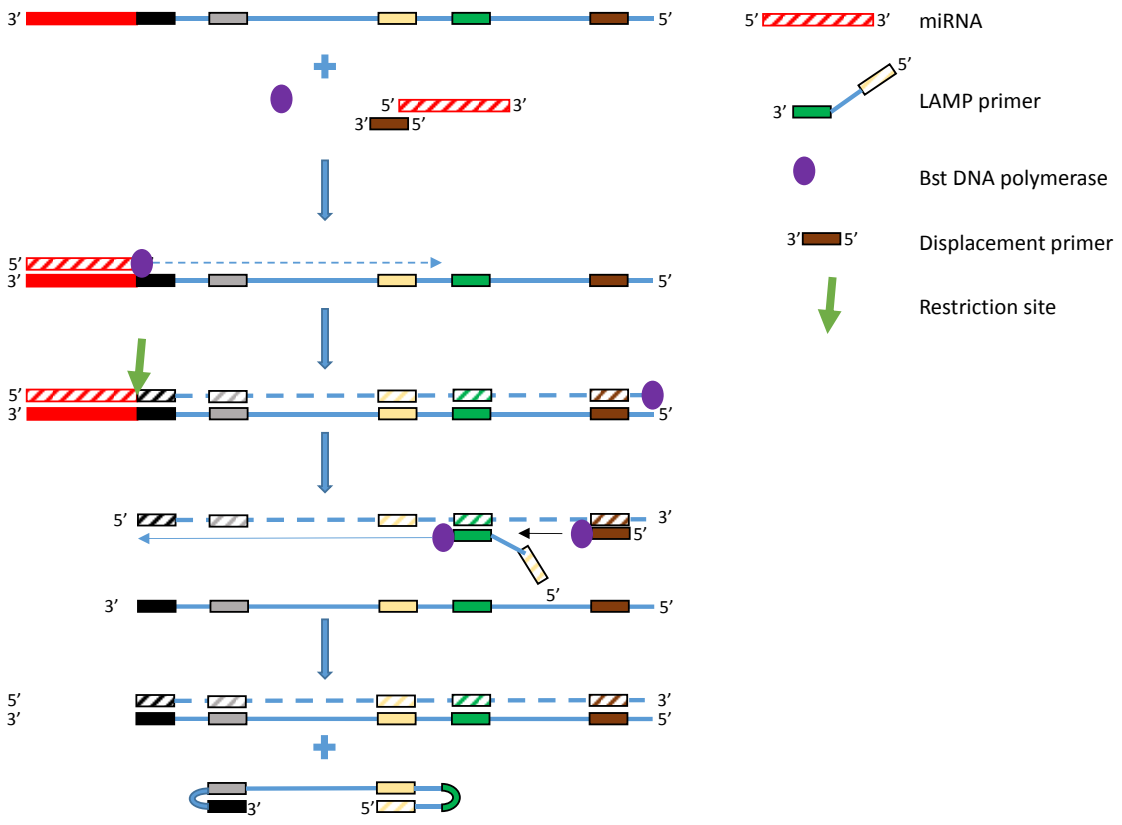

Figure 69. Graphic representation of an in-house designed endonuclease-based miRNA detection method utilising LAMP technology.

Synthesis of the complementary strand is initiated by the target miRNA hybridisation to the recognition site (red rectangle). Once a double-stranded product is generated, the restriction site between the miRNA and the F2 binding sites (black rectangle) is recognised by a specific restriction enzyme (BstUI)(green arrow). The restriction digest results in generation of a double stranded DNA product with both LAMP and displacement binding sites (green and brown striped rectangles). Strand invasion by the two primers results in a formation of single stranded dumbbell.

6.3.2.1 Assessment of the performance of the in-house designed restriction endonuclease-mediated miRNA detection system

Performance of the restriction enzyme-mediated miRNA detection system, was assessed in this study. Various restriction enzymes (BssKI, BstUI, BstWI and BsaWI) were tested, in order to determine the most suitable candidate enzyme to couple with the LAMP-BART reaction.

Figure 70 shows polyacrylamide gel results of a 10 min restriction digest performed using four restriction enzymes. The restriction digest was tested using both, LAMP-BART and NEB buffering conditions in this study. The performance of each enzyme was assessed by looking at the brightness of the DNA bands and fragmentation before and after digestion. Surprisingly, all of the restriction enzymes performed more efficiently under the LAMP-BART chemistry compared to NEBs recommended conditions. (**Figure 70 lanes E-H**). BssKI restricted the DNA more efficiently than the other enzymes tested under NEB recommended conditions (**Figure 70 lanes B and F**); under the LAMP-BART buffering conditions, the BstUI enzyme was found to be the most efficient.

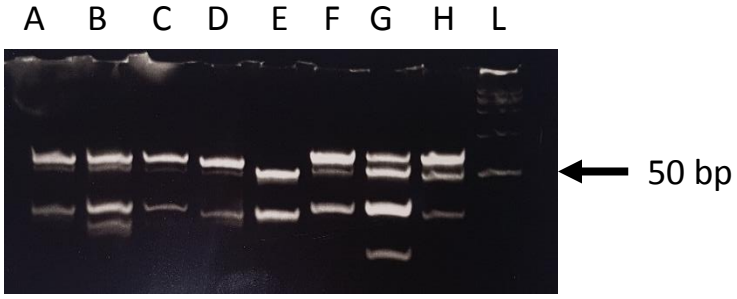

Figure 70. Polyacrylamide gel electrophoresis showing restriction digest of 4 in-house designed double-stranded DNA probes.

Lanes A-D show restriction digests carried out in recommended buffers; lanes E-H shows restriction digest performed under LAMP-BART chemistry (enzyme constituents of LAMP-BART were not added). Lanes A and E – BstUI; lanes B and F – BssKI; lanes C and G – BsaWI; lanes D and H – BstNI; lane L contained 50bp ladder (NEB). Refer to **Appendix 42** for undigested controls.

After digestion, very little evidence was left of the initial template on the polyacrylamide gel, with only 2 lower molecular weight bands evident, and this indicated complete digestion of the

original template DNA. BssKI and BstWI were the least efficient of the restriction enzymes tested (**Figure 70 lanes B and F, D and H**). BsaWI generated good quantities of digested product but was not considered for the miRNA amplification due to its non-specific restriction cutting, reflected in the observed star activity and the generation of a small MW 4th band (**Figure 70 lane G**).

Figure 71 shows LAMP-BART profiles generated using the BstUI-mediated (endonuclease) miRNA detection system.

Surprisingly, positive amplification profiles were detected whether the miRNA was included in the reaction or not. The same amplification rates were also detected in the NTC samples, suggesting possible contamination of the reagents.

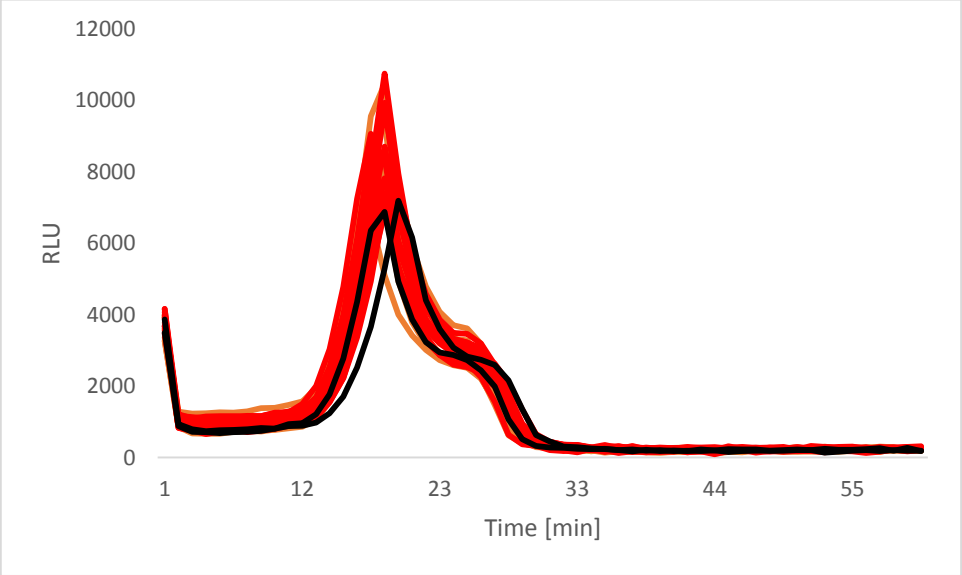

Figure 71. LAMP-BART profiles generated using the endonuclease-based miRNA detection system. Red curves represent the reactions containing the target miRNA; orange curves show profiles generated in the absence of the target miRNA; black curves represent reactions lacking both the miRNA and the detection probe. Note that all of the reactions contained 8 U of BstUI restriction enzyme and 1.6 and 0.8 uM LAMP and displacement primer, respectively.

A similar experimental set up, using the same aliquots of reagents, was then performed and comparable observations were made.

Figure 72 shows LAMP-BART profiles generated using BstUI mediated miRNA detection chemistry. Note that the amount of enzyme in each reaction, was 5x lower than previously used. In addition, no BstUI was added to the NTC control samples.

No difference in TTM was detected between the true and false positive profiles, generated using BstUI. Reducing the BstUI 2-fold, caused a 5 min delay in amplification time compared to assays utilising 1.6 U (**Figure 72A-B**). Despite the reduced speed no discrimination between miRNA dependent and independent amplifications was possible.

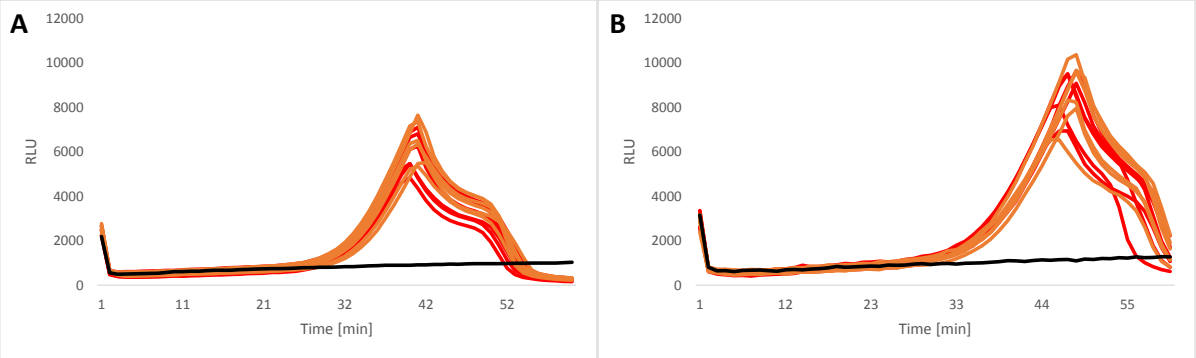

Figure 72. LAMP-BART profiles generated using the endonuclease-based miRNA detection system. Red curves represent the reactions containing the target miRNA; orange curves show profiles generated in the absence of the target miRNA; black curves represent reactions lacking both the miRNA and the detection probe as well as the restriction enzyme. A – amplification profiles generated with the reactions containing 1.6 U BstUI; B – amplification profiles generated using 0.8 U BstUI

Interestingly, when BstUI was completely eliminated, no amplification was observed in the reactions lacking the miRNA, yet the true positives were successfully detected (**Figure 73**). The amplifications are therefore working independently of the restriction enzyme.

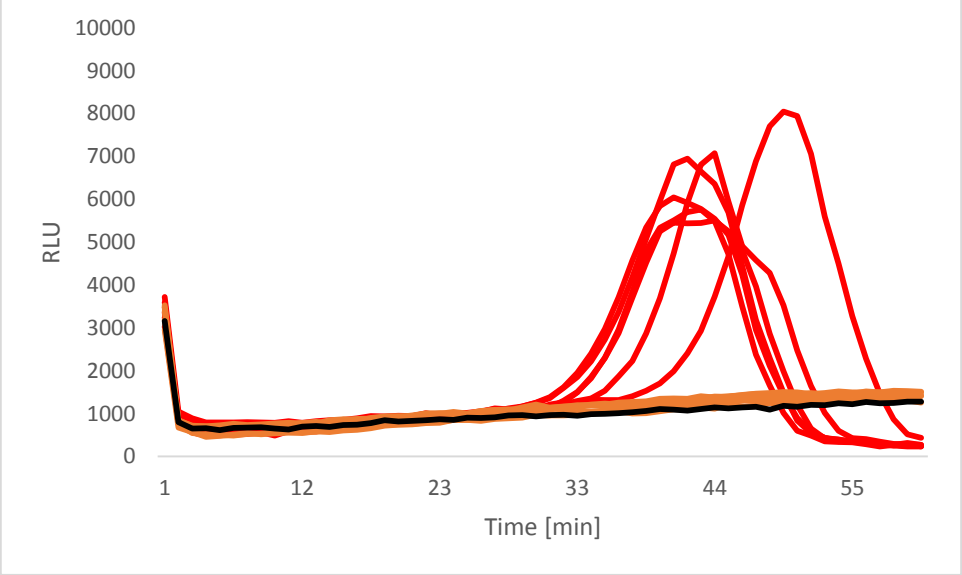

Figure 73. LAMP-BART profiles generated using the endonuclease-based miRNA detection system. Red curves represent the reactions containing the target miRNA; orange curves show profiles generated in the absence of the target miRNA; black curves represent reactions lacking both the miRNA and the detection probe. Note that the BstUI restriction enzyme was not present.

6.3.3 Nickase-mediated miRNA detection

As shown in **figure 74**, the nicking enzyme mediated method is very similar to the previously described miRNA detection technique (**Figure 69**). Instead of removing the fragment of miRNA bound to the dumbbell probe, a single-stranded nick is generated between the miRNA and the F2 site (red and black striped rectangles, respectively (**Figure 74**)). DNA polymerase then binds to the nick site and proceeds with extension and displacement of the synthesised strand which now contains the LAMP and the displacement binding sites. From this point onwards, the DNA synthesis proceeds as described in the endonuclease-mediated miRNA detection method (see above for details). In contrast with the previous method, nicking enzyme should allow continuous generation of single-stranded complementary to the probe DNA fragments that can be targeted by the LAMP and displacement primers. This could increase the sensitivity of the entire system since several dumbbell structures could be generated from a single miRNA binding event.

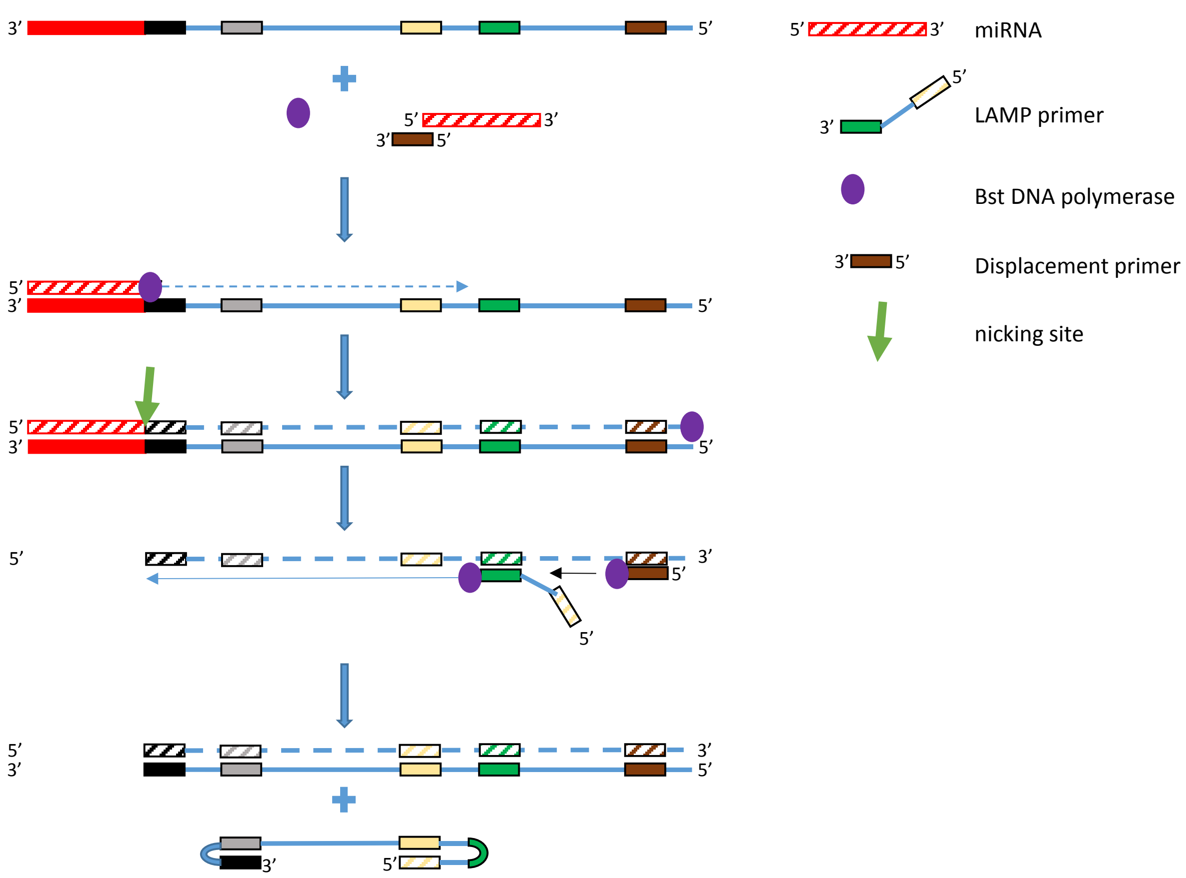

Figure 74. Graphic representation of an in-house designed nickase-based miRNA detection method utilising LAMP technology.

Synthesis of the complementary strand is initiated by the target miRNA hybridisation to the recognition site (red rectangle). Once a double-stranded product is generated, the nickase recognition site between the miRNA and the F2 binding sites (black rectangle) is recognised by the chosen enzyme (green arrow) which introduces a single stranded break (a nick). Bst DNA polymerase binds to the nicks initiating synthesis of the complementary strand resulting in generation of a double stranded DNA product with both LAMP and displacement binding sites (green and brown striped rectangles). Strand invasion by the two primers results in a formation of single stranded dumbbell. This process can potentially be repeated throughout the duration of the assay since the miRNA recognition site is not removed upon nicking.

6.3.3.1 Assessment of the performance of the in-house developed nickase-mediated miRNA detection systems

The performance of the nicking enzyme-mediated miRNA detection was then tested. The mechanism described earlier is known to be similar to the restriction mediated miRNA mediated detection method that could not differentiate between the reactions containing miRNA and the false positives (**see Figure 75**).

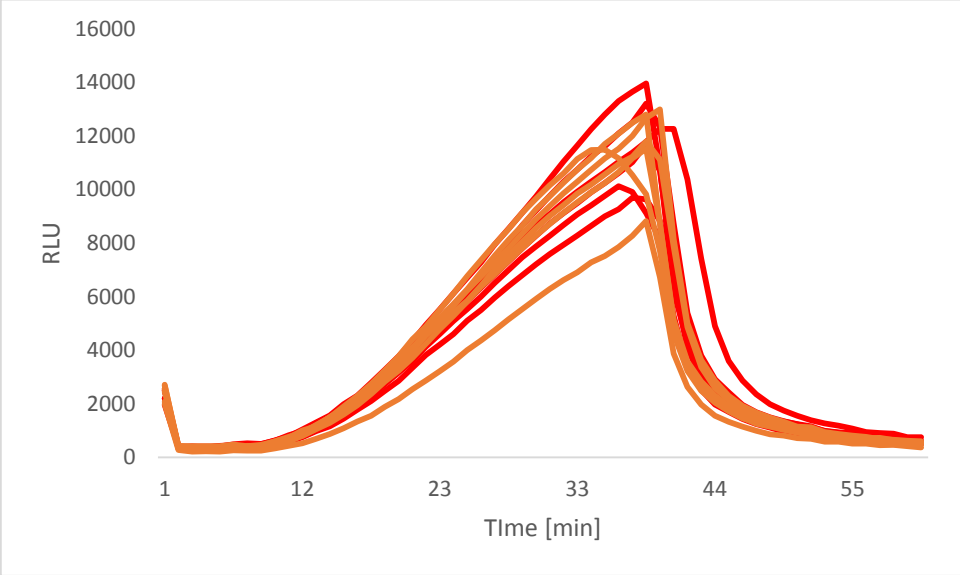

Figure 75. LAMP-BART profiles generated using the nickase-based miRNA detection system. Red curves represent the reactions containing the target miRNA; orange curves show profiles generated in the absence of the target miRNA. Note that each amplification reaction was performed in the presence of 1 U of Nb.bsmI nickase.

Figure 76 shows LAMP-BART profiles generated using the standard nickase-mediated miRNA reactions prepared in the presence or absence of the Nb.BsmI nicking enzyme. All reactions contained equal amounts of detection template. Amplifications were not observed in the NTCs (no detection template, no nicking enzyme), nor in the reactions lacking the Nb.BsmI nickase. In contrast, reactions containing the miRNA were detected when nickase was added.

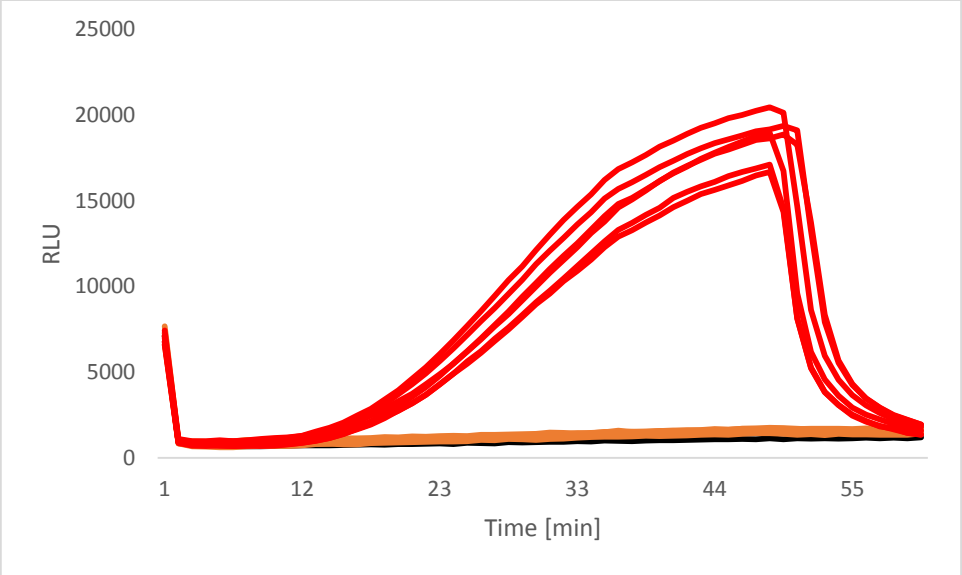

Figure 76. LAMP-BART profiles generated using the nickase-based miRNA detection system. Red curves represent the reactions containing the target miRNA and 1 U Nb.bsmI nickase; orange curves show profiles generated with the reactions containing miRNA in the absence of the nicking enzyme; black curves represents reactions lacking both the miRNA and the nicking enzyme.

Figure 77 shows LAMP-BART profiles generated using the standard nickase-mediated miRNA assay. In this experiment, the nicking enzyme was heat-inactivated in order to exclude possible contamination. No amplification was observed suggesting the requirement for an active nicking enzyme to generate false positive amplification profiles.

Further investigations demonstrated that the false positive amplification profiles was nickase-dependant, but also required a DNA polymerase. In addition, false positive amplification was found to be independent of primer, detection template and miRNA.

Figure 78 shows LAMP-BART profiles generated using the nickase-mediated miRNA assay in either the presence or absence of the Bst2.0 DNA polymerase. All assays were performed in the absence of miRNA. No detectable amplification was observed in reactions lacking Bst 2.0 DNA polymerase; this data suggests that the formation of the false positive amplifications requires the both the nickase and DNA polymerase.

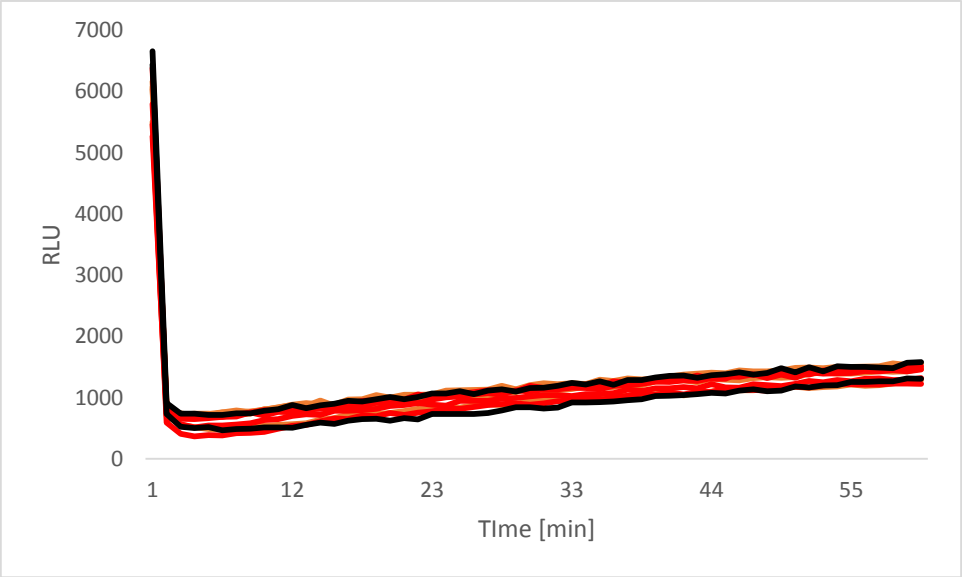

Figure 77. LAMP-BART profiles generated using the nickase-based miRNA detection system. Red curves represent the reactions containing the target miRNA and 1 U of heat-inactivated Nb.bsmI nickase; orange curves show profiles generated with the reactions containing miRNA in the absence of the nicking enzyme; black curves represents reactions lacking both the miRNA and the nicking

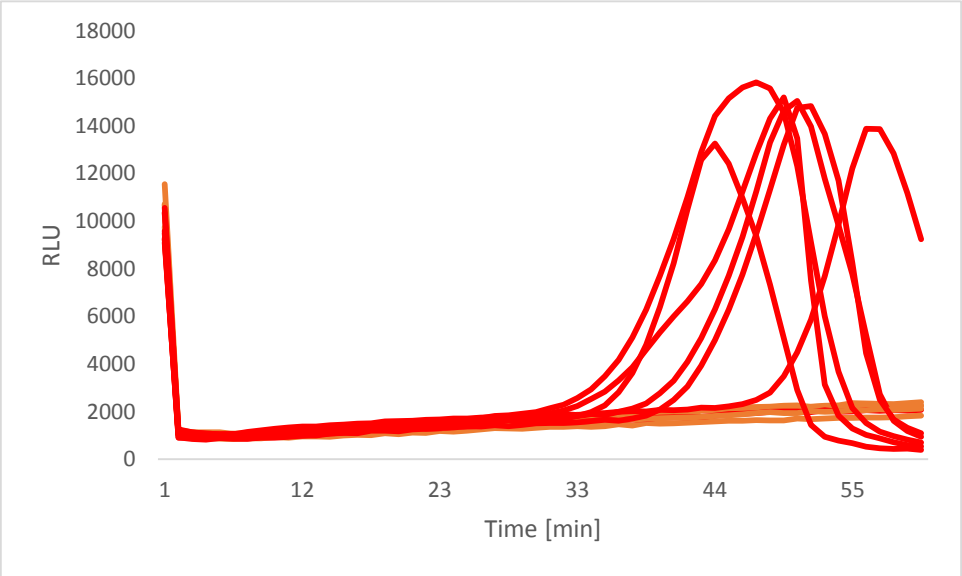

Figure 78. LAMP-BART profiles generated using the nickase-based miRNA detection system. Red curves represent the reactions containing Bst 2.0 DNA polymerase and 1 U Nb.bsmI nickase; orange curves show profiles generated with the reactions containing the nicking enzyme only.

Figure 79 shows LAMP-BART amplification curves generated using further controls of the nickase-mediated miRNA assay, where no detection template, primers and the target miRNA was added to the reactions.

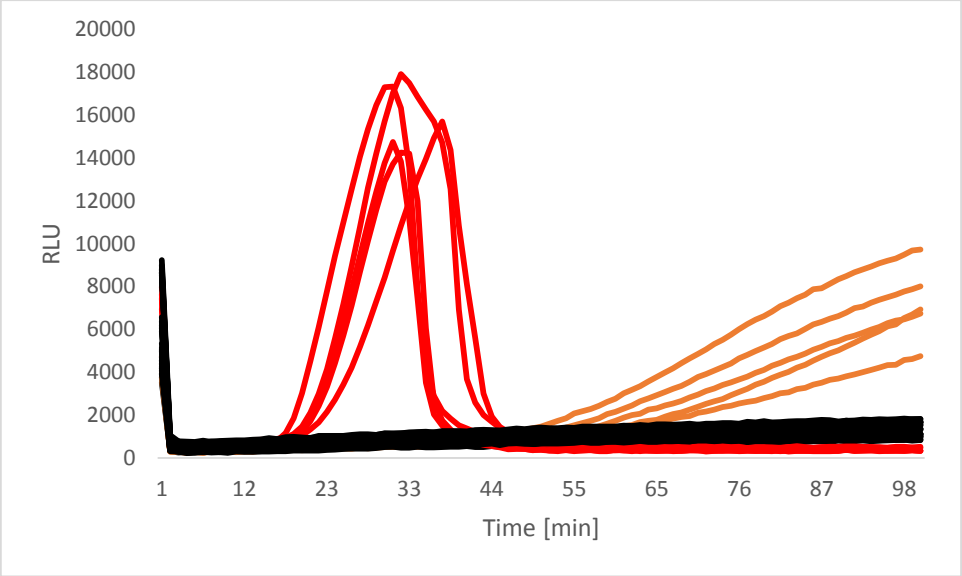

Figure 79. LAMP-BART profiles generated using the nickase-based miRNA detection system. Red curves represent the reactions containing active Nb.bsmI nicking enzyme; orange curves show profiles generated with the reactions containing the inactive version of the nicking enzyme that undergone pre-incubation; black curves represent reactions lacking Nb.bsmI nickase

In this study, the nicking enzyme was pre-incubated in a LAMP-BART reaction mixture, in the absence of Bst2.0, for 60 min at 60 °C followed by a heat-inactivation step. Two sets of reactions were then investigated, under a standard LAMP-BART set up (including Bst 2.0) where either the non-treated or the inactivated version of the nickase was used. It was already demonstrated, the reactions containing the non-treated version of the nickase showed typical amplification profile generated in a template- and miRNA-independent manner. Interestingly, positive amplifications were also detected in the samples utilising the heat-treated version of the nickase, although the amplification profiles differed considerably. The amplification in these controls were not only noticeably delayed, but also exhibited much slower assay kinetics with only gradual increases in BART over the course of the assay. In contrast, the BART switch off was extended with respect to a typical BART when the active version of the nickase was used.

Due to the non-specific effect that BstUI and Nb.BsmI nickase had on the BART reporter, a number of different endonucleases were tested under non-primer and detection template conditions.

Figure 80A-B demonstrates LAMP-BART profiles generated using the endonuclease / nickase-mediated miRNA assay using either Bst 1.0 (**A**) or Bst 2.0 (**B**) and six chosen endonucleases.

All of restriction and nicking enzymes showed similar non-specific activities to that already observed. Despite the lack of primers and the detection template, all of the reactions containing these enzymes generated positive amplification profiles, and this was also regardless of the type of the Bst DNA polymerase used. In addition, the reactions containing the DNA polymerase only (NTC) or lacking both the endonucleases and DNA polymerases (NEC), showed no signs of reactivity.

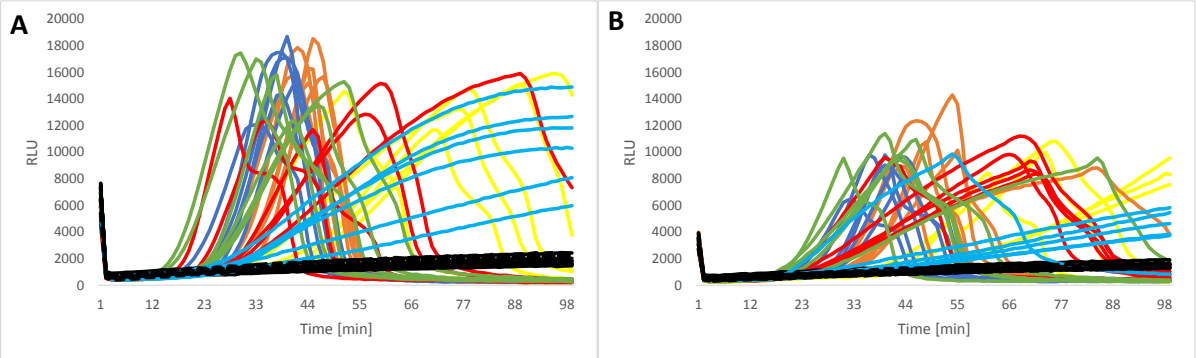

Figure 80. LAMP-BART profiles generated using the endonuclease-based miRNA detection system. A – represents the reactions utilising Bst large fragment and various endonucleases; B – represents reactions containing Bst 2.0 and various endonucleases.

Tested endonucleases were colour-coded as follows : yellow – BsaWI; orange – BssKI; dark blue – BstNI; red – BstUI; green – Nb.bsmI; light blue – Nt.bstNBI; black solid curves – No enzyme control (NEC); black dashed lines – no endonuclease

It was evident from this data that the type of DNA polymerase used did not affect the potential of each restriction or nicking enzyme to cause mis-amplification events. However, small differences in kinetics were observed between the profiles generated using Bst 1.0 and Bst 2.0 with the latter producing slower and shorter peaks.

6.4 Discussion

Recent advances in nucleic acid amplification technologies have resulted in a wide range of isothermal techniques being commercialised as molecular diagnostic assays (Craw and Balachandran, 2012). Of all the well-known isothermal amplification technologies, LAMP assays are the most prolific and well suited for a variety of diagnostic applications (Kiddle et al., 2012, Njiru, 2012, Li et al., 2011). The very design of the LAMP, and its reliance on a number of priming positions, makes this technology highly specific for the target of interest, but paradoxically prone to false positive backgrounds that can be caused by non-template amplifications (Tan et al., 2008). LAMP is highly sensitive and capable of detecting very small amounts of target template and is not prone to interference from non-template carrier DNA present in extracted samples, which makes this technology particularly suitable for GM detection, where the target concentration can be very limiting in high backgrounds of DNA (Kiddle et al., 2012). Since traditional LAMP requires a highly complex primer design, the adaption of this technology for miRNA screening has been immensely challenging, as will be discussed.

6.4.1 Ligation-based miRNA detection system

The results presented earlier demonstrate that it is possible to generate a LAMP intermediates (dumbbell-like structure) *via* a probe ligation-mediated strategy. This not only eliminates the need for a complex primer design, but also affords this technique reasonable analytical sensitivity. To test the viability of this and other miRNA detection systems lin-4 miRNA (one of the first discovered miRNA expressed by *Caenorhabditis elegans*) was selected and artificially synthesized as a model template (Esquela-Kerscher, 2014). Although the initial assessment of the ligation detection method showed this technology capable of detecting the target lin-4 microRNA, false positive results were routinely obtained.

It was demonstrated that the amplification efficiency and specificity was dependent on the efficiency of the ligation, the ligase used and the amount of probe in the reaction. The time difference of the LAMP-BART profiles generated by the true and the false positive samples ranged between 4 to 6 min, which had a significant impact on the dynamic range of this amplification mechanism. Several steps were taken to determine the cause of the false positive amplifications and to design methods for their control. **Figure 64** shows LAMP-BART profiles generated using different ligation reactions containing various combinations of the probes. It was demonstrated that only when both probes (with or without the target miRNA) were present during the ligation step, false positive peaks could be detected, suggesting the possibility of ligation events occurring in the absence of miRNA. As the proposed mechanism was entirely dependent on a miRNA driven ligation further work was undertaken to improve the specificity of the technique. Reducing the concentrations of each probe had a significant effect on the mis-amplification (**Figure 67**), a result that may be explained by the effect of molecular crowding on probe proximity and efficiencies of the miRNA independent ligation. Dilution of the probes prior to the ligation step had little effect on the detection time for the samples containing the target miRNA and this consequently increased the dynamic range of the method (**Figure 67-68**).

Our current probe ligation-mediated methodology, successfully detected as little as 125 fM of the target RNA within 40 min. Despite the analytical sensitivity demonstrated, biological samples, such as blood will pose additional problems for this type of technology, as the amount of available miRNA may be far more limiting than tested here (Parasramka et al., 2012). This technology may however afford increased resistance to inhibition compared to PCR based approaches, as LAMP and its associated displacement polymerase tolerate classical sample derived PCR inhibitors, such as haem, collagen or salts far more effectively than *Taq* polymerase (Kiddle et al., 2012).

In 2016, a ligation-based LAMP miRNA detection method was published by Du et al. that was based on a very similar ligation approach (Du et al., 2016). In his design, the dumbbell structure was also generated *via* ligation of two separate probes using a miRNA target, as a linker template. However, unlike our design, Du's method required the reverse transcription of the miRNA in order to successfully carry out the ligation. Thus, this method incorporated an additional step into the workflow, which increased the overall time required for detection compared to our assays. Similarly, to our findings, false positive results were also obtained in the reactions containing LAMP probes only suggesting miRNA-independent ligation events have occurred.

Although we showed that our current probe ligation-based system can successfully detect picomolar concentrations of miRNAs further optimization is required in order to enhance its sensitivity and specificity, as well as establishing its performance on template extracted from relevant biological samples.

6.4.2 Endonuclease-based microRNA detection

Unfortunately, both the restriction endonuclease and nickase-mediated methods for miRNA detection assessed failed to detect the target miRNA within a satisfactory time frame. Both restriction and nicking enzyme methods generated false positive results regardless of the presence of the miRNA.

Nonetheless, our work has shown a unique feature of both DNA polymerases when used in conjunction with endonucleases, as this coupling of activities appears to be capable of *de novo* DNA synthesis in the absence of templates and primers. There are several reports in the press regarding the same *de* novo synthesis, although it is unclear how the process is initiated (Antipova et al., 2014, Liang et al., 2004). For instance, Liang et al, suggested a potential mechanism of *de novo* amplification. In his model, short DNA fragments containing

palindromic repetitive sequences are *de novo* synthesised and then elongated by strand displacing DNA polymerases, which form long repetitive stretches of double-stranded DNAs. Those long molecules are then subjected to restriction or nicking digest that in turn generates more substrate for elongation. In concordance with our findings, Liang and co-workers have shown that DNA synthesis was not affected by nuclease treatment of any of the components used, suggesting a *de novo* origin of the template rather than a result of a pre-existing contamination of the enzymes used. Liang hypothesised that the DNA polymerase used in his studies was responsible for the *de novo* synthesis. Consequently, he showed that incubation of Vent DNA polymerases in the presence of dATP and dTTPs for 3 days could generate detectible amounts of short DNA fragments. Moreover, Ramadan et al. found that human DNA polymerase λ or deoxyribonucleotidyl transferase could synthesise DNA fragments *de novo* even in a presence of a single type of nucleotide such as dTTP (Ramadan et al., 2004).

The rate of de-novo synthesis described was extremely slow and could not explain the kinetic profiles generated in our experiments. Furthermore, each of the tested endonucleases required a unique recognition site in order to initiate either double- or single-stranded breaks. Even if we assume that the *de novo* synthesis originates from the DNA polymerase through synthesis of random stretches of repetitive sequences, the likelihood of synthesising perfect recognition sites in a quick and efficient manner that would allow generating such fast amplification profiles, is rather low. There is however a real possibility that due to imperfect chemical conditions, each of the tested endonucleases exhibited a star activity that resulted in non-specific cutting.

In contrast with the previously mentioned reports regarding *de novo* synthesis, our findings suggest an alternative origin of the synthesised DNA. However, it is evident that the native version of endonuclease enzyme is needed for this artefact, as we saw no amplification profiles when a heat-denatured version of the Nb.bsmI nickase was used. However, when the chosen

nickase was pre-incubated in typical LAMP buffering conditions, containing a full set of dNTPs, prior to heat-denaturation, amplification profiles were detected.

Following on, if Ling et al postulation that DNA polymerases were indeed responsible for *de novo* DNA synthesis observed in our experiments, we would expect to see no difference in amplification performance between reactions that utilise a heat-inactivated nickase and those that have undergone a pre-incubation step utilising nickase prior to heat denaturation. Instead, we saw full detection in the reactions containing the pre-incubated, inactive nicking enzyme. It is evident from this work that DNA is more likely to have originated from the endonuclease solution and/or the LAMP-BART components present during the pre-incubation step, which then was readily amplified by the DNA polymerases and this accelerated the overall miRNA detection mechanism in an unpredicted manner. In fact, we saw distinctly different BART amplification curves, when comparing reactions using the native nickase, compared to control reactions containing the denatured enzyme; this suggests that both are required for efficient amplification of the generated DNA.

Furthermore, to our understanding, the *de novo* synthesis phenomena was not limited to a few endonucleases, but is rather a common feature amongst of these enzymes, as over 10 different restriction and nicking enzymes were tested, all demonstrating a capacity for de novo DNA synthesis. Further work is now needed to prove our hypothesis. Particularly since successful incorporation of strand displacement DNA polymerases and nicking enzymes have been reported (SDA, EXPAR). However, most of these technologies utilise probe-based detection systems thus are immune to the non-specific backgrounds.

Chapter 7

7 Discussion and conclusions

7.1 Development of RT-LAMP assays

The advent of reverse transcription technologies has empowered scientists to study gene expression and these have proved extremely useful in the field of molecular diagnostics. However, despite their widespread use, there is little working knowledge of their optimisation in the literature. It is well established that all single stranded RNA molecules are prone to a high degree of secondary and tertiary structure that is often attributed to biological function, yet primer design rarely accounts for RNA folding (Jubin, 2001, Lukavsky, 2009), and to-date no specific RT primer design software is publicly or commercially available.

In chapter 3, different factors affecting reverse transcribed LAMP is explored, including enzymology, reaction chemistry and primer design. This research demonstrated the importance of a highly optimised chemistry and the right choice of enzymes, but also highlighted the need for bespoke RT primers that could negotiate RNA secondary structure and DNA polymerases, which could adequately displace the primed entities of the initiated DNA propagators of these reactions.

Following on, it was shown that RNA structure could impede the performance of the 5' UTR HCV RT-LAMP. *In silico* analysis of 5' UTR RNA showed a high degree of secondary structure, predicted by the Vienna RNA folding software. Even so, there were certain domains of the RNA sequence that showed only a moderate level of folding, and thus these regions were predicted to be more suited for primer annealing positions that could initiate amplification via reverse transcriptase. All of the designed RT-LAMP primer sets performed efficiently when

the RNA secondary structure was negotiated (Set 34-40), while LAMP RT primers targeting highly structured regions of the HCV 5'UTR failed to amplify (13-18 and 13-20) altogether.

In this thesis, two versions of the recombinant Bst 2.0 DNA polymerase (Bst 2.0 / Bst 2WS) were compared to a highly displacing combined DNA / RT polymerase (GSP-SSD). This work was carried out, to appropriate evaluate any differences in performance that could be attributed to the displacement activity associated with polymerases. Of the DNA polymerases tested, GSP-SSD proved to be the most optimal for the current 5'UTR RT-LAMP HCV. This polymerase not only increased the kinetics of amplification, but also generated far fewer NTCs compared to either Bst 2.0 tested.

Primer dimerization, is a very well-known cause of non-specific activity, and when combined with highly efficient DNA polymerisation, increased rates of primer-derived amplification are more likely to occur (Friedberg et al., 2000, Poritz and Ririe, 2014). Despite the increased polymerisation efficiency of GSP-SSD, primer and target derived amplification specificities were maintained. This may be attributed to reduced activity of the enzyme at low temperatures, which would prevent mis-priming events from occurring during the reaction set up, without affecting performance of specific priming at optimal assay temperatures. In contrast, amplifications tested using Bst 2.0 at similar concentrations resulted in nonspecific amplifications, suggesting a higher degree of activity exhibited by the enzyme at lower temperatures. An alternative version of Bst 2.0 (Bst 2.0 WS) designed to avoid mis-priming during reaction set ups makes use of aptamers attached to the active site. It was demonstrated that modified enzymes, such as Bst 2.0 WS, can negatively affect performance of RT-LAMP, but not LAMP amplifications. This was observed for both the 5'UTR HCV RT-LAMP and the 23S TB RT-LAMP but the LAMP amplifications were unaffected.

This optimisations of the RT-LAMP polymerisation and RT priming resulted in highly sensitive reactions capable of detecting as little as 5 cps. Despite this success further evaluations would still be needed to optimise assay chemistry and performance when challenged with inhibitory / extracted RNA from clinical samples.

7.2 Inhibition of RT-LAMP assays

One of the major drawbacks of any NAAT amplification, is their sensitivity to inhibitory substances, which result in either a reduction in amplification kinetics or a complete failure in detection (Bustin and Nolan, 2004, Schrader et al., 2012). Thus the inhibitory substances pose a real risk to amplification performance, particularly in the field of molecular diagnostics, where a failure to detect a true positive can lead to a mis-diagnosis and have a direct effects on a patients' wellbeing and the downstream disease transmission rates (Huggett et al., 2008, Drosten et al., 2002). Although, inhibition of amplification has been widely studied and is thought to be a result of many factors, research has mainly focused on the inhibition of DNA polymerase function (Opel et al., 2010, Al-Soud and Rådström, 2001), and not reverse transcription.

The main focus of the study presented in the chapter 4 was to determine the inhibitory effect of the chosen and commonly encountered polymerase inhibitors, including potassium and sodium salts, detergents and non-target nucleic acids, on the performance of RT assays specifically. In this study it was demonstrated that inhibition of polymerization not only depends upon the type of substance but also its concentration the effects of which can sometimes be mitigated by the assay chemistry. A clear correlation was between the concentration of the inhibitory salt tested and the impact on the amplification. However, it was noted that LAMP assays utilizing the Bst 2.0 DNA polymerase were less affected by salt inhibition when compared to GSP-SSD. Interestingly, the addition of 10 mM of either potassium chloride or acetate resulted in significant increases in the amplification speed for

both tested assay chemistries but was not observed in the reactions challenged with equal amounts of sodium chloride.

The acidic detergent LDS was shown to have no effect on the polymerization. Yet a large impact upon BART reporting was observed. Interestingly, the choice of buffer could modulate the effect of LDS on BART. It was concluded that low buffering capacities of certain buffers, which were insufficient to overcome the low pH of LDS (4≥pH), caused the decline in the light emission observed. Further work is however recommended to ascertain the impact of these detergents on RT-LAMP enzymology.

The inhibitory effect of carrier non-target nucleic acids was also gauged in this study. Unlike all other inhibitory substances tested, carrier NA showed an increased inhibitory potency towards RNA assays specifically. Although, a significant inhibition of amplification of both, DNA and RNA templates was observed when challenged with salmon sperm DNA and tRNA, RNA assays suffered to a much higher extent. The reaction containing RNA templates not only suffered a significant reduction in the amplification speed but also a dramatic reduction in the overall assay sensitivity. In contrast, no effect on the assay sensitivity was detected under identical inhibitory conditions, when DNA template were amplified. This work has categorically established clear differences between the effects of commonly encountered polymerase inhibitors and their impact on RT and DNA polymerizations.

7.3 Development of amplification controls for RT-LAMP assays

The main focus of the study presented in the chapter 5, was to develop a mechanism for controlling RT-LAMP amplification in a single-tube format, without causing interference of true positive activities or preferential amplification with respect to the IAC template.

Due to high complexity of the RT-LAMP priming mechanism, and a requirement for an abundance of primers to drive efficient amplification of the RNA target, a competitive IAC mechanism was adopted. It was demonstrated that a significant reduction in amplification speed can be achieved by introducing mismatches, without compromising on the reproducibility. As expected, all of the tested mutations introduced into the BIP and FIP primers affected the performance of *M*ycobacterium complex 23s rRNA RT-LAMP amplification, regardless of the extent or location of the mutations. However, mutations introduced into specific poles of the LAMP primers (B1 and F1) had a greater impact on the kinetics compared to corresponding alterations in F2 and B2. Thus, it was concluded that the observed differences could be correlated with distinct roles each pole of the LAMP inchworm primers played within the initiation and propagation of target sequence amplification.

The impact of these mutations was associated with the ability to form stable dumbbell intermediates – molecules crucial for propagation of isothermal LAMP reactions. Mismatches introduced within the B1 and F1 persist throughout the amplification reaction, since they are incorporated into the freshly synthesised target amplicon, and are not directly targeted by the primers. In contrast, mutation in the F2 and B2 sites could only affect the initiation rather than propagation, since once extended, the synthesised complementary strand will retain those exact same mutations thus resulting in a template containing full complementarity with the primers.

The developed IAC model was tested under various inhibitory conditions. The initial assessment showed a significant delay in amplification time under unchallenged conditions,

and proved the potential of the test to report on the inhibitory nature of sample and sample preparation derived substances such as sodium chloride and carrier DNA, without affecting the core RT-LAMP amplification. The designed IAC model responded to most of the tested inhibitory substances such as carrier NA or salts, proving its viability as an amplification control. However, significant differences in the response of RT-LAMP and the IAC to sodium hydroxide inhibition were also observed. The developed IAC assay remained unaffected by sodium hydroxide, whereas the sensitivity of 23s rRNA detection was significantly compromised. The difference in sensitivity of RT-LAMP and IAC to certain inhibitory substances poses real risks for diagnostic assays. In our model, the IAC was determined to contain as much as 10 % DNA contamination originating from the *in vitro* transcription process. Since the effects of sodium hydroxide on the integrity of RNA targets has been widely reported, the differences in the response to this inhibitor could be attributed to the presence of this contaminant.

Furthermore, it was observed that certain reactions containing limiting amounts of the target 23s rRNA amplified significantly slower under inhibitory conditions. Thus, in a molecular diagnostic setting where unknown samples are tested, such result could indicate amplification of the IAC rather than an inhibited sample, if the assessment was done solely on the basis of the TTM under BART detection system. It was then concluded that an efficient method of differentiating between the IAC and both inhibited and non-challenged true target amplification was crucial for this technology. However, one of the main limitations of BART is its lack of multiplexing capabilities. Thus, an alternative method of differentiation was explored.

It was hypothesised that by taking advantage of the high amounts of IAC used in each assay, a differentiation between the two targets could be performed when taking both the TTM and amplification frequencies into consideration.

A system was proposed, where standard 50 uL reactions containing the LAMP-BART reagents and the tested sample (including the IAC target) were split into 5 10 uL reactions and their amplification monitored in real time by BART platforms. However, an assessment of TTM and amplification frequencies would be performed based on a collective data from all 5 reactions as well as each reaction individually. Thus, in the proposed approach, if all 5 reactions amplified in a characteristic to 23s rRNA TTM then such sample would be considered true positive amplification likely to contain large amounts of the target RNA. Similarly, if only 1 out of 5 10 uL reactions showed positive amplification profiles for 23s rRNA, and 4 amplified significantly slower, the overall result would still lead to positive diagnosis of the disease based on the single positive replicate. However, since the full detection was not achieved then the amount of present RNA was most likely at the limit of detection. In contrast, in a scenario where none of the reactions amplified the target in a characteristic to the 23s rRNA manner, but still managed to generated late positive profiles corresponding to the IAC amplification, such result would then be marked as a true negative. Thus using this approach, the samples containing limited copy number of the core target or those compromised by inhibition are less likely to fully amplify in all 5 reactions. Consequently, the TTM as well as amplification frequencies generated by such samples are less likely to be mistaken for the IAC detection profiles.

In this chapter, it was demonstrated that reaction volume had no effect on the kinetics of the amplification, regardless of the type and amount of the template used. However, when limited amounts of the RT-LAMP template RNA was used, a reduction in amplification frequency was observed with the reduced reaction volume. Thus, it was concluded that the observed detrition in sensitivity of the RT-LAMP was caused by a limited amount of target available in the smaller reaction partition and was most likely further affected by stochastic variation. Furthermore, similar observations were made when amplification of the target RNA was performed in the

presence of impeded IAC template. When RT-LAMP amplifications were conducted in 10 uL reactions, two populations of peaks were generated, indicating that IAC had no effect on the overall sensitivity of the target RT-LAMP RNA. Thus, enabling full discrimination between the amplification of the core target and the IAC template.

Fluorescent detection using a probe-based system was also explored as an alternative to BART.

For over a decade, PCR based technologies have benefited from the specificity and multiplexing capabilities of fluorescent probes, but greatly limiting their use in the isothermal setting. In this study, the capability of dually labelled loop primers to detect nucleic acid amplification in a *Taq* independent manner, was reported. It was shown that full detection of the IAC can be achieved using this technology without accelerating the amplification.

Fluorescent detection of LAMP using such probes would not only simplify the analysis but also increase the specificity of detection.

7.4 Isothermal mechanisms of miRNA detection

Since disruption in miRNAs expression profiles have been associated with a wide range of different diseases, an efficient detection method could provide valuable insights into disease progression and early diagnosis. The main focus of this study was to develop a LAMP-based miRNA detection system that would offer a cost-effective, highly accessible detection platform.

Due to the complexity of LAMP primer design, the use of this technology has been limited and used rarely for miRNA detection (Li at el. 2013).

In chapter 6, we present an alternative method of miRNA detection, where the LAMP target was generated using a ligation-mediated step dependant on miRNA as a linker. Although, the specificity of the amplification was poor, this method was capable of successfully detecting 125 fM of the target miRNA.

Alternative methods of generating the dumbbell template using restriction mediated approaches were also presented in chapter 6. However, these methods failed due to the extent of non-specific amplification observed. The fidelity of both restriction mediated methods appeared to be compromised as a consequence of *de novo* DNA synthesis caused by activities associated with endonuclease and displacement polymerases. Although, this *de novo* synthesis artefact has already been reported, it is still unclear how the DNA synthesis is initiated. Most of the published accounts suggest the DNA polymerase is responsible for activity. This study has shown that the synthesised DNA originated from the tested endonucleases and was most likely amplified by the DNA polymerase. In addition, the observed effect was not limited to a chosen endonuclease but was likely a common feature when combined with displacing DNA polymerases.

However, several reports have already been published where nicking enzymes and strand displacement polymerases were successfully used for NA amplification using EXPAR or SDA. Nonetheless, most of these technologies utilise probe-based detection systems, thus are immune to the non-specific backgrounds.

References

1) Abdel-Hamid, M., El-Daly, M., El-Kafrawy, S., Mikhail, N., Strickland, G. T. and Fix, A. D. (2002) 'Comparison of second- and third-generation enzyme immunoassays for detecting antibodies to hepatitis C virus', *J Clin Microbiol,* 40(5), pp. 1656-9.
2) Abdelwahab, K. S. and Ahmed Said, Z. N. (2016) 'Status of hepatitis C virus vaccination: Recent update', *World J Gastroenterol,* 22(2), pp. 862-73.
3) Abdulmawjood, A., Roth, S. and Bülte, M. (2002) 'Two methods for construction of internal amplification controls for the detection of Escherichia coli O157 by polymerase chain reaction', *Mol Cell Probes,* 16(5), pp. 335-9.
4) Abergel, A., Asselah, T., Metivier, S., Loustaud-Ratti, V. and et al. (2016) 'Ledipasvir-sofosbuvir in patients with hepatitis C virus genotype 5 infection: an open-label, multicentre, single-arm, phase 2 study', *Lancet Infect Dis.,* 16(4), pp. 459-464.
5) Abu Al-Soud, W. and Radstrom, P. (1998) 'Capacity of nine thermostable DNA polymerases To mediate DNA amplification in the presence of PCR-inhibiting samples', *Appl Environ Microbiol,* 64(10), pp. 3748-53.
6) Adams, N. M., Bordelon, H., Wang, K. K., Albert, L. E., Wright, D. W. and Haselton, F. R. (2015) 'Comparison of three magnetic bead surface functionalities for RNA extraction and detection', *ACS Appl Mater Interfaces,* 7(11), pp. 6062-9.
7) Aebischer, A., Wernike, K., Hoffmann, B. and Beer, M. (2014) 'Rapid genome detection of Schmallenberg virus and bovine viral diarrhea virus by use of isothermal amplification methods and high-speed real-time reverse transcriptase PCR', *J Clin Microbiol,* 52(6), pp. 1883-92.
8) Akane, A., Matsubara, K., Nakamura, H., Takahashi, S. and Kimura, K. (1994) 'Identification of the heme compound copurified with deoxyribonucleic acid (DNA) from bloodstains, a major inhibitor of polymerase chain reaction (PCR) amplification', *J Forensic Sci,* 39(2), pp. 362-72.
9) Al-Soud, W. A. and Rådström, P. (2001) 'Purification and characterization of PCR-inhibitory components in blood cells', *J Clin Microbiol,* 39(2), pp. 485-93.
10) Alaeddini, R. (2012) 'Forensic implications of PCR inhibition--A review', *Forensic Sci Int Genet,* 6(3), pp. 297-305.
11) Ali, P. S., Ghoshdastider, U., Hoffmann, J., Brutschy, B. and Filipek, S. (2012) 'Recognition of the let-7g miRNA precursor by human Lin28B', *FEBS Lett,* 586(22), pp. 3986-90.
12) Alter, M. J. (2007) 'Epidemiology of hepatitis C virus infection', *World J Gastroenterol,* 13(17), pp. 2436-41.
13) Ambros, V. (2004) 'The functions of animal microRNAs', *Nature,* 431(7006), pp. 350-5.
14) André, P., Perlemuter, G., Budkowska, A., Bréchot, C. and Lotteau, V. (2005) 'Hepatitis C virus particles and lipoprotein metabolism', *Semin Liver Dis,* 25(1), pp. 93-104.
15) Antao, V. P., Lai, S. Y. and Tinoco, I. (1991) 'A thermodynamic study of unusually stable RNA and DNA hairpins', *Nucleic Acids Res,* 19(21), pp. 5901-5.
16) Antipova, V. N., Zheleznaya, L. A. and Zyrina, N. V. (2014) 'Ab initio DNA synthesis by Bst polymerase in the presence of nicking endonucleases Nt.AlwI, Nb.BbvCI, and Nb.BsmI', *FEMS Microbiol Lett,* 357(2), pp. 144-50.
17) Ardekani, A. M. and Naeini, M. M. (2010) 'The Role of MicroRNAs in Human Diseases', *Avicenna J Med Biotechnol,* 2(4), pp. 161-79.

18) Ashfaq, U. A., Javed, T., Rehman, S., Nawaz, Z. and Riazuddin, S. (2011) 'An overview of HCV molecular biology, replication and immune responses', *Virology Journal,* 8(1), pp. 161.
19) Auyeung, V. C., Ulitsky, I., McGeary, S. E. and Bartel, D. P. (2013) 'Beyond secondary structure: primary-sequence determinants license pri-miRNA hairpins for processing', *Cell,* 152(4), pp. 844-58.
20) Bagga, S., Bracht, J., Hunter, S., Massirer, K., Holtz, J., Eachus, R. and Pasquinelli, A. E. (2005) 'Regulation by let-7 and lin-4 miRNAs results in target mRNA degradation', *Cell,* 122(4), pp. 553-63.
21) Balmer, C. T. (*2007*2007) '"PCR biocompatibility of lab-on-a-chip and MEMS materials."' 17(8).
22) Bartel, D. P. (2004) 'MicroRNAs: genomics, biogenesis, mechanism, and function', *Cell,* 116(2), pp. 281-97.
23) Bartel, D. P. (2009) 'MicroRNAs: target recognition and regulatory functions', *Cell,* 136(2), pp. 215-33.
24) Barth, H., Liang, T. J. and Baumert, T. F. (2006) 'Hepatitis C virus entry: molecular biology and clinical implications', *Hepatology,* 44.
25) Bashiardes, S., Richter, J. and Christodoulou, C. G. (2008) 'An in-house method for the detection and quantification of HCV in serum samples using a TaqMan assay real time PCR approach', *Clin Chem Lab Med,* 46.
26) Baskerville, S. and Bartel, D. P. (2005) 'Microarray profiling of microRNAs reveals frequent coexpression with neighboring miRNAs and host genes', *RNA,* 11(3), pp. 241-7.
27) Bavamian, S., Mellios, N., Lalonde, J., Fass, D. M., Wang, J., Sheridan, S. D., Madison, J. M., Zhou, F., Rueckert, E. H., Barker, D., Perlis, R. H., Sur, M. and Haggarty, S. J. (2015) 'Dysregulation of miR-34a links neuronal development to genetic risk factors for bipolar disorder', *Mol Psychiatry,* 20(5), pp. 573-84.
28) Bazzini, A. A., Lee, M. T. and Giraldez, A. J. (2012) 'Ribosome profiling shows that miR-430 reduces translation before causing mRNA decay in zebrafish', *Science,* 336(6078), pp. 233-7.
29) Bedford, E., Tabor, S. and Richardson, C. C. (1997) 'The thioredoxin binding domain of bacteriophage T7 DNA polymerase confers processivity on Escherichia coli DNA polymerase I', *Proc Natl Acad Sci U S A,* 94(2), pp. 479-84.
30) Behrens, S. E., Tomei, L. and De Francesco, R. (1996) 'Identification and properties of the RNA-dependent RNA polymerase of hepatitis C virus', *Embo J,* 15.
31) Benes, V. and Castoldi, M. (2010) 'Expression profiling of microRNA using real-time quantitative PCR, how to use it and what is available', *Methods,* 50(4), pp. 244-249.
32) Berensmeier, S. (2006) 'Magnetic particles for the separation and purification of nucleic acids', *Applied microbiology and biotechnology,* 73(3), pp. 495-504.
33) Berry, K. E., Waghray, S., Mortimer, S. A., Bai, Y. and Doudna, J. A. (2011) 'Crystal structure of the HCV IRES central domain reveals strategy for start-codon positioning', *Structure,* 19(10), pp. 1456-66.
34) Bessetti, J. (2007) 'An introduction to PCR inhibitors', *J Microbiol Methods,* 28, pp. 159-67.
35) Bickley, J., Short, J., McDowell, D. and Parkes, H. (1996a) 'Polymerase chain reaction (PCR) detection of Listeria monocytogenes in diluted milk and reversal of PCR inhibition caused by calcium ions', *Letters in Applied Microbiology,* 22(2), pp. 153-158.
36) Bickley, J., Short, J. K., McDowell, D. G. and Parkes, H. C. (1996b) 'Polymerase chain reaction (PCR) detection of Listeria monocytogenes in diluted milk and reversal of PCR inhibition caused by calcium ions', *Lett Appl Microbiol,* 22(2), pp. 153-8.
37) Braid, M. D., Daniels, L. M. and Kitts, C. L. (2003) 'Removal of PCR inhibitors from soil DNA by chemical flocculation', *Journal of Microbiological Methods,* 52(3), pp. 389-393.

38) Brown, R. B. and Audet, J. (2008) 'Current techniques for single-cell lysis', *J R Soc Interface,* 5 Suppl 2, pp. S131-8.
39) Buhlmann, A., Pothier, J. F., Rezzonico, F., Smits, T. H., Andreou, M., Boonham, N., Duffy, B. and Frey, J. E. (2013) 'Erwinia amylovora loop-mediated isothermal amplification (LAMP) assay for rapid pathogen detection and on-site diagnosis of fire blight', *J Microbiol Methods,* 92(3), pp. 332-9.
40) Burkhart, C. A., Norris, M. D. and Haber, M. (2002) 'A simple method for the isolation of genomic DNA from mouse tail free of real-time PCR inhibitors', *J Biochem Biophys Methods,* 52(2), pp. 145-9.
41) Bustin, S. A. and Nolan, T. (2004) 'Pitfalls of quantitative real-time reverse-transcription polymerase chain reaction', *J Biomol Tech,* 15(3), pp. 155-66.
42) Butot, S., Putallaz, T., Croquet, C., Lamothe, G., Meyer, R., Joosten, H. and Sánchez, G. (2007) 'Attachment of enteric viruses to bottles', *Appl Environ Microbiol,* 73(16), pp. 5104-10.
43) Cacopardo, B., Nunnari, G. and Nigro, L. (2009) 'Clearance of HCV RNA following acute hepatitis A superinfection', *Dig Liver Dis,* 41(5), pp. 371-4.
44) Cai, X., Hagedorn, C. H. and Cullen, B. R. (2004) 'Human microRNAs are processed from capped, polyadenylated transcripts that can also function as mRNAs', *RNA,* 10(12), pp. 1957-66.
45) Calin, G. A., Ferracin, M., Cimmino, A., Di Leva, G., Shimizu, M., Wojcik, S. E., Iorio, M. V., Visone, R., Sever, N. I., Fabbri, M., Iuliano, R., Palumbo, T., Pichiorri, F., Roldo, C., Garzon, R., Sevignani, C., Rassenti, L., Alder, H., Volinia, S., Liu, C. G., Kipps, T. J., Negrini, M. and Croce, C. M. (2005) 'A MicroRNA signature associated with prognosis and progression in chronic lymphocytic leukemia', *N Engl J Med,* 353(17), pp. 1793-801.
46) Calin, G. A., Liu, C. G., Sevignani, C., Ferracin, M., Felli, N., Dumitru, C. D., Shimizu, M., Cimmino, A., Zupo, S., Dono, M., Dell'Aquila, M. L., Alder, H., Rassenti, L., Kipps, T. J., Bullrich, F., Negrini, M. and Croce, C. M. (2004) 'MicroRNA profiling reveals distinct signatures in B cell chronic lymphocytic leukemias', *Proc Natl Acad Sci U S A,* 101(32), pp. 11755-60.
47) Cao, X., Yeo, G., Muotri, A. R., Kuwabara, T. and Gage, F. H. (2006) 'Noncoding RNAs in the mammalian central nervous system', *Annu Rev Neurosci,* 29, pp. 77-103.
48) Cao, Y., Kim, H. J., Li, Y., Kong, H. and Lemieux, B. (2013) 'Helicase-dependent amplification of nucleic acids', *Curr Protoc Mol Biol,* 104, pp. Unit 15.11.
49) Chan, E. L., Brandt, K., Olienus, K., Antonishyn, N. and Horsman, G. B. (2000) 'Performance characteristics of the Becton Dickinson ProbeTec System for direct detection of Chlamydia trachomatis and Neisseria gonorrhoeae in male and female urine specimens in comparison with the Roche Cobas System', *Arch Pathol Lab Med,* 124(11), pp. 1649-52.
50) Chandler, D. P., Stults, J. R., Cebula, S., Schuck, B. L., Weaver, D. W., Anderson, K. K., Egholm, M. and Brockman, F. J. (2000) 'Affinity purification of DNA and RNA from environmental samples with peptide nucleic acid clamps', *Appl Environ Microbiol,* 66(8), pp. 3438-45.
51) Chase, J. W. and Williams, K. R. (1986) 'Single-stranded DNA binding proteins required for DNA replication', *Annu Rev Biochem,* 55, pp. 103-36.
52) Chen, A. A. and García, A. E. (2013) 'High-resolution reversible folding of hyperstable RNA tetraloops using molecular dynamics simulations', *Proceedings of the National Academy of Sciences,* 110(42), pp. 16820-16825.
53) Chen, C., Ridzon, D. A., Broomer, A. J., Zhou, Z., Lee, D. H., Nguyen, J. T., Barbisin, M., Xu, N. L., Mahuvakar, V. R., Andersen, M. R., Lao, K. Q., Livak, K. J. and Guegler, K. J. (2005) 'Real-time quantification of microRNAs by stem-loop RT-PCR', *Nucleic Acids Res,* 33(20), pp. e179.

54) Chen, H., Lan, H. Y., Roukos, D. H. and Cho, W. C. (2014) 'Application of microRNAs in diabetes mellitus', *J Endocrinol,* 222(1), pp. R1-R10.
55) Chevaliez, S., Bouvier-Alias, M., Brillet, R. and Pawlotsky, J. M. (2007) 'Overestimation and underestimation of hepatitis C virus RNA levels in a widely used real-time polymerase chain reaction-based method', *Hepatology,* 46.
56) Chien, Y. H. and Davidson, N. (1978) 'RNA:DNA hybrids are more stable than DNA:DNA duplexes in concentrated perchlorate and trichloroacetate solutions', *Nucleic Acids Res,* 5(5), pp. 1627-37.
57) Chomczynski, P. and Sacchi, N. (1987) 'Single-step method of RNA isolation by acid guanidinium thiocyanate-phenol-chloroform extraction', *Analytical biochemistry,* 162(1), pp. 156-159.
58) Choo, Q. L., Kuo, G., Weiner, A. J., Overby, L. R., Bradley, D. W. and Houghton, M. (1989) 'Isolation of a cDNA clone derived from a blood-borne non-A, non-B viral hepatitis genome', *Science,* 244(4902), pp. 359-62.
59) Chua, K. B. and Gubler, D. J. (2013) 'Perspectives of public health laboratories in emerging infectious diseases', *Emerg Microbes Infect,* 2(6), pp. e37.
60) Cloherty, G., Talal, A., Coller, K., Steinhart, C., Hackett, J., Dawson, G., Rockstroh, J. and Feld, J. (2016) 'Role of Serologic and Molecular Diagnostic Assays in Identification and Management of Hepatitis C Virus Infection', *J Clin Microbiol,* 54(2), pp. 265-73.
61) Compton, J. (1991) 'Nucleic acid sequence-based amplification', *Nature,* 350(6313), pp. 91-2.
62) Conrad, T., Marsico, A., Gehre, M. and Orom, U. A. (2014) 'Microprocessor activity controls differential miRNA biogenesis In Vivo', *Cell Rep,* 9(2), pp. 542-54.
63) Cook, P. (1984) 'A general method for preparing intact nuclear DNA', *The EMBO journal,* 3(8), pp. 1837.
64) Craw, P. and Balachandran, W. (2012) 'Isothermal nucleic acid amplification technologies for point-of-care diagnostics: a critical review', *Lab Chip,* 12(14), pp. 2469-86.
65) Cubero, J., van der Wolf, J., van Beckhoven, J. and López, M. M. (2002) 'An internal control for the diagnosis of crown gall by PCR', *J Microbiol Methods,* 51(3), pp. 387-92.
66) Curtis, K. A., Rudolph, D. L. and Owen, S. M. (2008) 'Rapid detection of HIV-1 by reverse-transcription, loop-mediated isothermal amplification (RT-LAMP)', *J Virol Methods,* 151(2), pp. 264-70.
67) Cuypers, L., Li, G., Libin, P., Piampongsant, S., Vandamme, A. M. and Theys, K. (2015) 'Genetic Diversity and Selective Pressure in Hepatitis C Virus Genotypes 1-6: Significance for Direct-Acting Antiviral Treatment and Drug Resistance', *Viruses,* 7(9), pp. 5018-39.
68) de Vega, M., Lázaro, J. M., Mencía, M., Blanco, L. and Salas, M. (2010) 'Improvement of ϕ29 DNA polymerase amplification performance by fusion of DNA binding motifs', *Proc Natl Acad Sci U S A,* 107(38), pp. 16506-11.
69) Dean, F. B., Nelson, J. R., Giesler, T. L. and Lasken, R. S. (2001) 'Rapid amplification of plasmid and phage DNA using Phi 29 DNA polymerase and multiply-primed rolling circle amplification', *Genome Res,* 11(6), pp. 1095-9.
70) Ding, M., Bullotta, A., Caruso, L., Gupta, P., Rinaldo, C. R. and Chen, Y. (2011) 'An optimized sensitive method for quantitation of DNA/RNA viruses in heparinized and cryopreserved plasma', *J Virol Methods,* 176(1-2), pp. 1-8.
71) Dingle, K. E., Crook, D. and Jeffery, K. (2004) 'Stable and noncompetitive RNA internal control for routine clinical diagnostic reverse transcription-PCR', *J Clin Microbiol,* 42.
72) Dragan, A. I., Pavlovic, R., McGivney, J. B., Casas-Finet, J. R., Bishop, E. S., Strouse, R. J., Schenerman, M. A. and Geddes, C. D. (2012) 'SYBR Green I: fluorescence properties and interaction with DNA', *J Fluoresc,* 22(4), pp. 1189-99.

73) Drosten, C., Panning, M., Guenther, S. and Schmitz, H. (2002) 'False-negative results of PCR assay with plasma of patients with severe viral hemorrhagic fever', *J Clin Microbiol,* 40(11), pp. 4394-5.
74) Du, W., Lv, M., Li, J., Yu, R. and Jiang, J. (2016) 'A ligation-based loop-mediated isothermal amplification (ligation-LAMP) strategy for highly selective microRNA detection', *Chem Commun (Camb),* 52(86), pp. 12721-12724.
75) Eckhart, L., Bach, J., Ban, J. and Tschachler, E. (2000) 'Melanin binds reversibly to thermostable DNA polymerase and inhibits its activity', *Biochem Biophys Res Commun,* 271(3), pp. 726-30.
76) Edwards, T., Burke, P. A., Smalley, H. B., Gillies, L. and Hobbs, G. (2014) 'Loop-mediated isothermal amplification test for detection of Neisseria gonorrhoeae in urine samples and tolerance of the assay to the presence of urea', *J Clin Microbiol,* 52(6), pp. 2163-5.
77) Elazar, M., Cheong, K. H., Liu, P., Greenberg, H. B., Rice, C. M. and Glenn, J. S. (2003) 'Amphipathic helix-dependent localization of NS5A mediates hepatitis C virus RNA replication', *J Virol,* 77.
78) Elshawadfy, A. M., Keith, B. J., Ee Ooi, H., Kinsman, T., Heslop, P. and Connolly, B. A. (2014) 'DNA polymerase hybrids derived from the family-B enzymes of Pyrococcus furiosus and Thermococcus kodakarensis: improving performance in the polymerase chain reaction', *Front Microbiol,* 5, pp. 224.
79) Esquela-Kerscher, A. (2014) 'The lin-4 microRNA: The ultimate micromanager', *Cell Cycle,* 13(7), pp. 1060-1.
80) Estes, M. D., Yang, J., Duane, B., Smith, S., Brooks, C., Nordquist, A. and Zenhausern, F. (2012) 'Optimization of multiplexed PCR on an integrated microfluidic forensic platform for rapid DNA analysis', *Analyst,* 137(23), pp. 5510-9.
81) Euler, M., Wang, Y., Nentwich, O., Piepenburg, O., Hufert, F. T. and Weidmann, M. (2012) 'Recombinase polymerase amplification assay for rapid detection of Rift Valley fever virus', *J Clin Virol,* 54(4), pp. 308-12.
82) Fabian, M. R., Sonenberg, N. and Filipowicz, W. (2010) 'Regulation of mRNA translation and stability by microRNAs', *Annu Rev Biochem,* 79, pp. 351-79.
83) Faller, M. and Guo, F. (2008) 'MicroRNA biogenesis: there's more than one way to skin a cat', *Biochim Biophys Acta,* 1779(11), pp. 663-7.
84) Fenton, K. A. and Lowndes, C. M. (2004) 'Recent trends in the epidemiology of sexually transmitted infections in the European Union', *Sex Transm Infect,* 80(4), pp. 255-63.
85) Fierz, W. (2004) 'Basic problems of serological laboratory diagnosis', *Methods Mol Med,* 94, pp. 393-427.
86) Filipowicz, W., Bhattacharyya, S. N. and Sonenberg, N. (2008) 'Mechanisms of post-transcriptional regulation by microRNAs: are the answers in sight?', *Nat Rev Genet,* 9(2), pp. 102-14.
87) Firdaus, R., Saha, K., Biswas, A. and Sadhukhan, P. C. (2015) 'Current molecular methods for the detection of hepatitis C virus in high risk group population: A systematic review', *World J Virol,* 4(1), pp. 25-32.
88) Fire, A. and Xu, S. Q. (1995) 'Rolling replication of short DNA circles', *Proc Natl Acad Sci U S A,* 92(10), pp. 4641-5.
89) Forsell, J., Koskiniemi, S., Hedberg, I., Edebro, H., Evengård, B. and Granlund, M. (2015) 'Evaluation of factors affecting real-time PCR performance for diagnosis of Entamoeba histolytica and Entamoeba dispar in clinical stool samples', *J Med Microbiol,* 64(9), pp. 1053-62.
90) Fortes, E. D., David, J., Koeritzer, B. and Wiedmann, M. (2013) 'Validation of the 3M molecular detection system for the detection of listeria in meat, seafood, dairy, and retail environments', *J Food Prot,* 76(5), pp. 874-8.

91) Fox, D. H., Huang, C. K., Du, J., Chang, T. Y. and Pan, Q. (2007) 'Profound inhibition of the PCR step of CF V3 multiplex PCR/OLA assay by the use of UV-irradiated plastic reaction tubes', *Diagn Mol Pathol,* 16(2), pp. 121-3.
92) Freeman, W. M., Walker, S. J. and Vrana, K. E. (1999) 'Quantitative RT-PCR: pitfalls and potential', *Biotechniques,* 26(1), pp. 112-22, 124-5.
93) Freiman, J. M., Tran, T. M., Schumacher, S. G., White, L. F., Ongarello, S., Cohn, J., Easterbrook, P. J., Linas, B. P. and Denkinger, C. M. (2016) 'Hepatitis C Core Antigen Testing for Diagnosis of Hepatitis C Virus Infection: A Systematic Review and Meta-analysis', *Ann Intern Med,* 165(5), pp. 345-55.
94) Friedberg, E. C., Feaver, W. J. and Gerlach, V. L. (2000) 'The many faces of DNA polymerases: strategies for mutagenesis and for mutational avoidance', *Proc Natl Acad Sci U S A,* 97(11), pp. 5681-3.
95) Funes-Huacca, M. E., Opel, K., Thompson, R. and McCord, B. R. (2011) 'A comparison of the effects of PCR inhibition in quantitative PCR and forensic STR analysis', *Electrophoresis,* 32(9), pp. 1084-9.
96) Gabriel, G. V. and Viviani, V. R. (2014) 'Novel application of pH-sensitive firefly luciferases as dual reporter genes for simultaneous ratiometric analysis of intracellular pH and gene expression/location', *Photochem Photobiol Sci,* 13(12), pp. 1661-70.
97) Gandelman, O., Jackson, R., Kiddle, G. and Tisi, L. (2011) 'Loop-mediated amplification accelerated by stem primers', *Int J Mol Sci,* 12(12), pp. 9108-24.
98) Gandelman, O. A., Church, V. L., Moore, C. A., Kiddle, G., Carne, C. A., Parmar, S., Jalal, H., Tisi, L. C. and Murray, J. A. (2010) 'Novel bioluminescent quantitative detection of nucleic acid amplification in real-time', *PLoS One,* 5(11), pp. e14155.
99) Ghany, M. G., Strader, D. B., Thomas, D. L., Seeff, L. B. and Diseases, A. A. f. t. S. o. L. (2009) 'Diagnosis, management, and treatment of hepatitis C: an update', *Hepatology,* 49(4), pp. 1335-74.
100) Gieffers, J., Reusche, E., Solbach, W. and Maass, M. (2000) 'Failure to detect Chlamydia pneumoniae in brain sections of Alzheimer's disease patients', *J Clin Microbiol,* 38(2), pp. 881-2.
101) Gill, P. and Ghaemi, A. (2008) 'Nucleic acid isothermal amplification technologies: a review', *Nucleosides Nucleotides Nucleic Acids,* 27(3), pp. 224-43.
102) Giza, D. E., Vasilescu, C. and Calin, G. A. (2014) 'Key principles of miRNA involvement in human diseases', *Discoveries (Craiova),* 2(4), pp. e34.
103) Godfrey, T. E. and Kelly, L. A. (2005) 'Development of quantitative reverse transcriptase PCR assays for measuring gene expression', *Methods Mol Biol,* 291, pp. 423-45.
104) Goldenberger, D., Perschil, I., Ritzler, M. and Altwegg, M. (1995) 'A simple "universal" DNA extraction procedure using SDS and proteinase K is compatible with direct PCR amplification', *PCR Methods Appl,* 4(6), pp. 368-70.
105) Goldschmidt, V., Didierjean, J., Ehresmann, B., Ehresmann, C., Isel, C. and Marquet, R. (2006) 'Mg2+ dependency of HIV-1 reverse transcription, inhibition by nucleoside analogues and resistance', *Nucleic Acids Res,* 34(1), pp. 42-52.
106) Gregory, R. I., Chendrimada, T. P. and Shiekhattar, R. (2006) 'MicroRNA biogenesis: isolation and characterization of the microprocessor complex', *Methods Mol Biol,* 342, pp. 33-47.
107) Gu, S., Jin, L., Zhang, F., Sarnow, P. and Kay, M. A. (2009) 'Biological basis for restriction of microRNA targets to the 3' untranslated region in mammalian mRNAs', *Nat Struct Mol Biol,* 16(2), pp. 144-50.
108) Gudnason, H., Dufva, M., Bang, D. D. and Wolff, A. (2007) 'Comparison of multiple DNA dyes for real-time PCR: effects of dye concentration and sequence composition on DNA amplification and melting temperature', *Nucleic Acids Res,* 35(19), pp. e127.

109) Guo, H., Ingolia, N. T., Weissman, J. S. and Bartel, D. P. (2010) 'Mammalian microRNAs predominantly act to decrease target mRNA levels', *Nature,* 466(7308), pp. 835-40.
110) Gupta, E., Bajpai, M. and Choudhary, A. (2014) 'Hepatitis C virus: Screening, diagnosis, and interpretation of laboratory assays', *Asian J Transfus Sci,* 8(1), pp. 19-25.
111) Hagan, H., Pouget, E. R. and Des Jarlais, D. C. (2011) 'A systematic review and meta-analysis of interventions to prevent hepatitis C virus infection in people who inject drugs', *J Infect Dis,* 204(1), pp. 74-83.
112) Hata, A., Katayama, H., Kitajima, M., Visvanathan, C., Nol, C. and Furumai, H. (2011) 'Validation of internal controls for extraction and amplification of nucleic acids from enteric viruses in water samples', *Appl Environ Microbiol,* 77(13), pp. 4336-43.
113) He, H., Li, R., Chen, Y., Pan, P., Tong, W., Dong, X. and Yu, D. (2017) 'Integrated DNA and RNA extraction using magnetic beads from viral pathogens causing acute respiratory infections', *Sci Rep,* 7, pp. 45199.
114) He, L. and Hannon, G. J. (2004) 'MicroRNAs: small RNAs with a big role in gene regulation', *Nat Rev Genet,* 5(7), pp. 522-531.
115) He, M., Liu, Y., Wang, X., Zhang, M. Q., Hannon, G. J. and Huang, Z. J. (2012) 'Cell-type-based analysis of microRNA profiles in the mouse brain', *Neuron,* 73(1), pp. 35-48.
116) Herrick, J. B., Madsen, E. L., Batt, C. A. and Ghiorse, W. C. (1993) 'Polymerase chain reaction amplification of naphthalene-catabolic and 16S rRNA gene sequences from indigenous sediment bacteria', *Appl Environ Microbiol,* 59(3), pp. 687-94.
117) Hilz, H., Wiegers, U. and Adamietz, P. (1975) 'Stimulation of proteinase K action by denaturing agents: application to the isolation of nucleic acids and the degradation of 'masked' proteins', *Eur J Biochem,* 56(1), pp. 103-8.
118) Hoffmann, B., Depner, K., Schirrmeier, H. and Beer, M. (2006) 'A universal heterologous internal control system for duplex real-time RT-PCR assays used in a detection system for pestiviruses', *Journal of virological methods,* 136(1), pp. 200-209.
119) Holland, B., Wong, J., Li, M. and Rasheed, S. (2013) 'Identification of human microRNA-like sequences embedded within the protein-encoding genes of the human immunodeficiency virus', *PLoS One,* 8(3), pp. e58586.
120) Holland, P. M., Abramson, R. D., Watson, R. and Gelfand, D. H. (1991) 'Detection of specific polymerase chain reaction product by utilizing the 5'----3' exonuclease activity of Thermus aquaticus DNA polymerase', *Proc Natl Acad Sci U S A,* 88(16), pp. 7276-80.
121) Hoorfar, J., Malorny, B., Abdulmawjood, A., Cook, N., Wagner, M. and Fach, P. (2004a) 'Practical considerations in design of internal amplification controls for diagnostic PCR assays', *J Clin Microbiol,* 42.
122) Hoorfar, J., Malorny, B., Abdulmawjood, A., Cook, N., Wagner, M. and Fach, P. (2004b) 'Practical considerations in design of internal amplification controls for diagnostic PCR assays', *J Clin Microbiol,* 42(5), pp. 1863-8.
123) Huggett, J. F., Novak, T., Garson, J. A., Green, C., Morris-Jones, S. D., Miller, R. F. and Zumla, A. (2008) 'Differential susceptibility of PCR reactions to inhibitors: an important and unrecognised phenomenon', *BMC Res Notes,* 1, pp. 70.
124) Hussain, Z. (2013) 'Genomic Heterogeneity of Hepatitis Viruses (A-E): Role in Clinical Implications and Treatment', in Serviddio, G. (ed.) *Practical Management of Chronic Viral Hepatitis*. Rijeka: InTech, pp. Ch. 02.
125) Imani, M., Hosseinkhani, S., Ahmadian, S. and Nazari, M. (2010) 'Design and introduction of a disulfide bridge in firefly luciferase: increase of thermostability and decrease of pH sensitivity', *Photochemical & Photobiological Sciences,* 9(8), pp. 1167-1177.
126) Jing, Q., Huang, S., Guth, S., Zarubin, T., Motoyama, A., Chen, J., Di Padova, F., Lin, S. C., Gram, H. and Han, J. (2005) 'Involvement of microRNA in AU-rich element-mediated mRNA instability', *Cell,* 120(5), pp. 623-34.

127) Jones-Rhoades, M. W., Bartel, D. P. and Bartel, B. (2006) 'MicroRNAS and their regulatory roles in plants', *Annu Rev Plant Biol,* 57, pp. 19-53.
128) Jonstrup, S. P., Koch, J. and Kjems, J. (2006) 'A microRNA detection system based on padlock probes and rolling circle amplification', *RNA,* 12(9), pp. 1747-52.
129) Jopling, C. L., Yi, M., Lancaster, A. M., Lemon, S. M. and Sarnow, P. (2005) 'Modulation of hepatitis C virus RNA abundance by a liver-specific MicroRNA', *Science,* 309(5740), pp. 1577-81.
130) Jubin, R. (2001) 'Hepatitis C IRES: translating translation into a therapeutic target', *Curr Opin Mol Ther,* 3(3), pp. 278-87.
131) Kalle, E., Gulevich, A. and Rensing, C. (2013) 'External and semi-internal controls for PCR amplification of homologous sequences in mixed templates', *J Microbiol Methods,* 95(2), pp. 285-94.
132) Kargar, M., Askari, A., Doosti, A. and Ghorbani-Dalini, S. (2012) 'Loop-Mediated Isothermal Amplification Assay for Rapid Detection of Hepatitis C virus', *Indian J Virol,* 23(1), pp. 18-23.
133) Karoney, M. J. and Siika, A. M. (2013) 'Hepatitis C virus (HCV) infection in Africa: a review', *Pan Afr Med J,* 14, pp. 44.
134) Kato, N. (2000) 'Genome of human hepatitis C virus (HCV): gene organization, sequence diversity, and variation', *Microb Comp Genomics,* 5(3), pp. 129-51.
135) Kersting, S., Rausch, V., Bier, F. F. and von Nickisch-Rosenegk, M. (2014) 'Rapid detection of Plasmodium falciparum with isothermal recombinase polymerase amplification and lateral flow analysis', *Malar J,* 13, pp. 99.
136) Kevil, C. G., Walsh, L., Laroux, F. S., Kalogeris, T., Grisham, M. B. and Alexander, J. S. (1997) 'An improved, rapid Northern protocol', *Biochem Biophys Res Commun,* 238(2), pp. 277-9.
137) Khan, G., Kangro, H. O., Coates, P. J. and Heath, R. B. (1991) 'Inhibitory effects of urine on the polymerase chain reaction for cytomegalovirus DNA', *J Clin Pathol,* 44(5), pp. 360-5.
138) Kharsany, A. B., Hancock, N., Frohlich, J. A., Humphries, H. R., Abdool Karim, S. S. and Abdool Karim, Q. (2010) 'Screening for 'window-period' acute HIV infection among pregnant women in rural South Africa', *HIV Med,* 11(10), pp. 661-5.
139) Kiddle, G., Hardinge, P., Buttigieg, N., Gandelman, O., Pereira, C., McElgunn, C. J., Rizzoli, M., Jackson, R., Appleton, N., Moore, C., Tisi, L. C. and Murray, J. A. (2012) 'GMO detection using a bioluminescent real time reporter (BART) of loop mediated isothermal amplification (LAMP) suitable for field use', *BMC Biotechnol,* 12, pp. 15.
140) Kim, A. (2016) 'Hepatitis C Virus', *Ann Intern Med,* 165(5), pp. ITC33-ITC48.
141) Kim, S., Labbe, R. G. and Ryu, S. (2000) 'Inhibitory effects of collagen on the PCR for detection of Clostridium perfringens', *Applied and environmental microbiology,* 66(3), pp. 1213-1215.
142) Kim, Y. K. and Kim, V. N. (2007) 'Processing of intronic microRNAs', *EMBO J,* 26(3), pp. 775-83.
143) Kitayama, A., Yoshizaki, H., Ohmiya, Y., Ueda, H. and Nagamune, T. (2003) 'Creation of a thermostable firefly luciferase with pH-insensitive luminescent color', *Photochem Photobiol,* 77(3), pp. 333-8.
144) Kleiboeker, S. B. (2003) 'Applications of competitor RNA in diagnostic reverse transcription-PCR', *J Clin Microbiol,* 41(5), pp. 2055-61.
145) Kochan, K. J., Amaral, M. E., Agarwala, R., Schäffer, A. A. and Riggs, P. K. (2008) 'Application of dissociation curve analysis to radiation hybrid panel marker scoring: generation of a map of river buffalo (B. bubalis) chromosome 20', *BMC Genomics,* 9, pp. 544.
146) Kontomanolis, E. N. and Koukourakis, M. I. (2015) 'MicroRNA: The Potential Regulator of Endometrial Carcinogenesis', *Microrna,* 4(1), pp. 18-25.

147) Koscianska, E., Starega-Roslan, J., Czubala, K. and Krzyzosiak, W. J. (2011) 'High-resolution northern blot for a reliable analysis of microRNAs and their precursors', *ScientificWorldJournal,* 11, pp. 102-17.

148) Kotewicz, M. L., Sampson, C. M., D'Alessio, J. M. and Gerard, G. F. (1988) 'Isolation of cloned Moloney murine leukemia virus reverse transcriptase lacking ribonuclease H activity', *Nucleic Acids Res,* 16(1), pp. 265-77.

149) Kramer, M. F. and Coen, D. M. (2006) 'Enzymatic amplification of DNA by PCR: standard procedures and optimization', *Curr Protoc Cytom,* Appendix 3, pp. Appendix 3K.

150) Kreader, C. A. (1996a) 'Relief of amplification inhibition in PCR with bovine serum albumin or T4 gene 32 protein', *Applied and environmental microbiology,* 62(3), pp. 1102-1106.

151) Kreader, C. A. (1996b) 'Relief of amplification inhibition in PCR with bovine serum albumin or T4 gene 32 protein', *Appl Environ Microbiol,* 62(3), pp. 1102-6.

152) Krsek, M. and Wellington, E. (1999) 'Comparison of different methods for the isolation and purification of total community DNA from soil', *Journal of Microbiological Methods,* 39(1), pp. 1-16.

153) Kunisaki, K. M. and Janoff, E. N. (2009) 'Influenza in immunosuppressed populations: a review of infection frequency, morbidity, mortality, and vaccine responses', *The Lancet infectious diseases,* 9(8), pp. 493-504.

154) Kurkela, S. and Brown, D. W. G. (2009) 'Molecular diagnostic techniques', *Medicine,* 37(10), pp. 535-540.

155) Kurzynska-Kokorniak, A., Pokornowska, M., Koralewska, N., Hoffmann, W., Bienkowska-Szewczyk, K. and Figlerowicz, M. (2016) 'Revealing a new activity of the human Dicer DUF283 domain in vitro', 6, pp. 23989.

156) Kwak, J., Shim, J. H., Tiwari, I. and Jang, K. L. (2016) 'Hepatitis C virus core protein inhibits E6AP expression via DNA methylation to escape from ubiquitin-dependent proteasomal degradation', *Cancer letters,* 380(1), pp. 59-68.

157) L. Lawson, G., L. Cummings, A. and Mecum, S. (2003) *AMINE PLANT CORROSION REDUCED BY REMOVAL OF BICINE.*

158) Lahiri, D. K. and Nurnberger Jr, J. I. (1991) 'A rapid non-enzymatic method for the preparation of HMW DNA from blood for RFLP studies', *Nucleic acids research,* 19(19), pp. 5444.

159) Lahr, D. J. and Katz, L. A. (2009) 'Reducing the impact of PCR-mediated recombination in molecular evolution and environmental studies using a new-generation high-fidelity DNA polymerase', *Biotechniques,* 47(4), pp. 857-66.

160) Larkin, A. and Harbison, S. (1999) 'An improved method for STR analysis of bloodstained denim', *Int J Legal Med,* 112(6), pp. 388-90.

161) Lee, D., Kim, E. J., Kilgore, P. E., Kim, S. A., Takahashi, H., Ohnishi, M., Anh, D. D., Dong, B. Q., Kim, J. S., Tomono, J., Miyamoto, S., Notomi, T., Kim, D. W. and Seki, M. (2015) 'Clinical evaluation of a loop-mediated isothermal amplification (LAMP) assay for rapid detection of Neisseria meningitidis in cerebrospinal fluid', *PLoS One,* 10(4), pp. e0122922.

162) Lee, M. S., Lin, Y. C., Lai, G. H., Lai, S. Y., Chen, H. J. and Wang, M. Y. (2011) 'One-step reverse-transcription loop-mediated isothermal amplification for detection of infectious bursal disease virus', *Can J Vet Res,* 75(2), pp. 122-7.

163) Lee, Y., Ahn, C., Han, J., Choi, H., Kim, J., Yim, J., Lee, J., Provost, P., Rådmark, O., Kim, S. and Kim, V. N. (2003) 'The nuclear RNase III Drosha initiates microRNA processing', *Nature,* 425(6956), pp. 415-9.

164) Lee, Y., Kim, M., Han, J., Yeom, K. H., Lee, S., Baek, S. H. and Kim, V. N. (2004) 'MicroRNA genes are transcribed by RNA polymerase II', *EMBO J,* 23(20), pp. 4051-60.

165) Lesnik, E. A. and Freier, S. M. (1995) 'Relative thermodynamic stability of DNA, RNA, and DNA:RNA hybrid duplexes: relationship with base composition and structure', *Biochemistry,* 34(34), pp. 10807-15.

166) Lewis, B. P., Burge, C. B. and Bartel, D. P. (2005) 'Conserved seed pairing, often flanked by adenosines, indicates that thousands of human genes are microRNA targets', *Cell,* 120(1), pp. 15-20.
167) Lewis, B. P., Shih, I. H., Jones-Rhoades, M. W., Bartel, D. P. and Burge, C. B. (2003) 'Prediction of mammalian microRNA targets', *Cell,* 115(7), pp. 787-98.
168) Li, C., Li, Z., Jia, H. and Yan, J. (2011) 'One-step ultrasensitive detection of microRNAs with loop-mediated isothermal amplification (LAMP)', *Chem Commun (Camb),* 47(9), pp. 2595-7.
169) Li, M. P., Hu, Y. D., Hu, X. L., Zhang, Y. J., Yang, Y. L., Jiang, C., Tang, J. and Chen, X. P. (2016) 'MiRNAs and miRNA Polymorphisms Modify Drug Response', *Int J Environ Res Public Health,* 13(11).
170) Li, W. and Ruan, K. (2009) 'MicroRNA detection by microarray', *Anal Bioanal Chem,* 394(4), pp. 1117-24.
171) Li, Y., Kumar, N., Gopalakrishnan, A., Ginocchio, C., Manji, R., Bythrow, M., Lemieux, B. and Kong, H. (2013) 'Detection and species identification of malaria parasites by isothermal tHDA amplification directly from human blood without sample preparation', *J Mol Diagn,* 15(5), pp. 634-41.
172) Liang, X., Jensen, K. and Frank-Kamenetskii, M. D. (2004) 'Very efficient template/primer-independent DNA synthesis by thermophilic DNA polymerase in the presence of a thermophilic restriction endonuclease', *Biochemistry,* 43(42), pp. 13459-66.
173) Lienert, K. and Fowler, J. C. (1992) 'Analysis of mixed human/microbial DNA samples: a validation study of two PCR AMP-FLP typing methods', *Biotechniques,* 13(2), pp. 276-81.
174) Lim, L. P., Lau, N. C., Garrett-Engele, P., Grimson, A., Schelter, J. M., Castle, J., Bartel, D. P., Linsley, P. S. and Johnson, J. M. (2005) 'Microarray analysis shows that some microRNAs downregulate large numbers of target mRNAs', *Nature,* 433(7027), pp. 769-73.
175) Lim, L. P., Lau, N. C., Weinstein, E. G., Abdelhakim, A., Yekta, S., Rhoades, M. W., Burge, C. B. and Bartel, D. P. (2003) 'The microRNAs of Caenorhabditis elegans', *Genes Dev,* 17(8), pp. 991-1008.
176) Lim, N. Y., Roco, C. A. and Frostegård, Å. (2016) 'Transparent DNA/RNA Co-extraction Workflow Protocol Suitable for Inhibitor-Rich Environmental Samples That Focuses on Complete DNA Removal for Transcriptomic Analyses', *Front Microbiol,* 7, pp. 1588.
177) Liolios, L., Jenney, A., Spelman, D., Kotsimbos, T., Catton, M. and Wesselingh, S. (2001) 'Comparison of a multiplex reverse transcription-PCR-enzyme hybridization assay with conventional viral culture and immunofluorescence techniques for the detection of seven viral respiratory pathogens', *J Clin Microbiol,* 39(8), pp. 2779-83.
178) Lion, T. (2001) 'Current recommendations for positive controls in RT-PCR assays', *Leukemia,* 15(7), pp. 1033.
179) Liu, Q. Y., Chang, M. N., Lei, J. X., Koukiekolo, R., Smith, B., Zhang, D. and Ghribi, O. (2014a) 'Identification of microRNAs involved in Alzheimer's progression using a rabbit model of the disease', *Am J Neurodegener Dis,* 3(1), pp. 33-44.
180) Liu, Y., Gao, G., Yang, C., Zhou, K., Shen, B., Liang, H. and Jiang, X. (2014b) 'The role of circulating microRNA-126 (miR-126): a novel biomarker for screening prediabetes and newly diagnosed type 2 diabetes mellitus', *Int J Mol Sci,* 15(6), pp. 10567-77.
181) Lucchi, N. W., Gaye, M., Diallo, M. A., Goldman, I. F., Ljolje, D., Deme, A. B., Badiane, A., Ndiaye, Y. D., Barnwell, J. W., Udhayakumar, V. and Ndiaye, D. (2016) 'Evaluation of the Illumigene Malaria LAMP: A Robust Molecular Diagnostic Tool for Malaria Parasites', *Sci Rep,* 6, pp. 36808.
182) Lukavsky, P. J. (2009) 'Structure and function of HCV IRES domains', *Virus Res,* 139(2), pp. 166-71.
183) Lund, E. and Dahlberg, J. E. (2006) 'Substrate selectivity of exportin 5 and Dicer in the biogenesis of microRNAs', *Cold Spring Harb Symp Quant Biol,* 71, pp. 59-66.

184) Maheshwari, A. and Thuluvath, P. J. (2010) 'Management of acute hepatitis C', *Clin Liver Dis,* 14(1), pp. 169-76; x.
185) Maillard, P., Krawczynski, K., Nitkiewicz, J., Bronnert, C., Sidorkiewicz, M., Gounon, P., Dubuisson, J., Faure, G., Crainic, R. and Budkowska, A. (2001) 'Nonenveloped nucleocapsids of hepatitis C virus in the serum of infected patients', *J Virol,* 75(17), pp. 8240-50.
186) Malorny, B., Hoorfar, J., Bunge, C. and Helmuth, R. (2003) 'Multicenter validation of the analytical accuracy of Salmonella PCR: towards an international standard', *Appl Environ Microbiol,* 69(1), pp. 290-6.
187) Maroney, P. A., Yu, Y., Fisher, J. and Nilsen, T. W. (2006) 'Evidence that microRNAs are associated with translating messenger RNAs in human cells', *Nat Struct Mol Biol,* 13(12), pp. 1102-7.
188) Marwaha, N. and Sachdev, S. (2014) 'Current testing strategies for hepatitis C virus infection in blood donors and the way forward', *World J Gastroenterol,* 20(11), pp. 2948-54.
189) Mathonnet, G., Fabian, M. R., Svitkin, Y. V., Parsyan, A., Huck, L., Murata, T., Biffo, S., Merrick, W. C., Darzynkiewicz, E., Pillai, R. S., Filipowicz, W., Duchaine, T. F. and Sonenberg, N. (2007) 'MicroRNA inhibition of translation initiation in vitro by targeting the cap-binding complex eIF4F', *Science,* 317(5845), pp. 1764-7.
190) Mayer, C. L. and Palmer, C. J. (1996) 'Evaluation of PCR, nested PCR, and fluorescent antibodies for detection of Giardia and Cryptosporidium species in wastewater', *Appl Environ Microbiol,* 62(6), pp. 2081-5.
191) Mazière, P. and Enright, A. J. (2007) 'Prediction of microRNA targets', *Drug Discov Today,* 12(11-12), pp. 452-8.
192) Meng, S. and Li, J. (2010) 'A novel duplex real-time reverse transcriptase-polymerase chain reaction assay for the detection of hepatitis C viral RNA with armored RNA as internal control', *Virology Journal,* 7(1), pp. 117.
193) Mertens, K., Freund, L., Schmoock, G., Hänsel, C., Melzer, F. and Elschner, M. C. (2014) 'Comparative evaluation of eleven commercial DNA extraction kits for real-time PCR detection of Bacillus anthracis spores in spiked dairy samples', *International journal of food microbiology,* 170, pp. 29-37.
194) Mirihana Arachchilage, G., Dassanayake, A. C. and Basu, S. (2015) 'A potassium ion-dependent RNA structural switch regulates human pre-miRNA 92b maturation', *Chem Biol,* 22(2), pp. 262-72.
195) Mitchell, P. S., Parkin, R. K., Kroh, E. M., Fritz, B. R., Wyman, S. K., Pogosova-Agadjanyan, E. L., Peterson, A., Noteboom, J., O'Briant, K. C. and Allen, A. (2008) 'Circulating microRNAs as stable blood-based markers for cancer detection', *Proceedings of the National Academy of Sciences,* 105(30), pp. 10513-10518.
196) Modi, A. A. and Liang, T. J. (2008) 'Hepatitis C: a clinical review', *Oral Dis,* 14(1), pp. 10-4.
197) Montgomery, J. L. and Wittwer, C. T. (2014) 'Influence of PCR Reagents on DNA Polymerase Extension Rates Measured on Real-Time PCR Instruments', *Clinical Chemistry,* 60(2), pp. 334-340.
198) Moradpour, D., Brass, V. and Penin, F. (2005) 'Function follows form: the structure of the N-terminal domain of HCV NS5A', *Hepatology,* 42.
199) Moradpour, D. and Penin, F. (2013) 'Hepatitis C virus proteins: from structure to function', *Curr Top Microbiol Immunol,* 369, pp. 113-42.
200) Morata, P., Queipo-Ortuño, M. I. and de Dios Colmenero, J. (1998) 'Strategy for optimizing DNA amplification in a peripheral blood PCR assay used for diagnosis of human brucellosis', *J Clin Microbiol,* 36(9), pp. 2443-6.

201) Mori, Y. and Notomi, T. (2009) 'Loop-mediated isothermal amplification (LAMP): a rapid, accurate, and cost-effective diagnostic method for infectious diseases', *J Infect Chemother,* 15(2), pp. 62-9.
202) Morishima, C., Morgan, T. R., Everhart, J. E., Wright, E. C., Shiffman, M. L., Everson, G. T., Lindsay, K. L., Lok, A. S., Bonkovsky, H. L., Di Bisceglie, A. M., Lee, W. M., Dienstag, J. L., Ghany, M. G., Gretch, D. R. and Group, H.-C. T. (2006) 'HCV RNA detection by TMA during the hepatitis C antiviral long-term treatment against cirrhosis (Halt-C) trial', *Hepatology,* 44(2), pp. 360-7.
203) Mraz, M. and Pospisilova, S. (2012) 'MicroRNAs in chronic lymphocytic leukemia: from causality to associations and back', *Expert Rev Hematol,* 5(6), pp. 579-81.
204) Muldrew, K. L. (2009) 'Molecular diagnostics of infectious diseases', *Curr Opin Pediatr,* 21(1), pp. 102-11.
205) Murchison, E. P. and Hannon, G. J. (2004) 'miRNAs on the move: miRNA biogenesis and the RNAi machinery', *Curr Opin Cell Biol,* 16(3), pp. 223-9.
206) Musilova, K. and Mraz, M. (2015) 'MicroRNAs in B-cell lymphomas: how a complex biology gets more complex', *Leukemia,* 29(5), pp. 1004-17.
207) Nagamine, K., Hase, T. and Notomi, T. (2002) 'Accelerated reaction by loop-mediated isothermal amplification using loop primers', *Mol Cell Probes,* 16(3), pp. 223-9.
208) Nakon, R. and Krishnamoorthy, C. R. (1983) 'Free-metal ion depletion by "Good's" buffers', *Science,* 221(4612), pp. 749-50.
209) Nielsen, L. B., Wang, C., Sørensen, K., Bang-Berthelsen, C. H., Hansen, L., Andersen, M. L., Hougaard, P., Juul, A., Zhang, C. Y., Pociot, F. and Mortensen, H. B. (2012) 'Circulating levels of microRNA from children with newly diagnosed type 1 diabetes and healthy controls: evidence that miR-25 associates to residual beta-cell function and glycaemic control during disease progression', *Exp Diabetes Res,* 2012, pp. 896362.
210) Niemz, A., Ferguson, T. M. and Boyle, D. S. (2011) 'Point-of-care nucleic acid testing for infectious diseases', *Trends Biotechnol,* 29(5), pp. 240-50.
211) Njiru, Z. K. (2012) 'Loop-mediated isothermal amplification technology: towards point of care diagnostics', *PLoS Negl Trop Dis,* 6(6), pp. e1572.
212) Notomi, T., Okayama, H., Masubuchi, H., Yonekawa, T., Watanabe, K., Amino, N. and Hase, T. (2000) 'Loop-mediated isothermal amplification of DNA', *Nucleic Acids Res,* 28(12), pp. E63.
213) Nottrott, S., Simard, M. J. and Richter, J. D. (2006) 'Human let-7a miRNA blocks protein production on actively translating polyribosomes', *Nat Struct Mol Biol,* 13(12), pp. 1108-14.
214) Nyan, D.-C. and Swinson, K. L. (2016) 'A method for rapid detection and genotype identification of hepatitis C virus 1–6 by one-step reverse transcription loop-mediated isothermal amplification', *International Journal of Infectious Diseases,* 43(Supplement C), pp. 30-36.
215) Nyrén, P., Pettersson, B. and Uhlén, M. (1993) 'Solid phase DNA minisequencing by an enzymatic luminometric inorganic pyrophosphate detection assay', *Analytical biochemistry,* 208(1), pp. 171-175.
216) Okuda, M., Li, K., Beard, M. R., Showalter, L. A., Scholle, F., Lemon, S. M. and Weinman, S. A. (2002) 'Mitochondrial injury, oxidative stress, and antioxidant gene expression are induced by hepatitis C virus core protein', *Gastroenterology,* 122(2), pp. 366-375.
217) Opel, K. L., Chung, D. and McCord, B. R. (2010) 'A study of PCR inhibition mechanisms using real time PCR', *J Forensic Sci,* 55(1), pp. 25-33.
218) Panel, A. I. H. G. (2015) 'Hepatitis C guidance: AASLD-IDSA recommendations for testing, managing, and treating adults infected with hepatitis C virus', *Hepatology,* 62(3), pp. 932-54.

219) Parasramka, M. A., Dashwood, W. M., Wang, R., Saeed, H. H., Williams, D. E., Ho, E. and Dashwood, R. H. (2012) 'A role for low-abundance miRNAs in colon cancer: the miR-206/Krüppel-like factor 4 (KLF4) axis', *Clin Epigenetics,* 4(1), pp. 16.
220) Park, J. E., Heo, I., Tian, Y., Simanshu, D. K., Chang, H., Jee, D., Patel, D. J. and Kim, V. N. (2011) 'Dicer recognizes the 5' end of RNA for efficient and accurate processing', *Nature,* 475(7355), pp. 201-5.
221) Pasloske, B. L., Walkerpeach, C. R., Obermoeller, R. D., Winkler, M. and DuBois, D. B. (1998) 'Armored RNA technology for production of ribonuclease-resistant viral RNA controls and standards', *J Clin Microbiol,* 36(12), pp. 3590-4.
222) Patel, P., Klausner, J. D., Bacon, O. M., Liska, S., Taylor, M., Gonzalez, A., Kohn, R. P., Wong, W., Harvey, S., Kerndt, P. R. and Holmberg, S. D. (2006) 'Detection of acute HIV infections in high-risk patients in California', *J Acquir Immune Defic Syndr,* 42(1), pp. 75-9.
223) Pawlotsky, J. M. (1999) 'Diagnostic tests for hepatitis C', *J Hepatol,* 31.
224) Penin, F., Brass, V., Appel, N., Ramboarina, S., Montserret, R., Ficheux, D., Blum, H. E., Bartenschlager, R. and Moradpour, D. (2004) 'Structure and function of the membrane anchor domain of hepatitis C virus nonstructural protein 5A', *J Biol Chem,* 279.
225) Perkins, D. O., Jeffries, C. D., Jarskog, L. F., Thomson, J. M., Woods, K., Newman, M. A., Parker, J. S., Jin, J. and Hammond, S. M. (2007) 'microRNA expression in the prefrontal cortex of individuals with schizophrenia and schizoaffective disorder', *Genome Biol,* 8(2), pp. R27.
226) Petersen, C. P., Bordeleau, M. E., Pelletier, J. and Sharp, P. A. (2006) 'Short RNAs repress translation after initiation in mammalian cells', *Mol Cell,* 21(4), pp. 533-42.
227) Petruzziello, A., Marigliano, S., Loquercio, G., Cozzolino, A. and Cacciapuoti, C. (2016) 'Global epidemiology of hepatitis C virus infection: An up-date of the distribution and circulation of hepatitis C virus genotypes', *World J Gastroenterol,* 22(34), pp. 7824-40.
228) Pondé, R. A. (2011) 'Hidden hazards of HCV transmission', *Med Microbiol Immunol,* 200(1), pp. 7-11.
229) Poritz, M. A. and Ririe, K. M. (2014) 'Getting things backwards to prevent primer dimers', *The Journal of Molecular Diagnostics,* 16(2), pp. 159-162.
230) Powell, H., Gooding, C., Garrett, S., Lund, B. and McKee, R. (1994) 'Proteinase inhibition of the detection of Listeria monocytogenes in milk using the polymerase chain reaction', *Letters in Applied Microbiology,* 18(1), pp. 59-61.
231) Pratt, A. J. and MacRae, I. J. (2009) 'The RNA-induced silencing complex: a versatile gene-silencing machine', *J Biol Chem,* 284(27), pp. 17897-901.
232) Qi, J., Wang, J., Katayama, H., Sen, S. and Liu, S. M. (2013) 'Circulating microRNAs (cmiRNAs) as novel potential biomarkers for hepatocellular carcinoma', *Neoplasma,* 60(2), pp. 135-42.
233) Radhakrishnan, B. and Alwin Prem Anand, A. (2016) 'Role of miRNA-9 in Brain Development', *J Exp Neurosci,* 10, pp. 101-120.
234) Radstrom, P., Knutsson, R., Wolffs, P., Lovenklev, M. and Lofstrom, C. (2004) 'Pre-PCR processing: strategies to generate PCR-compatible samples', *Mol Biotechnol,* 26(2), pp. 133-46.
235) Ramadan, K., Shevelev, I. V., Maga, G. and Hübscher, U. (2004) 'De novo DNA synthesis by human DNA polymerase lambda, DNA polymerase mu and terminal deoxyribonucleotidyl transferase', *J Mol Biol,* 339(2), pp. 395-404.
236) Robe, P., Nalin, R., Capellano, C., Vogel, T. M. and Simonet, P. (2003) 'Extraction of DNA from soil', *European Journal of Soil Biology,* 39(4), pp. 183-190.
237) Robinson, H., Gao, Y. G., Sanishvili, R., Joachimiak, A. and Wang, A. H. (2000) 'Hexahydrated magnesium ions bind in the deep major groove and at the outer mouth of A-form nucleic acid duplexes', *Nucleic Acids Res,* 28(8), pp. 1760-6.

238) Rodriguez, A., Griffiths-Jones, S., Ashurst, J. L. and Bradley, A. (2004) 'Identification of mammalian microRNA host genes and transcription units', *Genome Res,* 14(10A), pp. 1902-10.
239) Rohrman, B. and Richards-Kortum, R. (2015) 'Inhibition of recombinase polymerase amplification by background DNA: a lateral flow-based method for enriching target DNA', *Anal Chem,* 87(3), pp. 1963-7.
240) Rosenstraus, M., Wang, Z., Chang, S. Y., DeBonville, D. and Spadoro, J. P. (1998) 'An internal control for routine diagnostic PCR: design, properties, and effect on clinical performance', *J Clin Microbiol,* 36(1), pp. 191-7.
241) Rossen, L., Nørskov, P., Holmstrøm, K. and Rasmussen, O. F. (1992) 'Inhibition of PCR by components of food samples, microbial diagnostic assays and DNA-extraction solutions', *International journal of food microbiology,* 17(1), pp. 37-45.
242) Rouhibakhsh, A., Priya, J., Periasamy, M., Haq, Q. M. and Malathi, V. G. (2008) 'An improved DNA isolation method and PCR protocol for efficient detection of multicomponents of begomovirus in legumes', *J Virol Methods,* 147(1), pp. 37-42.
243) Rudi, K. and Jakobsen, K. S. (2006) 'Overview of DNA purification for nucleic acid-based diagnostics from environmental and clinical samples', *Methods Mol Biol,* 345, pp. 23-35.
244) Rådström, P., Löfström, C., Lövenklev, M., Knutsson, R. and Wolffs, P. (2008) 'Strategies for overcoming PCR inhibition', *CSH Protoc,* 2008, pp. pdb.top20.
245) Saeki, K., Ihyo, Y., Sakai, M. and Kunito, T. (2011) 'Strong adsorption of DNA molecules on humic acids', *Environmental Chemistry Letters,* 9(4), pp. 505-509.
246) Sambrook, J. and Russell, D. W. (2006) 'Purification of nucleic acids by extraction with phenol: chloroform', *Cold Spring Harbor Protocols,* 2006(1), pp. pdb. prot4455.
247) Sanders, R., Mason, D. J., Foy, C. A. and Huggett, J. F. (2013) 'Evaluation of digital PCR for absolute RNA quantification', *PLoS One,* 8(9), pp. e75296.
248) Scaria, V., Hariharan, M., Maiti, S., Pillai, B. and Brahmachari, S. K. (2006) 'Host-virus interaction: a new role for microRNAs', *Retrovirology,* 3, pp. 68.
249) Schrader, C., Schielke, A., Ellerbroek, L. and Johne, R. (2012) 'PCR inhibitors–occurrence, properties and removal', *Journal of applied microbiology,* 113(5), pp. 1014-1026.
250) Schwarz, D. S. and Zamore, P. D. (2002) 'Why do miRNAs live in the miRNP?', *Genes Dev,* 16(9), pp. 1025-31.
251) Scott, J. D. and Gretch, D. R. (2007) 'Molecular diagnostics of hepatitis C virus infection: a systematic review', *JAMA,* 297(7), pp. 724-32.
252) Seeff, L. B. and Hoofnagle, J. H. (2003) 'Appendix: The National Institutes of Health Consensus Development Conference Management of Hepatitis C 2002', *Clin Liver Dis,* 7(1), pp. 261-87.
253) Selvey, S., Thompson, E. W., Matthaei, K., Lea, R. A., Irving, M. G. and Griffiths, L. R. (2001) 'Beta-actin--an unsuitable internal control for RT-PCR', *Mol Cell Probes,* 15(5), pp. 307-11.
254) Serec, K., Babić, S. D., Podgornik, R. and Tomić, S. (2016) 'Effect of magnesium ions on the structure of DNA thin films: an infrared spectroscopy study', *Nucleic Acids Res,* 44(17), pp. 8456-64.
255) Sidstedt, M., Jansson, L., Nilsson, E., Noppa, L., Forsman, M., Rådström, P. and Hedman, J. (2015) 'Humic substances cause fluorescence inhibition in real-time polymerase chain reaction', *Anal Biochem,* 487, pp. 30-7.
256) Simmonds, P. (1995) 'Variability of hepatitis C virus', *Hepatology,* 21.
257) Simmonds, P. (2004) 'Genetic diversity and evolution of hepatitis C virus--15 years on', *J Gen Virol,* 85(Pt 11), pp. 3173-88.
258) Simmonds, P., Holmes, E. C., Cha, T. A., Chan, S. W., McOmish, F., Irvine, B., Beall, E., Yap, P. L., Kolberg, J. and Urdea, M. S. (1993) 'Classification of hepatitis C virus into six major genotypes and a series of subtypes by phylogenetic analysis of the NS-5 region', *J Gen Virol,* 74.

259) Simon, A. K., Hollander, G. A. and McMichael, A. (2015) 'Evolution of the immune system in humans from infancy to old age', *Proc Biol Sci,* 282(1821), pp. 20143085.
260) Sint, D., Raso, L. and Traugott, M. (2012) 'Advances in multiplex PCR: balancing primer efficiencies and improving detection success', *Methods Ecol Evol,* 3(5), pp. 898-905.
261) Sipahioglu, H. M., Usta, M. and Ocak, M. (2006) 'Use of dried high-phenolic laden host leaves for virus and viroid preservation and detection by PCR methods', *Journal of virological methods,* 137(1), pp. 120-124.
262) Smart, L. B., Nall, N. M. and Bennett, A. B. (1999) 'Isolation of RNA and Protein from Guard Cells of Nicotiana glauca', *Plant Molecular Biology Reporter,* 17(4), pp. 371-383.
263) Smith, R. M., Walton, C. M., Wu, C. H. and Wu, G. Y. (2002) 'Secondary structure and hybridization accessibility of hepatitis C virus 3'-terminal sequences', *J Virol,* 76(19), pp. 9563-74.
264) Smith, R. M. and Wu, G. Y. (2004) 'Secondary structure and hybridization accessibility of the hepatitis C virus negative strand RNA 5'-terminus', *J Viral Hepat,* 11(2), pp. 115-23.
265) Song, X., Yao, Z., Yang, J., Zhang, Z., Deng, Y., Li, M., Ma, C., Yang, L., Gao, X. and Li, W. (2016) 'HCV core protein binds to gC1qR to induce A20 expression and inhibit cytokine production through MAPKs and NF-κB signaling pathways', *Oncotarget,* 7(23), pp. 33796.
266) Speers, D. J. (2006) 'Clinical applications of molecular biology for infectious diseases', *Clinical Biochemist Reviews,* 27(1), pp. 39.
267) Stadhouders, R., Pas, S. D., Anber, J., Voermans, J., Mes, T. H. and Schutten, M. (2010) 'The effect of primer-template mismatches on the detection and quantification of nucleic acids using the 5' nuclease assay', *J Mol Diagn,* 12(1), pp. 109-17.
268) Streit, S., Michalski, C. W., Erkan, M., Kleeff, J. and Friess, H. (2009) 'Northern blot analysis for detection and quantification of RNA in pancreatic cancer cells and tissues', *Nat Protoc,* 4(1), pp. 37-43.
269) Su, A. I., Pezacki, J. P., Wodicka, L., Brideau, A. D., Supekova, L., Thimme, R., Wieland, S., Bukh, J., Purcell, R. H., Schultz, P. G. and Chisari, F. V. (2002) 'Genomic analysis of the host response to hepatitis C virus infection', *Proc Natl Acad Sci U S A,* 99(24), pp. 15669-74.
270) Suthar, A. B. and Harries, A. D. (2015) 'A public health approach to hepatitis C control in low- and middle-income countries', *PLoS Med,* 12(3), pp. e1001795.
271) Takamizawa, J., Konishi, H., Yanagisawa, K., Tomida, S., Osada, H., Endoh, H., Harano, T., Yatabe, Y., Nagino, M., Nimura, Y., Mitsudomi, T. and Takahashi, T. (2004) 'Reduced expression of the let-7 microRNAs in human lung cancers in association with shortened postoperative survival', *Cancer Res,* 64(11), pp. 3753-6.
272) Tam, W. (2008) 'The emergent role of microRNAs in molecular diagnostics of cancer', *J Mol Diagn,* 10(5), pp. 411-4.
273) Tan, E., Erwin, B., Dames, S., Ferguson, T., Buechel, M., Irvine, B., Voelkerding, K. and Niemz, A. (2008) 'Specific versus nonspecific isothermal DNA amplification through thermophilic polymerase and nicking enzyme activities', *Biochemistry,* 47(38), pp. 9987-9999.
274) Tan, S. C. and Yiap, B. C. (2009) 'DNA, RNA, and protein extraction: the past and the present', *J Biomed Biotechnol,* 2009, pp. 574398.
275) Tang, Y., Chen, H. and Diao, Y. (2016) 'Advanced uracil DNA glycosylase-supplemented real-time reverse transcription loop-mediated isothermal amplification (UDG-rRT-LAMP) method for universal and specific detection of Tembusu virus', *Sci Rep,* 6, pp. 27605.
276) Tanner, N. A. and Evans, T. C. (2014) 'Loop-mediated isothermal amplification for detection of nucleic acids', *Curr Protoc Mol Biol,* 105, pp. Unit 15.14.
277) Tebbe, C. C. and Vahjen, W. (1993) 'Interference of humic acids and DNA extracted directly from soil in detection and transformation of recombinant DNA from bacteria and a yeast', *Appl Environ Microbiol,* 59(8), pp. 2657-65.
278) Tibbs, C. J. (1995) 'Methods of transmission of hepatitis C', *J Viral Hepat,* 2(3), pp. 113-9.

279) Timm, J. and Roggendorf, M. (2007) 'Sequence diversity of hepatitis C virus: implications for immune control and therapy', *World J Gastroenterol,* 13(36), pp. 4808-17.
280) Tisi, L., White, P., Squirrell, D., Murphy, M., Lowe, C. and Murray, J. (2002) 'Development of a thermostable firefly luciferase', *Analytica Chimica Acta,* 457(1), pp. 115-123.
281) Tsai, Y. L. and Olson, B. H. (1992) 'Detection of low numbers of bacterial cells in soils and sediments by polymerase chain reaction', *Appl Environ Microbiol,* 58(2), pp. 754-7.
282) Tsugama, D., Liu, S. and Takano, T. (2011) 'A rapid chemical method for lysing Arabidopsis cells for protein analysis', *Plant Methods,* 7, pp. 22.
283) Tyagi, S. and Kramer, F. R. (2012) 'Molecular beacons in diagnostics', *F1000 Med Rep,* 4, pp. 10.
284) van der Werf, R., Wijmenga, S. S., Heus, H. A. and Olsthoorn, R. C. (2013) 'Structural and thermodynamic signatures that define pseudotriloop RNA hairpins', *RNA,* 19(12), pp. 1833-9.
285) Vandeventer, P. E., Lin, J. S., Zwang, T. J., Nadim, A., Johal, M. S. and Niemz, A. (2012) 'Multiphasic DNA adsorption to silica surfaces under varying buffer, pH, and ionic strength conditions', *J Phys Chem B,* 116(19), pp. 5661-70.
286) Vermehren, J., Kau, A., Gärtner, B. C., Göbel, R., Zeuzem, S. and Sarrazin, C. (2008) 'Differences between two real-time PCR-based hepatitis C virus (HCV) assays (RealTime HCV and Cobas AmpliPrep/Cobas TaqMan) and one signal amplification assay (Versant HCV RNA 3.0) for RNA detection and quantification', *J Clin Microbiol,* 46.
287) Viguera, E., Canceill, D. and Ehrlich, S. D. (2001) 'Replication slippage involves DNA polymerase pausing and dissociation', *EMBO J,* 20(10), pp. 2587-95.
288) Vincent, M., Xu, Y. and Kong, H. (2004) 'Helicase-dependent isothermal DNA amplification', *EMBO Rep,* 5(8), pp. 795-800.
289) Válóczi, A., Hornyik, C., Varga, N., Burgyán, J., Kauppinen, S. and Havelda, Z. (2004) 'Sensitive and specific detection of microRNAs by northern blot analysis using LNA-modified oligonucleotide probes', *Nucleic Acids Res,* 32(22), pp. e175.
290) Wakiyama, M., Takimoto, K., Ohara, O. and Yokoyama, S. (2007) 'Let-7 microRNA-mediated mRNA deadenylation and translational repression in a mammalian cell-free system', *Genes Dev,* 21(15), pp. 1857-62.
291) Walker, G. T., Fraiser, M. S., Schram, J. L., Little, M. C., Nadeau, J. G. and Malinowski, D. P. (1992) 'Strand displacement amplification--an isothermal, in vitro DNA amplification technique', *Nucleic Acids Res,* 20(7), pp. 1691-6.
292) Wang, J., Chen, J. and Sen, S. (2016) 'MicroRNA as Biomarkers and Diagnostics', *J Cell Physiol,* 231(1), pp. 25-30.
293) Wang, Q. Q., Zhang, J., Hu, J. S., Chen, H. T., Du, L., Wu, L. Q., Ding, Y. Z., Xiong, S. H., Huang, X. C., Zhang, Y. H. and Liu, Y. S. (2011) 'Rapid detection of hepatitis C virus RNA by a reverse transcription loop-mediated isothermal amplification assay', *FEMS Immunol Med Microbiol,* 63(1), pp. 144-7.
294) Weber, J. A., Baxter, D. H., Zhang, S., Huang, D. Y., Huang, K. H., Lee, M. J., Galas, D. J. and Wang, K. (2010) 'The microRNA spectrum in 12 body fluids', *Clin Chem,* 56(11), pp. 1733-41.
295) Weber, M. J. (2005) 'New human and mouse microRNA genes found by homology search', *FEBS J,* 272(1), pp. 59-73.
296) WHO (2017) *Hepatitis C*. Available at: http://www.who.int/mediacentre/factsheets/fs164/en/.
297) Wiedbrauk, D. L., Werner, J. C. and Drevon, A. M. (1995) 'Inhibition of PCR by aqueous and vitreous fluids', *Journal of clinical microbiology,* 33(10), pp. 2643-2646.
298) Williams, A. E. (2008) 'Functional aspects of animal microRNAs', *Cell Mol Life Sci,* 65(4), pp. 545-62.

299) Wilson, I. G. (1997) 'Inhibition and facilitation of nucleic acid amplification', *Appl Environ Microbiol,* 63(10), pp. 3741-51.
300) Wink, M. (2011) *An introduction to molecular biotechnology : fundamentals, methods, and applications.* 2nd ed. edn. Weinheim: Wiley-VCH.
301) Wu, L. R., Wang, J. S., Fang, J. Z., R Evans, E., Pinto, A., Pekker, I., Boykin, R., Ngouenet, C., Webster, P. J., Beechem, J. and Zhang, D. Y. (2015) 'Continuously tunable nucleic acid hybridization probes', *Nat Meth,* 12(12), pp. 1191-1196.
302) Xu, J. H., Fu, J. J., Wang, X. L., Zhu, J. Y., Ye, X. H. and Chen, S. D. (2013) 'Hepatitis B or C viral infection and risk of pancreatic cancer: a meta-analysis of observational studies', *World J Gastroenterol,* 19(26), pp. 4234-41.
303) Yan, K. S., Yan, S., Farooq, A., Han, A., Zeng, L. and Zhou, M. M. (2003) 'Structure and conserved RNA binding of the PAZ domain', *Nature,* 426(6965), pp. 468-74.
304) Yang, J., Fang, M. X., Li, J., Lou, G. Q., Lu, H. J. and Wu, N. P. (2011) 'Detection of hepatitis C virus by an improved loop-mediated isothermal amplification assay', *Arch Virol,* 156(8), pp. 1387-96.
305) Yang, S. and Rothman, R. E. (2004) 'PCR-based diagnostics for infectious diseases: uses, limitations, and future applications in acute-care settings', *Lancet Infect Dis,* 4(6), pp. 337-48.
306) Young, B. and Cotter, F. (1992) 'Molecular Diagnostics of Cancer', in Mathew, C. (ed.) *Protocols in Human Molecular Genetics Methods in Molecular Biology*: Springer New York, pp. 327-345.
307) Young, K. K., Resnick, R. M. and Myers, T. W. (1993) 'Detection of hepatitis C virus RNA by a combined reverse transcription-polymerase chain reaction assay', *J Clin Microbiol,* 31(4), pp. 882-6.
308) Yu, X. F., Pan, J. C., Ye, R., Xiang, H. Q., Kou, Y. and Huang, Z. C. (2008) 'Preparation of armored RNA as a control for multiplex real-time reverse transcription-PCR detection of influenza virus and severe acute respiratory syndrome coronavirus', *J Clin Microbiol,* 46(3), pp. 837-41.
309) Zhang, J., Nguyen, D. and Hu, K.-Q. (2016) 'Chronic Hepatitis C Virus Infection: A Review of Current Direct-Acting Antiviral Treatment Strategies', *North American journal of medicine & science,* 9(2), pp. 47-54.
310) Zhang, J., Wu, D., Chen, Q., Chen, M., Xia, Y., Cai, S., Zhang, X., Wu, F. and Chen, J. (2015) 'Label-free microRNA detection based on terbium and duplex-specific nuclease assisted target recycling', *Analyst,* 140(15), pp. 5082-9.
311) Zhang, L., Zong, Z. Y., Liu, Y. B., Ye, H. and Lv, X. J. (2011) 'PCR versus serology for diagnosing Mycoplasma pneumoniae infection: a systematic review & meta-analysis', *Indian J Med Res,* 134, pp. 270-80.
312) Zhang, Y. (2013) 'RNA-induced Silencing Complex (RISC)', in Dubitzky, W., Wolkenhauer, O., Cho, K.-H. & Yokota, H. (eds.) *Encyclopedia of Systems Biology*. New York, NY: Springer New York, pp. 1876-1876.
313) Zhang, Y., Jia, Y., Zheng, R., Guo, Y., Wang, Y., Guo, H., Fei, M. and Sun, S. (2010a) 'Plasma microRNA-122 as a biomarker for viral-, alcohol-, and chemical-related hepatic diseases', *Clin Chem,* 56(12), pp. 1830-8.
314) Zhang, Z., Kermekchiev, M. B. and Barnes, W. M. (2010b) 'Direct DNA amplification from crude clinical samples using a PCR enhancer cocktail and novel mutants of Taq', *J Mol Diagn,* 12(2), pp. 152-61.
315) Zhao, C., Sun, G., Li, S. and Shi, Y. (2009) 'A feedback regulatory loop involving microRNA-9 and nuclear receptor TLX in neural stem cell fate determination', *Nat Struct Mol Biol,* 16(4), pp. 365-71.
316) Zheng, X., Niu, L., Wei, D., Li, X. and Zhang, S. (2016) 'Label-free detection of microRNA based on coupling multiple isothermal amplification techniques', *Sci Rep,* 6, pp. 35982.

317) Zhou, X., Ruan, J., Wang, G. and Zhang, W. (2007) 'Characterization and identification of microRNA core promoters in four model species', *PLoS Comput Biol,* 3(3), pp. e37.
318) Zipper, H., Buta, C., Lämmle, K., Brunner, H., Bernhagen, J. and Vitzthum, F. (2003) 'Mechanisms underlying the impact of humic acids on DNA quantification by SYBR Green I and consequences for the analysis of soils and aquatic sediments', *Nucleic Acids Res,* 31(7), pp. e39.

Appendix

Appendix 1

Protocol 1: Standard HCV LAMP-BART assay

Reaction mix setup:

Dispense volume [µL]:	15					
		Final conc				
Component	Stock	Mix+sample	Units	Spec	[µL]	Added
MGW				MS00001	464	
Trehalose (25% solution)	250	75	mg/mL	SS008	600	
10 Isothermal Buffer	10	1	x	MS00043	200	
Dithiothreitol 1M	1000	10	mM	SS003	20	
Luciferin, 10 mg/mL solution	10	0.1	mg/mL	SS0004	20	
10 mM APS	10000	250	µM	MS00015	50	
Ultraglow luciferase	46.6	0.05	RLU/mL	MS00011	1.1	
300U/ml ATP sulphurylase	300000	375	mU/mL	MS00012	2.5	
100 mM dNTP mix	25000	300	µM	MS00032	24	
HCV BIP	100	1.6	µM	Eurofins	32	
HCV FIP	100	1.6	µM		32	
HCV F3	100	0.4	µM		8	
HCV B3	100	0.4	µM		8	
HCV LoopF	100	0.8	µM		16	
HCV LoopB	100	0.8	µM		16	
Ribolock	40	0.05	U/µl	MS00042	2.5	
Gsp SSD pol	100	0.1	U/µl	MS00041	2	
Maxima RTase H -	200	0.2	u/µl	MS00030	2.0	
*HPLC Purified Primers					1500	Total volume

Master mix was prepared according to the reaction mix set up shown above. 15 uL of the master mix was then mixed with 5 uL of the appropriate HCV template in a 96-well plate (white) followed by an addition of two drops of mineral oil. Samples were sealed using a clear adhesive film and loaded onto BISON set at 60 °C and ran for 90 min.

Appendix 2

Protocol 2: Primer screening procedure using standard HCV LAMP-BART assay

Reaction mix set up:

Dispense volume [µL]:	15					
		Final conc				
Component	Stock	Mix+sample	Units	Spec	[µL]	Added
MGW				MS00001	464	
Trehalose (25% solution)	250	75	mg/mL	SS008	600	
10 Isothermal Buffer	10	1	x	MS00043	200	
Dithiothreitol 1M	1000	10	mM	SS003	20	
Luciferin, 10 mg/mL solution	10	0.1	mg/mL	SS0004	20	
10 mM APS	10000	250	µM	MS00015	50	
Ultraglow luciferase	46.6	0.05	RLU/mL	MS00011	1.1	
300U/ml ATP sulphurylase	300000	375	mU/mL	MS00012	2.5	
100 mM dNTP mix	25000	300	µM	MS00032	24	
HCV BIP	100	1.6	µM	Eurofins		
HCV FIP	100	1.6	µM			
HCV F3	100	0.4	µM			
HCV B3	100	0.4	µM			
HCV LoopF	100	0.8	µM			
HCV LoopB	100	0.8	µM			
Ribolock	40	0.05	U/µl	MS00042	2.5	
Gsp SSD pol	100	0.1	U/µl	MS00041	2	
Maxima RTase H -	200	0.2	u/µl	MS00030	2.0	
*HPLC Purified Primers					1388	Total volume

Initial master mix was prepared according to the reaction mix set up shown above. 1388 uL of the initial reaction mix was then split into four aliquots of 347 uL each. Final master mix was prepared by adding 2 uL of F3 and B3, 4 uL of Loop B and F and 8 uL of FIP and BIP of the appropriate LAMP primer sets to the aliquots containing 347 uL of the initial master mix. 15 uL of the final master mix was then mixed with 5 uL of the appropriate HCV template [10^4 cp/5uL] in a 96-well plate (white) followed by an addition of two drops of mineral oil. Samples were sealed using a clear adhesive film and loaded onto BISON set at 60 °C and ran for 90 min.

Note: 100 uM primer stocks were used

Appendix 3

Protocol 3: DNA polymerase screening procedure using standard HCV LAMP-BART assay

Reaction mix set up:

Dispense volume [µL]:	15					
		Final conc				
Component	Stock	Mix+sample	Units	Spec	[µL]	Added
MGW				MS00001	464	
Trehalose (25% solution)	250	75	mg/mL	SS008	600	
10 Isothermal Buffer	10	1	x	MS00043	200	
Dithiothreitol 1M	1000	10	mM	SS003	20	
Luciferin, 10 mg/mL solution	10	0.1	mg/mL	SS0004	20	
10 mM APS	10000	250	µM	MS00015	50	
Ultraglow luciferase	46.6	0.05	RLU/mL	MS00011	1.1	
300U/ml ATP sulphurylase	300000	375	mU/mL	MS00012	2.5	
100 mM dNTP mix	25000	300	µM	MS00032	24	
HCV BIP	100	1.6	µM	Eurofins	32	
HCV FIP	100	1.6	µM		32	
HCV F3	100	0.4	µM		8	
HCV B3	100	0.4	µM		8	
HCV LoopF	100	0.8	µM		16	
HCV LoopB	100	0.8	µM		16	
Ribolock	40	0.05	U/µl	MS00042	2.5	
Gsp SSD pol	100	0.1	U/µl	MS00041		
Maxima RTase H -	200	0.2	u/µl	MS00030	2.0	
*HPLC Purified Primers					1498	Total volume

Initial master mixes (2x) were prepared according to the reaction mix set up shown above. 1498 uL of each of the prepared initial reaction mixes were then split into two aliquots of 749 uL. Final master mixes were prepared by adding 1 uL of either GSP-SSD [100 U/uL], Bst 2.0 [200 U/uL] or Bst 2.0WS [200 U/uL], or 1.5 uL of Bst large fragment [160 U/uL] to separate aliquots containing 749 uL of the initial master mix. 15 uL of the final master mix was then mixed with 5 uL of the appropriate HCV template in a 96-well plate (white) followed by an addition of two drops of mineral oil. Samples were sealed using a clear adhesive film and loaded onto BISON set at 60 °C and ran for 90 min.

HCV RNA at concentrations 10^4, 10^3, 100, 50 and 10 cps/5uL were used in this study.

Appendix 4

Protocol 4: Reverse transcriptases screening procedure using standard HCV LAMP-BART assay

Reaction mix set up:

Dispense volume [µL]:	15					
		Final conc				
Component	Stock	Mix+sample	Units	Spec	[µL]	Added
MGW				MS00001	464	
Trehalose (25% solution)	250	75	mg/mL	SS008	600	
10 Isothermal Buffer	10	1	x	MS00043	200	
Dithiothreitol 1M	1000	10	mM	SS003	20	
Luciferin, 10 mg/mL solution	10	0.1	mg/mL	SS0004	20	
10 mM APS	10000	250	µM	MS00015	50	
Ultraglow luciferase	46.6	0.05	RLU/mL	MS00011	1.1	
300U/ml ATP sulphurylase	300000	375	mU/mL	MS00012	2.5	
100 mM dNTP mix	25000	300	µM	MS00032	24	
HCV BIP	100	1.6	µM	Eurofins	32	
HCV FIP	100	1.6	µM		32	
HCV F3	100	0.4	µM		8	
HCV B3	100	0.4	µM		8	
HCV LoopF	100	0.8	µM		16	
HCV LoopB	100	0.8	µM		16	
Ribolock	40	0.05	U/µl	MS00042	2.5	
Gsp SSD pol	100	0.1	U/µl	MS00041	2	
Maxima RTase H -	200	0.2	u/µl	MS00030		
*HPLC Purified Primers					1498	Total volume

Initial master mixes (2x) were prepared according to the reaction mix set up shown above. 1498 uL of each of the prepared initial reaction mixes were then split into two aliquots of 749 uL. Final master mixes were prepared by adding 1 uL of either Maxima RNaseH+ [200 U/uL], Maxima RNaseH+ [200 U/uL] or SuperScriptIV [200 U/uL] to separate aliquots containing 749 uL of the initial master mix. 15 uL of the final master mix was then mixed with 5 uL of the appropriate HCV template in a 96-well plate (white) followed by an addition of two drops of mineral oil. Samples were sealed using a clear adhesive film and loaded onto BISON set at 60 °C and ran for 90 min.

HCV RNA at concentrations 10^4, 10^3, 100, 50, 10 and 1 cps/5uL were used in this study.

Appendix 5

Protocol 5: Reaction buffers screening procedure using standard HCV LAMP-BART assay

Reaction mix set up:

Dispense volume [µL]:	15					
		Final conc				
Component	Stock	Mix+sample	Units	Spec	[µL]	Added
MGW				MS00001	464	
Trehalose (25% solution)	250	75	mg/mL	SS008	600	
10 Isothermal Buffer	10	1	x	MS00043		
Dithiothreitol 1M	1000	10	mM	SS003	20	
Luciferin, 10 mg/mL solution	10	0.1	mg/mL	SS0004	20	
10 mM APS	10000	250	µM	MS00015	50	
Ultraglow luciferase	46.6	0.05	RLU/mL	MS00011	1.1	
300U/ml ATP sulphurylase	300000	375	mU/mL	MS00012	2.5	
100 mM dNTP mix	25000	300	µM	MS00032	24	
HCV BIP	100	1.6	µM	Eurofins	32	
HCV FIP	100	1.6	µM		32	
HCV F3	100	0.4	µM		8	
HCV B3	100	0.4	µM		8	
HCV LoopF	100	0.8	µM		16	
HCV LoopB	100	0.8	µM		16	
Ribolock	40	0.05	U/µl	MS00042	2.5	
Gsp SSD pol	100	0.1	U/µl	MS00041	2	
Maxima RTase H -	200	0.2	u/µl	MS00030	2.0	
*HPLC Purified Primers					1300	Total volume

Initial master mix was prepared according to the reaction mix set up shown above. 1300 uL of the prepared initial reaction mixes was then split into two aliquots of 650 uL each. Final master mix was prepared by adding 100 uL of either Isothermal [10x] or Thermopol [10x] buffers to separate aliquots containing 650 uL of the initial master mix. 15 uL of the final master mix was then mixed with 5 uL of the appropriate HCV template in a 96-well plate (white) followed by an addition of two drops of mineral oil. Samples were sealed using a clear adhesive film and loaded onto BISON set at 60 °C and ran for 90 min.

HCV RNA at concentrations 10^4, 10^3, 100, 50, 10 and 1 cps/5uL were used in this study.

Appendix 6

Protocol 6: Inhibitory substances screening procedure using standard HCV LAMP-BART assay

Reaction mix set up:

Dispense volume [µL]:	15					
		Final conc				
Component	Stock	Mix+sample	Units	Spec	[µL]	Added
MGW				MS00001	462	
Trehalose (25%solution)	250	75	mg/mL	SS008	600	
10 Isothermal Buffer	10	1	x	MS00043	200	
Dithiothreitol 1M	1000	10	mM	SS003	20	
Luciferin, 10 mg/mL solution	10	0.1	mg/mL	SS0004	20	
10 mM APS	10000	250	µM	MS00015	50	
Ultraglow luciferase	46.6	0.05	RLU/mL	MS00011	1.1	
300U/ml ATP sulphurylase	300000	375	mU/mL	MS00012	2.5	
100 mM dNTP mix	25000	300	µM	MS00032	24	
HCV BIP	100	1.6	µM	Eurofins	32	
HCV FIP	100	1.6	µM		32	
HCV F3	100	0.4	µM		8	
HCV B3	100	0.4	µM		8	
HCV LoopF	100	0.8	µM		16	
HCV LoopB	100	0.8	µM		16	
Ribolock	40	0.05	U/µl	MS00042	2.5	
Gsp SSD pol	100	0.1	U/µl	MS00041		
HCV 5'UTR RNA	200000	100	cps/µl		2	
Maxima RTase H -	200	0.2	u/µl	MS00030	2.0	
*HPLC Purified Primers					1498	Total volume

Initial master mix was prepared according to the reaction mix set up shown above. 1498 uL of the initial reaction mixes was then split into two aliquots of 749 uL each. Final master mix was prepared by adding 1 uL of either GSP-SSD [100 U/uL] or Bst 2.0 [200 U/uL] to separate aliquots containing 749 uL of the initial master mix. 15 uL of the final master mix was then mixed with 5 uL of the appropriate inhibitory substance in a 96-well plate (white) followed by an addition of two drops of mineral oil. Samples were sealed using a clear adhesive film and loaded onto BISON set at 60 °C and ran for 90 min.

Potassium and sodium chloride and Potassium acetate at concentrations 0 to 50 mM, were tested in this study.

Appendix 7

Protocol 7: Standard TB LAMP-BART assay (20 uL)

Reaction mix set up:

Dispense volume [µL]:	15					
Component	Stock	Final conc Mix+sample	Units	Spec	[µL]	Added
MGW				MS00001	325	
Trehalose (25% solution)	250	50	mg/mL	SS008	400	
Bicine Buffer	4x	1x			500	
Mg2SO4, 100mM	100	2	mM	MS00017	40	
Dithiothreitol 1M	1000	10	mM	SS003	20	
Luciferin, 10 mg/mL solution	10	0.1	mg/mL	SS0004	20	
10 mM APS	10000	250	µM	MS00015	50	
Ultraglow luciferase	50.7	0.025	µg/mL	MS00011	2.0	
300U/ml ATP sulphurylase	300000	375	mU/mL	MS00012	2.5	
100mM dNTP mix (25mM eac	25000	300	µM	MS00032	24	
Bst LF DNA polymerase	160000	200	u/mL	MS00029	2.5	
Lamp F TB103	100	1.6	µM	MWG	32	
LAMP B TB087	100	1.6	µM		32	
Loop B TB083	100	0.8	µM		16	
LoopF TB101	100	0.8	µM		16	
Disp B TB100	100	0.4	µM		8	
Disp F TB115	100	0.4	µM		8	
Maxima RtaseH +	200	0.2	u/µl	MS00030	2	
				Total Volume	1500	[µL]

Master mix was prepared according to the reaction mix set up shown above. 15 uL of the master mix was then mixed with 5 uL of the appropriate *M. bovi* template in a 96-well plate (white) followed by an addition of two drops of mineral oil. Samples were sealed using a clear adhesive film and loaded onto BISON set at 60 °C and ran for 90 min.

Appendix 8

Protocol 8: DNA polymerase screening procedure using standard TB LAMP-BART assay

Reaction mix set up:

Dispense volume [µL]:	15					
		Final conc				
Component	Stock	Mix+sample	Units	Spec	[µL]	Added
MGW				MS00001	325	
Trehalose (25% solution)	250	50	mg/mL	SS008	400	
Bicine Buffer	4x	1x			500	
Mg2SO4, 100mM	100	2	mM	MS00017	40	
Dithiothreitol 1M	1000	10	mM	SS003	20	
Luciferin, 10 mg/mL solution	10	0.1	mg/mL	SS0004	20	
10 mM APS	10000	250	µM	MS00015	50	
Ultraglow luciferase	50.7	0.025	µg/mL	MS00011	2.0	
300U/ml ATP sulphurylase	300000	375	mU/mL	MS00012	2.5	
100mM dNTP mix (25mM eac	25000	300	µM	MS00032	24	
Bst LF DNA polymerase	160000	200	u/mL	MS00029		
Lamp F TB103	100	1.6	µM	MWG	32	
LAMP B TB087	100	1.6	µM		32	
Loop B TB083	100	0.8	µM		16	
LoopF TB101	100	0.8	µM		16	
Disp B TB100	100	0.4	µM		8	
Disp F TB115	100	0.4	µM		8	
Maxima RtaseH +	200	0.2	u/µl	MS00030	2	
				Total Volume	1498	[µL]

Initial master mixes (2x) were prepared according to the reaction mix set up shown above. 1498 uL of each of the prepared initial reaction mixes were then split into two aliquots of 749 uL. Final master mixes were prepared by adding 1 uL of either GSP-SSD [100 U/uL], Bst 2.0 [200 U/uL] or Bst 2.0WS [200 U/uL], or 1.3 uL Bst large fragment [160 U/uL] to separate aliquots containing 749 uL of the initial master mix. 15 uL of the final master mix was then mixed with 5 uL of the appropriate TB *M. bovis* template in a 96-well plate (white) followed by an addition of two drops of mineral oil. Samples were sealed using a clear adhesive film and loaded onto BISON set at 60 °C and ran for 90 min.

M. bovis nucleic acids concentrations of 1000 and 100 cps/5uL were used in this study.

Both genomic DNA and 23s rRNA were used.

Appendix 9

Protocol 9: Inhibitory substances screening procedure using standard TB LAMP-BART assay (no IAC) - LDS

Reaction mix set up:

Dispense volume [µL]:	15					
		Final conc				
Component	Stock	Mix+sample	Units	Spec	[µL]	Added
MGW				MS00001	325	
Trehalose (25%solution)	250	50	mg/mL	SS008	400	
Bicine Buffer	4x	1x			500	
Mg2SO4, 100mM	100	2	mM	MS00017	40	
Dithiothreitol 1M	1000	10	mM	SS003	20	
Luciferin, 10 mg/mL solution	10	0.1	mg/mL	SS0004	20	
10 mM APS	10000	250	µM	MS00015	50	
Ultraglow luciferase	50.7	0.025	µg/mL	MS00011	2.0	
300U/ml ATP sulphurylase	300000	375	mU/mL	MS00012	2.5	
100mM dNTP mix (25mM eac	25000	300	µM	MS00032	24	
Bst LF DNA polymerase	160000	200	u/mL	MS00029	2.5	
Lamp F TB103	100	1.6	µM	MWG	32	
LAMP B TB087	100	1.6	µM		32	
Loop B TB083	100	0.8	µM		16	
LoopF TB101	100	0.8	µM		16	
Disp B TB100	100	0.4	µM		8	
Disp F TB115	100	0.4	µM		8	
Maxima RtaseH +	200	0.2	u/µl	MS00030	2	
				Total Volume	1500	[µL]

Master mix was prepared according to the reaction mix set up shown above. 15 uL of the master mix was then mixed with 5 uL of the appropriate *M. bovis* template* in a 96-well plate (white) followed by an addition of two drops of mineral oil. Samples were sealed using a clear adhesive film and loaded onto BISON set at 60 °C and ran for 90 min.

*- dilutions of the templates were performed using the appropriate concentrations of the tested inhibitors as diluents.

M. bovis 23s rRNA at concentration 1000 and 100 cps/5uL was used in this study.

Serial dilutions (20 uL sample + 180 uL diluent) of the 23s rRNA top stock [10^6 cps/5uL] were carried out in order to obtain the appropriate template concentrations.

For the inhibitory samples, 0.01 and 0.05% LDS was used as diluents.

Appendix 10

Protocol 10: Inhibitory substances screening procedure using standard TB LAMP-BART assay (no IAC) – Bicine buffers comparison

Reaction mix set up:

Dispense volume [µL]:	15					
		Final conc				
Component	Stock	Mix+sample	Units	Spec	[µL]	Added
MGW				MS00001	325	
Trehalose (25% solution)	250	50	mg/mL	SS008	400	
Bicine Buffer	4x	1x				
Mg2SO4, 100mM	100	2	mM	MS00017	40	
Dithiothreitol 1M	1000	10	mM	SS003	20	
Luciferin, 10 mg/mL solution	10	0.1	mg/mL	SS0004	20	
10 mM APS	10000	250	µM	MS00015	50	
Ultraglow luciferase	50.7	0.025	µg/mL	MS00011	2.0	
300U/ml ATP sulphurylase	300000	375	mU/mL	MS00012	2.5	
100mM dNTP mix (25mM eac	25000	300	µM	MS00032	24	
Bst LF DNA polymerase	160000	200	u/mL	MS00029	2.5	
Lamp F TB103	100	1.6	µM	MWG	32	
LAMP B TB087	100	1.6	µM		32	
Loop B TB083	100	0.8	µM		16	
LoopF TB101	100	0.8	µM		16	
Disp B TB100	100	0.4	µM		8	
Disp F TB115	100	0.4	µM		8	
Maxima RtaseH +	200	0.2	u/µl	MS00030	2	
				Total Volume	1000	[µL]

Initial master mix was prepared according to the reaction mix set up shown above. 1000 uL of the initial reaction mix was then split into two aliquots of 500 uL each. Final master mix was prepared by adding 250 uL of either 500 mM [4x] or 50 mM [4x] Bicine buffers to separate aliquots containing 500 uL of the initial master mix. 15 uL of the final master mix was then mixed with 5 uL of the appropriate *M. bovis* template* in a 96-well plate (white) followed by an addition of two drops of mineral oil. Samples were sealed using a clear adhesive film and loaded onto BISON set at 60 °C and ran for 90 min.

*- dilutions of the templates were performed using the appropriate concentrations of the tested inhibitors as diluents.

M. bovis 23s rRNA at concentration 10000 and 1000 cps/5uL was used in this study.

Serial dilutions (20 uL sample + 180 uL diluent) of the 23s rRNA top stock [10^6 cps/5uL] were carried out in order to obtain the appropriate template concentrations.

For the inhibitory samples, 0.05% LDS was used as diluent.

Appendix 11

Protocol 11: Inhibitory substances screening procedure using standard TB LAMP-BART assay (no IAC) – carrier DNA

Reaction mix set up:

Dispense volume [µL]:	15					
		Final conc				
Component	Stock	Mix+sample	Units	Spec	[µL]	Added
MGW				MS00001	325	
Trehalose (25% solution)	250	50	mg/mL	SS008	400	
Bicine Buffer	4x	1x			500	
Mg2SO4, 100mM	100	2	mM	MS00017	40	
Dithiothreitol 1M	1000	10	mM	SS003	20	
Luciferin, 10 mg/mL solution	10	0.1	mg/mL	SS0004	20	
10 mM APS	10000	250	µM	MS00015	50	
Ultraglow luciferase	50.7	0.025	µg/mL	MS00011	2.0	
300U/ml ATP sulphurylase	300000	375	mU/mL	MS00012	2.5	
100mM dNTP mix (25mM eac	25000	300	µM	MS00032	24	
Bst LF DNA polymerase	160000	200	u/mL	MS00029	2.5	
Lamp F TB103	100	1.6	µM	MWG	32	
LAMP B TB087	100	1.6	µM		32	
Loop B TB083	100	0.8	µM		16	
LoopF TB101	100	0.8	µM		16	
Disp B TB100	100	0.4	µM		8	
Disp F TB115	100	0.4	µM		8	
Maxima RtaseH +	200	0.2	u/µl	MS00030	2	
				Total Volume	1500	[µL]

Master mix was prepared according to the reaction mix set up shown above. 15 uL of the master mix was then mixed with 5 uL of the appropriate *M. bovis* template* in a 96-well plate (white) followed by an addition of two drops of mineral oil. Samples were sealed using a clear adhesive film and loaded onto BISON set at 60 °C and ran for 90 min.

*- dilutions of the templates were performed using the appropriate concentrations of the tested inhibitors as diluents.

M. bovis 23s rRNA at concentration 1000 and 100 cps/5uL was used in this study.

Serial dilutions (20 uL sample + 180 uL diluent) of the 23s rRNA top stock [10^6 cps/5uL] were carried out in order to obtain the appropriate template concentrations.

For the inhibitory samples, 1000 ng/5uL of salmon sperm DNA was used as diluent.

Appendix 12

Protocol 12: Primer mutations screening procedure using standard TB LAMP-BART assay

Reaction mix set up:

Dispense volume [µL]:	15					
		Final conc				
Component	Stock	Mix+sample	Units	Spec	[µL]	Added
MGW				MS00001	325	
Trehalose (25% solution)	250	50	mg/mL	SS008	400	
Bicine Buffer	4x	1x			500	
Mg2SO4, 100mM	100	2	mM	MS00017	40	
Dithiothreitol 1M	1000	10	mM	SS003	20	
Luciferin, 10 mg/mL solution	10	0.1	mg/mL	SS0004	20	
10 mM APS	10000	250	µM	MS00015	50	
Ultraglow luciferase	50.7	0.025	µg/mL	MS00011	2.0	
300U/ml ATP sulphurylase	300000	375	mU/mL	MS00012	2.5	
100mM dNTP mix (25mM eac	25000	300	µM	MS00032	24	
Bst LF DNA polymerase	160000	200	u/mL	MS00029	2.5	
Lamp F TB103	100	1.6	µM	MWG		
LAMP B TB087	100	1.6	µM		32	
Loop B TB083	100	0.8	µM		16	
LoopF TB101	100	0.8	µM		16	
Disp B TB100	100	0.4	µM		8	
Disp F TB115	100	0.4	µM		8	
Maxima RtaseH +	200	0.2	u/µl	MS00030	2	
				Total Volume	1468	[µL]

Initial master mix was prepared according to the reaction mix set up shown above. 1468 uL of the initial reaction mix was then split into four aliquots of 367 uL each. Final master mix was prepared by adding 8 uL of the appropriate version of the LAMP F primer to separate aliquots containing 367 uL of the initial master mix. 15 uL of the final master mix was then mixed with 5 uL of the appropriate *M. bovis* template [10^4 cps/5uL] in a 96-well plate (white) followed by an addition of two drops of mineral oil. Samples were sealed using a clear adhesive film and loaded onto BISON set at 60 °C and ran for 90 min.

Note that the loop primers were not added.

Appendix 13

Protocol 13: Assessment of DNA contamination in IAC RNA samples

Initial master mix was prepared according to the reaction mix set up shown in appendix 7. However, Maxima RNaseH+ was not added to the initial master mix. 1498 uL of the initial master mix was then split into two aliquots of 749 uL each followed by an addition of 1 uL of either Maxima RNaseH+ [200 U/uL] or MGW. 15 uL of the final master mix was then mixed with 5 uL of the appropriate *IAC* template in a 96-well plate (white) followed by an addition of two drops of mineral oil. Samples were sealed using a clear adhesive film and loaded onto BISON set at 60 °C and ran for 90 min.

IAC RNA and DNA concentrations of 10^8, 10^7, 10^6 and 10^5 cps/5uL, were used in this study

Appendix 14

Protocol 14: Standard TB LAMP-BART assay with IAC RNA at 10^6 cps/rxn

Reaction mix set up:

Dispense volume [µL]:	15					
		Final conc				
Component	Stock	Mix+sample	Units	Spec	[µL]	Added
IAC RNA	10^7	5 x 10^4	cps/µl		10	
MGW				MS00001	315	
Trehalose (25% solution)	250	50	mg/mL	SS008	400	
Bicine Buffer	4x	1x			500	
Mg2SO4, 100mM	100	2	mM	MS00017	40	
Dithiothreitol 1M	1000	10	mM	SS003	20	
Luciferin, 10 mg/mL solution	10	0.1	mg/mL	SS0004	20	
10 mM APS	10000	250	µM	MS00015	50	
Ultraglow luciferase	50.7	0.025	µg/mL	MS00011	2.0	
300U/ml ATP sulphurylase	300000	375	mU/mL	MS00012	2.5	
100mM dNTP mix (25mM eac	25000	300	µM	MS00032	24	
Bst LF DNA polymerase	160000	200	u/mL	MS00029	2.5	
Lamp F TB103	100	1.6	µM	MWG	32	
LAMP B TB087	100	1.6	µM		32	
Loop B TB083	100	0.8	µM		16	
LoopF TB101	100	0.8	µM		16	
Disp B TB100	100	0.4	µM		8	
Disp F TB115	100	0.4	µM		8	
Maxima RtaseH +	200	0.2	u/µl	MS00030	2	
				Total Volume	1500	[µL]

Master mix was prepared according to the reaction mix set up shown above. 15 uL of the master [10^6 cp/rxn IAC RNA] mix was then mixed with 5 uL of the appropriate *M. bovis* template in a 96-well plate (white) followed by an addition of two drops of mineral oil. Samples were sealed using a clear adhesive film and loaded onto BISON set at 60 °C and ran for 90 min.

M. bovis 23s rRNA at concentrations 10^4, 10^3 and 100 cps/5uL were used in this study.

Appendix 15

Protocol 15: Standard TB IAC LAMP-BART assay with ROX-HIV probe

Reaction mix set up:

Dispense volume [µL]:	15					
		Final conc				
Component	Stock	Mix+sample	Units	Spec	[µL]	Added
MGW				MS00001	309	
Trehalose (25% solution)	250	50	mg/mL	SS008	400	
Bicine Buffer	4x	1x			500	
Mg2SO4, 100mM	100	2	mM	MS00017	40	
Dithiothreitol 1M	1000	10	mM	SS003	20	
Luciferin, 10 mg/mL solution	10	0.1	mg/mL	SS0004	20	
10 mM APS	10000	250	µM	MS00015	50	
Ultraglow luciferase	50.7	0.025	µg/mL	MS00011	2.0	
300U/ml ATP sulphurylase	300000	375	mU/mL	MS00012	2.5	
100mM dNTP mix (25mM eac	25000	300	µM	MS00032	24	
Bst LF DNA polymerase	160000	200	u/mL	MS00029		
Lamp F TB103	100	1.6	µM	MWG	32	
LAMP B TB087	100	1.6	µM		32	
Loop B TB083	100	0.8	µM		16	
LoopF TB101	100	0.8	µM		16	
Disp B TB100	100	0.4	µM		8	
HIV probe	100	0.8	µM			
Disp F TB115	100	0.4	µM		8	
Maxima RtaseH +	200	0.2	u/µl	MS00030	2	
				Total Volume	1482	[µL]

Initial master mix was prepared according to the reaction mix set up shown above. 1482 uL of the initial reaction mix was then split into two aliquots of 741 uL each, followed by an addition of either 1 uL GSP-SSD or 1.3 uL Bst large fragment. Each of the two prepared aliquots was then split into two smaller aliquots of 370.5 uL each. Final master mix was prepared by adding 4 uL of either HIV probe or MGW to the separate aliquots containing 370.5 uL of the initial master mix with either GSP-SSD or Bst large fragment. 15 uL of the final master mix was then mixed with 5 uL of the IAC RNA template [10^6 cps/5uL] in a 96-well plate (white) followed by an addition of two drops of mineral oil. Samples were sealed using a clear adhesive film and loaded onto BISON set at 60 °C and ran for 90 min.

Note: 50 mM Bicine buffer was used in this study

Appendix 16

Protocol 16: Inhibitory substances screening procedure using modified TB LAMP-BART assay – Sodium chloride

Reaction mix set up:

Dispense volume [µL]:	15					
		Final conc				
Component	Stock	Mix+sample	Units	Spec	[µL]	Added
M. bovis RNA	1000	5	cps/µl			
IAC RNA	10^7	5 x 10^4	cps/µl			
MGW				MS00001	305	
Trehalose (25% solution)	250	50	mg/mL	SS008	400	
Bicine Buffer	4x	1x			500	
Mg2SO4, 100mM	100	2	mM	MS00017	40	
Dithiothreitol 1M	1000	10	mM	SS003	20	
Luciferin, 10 mg/mL solution	10	0.1	mg/mL	SS0004	20	
10 mM APS	10000	250	µM	MS00015	50	
Ultraglow luciferase	50.7	0.025	µg/mL	MS00011	2.0	
300U/ml ATP sulphurylase	300000	375	mU/mL	MS00012	2.5	
100mM dNTP mix (25mM eac	25000	300	µM	MS00032	24	
Bst LF DNA polymerase	160000	200	u/mL	MS00029	2.5	
Lamp F TB103	100	1.6	µM	MWG	32	
LAMP B TB087	100	1.6	µM		32	
Loop B TB083	100	0.8	µM		16	
LoopF TB101	100	0.8	µM		16	
Disp B TB100	100	0.4	µM		8	
Disp F TB115	100	0.4	µM		8	
Maxima RtaseH +	200	0.2	u/µl	MS00030	2	
				Total Volume	1480	[µL]

Initial master mix was prepared according to the reaction mix set up shown above. 1480 uL of the initial reaction mix was then split into two aliquots of 740 uL each. Final master mix was prepared by adding 5 uL of both MGW and IAC RNA or 5 uL of IAC and TB RNA to the separate aliquots containing 740 uL of the initial master mix. 15 uL of the final master mix was then mixed with 5 uL of the appropriate inhibitory substance in a 96-well plate (white) followed by an addition of two drops of mineral oil. Samples were sealed using a clear adhesive film and loaded onto BISON set at 60 °C and ran for 90 min.

Sodium chloride at concentrations 20, 30 and 40 mM was used in this study.

Appendix 17

Protocol 17: Inhibitory substances screening procedure using modified TB LAMP-BART assay – carrier DNA

Reaction mix set up:

Dispense volume [µL]:	15					
		Final conc				
Component	Stock	Mix+sample	Units	Spec	[µL]	Added
M. bovis RNA	1000	5	cps/µl			
IAC RNA	10^7	5 x 10^4	cps/µl			
MGW				MS00001	305	
Trehalose (25% solution)	250	50	mg/mL	SS008	400	
Bicine Buffer	4x	1x			500	
Mg2SO4, 100mM	100	2	mM	MS00017	40	
Dithiothreitol 1M	1000	10	mM	SS003	20	
Luciferin, 10 mg/mL solution	10	0.1	mg/mL	SS0004	20	
10 mM APS	10000	250	µM	MS00015	50	
Ultraglow luciferase	50.7	0.025	µg/mL	MS00011	2.0	
300U/ml ATP sulphurylase	300000	375	mU/mL	MS00012	2.5	
100mM dNTP mix (25mM eac	25000	300	µM	MS00032	24	
Bst LF DNA polymerase	160000	200	u/mL	MS00029	2.5	
Lamp F TB103	100	1.6	µM	MWG	32	
LAMP B TB087	100	1.6	µM		32	
Loop B TB083	100	0.8	µM		16	
LoopF TB101	100	0.8	µM		16	
Disp B TB100	100	0.4	µM		8	
Disp F TB115	100	0.4	µM		8	
Maxima RtaseH +	200	0.2	u/µl	MS00030	2	
				Total Volume	1480	[µL]

Initial master mix was prepared according to the reaction mix set up shown above. 1480 uL of the initial reaction mix was then split into two aliquots of 740 uL each. Final master mix was prepared by adding 5 uL of MGW and 5 uL of either IAC or TB RNA to the separate aliquots containing 740 uL of the initial master mix. 15 uL of the final master mix was then mixed with 5 uL of the appropriate inhibitory substance in a 96-well plate (white) followed by an addition of two drops of mineral oil. Samples were sealed using a clear adhesive film and loaded onto BISON set at 60 °C and ran for 90 min.

Salmon sperm DNA at concentrations 50, 500 and 1000 ng/5uL was used in this study.

Appendix 18

Protocol 18: Standard TB LAMP-BART assay (50 uL)

Reaction mix set up:

Dispense volume [µL]:	50					
		Final conc				
Component	Stock	Mix+sample	Units	Spec	[µL]	Added
MGW				MS00001	583	
Trehalose (25% solution)	250	50	mg/mL	SS008	300	
TB RNA	10^4	100	cp/5uL			
IAC RNA	10^7	10^6	cp/5uL			
Bicine Buffer	4x	1x		STD	375	
MgCl2, 100mM	100	2	mM	MS00017	30	
Dithiothreitol 1M	1000	10	mM	SS003	15	
Luciferin, 10 mg/mL solution	10	0.1	mg/mL	SS0004	15	
10 mM APS	10000	250	µM	MS00015	37.5	
Ultraglow luciferase	50.7	0.025	µg/mL	MS00011	1.2	
300U/ml ATP sulphurylase	300000	375	mU/mL	MS00012	1.8	
100mM dNTP mix (25mM eac	25000	400	µM	MS00032	24	
GSP	100	0.1	U/uL	MS00029	1.5	
Lamp F TB103	100	1.6	µM	MWG	24	
LAMP B TB087	100	1.6	µM		24	
LoopB 083	100	0.8	µM		12	
LoopF TB101	100	0.8	µM		12	
Disp B TB100	100	0.4	µM		6	
Disp F TB115	100	0.4	µM		6	
Maxima RtaseH +	200	0.2	u/µl	MS00030	1.5	
				Total Volume	1470	[µL]

Initial master mix was prepared according to the reaction mix set up shown above. 1470 uL of the initial reaction mixes was then split into two aliquots of 735 uL each. Final master mix was prepared by adding 7.5 uL of MGW and 7.5 uL of either *M. bovis* TB template [10^4 cps/5uL] or IAC RNA [10^7 cps/5uL] to separate aliquots containing 735 uL of the initial master mix. 50 uL of the final reaction mix (including templates) was then dispensed across 30 wells of a 96-well plate (white) covered with 2 drops of mineral oil and sealed using adhesive clear film. Samples were run at 60 °C for 90 min on BISON.

Appendix 19

Protocol 19: Inhibitory substances screening procedure using standard TB LAMP-BART assay (50 uL) – carrier DNA (500ng)

Reaction mix set up:

Dispense volume [µL]:	50					
		Final conc				
Component	Stock	Mix+sample	Units	Spec	[µL]	Added
MGW				MS00001	568	
Carrier DNA	1000	10	ng/µl			
Trehalose (25%solution)	250	50	mg/mL	SS008	300	
TB RNA	2 x 10^3	2	cps/uL			
IAC RNA	2 x 10^6	2 x 10^4	cps/uL		15	
Bicine Buffer	4x	1x		STD	375	
MgCl2, 100mM	100	2	mM	MS00017	30	
Dithiothreitol 1M	1000	10	mM	SS003	15	
Luciferin, 10 mg/mL solution	10	0.1	mg/mL	SS0004	15	
10 mM APS	10000	250	µM	MS00015	37.5	
Ultraglow luciferase	50.7	0.025	µg/mL	MS00011	1.2	
300U/ml ATP sulphurylase	300000	375	mU/mL	MS00012	1.8	
100mM dNTP mix (25mM eac	25000	400	µM	MS00032	24	
GSP	100	0.1	U/uL	MS00029	1.5	
Lamp F TB103	100	1.6	µM	MWG	24	
LAMP B TB087	100	1.6	µM		24	
LoopB 083	100	0.8	µM		12	
LoopF TB101	100	0.8	µM		12	
Disp B TB100	100	0.4	µM		6	
Disp F TB115	100	0.4	µM		6	
Maxima RtaseH +	200	0.2	u/µl	MS00030	1.5	
				Total Volume	1470	[µL]

Initial master mix was prepared according to the reaction mix set up shown above. 1470 uL of the initial reaction mixes was then split into two aliquots of 735 uL each followed by an addition of 7.5 uL either MGW or TB *M. bovis* RNA. The two prepared initial master mixes (after additions) were then split into two smaller aliquots of 371.25 uL each. Final master mix was prepared by adding 3.75 uL of either MGW or carrier DNA [1000 ng/uL] to separate aliquots containing 371.25 uL of the initial master mix with either added TB RNA or MGW. 50 uL and 10 uL of the final reaction mix (including templates) were then dispensed across a 96-well plate (white) covered with 2 drops of mineral oil and sealed using adhesive clear film. Samples were run at 60 °C for 90 min on BISON.

Appendix 20

Protocol 20: Standard HBV LAMP-BART assay

Reaction mix set up:

Dispence valume	15					
		Final conc				
Component	**Stock**	**Mix+sample**	**Units**	**Spec**	**uL required**	**Added**
MGW				MS00001	466	
25% w/v trehalose	250	75	mg/mL	SS008	600	
Isothermal buffer	10	1	x		200	
1M DTT	1000	10	mM	SS003	20	
Luciferin, 10 mg/mL solution	10	0.1	mg/mL	SS0004	20	
10 mM APS (Biolog)	10000	250	µM	MS00015	50	
Ultraglow luciferase	50.7	0.05	ug/mL	MS00011	2.0	
300U/ml ATP sulphurylase	300000	375	mu/mL	MS00012	2.5	
dATP 100mM	100000	300	µM	MS00008	6	
dTTP 100mM	100000	300	µM		6	
dCTP 100mM	100000	300	µM		6	
dGTP 100mM	100000	300	µM		6	
Bst 2.0 WS	200000	200	units/mL	MS00010	3.0	
HBV-019 (DispB)	100	1.6	µM		8	
HBV-024 (DispF)	100	1.6	µM		8	
HBV-021(Bloop)	100	0.8	µM		16	
HBV-023 (Floop)	100	0.8	µM		16	
HBV-020 (BIP)	100	0.4	µM		32	
HBV-022 (FIP)	100	0.4	µM	Supertempla	32	
				Total Volume	1500	(µL)

Master mix was prepared according to the reaction mix set up shown above. 15 uL of the master mix was then mixed with 5 uL of the appropriate *HBV* template in a 96-well plate (white) followed by an addition of two drops of mineral oil. Samples were sealed using a clear adhesive film and loaded onto BISON set at 60 °C and ran for 90 min.

Appendix 21

Protocol 21: Modified HBV LAMP-BART assay (no BART)

Reaction mix set up:

Dispense volume [µL]:	15					
		Final conc				
Component	**Stock**	**Mix+sample**	**Units**	**Spec**	**uL required**	**Added**
MGW				MS00001	281	
25% w/v trehalose	250	75	mg/mL	SS008	300	
Isothermal buffer	10	1	x		100	
1M DTT	1000	10	mM	SS003		
Luciferin, 10 mg/mL solution	10	0.1	mg/mL	SS0004		
10 mM APS (Biolog)	10000	250	µM	MS00015		
Ultraglow luciferase	50.7	0.05	ug/mL	MS00011		
300U/ml ATP sulphurylase	300000	375	mu/mL	MS00012		
dATP 100mM	100000	300	µM	MS00008	3	
dTTP 100mM	100000	300	µM		3	
dCTP 100mM	100000	300	µM		3	
dGTP 100mM	100000	300	µM		3	
GSP	100000	200	units/mL	MS00010	1.0	
HBV-019 (DispB)	100	0.4	µM		4	
HBV-024 (DispF)	100	0.4	µM		4	
HBV-021(Bloop)	100	0.8	µM		8	
HBV-023 (Floop)	100	0.8	µM			
HBV-020 (BIP)	100	1.6	µM		16	
HBV-022 (FIP)	100	1.6	µM	Supertempla	16	
				Total Volume	742	(µL)

Initial master mix was prepared according to the reaction mix set up shown above. 742 uL of the initial reaction mixes was then split into two aliquots of 371 uL each. Final master mix was prepared by adding 4 uL of either MGW or ROX-labelled loopF probe [100 uM] to separate aliquots containing 371 uL of the initial master mix. 15 uL of the final reaction mix was then mixed with 5 uL of the appropriate HBV template in a 96-well plate (white) covered with 2 drops of mineral oil and sealed using adhesive clear film. Samples were run at 60 °C for 90 cycles on Strategene. Note: each cycle was set to run for 1 min.

Appendix 22

Protocol 22: Modified HBV LAMP-BART assay

Reaction mix set up:

Dispense volume [µL]:	15					
		Final conc				
Component	**Stock**	**Mix+sample**	**Units**	**Spec**	**uL required**	**Added**
MGW				MS00001	234	
25% w/v trehalose	250	75	mg/mL	SS008	300	
Isothermal buffer	10	1	x		100	
1M DTT	1000	10	mM	SS003	10	
Luciferin, 10 mg/mL solution	10	0.1	mg/mL	SS0004	10	
10 mM APS (Biolog)	10000	250	µM	MS00015	25	
Ultraglow luciferase	50.7	0.05	ug/mL	MS00011	1.0	
300U/ml ATP sulphurylase	300000	375	mu/mL	MS00012	1.3	
dATP 100mM	100000	300	µM	MS00008	3	
dTTP 100mM	100000	300	µM		3	
dCTP 100mM	100000	300	µM		3	
dGTP 100mM	100000	300	µM		3	
GSP	100000	200	units/mL	MS00010	1.0	
HBV-019 (DispB)	100	0.4	µM		4	
HBV-024 (DispF)	100	0.4	µM		4	
HBV-021(Bloop)	100	0.8	µM		8	
HBV-023 (Floop)	100	0.8	µM			
ST 35-2	100	1.6	µM		16	
ST 37-2	100	1.6	µM	Supertempla	16	
				Total Volume	742	(µL)

Initial master mix was prepared according to the reaction mix set up shown above. 742 uL of the initial reaction mixes was then split into two aliquots of 371 uL each. Final master mix was prepared by adding 4 uL of either MGW or ROX-labelled loopF probe [100 uM] to separate aliquots containing 371 uL of the initial master mix. 15 uL of the final reaction mix was then mixed with 5 uL of the appropriate HBV template in a 96-well plate (white) covered with 2 drops of mineral oil and sealed using adhesive clear film. Samples were run at 60 °C for 90 cycles on Strategene. Note: each cycle was set to run for 1 min.

Appendix 23

Protocol 23: Standard fluorescent TB LAMP assay

Reaction mix set up:

Dispense volume [µL]:	15					
		Final conc				
Component	Stock	Mix+sample	Units	Spec	[µL]	Added
SYBR	10x	0.1x			20	
HIV probe	10^7	5 x 10^4	cps/µl		16	
MGW				MS00001	416	
Trehalose (25% solution)	250	50	mg/mL	SS008	400	
Bicine Buffer	4x	1x			500	
Mg2SO4, 100mM	100	2	mM	MS00017	40	
Dithiothreitol 1M	1000	10	mM	SS003		
Luciferin, 10 mg/mL solution	10	0.1	mg/mL	SS0004		
10 mM APS	10000	250	µM	MS00015		
Ultraglow luciferase	50.7	0.025	µg/mL	MS00011		
300U/ml ATP sulphurylase	300000	375	mU/mL	MS00012		
100mM dNTP mix (25mM eac	25000	300	µM	MS00032	24	
Bst LF DNA polymerase	160000	200	u/mL	MS00029		
Lamp F TB103	100	1.6	µM	MWG	32	
LAMP B TB087	100	1.6	µM		32	
Loop B TB083	100	0.8	µM			
LoopF TB101	100	0.8	µM			
Disp B TB100	100	0.4	µM		8	
Disp F TB115	100	0.4	µM		8	
Maxima RtaseH +	200	0.2	u/µl	MS00030	2	
				Total Volume	1498	[µL]

Initial master mix was prepared according to the reaction mix set up shown above. 1498 uL of the initial reaction mixes was then split into two aliquots of 749 uL each. Final master mix was prepared by adding 1 uL of GSP-SSD [100 U/uL] or 1.3 uL Bst large fragment [160 U/uL] to separate aliquots containing 749 uL of the initial master mix. 15 uL of the final reaction mix was then mixed with 5 uL of the appropriate IAC template in a 96-well plate (white) covered with 2 drops of mineral oil and sealed using adhesive clear film. Samples were run at 60 °C for 90 cycles on Strategene. Note: each cycle was set to run for 1 min.

Appendix 24

Protocol 24: Standard miRNA LAMP-BART assay

Reaction mix set up:

Reaction set-up	
Volume/reaction [ul]:	20
Number reactions (inc. extra):	50
Bulk mix	**µl for bulk mix**
MGW	**142.0**
10x Thermopol buffer	**100**
25% Trehalose	**200**
1M DTT	**5**
40mg/ml PVP	**10**
1.2 M KCl	**33**
5mM dNTPs (5mM of each)	**60**
10mg/ml LH2	**10**
10 mM APS (Biolog)	**25**
0.55mg/ml rLuc Ultraglo	**10**
25U/ml ATP sulphurylase NEB*	**15**
8U/µl Bst DNA polymerase	**40**
10x primer combinations	**100**
Total mix volume, ul	**750**

Master mix was prepared according to the reaction mix set up shown above. 15 uL of the master mix was then mixed with 5 uL of the appropriate *miRNA* template in a 96-well plate (white) followed by an addition of two drops of mineral oil. Samples were sealed using a clear adhesive film and loaded onto "Lucy" set at 60 °C and ran for 90 min.

Appendix 25

Protocol 25: 10x primer combination

Primer mix set up:

Primer	volume added [uL]
F3	**2**
B3	**2**
FIP	**8**
BIP	**8**
Loop B	**4**
Loop F	**4**
MGW	**72**
Total mix volume, ul	**100**

Note: all primers used were stored at 100 uM

Appendix 26

Protocol 26: Reagent preparation for miRNA and LAMP assays

1) Salmon sperm carrier DNA
supplied by Invitrogen at 10mg/ml but NanoDrop for more accurate concentration, dilute 1/100 in serial dilution to ng/µl (typically 142ng/µl) use in assay at 100ng per partition, label and store at -20°C

2) Molecular grade water
supplied by Fisher (not Milli-Q or ELIX water), approximately 1.5ml per 2ml screw-top tube, label and store at -20°C

3) 10x Thermopol buffer
supplied by NEB at 10X concentration and used directly

4) 25% Trehalose
supplied by Sigma as a powder, prepare by adding 12.5g to 50ml MGW, produces approximately 80 aliquots of 420µl per batch, label and store at -20°C

5) 1M DTT
supplied by Sigma as a powder, prepare by adding 1.54g to 10ml MGW, produces approximately 100 aliquots of 100µl per batch, label and store at -20°C

6) 40mg/ml PVP
supplies by Sigma as a powder, prepare by adding 0.4g to 10ml MGW, produces approximately 100 aliquots of 100µl per batch, label and store at -20°C

7) 1.2M KCl
supplied by Fisher as a powder, prepare by adding 0.895g to 10ml MGW, produces approximately 80 aliquots of 100µl per batch, label and store at -20°C

8) 5mM dNTPs
supplied by Invitrogen at 100mM for each dNTP, prepare by adding 10µl of each to 160µl MGW in 8 tubes, produces 24 aliquots of 65µl per batch, label and store at -20°C

9) 10mg/ml Luciferin
D-luciferin K salt supplied by Europa Bioproducts, prepare by adding 10mg to 1ml MGW, produces 40 aliquots of 25µl per batch, label and store at -20°C

10) 10mM APS
supplied by Biolog at desired concentration, each vial produces 16 aliquots of 60µl, label and store at -20°C

11) 0.55mg/ml Ultra-Glo Luciferase
Ultra-glo luciferase supplied by Promega at 5.5mg/ml, prepare 100µl luciferase with 10µl 1M DTT, 100µl NEB Thermopol (10X) and 790µl MGW, produces 40 aliquots of 25µl per batch, label and store at -20°C

12) 25U/ml ATP sulphurylase
supplied by NEB at 300U/ml, dilute 4µl ATP-S with 44µl Diluent D or VENT Diluent when required

13) 8U/ml Bst DNA polymerase
supplied by NEB at 8000U/ml and used directly

14) mineral oil
supplied by Fisher, approximately 1.5ml per 2ml screw-top tube, label and store at room temperature

15) primers
supplied by Sigma or MWG Operon, dilute as indicated with MGW to 100µM, label and store at -20°C, enter details on Lab Collector

Appendix 27

Protocol 27: SplintR ligation protocol

Reagent	Volume [ul]
P1 [100uM]	1
P2 [100uM]	1
miRNA [100uM]	1
SplintR Buffer [10x]	2
SplintR [25 U/uL]	1
MGW	14
Total volume	20

Appendix 28

Protocol 28: Ampligase ligation protocol

Reagent	Volume [ul]
P1 [100uM]	1
P2 [100uM]	1
miRNA [100uM]	1
Ampligase Buffer [10	2
Ampligase [5 U/uL]	1
MGW	14
Total volume	20

Appendix 29

Protocol 29: T4 ligation protocol

Reagent	Volume [ul]
P1 [100uM]	1
P2 [100uM]	1
miRNA [100uM]	1
T4 Buffer [10x]	2
T4 ligase [400 U/uL]	1
MGW	14
Total volume	20

Appendix 30

Protocol 30: T7 ligation protocol

Reagent	Volume [ul]
P1 [100uM]	1
P2 [100uM]	1
miRNA [100uM]	1
T7 Buffer [2x]	10
T7 ligase [3000 U/uL]	1
MGW	4
Total volume	20

Appendix 31

Protocol 31: Restriction digest protocol

Reagent	Volume [ul]
Template	1
Buffer	5
Restriction Enzyme	1
MGW	43
Total volume	50

Appendix 32

Protocol 32: Restriction digest protocol under LAMP-BART reaction set up

Bulk mix	µl for bulk mix
MGW	**109.6**
10x Thermopol buffer	**20**
25% Trehalose	**40**
1M DTT	**2**
40mg/ml PVP	**2**
1.2 M KCl	**6.4**
5mM dNTPs (5mM of each)	**12**
10mg/ml LH2	
10 mM APS (Biolog)	**5**
0.55mg/ml rLuc Ultraglo	
25U/ml ATP sulphurylase NEB*	**3**
8U/µl Bst DNA polymerase	
10x primer combinations	
Total mix volume, ul	**200**

44 uL of the reaction mix was then mixed with 5 uL of the restriction template and 1 uL of the appropriate endonuclease

Appendix 33

Protocol 33: Preparation of restriction templates

Reagent	Volume [ul]				
2x QI MasterMix	50		PCR cycling conditions		
Lin-DNA primer	10		94 °C 3 min		
Template [100uM]	10		94 °C 30 sec		35 cycles
MGW	30		55 °C 30 sec		
			72 °C 30 sec		
Total volume	100		72 °C 10 min		

Each template was purchased from Sigma and reconstituted at 100 uM concentration

Appendix 34

Protocol 34: SDS-PAGE protocol

SDS page Gels (For 2 gels, 0.75mm plates or 1 gel, 1.5mm plates)

10% Gel

- 4.1ml H_2O
- 2.5ml Tris 1.5M pH 8.8
- 3.3ml Acrylamide (33%)
- 100ul SDS (10%)
- 50ul APS (10%)
- 10ul TEMED

Run at 45 V for 85 min

Appendix 35

Protocol 35: Endonuclease-based miRNA detection protocol

Reaction set up:

Volume/reaction [ul]:	20
Number reactions (inc. extra):	**25**
Bulk mix	**µl for bulk mix**
MGW	**50.0**
10x Thermopol buffer	**50**
25% Trehalose	**100**
1M DTT	**5**
40mg/ml PVP	**5**
BstUI	**8**
1.2 M KCl	**16.5**
5mM dNTPs (5mM of each)	**30**
10mg/ml LH2	**5**
10 mM APS (Biolog)	**12.5**
0.55mg/ml rLuc Ultraglo	**5**
25U/ml ATP sulphurylase NEB*	**7.5**
BstUI template	**10**
8U/µl Bst DNA polymerase	**20**
10x primer combinations	**50**
Total mix volume, ul	**375**

Master mix was prepared according to the reaction mix set up shown above. 15 uL of the master mix was then mixed with 5 uL of the appropriate *miRNA* template in a 96-well plate (white) followed by an addition of two drops of mineral oil. Samples were sealed using a clear adhesive film and loaded onto "Lucy" set at 60 °C and ran for 90 min.

Appendix 36

SDS-PAGE showing probe ligation via miRNA using SplintR ligase

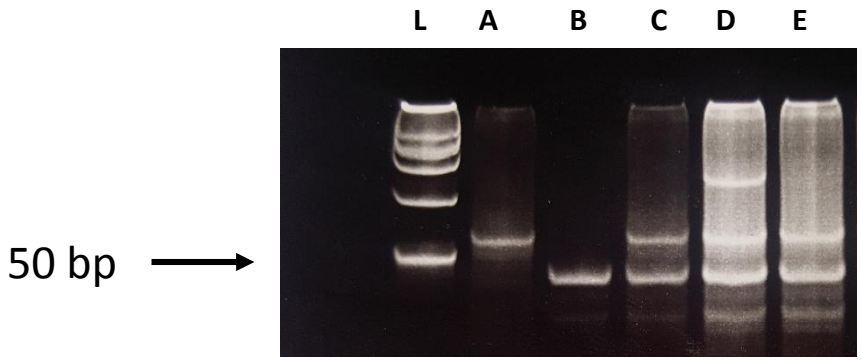

Lanes:

L – 50 bp ladder (NEB)

A – P1

B – P2

C – P1 + P2

D – P1 + P2 + miRNA

E – P1 + P2

Note: lanes D and E show samples that underwent ligation reactions

Appendix 37

Primer and probes sequences used in the ligation-based miRNA detection system

Primer	Sequence (5'→3')
Probe 1	Phos-GTCTCAGGGAATTTTCCACGTCTTCAAAGCAAGTGGTTTTTCCACTGACGTAAG GGTTTTGACGCACAATCCCACTATCCTTTTCCACTTGCTTTGAAGACGTGG
Probe 2	TTCCACGATGCTCCTCGTTTTCCTCTGCCGACAGTGGTTTTCCCAAAGATGGACC CCTTTTCGAGGAGCATCGTGGAATTTTTCACACTTGAG
FIP	CCACGTCTTCAAAGCAAGTGGTTTTGGATAGTGGGATTGTGCGTC
BIP	TTCCACGATGCTCCTCGTTTTCCTCTGCCGACAGTGG

Appendix 38

Primer and probes sequences used in the endonuclease-based miRNA detection system

Probe (5’ → 3’)

P1BstUI- TTTT-GTTCTATAGAGGAAGGGTCA-AGACTAT-TAGTCCTAGGCTGATCAGTG-TTTT-ATATCCTGAGTGACTCCAA-CTAATGGGTCTATGT-CG-TAAGTCCAACTGGACTCCTT-TTTT-AAGGAGTCCAGTTGGACTTA-CGCG-TCACACTTGAGGTCTCAGGGAA

P1BsaWI- TTTT-GTTCTATAGAGGAAGGGTCA-AGACTAT-TAGTCCTAGGCTGATCAGTG-TTTT-ATATCCTGAGTGACTCCAA-CTAATGGGTCTATGT-TAAGTCCAACTGGACTCCTT-TTTT-AAGGAGTCCAGTTGGACTTA-CCGG-TCACACTTGAGGTCTCAGGGAA

P1Nb.BsmI
TTaaTTGTTCTATAGAGGAAGGGTCAAGACTATTAGTCCTAGGCTGATCAGTGTTTTATATCCTGAGcGAgacCTtgTAATGGGTCTATGTCcattcTAAGTCCAACTGGACTCCTTTTTTAAGGAGTCCAGTTGGACTTAgaatGCattTCACACTTGAGGTCTCAGGGAA

UUCCCUGAGACCUCAAGUGUGA- miRNA

5’ – gttctcgctcagttgtgtt-tttt-tagaggggaagcgtaatcag – 3’ Primer L1v1

5’-TTGGAGTCACTCAGGATAT-TTTT-TAGTCCTAGGCTGATCAGTG-3’ - Primer L1

5’-GTTCTATAGAGGAAGGGTCA-3’- Displacement primer

Appendix 39

HBV primers

Primer	Sequence 5' -> 3 '
HBV-019	GCTCAAGGCAACTCTATG
HBV-020	cccataggtattttgcgaaagGGATGGAAATTGCACCTG
HBV-021	caagatgatgggatgggaat
HBV-022	TCAGTGGTTCGTAGGGCccaataccacatcatccata
HBV-023	CCACTGTTTGGCTTTCAG
HBV-024	ctcaagatgctgcacag

TB primers

Primer	5'→3' sequence
Lamp B TB087	ACTCGCAGGCTCATTCTTTTTTCCGGAGGAGGGTG
Lamp F TB103	AAGGTTAACCCGTGTGGTTTTCGCGTGTGGGTCGC
Loop B TB083	CAAAAGGCACGCCATCA
LoopF TB101	CGAAAGCGAGTCTGAATAG
Disp B TB100	AGAGTACCTGAAACCGTG
Disp F TB115	ATTCACACGCGCGTAT

Appendix 40

Development of internal amplification controls for LAMP assays.

Objectives: Slowing down the amplification of IC templates by mutating FIP primers.

Materials and Methods

Reaction mixture was prepared according to the "HBV set-up160916". 1468 uL of the LAMP-BART mix was split into 4 aliquots of 367 uL each followed by the addition of 8 uL of the appropriate FIP primer [100mM]. 5 uL of the dsHBV template (LOT: 1529406) of 10000 cp/5uL was added to 15 uL of the final LAMP-BART reaction mix followed by an addition of mineral oil and ran for 90 min at 60°C on BISON 5.

NOTE: HBV template was prepared by adding 500 uL of MGW into a dried HBV pellet of 10^8 cp resulting in a final concentration of 10^6 cp/5ul. 3 x 10-fold serial dilutions (10 uL Sample + 90 uL MGW) were prepared in order to achieve final concentrations of 1000 and 10000 cp/5 uL.

		Final conc				
Component	Stock	Mix+sample	Units	Spec	uL required	Added
MGW				MS00001	498	
25% w/v trehalose	250	75	mg/mL	SS008	600	
Isothermal buffer	10	1	x		200	
1M DTT	1000	10	mM	SS003	20	
Luciferin, 10 mg/mL solution	10	0.1	mg/mL	SS0004	20	
10 mM APS (Biolog)	10000	250	µM	MS00015	50	
Ultraglow luciferase	50.7	0.05	ug/mL	MS00011	2.0	
300U/ml ATP sulphurylase	300000	375	mu/mL	MS00012	2.5	
dATP 100mM	100000	300	µM	MS00008	6	
dTTP 100mM	100000	300	µM		6	
dCTP 100mM	100000	300	µM		6	
dGTP 100mM	100000	300	µM		6	
Warm Start Bst	120000	200	units/mL	MS00010	3.3	
HBV-019 (DispB)	100	1.6	µM		8	
HBV-024 (DispF)	100	1.6	µM		8	
HBV-021(Bloop)	100	0.8	µM		0	
HBV-023 (Floop)	100	0.8	µM		0	
HBV-020 (BIP)	100	0.4	µM		32	
HBV-022 (FIP)	100	0.4	µM	Supertempla	0	
				Total Volume	1468	(µL)

HBV-019	GCTCAAGGCAACTCTATG
HBV-020	cccataggtattttgcgaaagGGATGGAAATTGCACCTG
HBV-021	caagatgatgggatgggaat
HBV-022	TCAGTGGTTCGTAGGGCccaataccacatcatccata
HBV-023	CCACTGTTTGGCTTTCAG
HBV-024	ctcaagatgctgcacag
Mut-HBV022FIPa	TCAGTGGTTCGTAGCCGccaataccacatcatccata
Mut-HBV022FIPb	TCAGTGGTTCGTTCCCGccaataccacatcatccata
Mut-HBV022FIPc	TCAGTGGTTCCATCCCGccaataccacatcatccata

Results

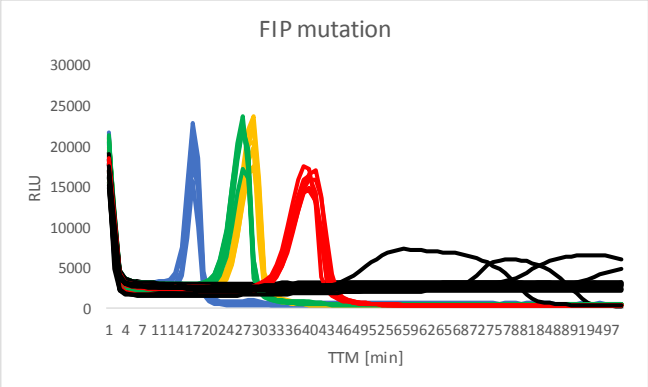

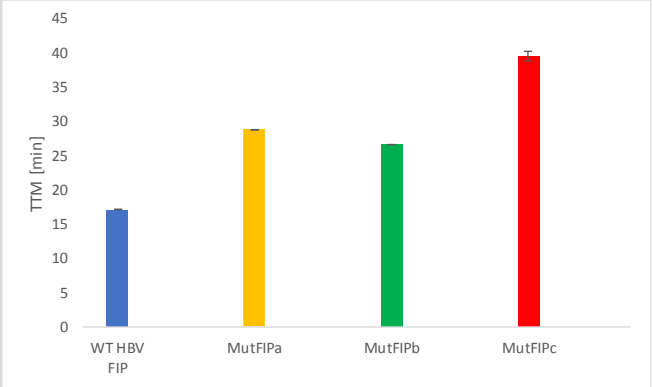

	DNA [cp/rxn]	Mean [min]	Stdev	Amp.Freq.[%]
WT HBV FIP	10000	17	0.0	100
MutFIPa	10000	29	0.0	100
MutFIPb	10000	27	0.0	100
MutFIPc	10000	40	0.7	100

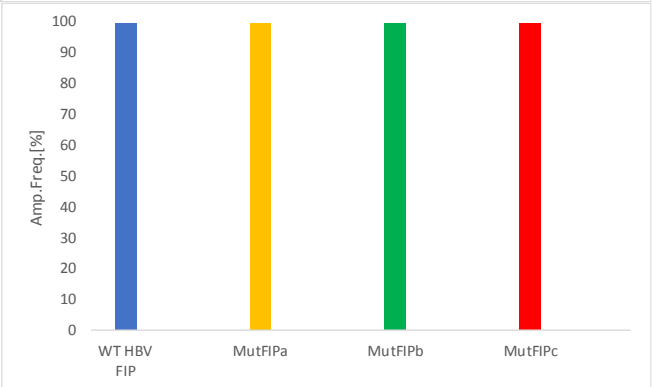

In this experiment, the amplification slow down via template mutation idea was tested on the dsHBV template using mutated FIP primers. Note that in this instance, the primers were mutated rather than the primer binding sides on the IC template due to the cost of the template synthesis.

In principle, the slow down technology is based on reduction of the Tms of the IC LAMP primers by mutating the F1 FIP biding side (or the primer F1 side itself) at the 3'ends. This reduction in Tm would then significantly impair the primer binding and folding to generate dumbbell structures thus impacting upon the amplification kinetics.

In this experiment, three different mutated FIP primers were tested where 3 to 7 bp were mutated at the 3' end of the F1 site. As expected, the TTMs were significantly affected regardless of the mutation introduced into the FIP primers. However, it was not surprising that the most significant delay in the amplification was observed in the reactions containing the FIP primer with 7 bp mutated. This mutation caused the most severe change to the Tm of the F1 site therefore impacting on the dumbbell generation most significantly.

Conclusions

The primer mutation experiment shows a huge promise as a potential IC method. Mutation of only one LAMP primer caused a major reduction in the amplification speed which could further be delayed by mutating the BIP primer.

Appendix 41

Protocol 35: Mucin preparation

Mucin from porcine stomach, type II, was purchased from Sigma-Aldrich, UK.

15mg/mL of Mucin solution was prepared by adding 75 g of mucin to 3 mL of 1M NaOH solution and vortexed at maximum speed for 5 min. The prepared solution was then topped up to the final volume of 5 mL using 1M NaOH and vortexed for additional 5 min.

The final mucin solution was stored at room temperature.

Appendix 42

SDS-PAGE showing four DNA probes designed for the endonuclease-based miRNA detection technology.

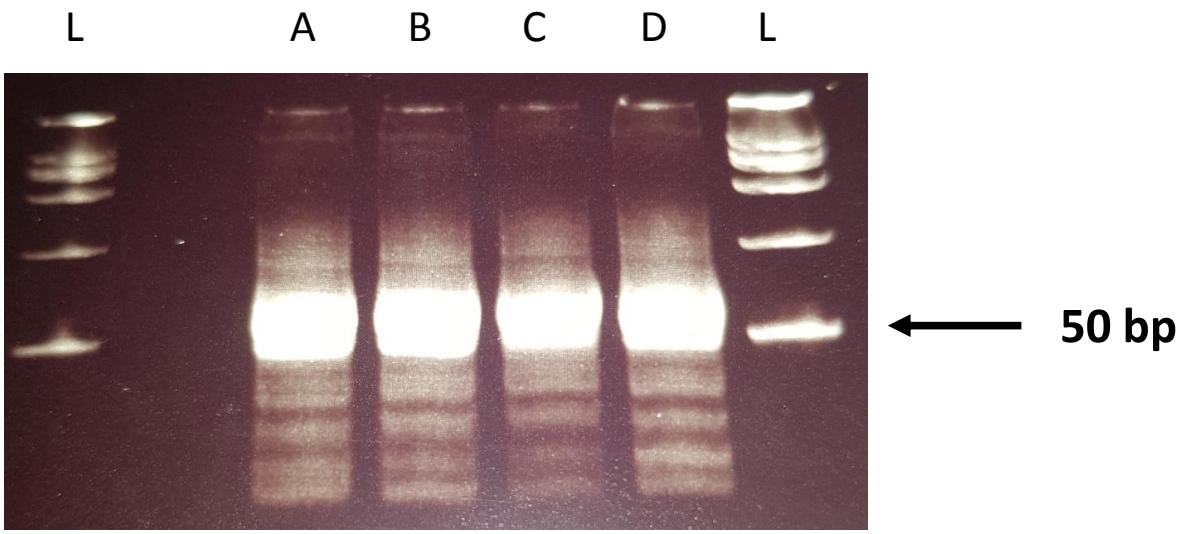

Lanes:

L – 50 bp ladder (NEB)

A – BstNI

B – BsaWI

C – BssKI

D – BstUI